Western&Graduate&PostdoctoralStudies

Electronic Thesis and Dissertation Repository

3-23-2021 11:45 AM

Uncovering Deficits in Auditory Processing and Cognition Following Hearing Loss and Prefrontal Cortex Dysfunction

Krystyna B. Wieczerzak, *The University of Western Ontario*

Follow this and additional works at: https://ir.lib.uwo.ca/etd

Part of the Systems Neuroscience Commons

Abstract

How the auditory cortex and higher-order cortical regions, e.g., the prefrontal cortex, interact for accurate auditory processing and perception is not fully understood. Furthermore, although hearing loss is correlated with cognitive impairment, and animal studies have shown that loud noise exposure causes hippocampal neuropathology, the effects of noise-induced hearing loss on the medial prefrontal cortex (mPFC) and higher-level cognitive functions have not been well studied. Using electrophysiological and cognitive-behavioural testing in rats, Chapter 2 provides the first evidence of noise-induced plasticity in the mPFC (e.g., loss of functional connectivity with the auditory cortex) and deficits in stimulus-response habit learning. Although the behavioural consequences of this plasticity remain unknown, past studies have suggested that functional connectivity between the auditory cortex and mPFC is crucial for sound detection in background noise. That said, the effect of permanent noise-induced hearing loss on sound detection in noisy environments has been studied comprehensively in rodent models. In Chapter 3 I first designed an operant conditioning-based behavioural task that required rats to detect a target sound in quiet or noisy backgrounds. Using this novel task, it was found that the same noise exposure that led to a decreased functional connectivity between the auditory cortex and mPFC did not necessarily lead to impaired sound detection. Finally, because the role of the mPFC in auditory processing and perception has not been fully elucidated, in Chapter 4 I used a battery of electrophysiological and behavioural experiments in rats to assess the effects of the mPFC (via pharmacological inactivation) on auditory functions. mPFC inactivation had limited effects on basic auditory processing; however, it significantly affected higher-order activity in the auditory cortex (e.g., diminished deviant effect, decreased mismatch response, and decreased spontaneous gamma oscillations) and worsened the rats' ability to detect sound in noise. Collectively, the novel findings in this thesis provide (1) further evidence of the complex and detrimental effects of noise exposure on higher-order cortical regions and cognitive functions, and (2) report exciting discoveries regarding the role of mPFC in sound

detection and processing, thereby opening possible new research paths into the field of auditory perception.

Keywords

Lay Person Summary

The sense of hearing allows us to chat with friends, listen to Freddy Mercury while taking a morning shower, or notice an upcoming emergency vehicle. Our brains are capable of processing sounds and making sense of them, including when we need to detect sounds that are important to us while ignoring background noise. Despite extensive research, the mechanisms giving rise to these common experiences are not fully known. Although we might be tempted to listen to our favourite song on maximum volume, we know it could lead to hearing loss. Beyond just damaging our hearing, studies report that noise exposure can also have detrimental effects on cognition. That said, which cognitive functions are most affected and the mechanisms linking hearing loss to those consequences remain unknown. Using a rat model, my first study found that noise exposure impaired the ability to learn a specific motor response following a visual stimulus (i.e., stimulus-response habit learning), and altered the way that sound information was processed across brain regions (i.e., functional connectivity between the auditory and prefrontal cortices). To further investigate how noise-induced hearing loss affects the brain, in my second study, I developed a task for rats to assess their ability to detect sounds in background noise. The results indicated that, although the severity of the rats' hearing loss was correlated with their performance, those rats with a mild hearing impairment did not exhibit a performance deficit. In my final study, I investigated how the prefrontal cortex—a higher-order brain region involved in cognitive processes such as attention—influences behaviours involving sound processing as well as the neural activity within the auditory system. By suppressing the activity of the prefrontal cortex using a drug manipulation, the rats had an impaired ability to detect sounds in a noisy background, and their brains were unable to effectively notice when a novel sound was presented. Taken together, the results of this thesis help to improve our understanding of how noise exposure can affect the brain, and the interactions between areas of the brain that ultimately contribute to the accurate processing of sounds within our environment.

Co-Authorship Statement

The first study of this thesis, entitled *Medial Prefrontal Cortex Plasticity and Cognitive-Behavioural Deficits Following Noise Exposure,* was accepted for publication in *Neuroscience,* and was co-authored by me, Salonee V. Patel, Hannah MacNeil, Kaela E. Scott, Ashley L. Schormans, Sarah H. Hayes, Björn Herrmann and Brian L. Allman. I designed the research project, performed all the hearing assessments, noise exposures, surgeries, electrophysiological recordings and analysis, and Morris water maze task, as well as performed all the statistical analyses, interpreted all of the data, and co-wrote and edited the manuscript. As noted in the publication, the co-authors assisted me in each of the following ways: Ashley Schormans and Brian Allman designed the research project; Salonee V. Patel, Hannah MacNeil, Kaela E. Scott, Ashley L. Schormans, Sarah H. Hayes and Björn Herrmann performed the data collection and analyses; Ashley L. Schormans, Sarah H. Hayes, Björn Herrmann and Brian L. Allman interpreted the data; Sarah Hayes, Björn Herrmann and Brian L. Allman co-wrote the manuscript; Ashley L. Schormans, Sarah Hayes and Brian Allman edited the manuscript. In particular, Hannah McNeil performed the operant conditioning-based lever task and analyzed the data. Salonee Patel analyzed the Morris water maze data. Björn Herrmann developed the original MATLAB scripts for analysis of the electrophysiological recordings.

The second study of this thesis, entitled *The Effects of Noise-Induced Hearing Loss on Sound Detection*, was designed by me Ashley L. Schormans and Brian L. Allman. I performed all behavioural experiments, data collection and analysis, statistical analysis, hearing assessments and noise exposures. Ashley L. Schormans and I designed the behavioural protocols. I designed the analysis scripts. Dr. Sarah H. Hayes provided valuable input on interpretation of the data. Kelly Yeung and Mohammed Al-Youzbaki assisted in behavioural training.

The third study of this thesis, entitled *The Effects of Medial Prefrontal Cortex Inactivation on Auditory Processing and Perception*, was designed by me and Brian L. Allman. Ashley L.

Schormans and I designed the protocols for the electrophysiological studies and sound detection behavioural task. Kaela E. Scott designed the acoustic startle response protocol. I designed all the analysis scripts and performed all the experiments, surgeries, drug deliveries, data collection and analysis, and statistical analysis. Mohammed Al-Youzbaki assisted in sound detection training and data collection. Niveen Fulcher and Alaa El-Cheikh Mohamad imaged the tissue slices for cannula placement confirmation.

The thesis was written by me, with valuable input from Drs. Brian L. Allman, Sarah H. Hayes, Ashley L. Schormans, Susanne Schmid, Björn Herrmann, Raj Rajakumar and Shawn Whitehead, that allowed for interpretation of the data and positioning it within the current literature. I created all the figures presented in this thesis. Furthermore, Drs. Brian L. Allman and Björn Herrmann edited the thesis.

Acknowledgments

First and foremost, I would like to thank my supervisor, Dr. Brian Allman, for his guidance and support over the last four years. He was excellent in helping me to learn how to relate my results to the literature. His devotion and enthusiasm for research and inspiring scientific conversations late in the lab provided many ideas for this thesis and perhaps for future projects.

I am grateful to the past and present members of the Allman lab for their emotional and scientific support for the past four years. I would particularly like to thank Dr. Ashley Schormans, who provided me with vital mentoring and scientific advice. Further, I would like to thank Dr. Sarah Hayes for sharing her expert audiologist insight and providing fantastic feedback into understanding the results of my studies, which was crucial in my training as a scientist. I would also like to thank Kaela Scott, Greg Sigel, Salonee Patel, Hanna MacNeil and Mohamed Al-Youzbaki for their scientific and emotional support. Moreover, I would like to thank you for the fantastic cupcakes, which kept me going during the hard times. I will miss them every birthday.

Furthermore, I would like to thank Dr. Björn Herrmann for his mentorship, guidance and support. He shared his vast scientific knowledge and much professional advice with me, for which I am forever grateful. Finally, I would also like to thank for his emotional support and always having my back, which made going through committee meetings so much less scary.

I would also like to thank the members of my advisory committee: Dr. Susanne Schmid, Dr. Raj Rajakumar, Dr. Shawn Whitehead and Dr. Björn Herrmann for their guidance and support through my graduate studies.

I am grateful to the students, staff and faculty of the Neuroscience Program, especially to the fantastic Ms. Susan Simpson, who provided great administrative support, but foremost always had time to listen and magically had solutions to all the troubles. I would also like to

Table of Contents

List of Tables

List of Figures

List of Appendices

List of Abbreviations and Symbols

2AFC	Two-Alternative Forced-Choice
ABR	Auditory Brainstem Recordings
AC	Amplitude of the carrier
aCSF	Artificial Cerebrospinal Fluid
ANOVA	Analysis of Variance
AM	Amplitude of the modulator
ASR	Acoustic Startle Response
ASR_{base}	Baseline Acoustic Startle Response
ASR_{max}	Maximum Acoustic Startle Response
ASR_{PP}	Acoustic Startle Response to a startle stimulus following a prepulse
ASR_t	Acoustic Startle Response at the sound level t
ASSR	Auditory Steady-State Response
BBN	Broad-Band noise
cm	centimeters
CTR_{seq}	Control sequence
CTR_{tone}	8 kHz tone presented as a control
CTR_{N85}	Wave N85 elicited by a control tone
D	depth
d'-score	d-prime score
dB SPL	decibels per Sound Pressure Level
DD	Deviance Detection
DEV_{seq}	An oddball sequence with the 8 kHz deviant tone
DEV_{tone}	8 kHz tone presented as a deviant
DEV_{N85}	Wave N85 elicited by a deviant tone
DV	dorsal-ventral plane
EEG	Electroencephalogram
ERP	Event-Related Potential
FFT	Fast-Fourier Transformation
fMRI	Functional Magnetic Resonance Imaging
g	grams
GABA	Gamma aminobutyric acid
$GABA_AR$	$GABA_A$ receptor

H	height
h	hour
Hz	Hertz
IM	Intramuscular
IP	Intraperitoneal
ITC	Intra-Trial Coherence
IR	Infrared
kg	kilograms
kHz	kilohertz
L	length
LED	Light Emitting Diode
LFP	Local Field Potential
L/min	Liters per minute
m	modulation index
mA	milliamperes
mg	milligrams
mg/kg	milligrams per kilogram
min	minutes
ML	medial-lateral plane
mm	millimeters
mM	millimolar
MMR	Mismatch Response
ms	milliseconds
mPFC	medial prefrtonal cortex
MWM	Morris water maze
N18	Sound-evoked potential elicited 16-20 ms following stimulus onset
N85	Sound-evoked potential elicited 65-105 ms following stimulus onset
n	Number of animals involved in the experiment
NBN	Narrow Band Noise
NE	Noise exposure
NIHL	Noise-induced hearing loss
Oth-A	*Other* training sound A
Oth-B	*Other* training sound B
Oth-C	*Other* training sound C
P30	Sound-evoked potential elicited 28-32 ms following stimulus onset
PB	Phosphate Buffer

Pc	Percentage correct
PE	Prediction error
PLV	Phase Locking Value
PP	Prepulse
PPI	Prepulse inhibition
RC	rostral-caudal plane
RD	Response Discrimination
RL	Reversal Learning
RM-ANOVA	Repeated Measures Analysis of Variance
RS	Repetition Suppression
s	seconds
SC	Subcutaneous
SEM	Standard Error of the Mean
SS	Set-Shifting
STD_{seq}	An oddball sequence with the 8 kHz standard tone
STD_{tone}	8 kHz tone presented as a standard
STD_{N85}	Wave N85 elicited by a standard tone
TDT	Tucker Davis Technologies
UN-I	*Unknown* testing sound I
UN-II	*Unknown* testing sound II
UN-III	*Unknown* testing sound III
VCD	Visual-Cue Discrimination
α	First two trials
αASR	Average Acoustic Startle Response to the first two trials
µL	microliters
µL/min	microliters per minute
µm	micrometres
µV	microvolts
ωASR	Average Acoustic Startle Response to the last two trials
ω	Last two trials
°	degrees
°C	Degrees of Celsius
%	percent

Chapter 1

1. General Introduction

1.1 Overview

Auditory perception is a crucial ability that allows for rich experience and interactions with our world, e.g., effective communication or identifying dangerous situations. When considering the anatomical regions that give rise to auditory perception, it is critical first to acknowledge the complex neurophysiological processes happening within (1) the peripheral auditory pathway, which transduces sound waves present within the environment into the electrical signals, and (2) the central auditory pathway, which processes and relays these electrical signals through the brainstem and thalamus to the auditory cortex (Pickles, 2013; Plack, 2018). Furthermore, it is essential to appreciate that for the brain to thoroughly perceive information in the environment, the processes happening along the auditory pathway (i.e., from the hair cells to the auditory cortex) alone are insufficient to explain the complexity of the auditory perception. For example, studies have shown that executive function, such as the prefrontal cortex-dependent attention, might play a significant role in sound detection in a noisy environment (Fritz, Elhilali and Shamma, 2007; Atiani *et al.*, 2009; Fritz *et al.*, 2010). Additionally, studies using animal models have identified that common auditory deficits (e.g., noise-induced hearing loss) can also have detrimental effects on brain functions beyond impaired sound processing, such as deficits in learning and memory (Cui, Wu and She, 2009; Cheng *et al.*, 2011; Liu *et al.*, 2016, 2018). Despite significant developments in the field of auditory perception, the physiological relationships between the auditory pathway and prefrontal cortex are still not fully understood. Furthermore, the direct role of the prefrontal cortex in the top-down modulation of sound perception and processing is also relatively unexplored. Toward that goal, this thesis used rat models to investigate these relationships using two main approaches: 1) studying neurophysiological changes within the medial prefrontal cortex and the cognitive consequences of noise-induced hearing

loss; and 2) investigating the effects of medial prefrontal cortex inactivation on auditory processing and perception.

1.2 From sensation to perception

1.2.1 Auditory pathway

The auditory system comprises a highly complex network of subcortical and cortical areas designed to register, process, and interpret the acoustic information present within the environment. This section will briefly describe the main anatomical structures along the auditory pathway through which acoustic information travels on its journey from sound waves to the auditory cortex. Given the focus of experiments included in this thesis, this introductory section aims to provide relevant anatomical and physiological information so that later discussions regarding noise exposure, hearing loss, and cortical plasticity are better contextualized.

Extensive research has investigated the auditory pathway by which variations in sound pressure waves within the environment are successively relayed to the auditory cortex (Joos *et al.*, 2014). Briefly, sound waves travel through the outer ear (auditory canal), causing vibration of the eardrum (tympanic membrane), which in turn causes movement of tiny bones – called ossicles – in the middle ear. These auditory ossicles (i.e., malleus, incus and stapes) effectively transmit the pressure variations in the air-filled, middle ear space into the fluid-filled snail-like compartment of the inner ear, called the cochlea. There are thousands of sensory hair cells in the cochlea, which transduce these fluid pressure variations containing the information about the original sound wave into the electrical signals transmitted to the brainstem through the cochlear (auditory) nerve. Now within the central auditory pathway, the afferent fibres in the cochlear nerve bifurcate and the information about the sound are sent to the ventral cochlear nucleus, which is located at the entrance of the cochlear nerve to the brainstem, and to the dorsal cochlear nucleus positioned posterior to the inferior cerebellar peduncle. Most fibres from the dorsal cochlear nucleus cross the midline and further ascend through the contralateral

lateral lemniscus, while the remaining fibres ascend through the ipsilateral lateral lemniscus. The majority of the fibres from the ventral cochlear nucleus decussate to the contralateral superior olivary complex, but some also project to the ipsilateral superior olivary complex. Furthermore, the neurons from the superior olive send projections to the ipsilateral and contralateral nuclei of the lateral lemniscus and the inferior colliculus (Pickles, 2013; Cant and Oliver, 2018; Plack, 2018).

The lateral lemniscus runs from the cochlear nucleus and superior olivary complex to the inferior colliculus. Furthermore, some neurons synapse with nuclei located in this region collectively referred to as *lateral lemniscus nuclei*. The neurons within the ventral lateral lemniscus nucleus receive input from the contralateral cochlear nucleus and project to the ipsilateral inferior colliculus. Simultaneously, the dorsal lateral lemniscus neurons receive the input from the ipsi- and contralateral superior olivary complex and contralateral cochlear nucleus and send an inhibitory connection to the ipsi and contra-lateral inferior colliculus (Pickles, 2013; Cant and Oliver, 2018). Next, the inferior colliculus projects ipsilaterally to the medial geniculate body in the thalamus and ultimately to the primary auditory cortex (Pickles, 2013; Cant and Oliver, 2018; Plack, 2018).

The pathway described in the previous paragraph is considered the primary auditory pathway and commonly referred to as the lemniscal pathway, originating from the fact that the sound-signal information is conveyed through the brainstem via the lateral lemniscus. The main characteristic of this pathway is its tonotopic organization, meaning that at each successive relay nucleus, there are neurons that are particularly sensitive to specific sound frequencies while being less sensitive to other frequencies (Cant and Oliver, 2018). This property arises from the anatomical arrangement of the sensory hair cells and their associated afferent nerve fibres within the cochlea, in which the high-frequency sounds are processed and transduced into the electrical signals at the entrance (base) of the cochlea. In contrast, lower-frequency sounds cause hair cell activation toward the apex of the cochlea. As a result, the specific neurons along the lemniscal pathway have their "preferred" frequency to which they respond the most, creating a tonotopic (i.e.,

"frequency-place") map, which is evident within each relay nucleus, all the way to the auditory cortex (Cant and Oliver, 2018).

Parallel to the lemniscal auditory pathway runs another auditory pathway, aptly referred to as a non-lemniscal auditory pathway. This phylogenetically oldest pathway does not exhibit a tonotopical distribution, has a longer response latency, and starts at the cochlear nucleus (Cervera-Paz, Saldaña and Manrique, 2007). At each station of the auditory pathway described above, the neurons of the non-lemniscal pathway create a belt wrapping around the core lemniscal neurons from which they receive inputs. For example, the non-lemniscal neurons at the level of the inferior colliculus receive inputs from the lemniscal inferior colliculus neurons and the non-lemniscal neurons from the superior olivary complex. (Cant and Oliver, 2018). Furthermore, non-lemniscal divisions of the medial geniculate body of the thalamus and the inferior colliculus project to the amygdala that connects to the auditory and association cortices (Aitkin, 1986; Moller, 2003). It also receives the descending, top-down projections from the non-lemniscal areas of the auditory cortex (Malmierca and Ryugo, 2011).

Ultimately, the lemniscal and non-lemniscal pathways are considered to engage in different auditory functions. The lemniscal pathway is thought to provide a high-fidelity, primary-like representation of sound features; it is referred to as the "primary auditory pathway" (Carbajal and Malmierca, 2018). On the other hand, the non-lemniscal pathway is considered to supply more context-dependent information, containing neurons that show the ability to detect change (Kraus *et al.*, 1994; Anderson, Christianson and Linden, 2009; Anderson and Linden, 2011), are sensitive to multimodal stimuli and reward stimuli (Komura *et al.*, 2001, 2005) and undergo rapid retuning following behavioural conditioning (Edeline, 1999; Hu, 2003). Therefore, the non-lemniscal auditory pathway is considered by some researchers as a higher-order stage of auditory processing (Carbajal and Malmierca, 2018).

1.2.2 Auditory processing and perception in noise

One of the proposed theories of how the brain "hears in noise" is an adaptation to stimulus statistics, in which neurons continually adapt their responses to match the statistics of the sound environment (Dean, Harper and McAlpine, 2005; Baccus, 2006; Nagel and Doupe, 2006; Dean *et al.*, 2008; Watkins and Barbour, 2008; Robinson and McAlpine, 2009; Zilany *et al.*, 2009; Rabinowitz *et al.*, 2011; Wen *et al.*, 2012). As a result, the neural response to a constant, unchanging background noise is attenuated, while the response to the less frequent sounds that carry important information is not (Willmore, Cooke and King, 2014). Furthermore, animal studies have also revealed that the ability to detect important sounds in noise depends not only on the way neurons adapt to the stimulus statistics but also on the level of attention to the task (Fritz, Elhilali and Shamma, 2007; Atiani *et al.*, 2009; Yin, Fritz and Shamma, 2014). For example, recordings from the primary cortical neurons within the auditory cortex of ferrets trained to discriminate tones in background noise show that the gain and shape of the spectrotemporal receptive field of those neurons changed within minutes of commencing the task in the background noise, perhaps improving the perceptual discrimination (Atiani *et al.*, 2009). As this change was correlated with the ferret's task performance requiring attention to the stimulus, it was concluded that the transient neural adaptation enhanced the contrast between the target stimuli and the background noise, indicating the effect of attention and the possible role of higher-order cortical regions in discriminating sounds in noise (Atiani *et al.*, 2009). At present, however, the cellular mechanisms and the role of the higher-order cortical regions (e.g., prefrontal cortex) in the attentional modulation of auditory processes and perception are still not fully understood.

1.2.3 From sensation to perception

In cognitive science, there are two main perception models: the first assumes that the brain passively absorbs and then processes the sensory information to generate the motor response (Freeman, 2003). The second theory of perception states that perception

is active, such that the brain intentionally and actively searches for sensory information, which it predicts to be present within the environment (Freeman, 2003). In other words, in the latter view, perception results from top-down indirect creation of information, depending on what is expected in the sensory environment and relying on the internal representation stored in the memory (Hume, 2003; Joos *et al.*, 2014; Merleau-Ponty, 1945). Furthermore, as expected, other scientists and philosophers argue that perception arises from both the bottom-up and top-down processes jointly. The example of this approach is based on Bayesian inference *predictive coding* theory, which states that the higher-order cortical regions create a prediction about the upcoming sensory information based on the previous sensory history. This predicted representation of the external world gets updated and recalibrated by the incoming bottom-up sensory inputs to create an accurate internal representation of the external world (Knill and Pouget, 2004; Friston, 2010; Joos *et al.*, 2014).

In conclusion, in the field of neuroscience and cognitive science, it is generally accepted that higher-order cortical regions play a significant role in the top-down modulation of sensory processing to ultimately give rise to conscious perception. That said, despite numerous theoretical and empirical indications of the influence of the higher-order cortical regions on sound processing and perception, the precise nature of these relationships remains relatively unexplored in animal models that allow for direct manipulations of neural activity.

1.3 Higher-order cortical regions in rats

The primate dorsolateral prefrontal cortex is considered to be the center of the complex cognitive functions, commonly referred to as executive functions (Brown and Bowman, 2002). For example, studies have shown that this cortical region is involved in working memory, attentional control, reasoning and decision-making (Miller and Cohen, 2001). Although clinical research and studies on non-human primates provide a more direct way of studying the functions of human brain, experiments using rodent models allow for

approaches involving more invasive procedures. Although there are inherent differences between the complexity of the primate versus rodent brain, it has been proposed that the rodent cortical regions of the anterior cingulate, pre-limbic area and infralimbic area, collectively referred to as medial prefrontal cortex (mPFC), are functionally equivalent to the primate dorsolateral prefrontal cortex (Brown and Bowman, 2002; Laubach *et al.*, 2018). For example, lesions of dorsolateral prefrontal cortex in humans and in marmosets (Milner, 1963; Owen *et al.*, 1991; Dias, Robbins and Roberts, 1996, 1996) and the mPFC in rodents (Floresco, Block and Tse, 2008) similarly result in impaired cognitive flexibility in tasks requiring an extradimensional shift in the animals' attention (section 1.6.2 includes additional details regarding cognitive flexibility).

1.4 Noise exposure and its consequences

1.4.1 Noise-induced hearing loss

Noise-induced hearing loss is the second most common (after age-related hearing loss) form of sensorineural hearing deficit, and affects nearly 10 million Americans. Furthermore, according to the Centers for Disease Control and Prevention, each year, ~22 million workers are exposed to noise levels that could lead to hearing impairment. Following the exposure to intense sound, noise-induced hearing loss may gradually recover over time. More specifically, depending on the severity of the exposure, hearing thresholds may fully recover (i.e., the subject experienced a temporary threshold shift) or eventually settle at an elevated level (i.e., a permanent threshold shift) (for review see Ryan *et al.*, 2016).

The underlying etiology of permanent noise-induced hearing loss is a degradation of the cochlear hair cells and/or damage to their mechano-sensory hair bundles (Liberman and Dodds, 1984). Excessive noise exposure triggers hair cell death, which can continue for days following the traumatic episode (Wang, Hirose and Liberman, 2002). In contrast, a loss of the cell bodies of the cochlear nerve (spiral ganglion cells) is delayed for months and can progress for years from the noise exposure (Kujawa and Liberman, 2006).

Interestingly, studies demonstrated that even exposure to a less intense noise that only resulted in a temporary threshold shift could still lead to a loss of afferent nerve terminals and delayed degeneration of the cochlear nerve, i.e., *cochlear synaptopathy* (Kujawa and Liberman, 2009)*,* further highlighting the insidious effects of noise.

Noise-induced damage to the peripheral auditory pathway is evident as an increased hearing threshold. Furthermore, following excessive noise exposure within the central auditory pathway, the neurons in the cochlear nucleus and the inferior colliculus demonstrate reduced firing rates to the acoustic stimulus played at the near-threshold intensities. However, when neurons in the inferior colliculus are presented acoustic stimuli at the suprathreshold intensities, they show higher firing rates than what would be expected based on the activity of the neurons within cochlear nucleus (Salvi, Hamernik and Henderson, 1978; Willott and Lu, 1982; Salvi *et al.*, 1990; Wang, Ding and Salvi, 2002). This hyperactivity to suprathreshold acoustic stimulation following a noise-induced hearing loss has been referred to as *central gain enhancement* (discussed in the following section), and ultimately manifests as enhanced sound-evoked responses recorded from the auditory cortex (Popelář, Syka and Berndt, 1987; Salvi *et al.*, 1990; Syka, Rybalko and Popelář, 1994; Syka and Rybalko, 2000).

1.4.2 Central gain enhancement

Triggered by the loss of afferent activity from the noise-damaged cochlea, the successive regions along the auditory pathway (e.g., inferior colliculus, medial geniculate body, auditory cortex) compensate by increasing neural sensitivity. This plasticity is most strongly manifested at the level of the auditory cortex as an amplification of sound-evoked responses (Popelář, Syka and Berndt, 1987; Syka, Rybalko and Popelář, 1994; Syka and Rybalko, 2000; Popelar *et al.*, 2008; Sun *et al.*, 2008; Schormans, Typlt and Allman, 2019). Thus, central gain enhancement is a paradoxical increase in gain or neural amplification within the central auditory system (e.g., inferior colliculus, medial geniculate body and auditory cortex), despite a reduction in the overall neural activity that is transmitted from

the cochlea to the central auditory pathway (Sun *et al.*, 2008, 2012; Chen *et al.*, 2013). Although central gain has been observed within various auditory areas, it is not fully understood where the hyperactivity is initiated, and whether this neural amplification is restricted to specific regions within the central auditory system or extends to other regions. Within the auditory cortex, it has been proposed that central gain enhancement may be due to decreased inhibitory synaptic responses, increased excitatory synaptic responses, or alterations to intrinsic neuronal excitability (Auerbach, Rodrigues and Salvi, 2014).

Numerous studies have confirmed that insults which cause hearing loss and central gain enhancement (e.g., noise exposure; ototoxic drugs), also disrupt inhibitory neurotransmission within the central auditory system (Wang *et al.*, 2006; Yang *et al.*, 2007; Gong *et al.*, 2008; Dong *et al.*, 2010; Lu *et al.*, 2011; Browne, Morley and Parsons, 2012; Sheppard *et al.*, 2014). For example, following noise exposure, there is an altered GABA receptor expression in the inferior colliculus (Dong *et al.*, 2010) and decreased inhibitory drive within the auditory cortex (Yang *et al.*, 2007). Furthermore, following unilateral noise exposure, there are significantly decreased $GABA_A$ receptor subunit α1 in both the contralateral and ipsilateral auditory cortex (Browne, Morley, and Parsons, 2012). The administration of sodium salicylate (a commonly used technique to induce central gain enhancement within the auditory system, as well as causing temporary hearing loss and tinnitus) demonstrated that hyperactivity of sound-evoked responses might depend on inhibition changes (Lu *et al.*, 2011). For example, sodium salicylate-induced enhancement of auditory cortex responses was suppressed after local application of vigabatrin, a drug that increases GABA levels in the brain (Lu *et al.*, 2011), indicating a potential role of the GABAergic system in the enhancement of sound-evoked responses. Recent studies have begun to investigate the specific subclasses of the inhibitory interneurons in mediating the central gain enhancement in the auditory cortex following noise exposure, such as parvalbumin-positive and vasoactive intestinal polypeptide expressing interneurons (Moore and Wehr, 2013).

Is it possible that noise-induced central gain enhancement in the auditory cortex is not solely the result of local changes in its synaptic properties, neuronal excitability or GABAergic neurotransmission? Previous studies on normal-hearing subjects have indicated that the prefrontal cortex exerts inhibitory output to multiple cortical and subcortical regions (Edinger, Siegel and Troiano, 1975; Alexander, Newman and Symmes, 1976), and it has been shown to gate input to primary sensory cortices (Skinner, 1984). To date, no preclinical studies have directly investigated whether alterations in top-down modulation from the prefrontal cortex could contribute to central gain enhancement observed at the level of the auditory cortex. In fact, it still remains unclear whether higher-order brain regions outside of the primary auditory pathway, such as the prefrontal cortex, actually show enhanced sound-evoked responses following noise exposure (i.e., central gain enhancement), or instead, if there is a differential plasticity that occurs in the auditory versus prefrontal cortices post-exposure.

1.4.3 Non-auditory effects of noise exposure

There is mounting evidence that the detrimental effects of noise exposure are not limited to the auditory system. For example, noise exposure has been shown to cause DNA damage and altered neurotransmitters in the cerebellum and striatum (Frenzilli *et al.*, 2017). Furthermore, studies have shown that noise exposure leads to neuropathology in the hippocampus, including impaired neurogenesis (Kraus *et al.*, 2010), neuroinflammation (Cui *et al.*, 2015), tau hyper-phosphorylation, and the formation of neurofibrillary tangles (Cui *et al.*, 2012). Related to these neuroanatomical findings, numerous studies in rodents have shown that noise exposure impairs hippocampus-driven spatial learning and memory (Cui, Wu and She, 2009; Cheng *et al.*, 2011; Liu *et al.*, 2016, 2018). As the majority of preclinical studies investigating the effects of noise exposure on cognitive functions have primarily focused on hippocampal-dependent behavioural performance, it remains unclear how excessive exposure to loud noise affects other cognitive abilities, such as executive functions mediated by the prefrontal cortex.

1.5 Electrophysiological approaches to study auditory processing, perception, and cognitive abilities

1.5.1 Auditory brainstem response recordings

Recordings of the auditory brainstem response recordings (ABR) are commonly used in clinical and translational studies to investigate auditory processing at the level of the brainstem nuclei and ultimately assess a subject's hearing sensitivity. In both humans and rats, an ABR is recorded from the scalp in response to repetitive presentation of acoustic stimuli (e.g., clicks or tones), and a typical waveform consists of five to seven positive peaks that appear within 10 ms of the stimulus presentation (Chiappa, Gladstone and Young, 1979; Chen and Chen, 1991; Reichmuth *et al.*, 2007; Parkkonen, Fujiki and Mäkelä, 2009; Alvarado *et al.*, 2012). Based on decades of research, it has been generally accepted that in humans, the waves I, II, III, IV, and V correspond to neuronal activity in the auditory nerve, cochlear nucleus, superior olivary complex, lateral lemniscus, and inferior colliculus, respectively (Simpson *et al.*, 1985; Chen and Chen, 1991; Reichmuth *et al.*, 2007; Alvarado *et al.*, 2012). Rats' ABR wave profile is essentially the same as humans'. The difference is that peak IV has been proposed to be generated by the lateral lemniscus and inferior colliculus together, while wave V by the medial geniculate body and thalamo-cortical activity (R. Henry, 1979). Most relevant for this thesis, because the first wave of the ABR (wave I) in rats represents the activity in the auditory nerve (Alvarado *et al.*, 2012), ABR recordings before and after noise exposure not only provide a metric of the change in hearing threshold (i.e., the lowest intensity of the acoustic stimulus capable of eliciting a visible deflection of the waveform) but also offer valuable information about noise-induced changes in the cochlear output to the central auditory system.

1.5.2 Spontaneous Oscillations and Auditory Steady-State Response

Spontaneous and sound-evoked oscillations can be obtained through electroencephalogram recordings (EEG) in humans and local field potential (LFP) recordings in rodents. These recordings provide valuable information about the

physiological state of the cortex. Furthermore, recordings of these cortical activities can offer insights into perceptual and cognitive abilities of subjects, and indicate possible explanations underlying perceptual and cognitive deficits (for review: Karakaş and Barry, 2017).

Extracellular LFP recordings from rats reported in this thesis can be related to EEG recordings in humans, where cortical activity representing a synaptic input across large neuronal populations is recorded from the surface of the skull (Buzsaki, 2006; Buzsáki and Wang, 2012). This rhythmic synaptic activity causes temporally synchronized changes across the membrane potentials of neuronal populations, ultimately manifesting as neuronal oscillations. Oscillations are typically grouped into frequency bands that include delta (0 – 4 Hz), theta (4 – 8 Hz), alpha (8 – 12 Hz), and gamma (> 30 Hz), and are believed to be crucial for normal cortical functions (Başar *et al.*, 2001; Uhlhaas *et al.*, 2008; Karakaş and Barry, 2017). Although the exact origin and functions of spontaneous oscillations are not clear and are a current topic of scientific debate and research, it has been suggested that oscillations within specific frequency bands might be associated with specific cognitive functions (Karakaş and Barry, 2017). For example, delta oscillations are commonly associated with functional uncoupling between cortical regions and their thalamocortical afferents (Steriade, 2006) and are most prominent during the deep sleep cycle (Başar *et al.*, 2001; Karakaş and Barry, 2017). The oscillations within the theta band are crucial for communication between distant brain regions, such as the thalamus and the cortex (Uhlhaas *et al.*, 2008). Alpha oscillations are the most prominent resting-state oscillation in the human brain, and are considered to represent a balance between inhibitory and excitatory activity within a brain region, where increased alpha-band power signifies increased inhibition (i.e., decreased excitatory activity) (Klimesch, Sauseng and Hanslmayr, 2007; Weisz *et al.*, 2011). Gamma oscillations are crucial for short-range neuronal communication within a particular cortical region and are believed to be driven by the activity of the fast-spiking interneurons (Cardin *et al.*, 2009; Sohal *et al.*, 2009). It has been proposed that gamma oscillations are responsible for coordinating multiple

sensory stimuli into a single, cognitively relevant percept giving rise to a conscious awareness of the stimulus (Joliot, Ribary and Llinás, 1994; Cardin, 2016; Sohal, 2016). Notably, changes related to oscillations have been reported in several clinical conditions, such as schizophrenia (Uhlhaas *et al.*, 2008), autism spectrum disorder (Gandal *et al.*, 2010; An *et al.*, 2018; Ronconi *et al.*, 2020), Alzheimer's disease (Osipova *et al.*, 2005; Montez *et al.*, 2009; Palop and Mucke, 2016), bipolar disorder (Özerdem *et al.*, 2010; Atagün, 2016; Başar *et al.*, 2016; Canali *et al.*, 2017), ADHD (Robertson *et al.*, 2019; Shephard *et al.*, 2019; Zamorano *et al.*, 2020), and have been proposed as neurophysiological indications of cognitive and perceptual dysfunction (Başar *et al.*, 2001, 2016).

Using electrophysiological recordings, cortical activity can be investigated during periods of no external stimuli (i.e., "resting state," commonly called *spontaneous oscillations*) or during periods of stimulus-evoked activity, commonly referred to as *evoked oscillations*. One of the common methods to study such evoked oscillations is via steady-state auditory response (ASSR) recordings. During ASSR recordings, the subject is presented with an acoustic stimulus that is repeated in a train at a specific frequency (e.g., 40 times per second, Hz), and the extent to which the evoked response maintains its consistency over several trials can be assessed (Picton *et al.*, 2003; Brenner *et al.*, 2009; Uhlhaas and Singer, 2010; Uhlhaas *et al.*, 2010). ASSR recordings can be a handy tool for uncovering abnormalities within neuronal populations (Brenner *et al.*, 2009). As mentioned above, because gamma oscillations are thought to be crucial for conscious perception, failure to sustain gamma oscillations might indicate perceptual deficits (Joliot, Ribary and Llinás, 1994; Cardin *et al.*, 2009; Cardin, 2016; Sohal, 2016). Clinical studies reveal that some psychiatric conditions in which auditory perception and processing are known to be disrupted, such as schizophrenia (Uhlhaas *et al.*, 2008; Thuné, Recasens and Uhlhaas, 2016; Baradits *et al.*, 2019; Kim *et al.*, 2019) and autism spectrum disorder (Edgar *et al.*, 2016; Ono *et al.*, 2020; Seymour *et al.*, 2020), exhibit deficits in sustained gamma oscillations as indicated by reduced ASSR to 40-Hz click stimulus.

1.5.3 Mismatch response

Although auditory cortical responses to sound are necessary for its perception, it does not necessarily imply that a person becomes aware. Studies suggest that in order to perceive an auditory event consciously, higher-order "awareness" and "salience" neural networks have to be co-activated (Loo *et al.*, 2009; Langguth *et al.*, 2012). Interestingly, studies imply that the electrophysiological characteristics of higher-order neural networks are evident in the auditory late-latency responses that occur at >50 ms after the stimulus onset, rather than in the immediate sound-evoked response (Boly *et al.*, 2011; Joos *et al.*, 2014).

One example of a late-latency event-related response is the *mismatch response* (Joos *et al.*, 2014). The mismatch response is defined as a component of the sound-evoked potential elicited by an unexpected, *deviant* stimulus occurring within a stream of predictable, *standard* stimuli (Näätänen *et al.*, 2001; Paavilainen *et al.*, 2001; Näätänen, Jacobsen and Winkler, 2005; Harms *et al.*, 2014, 2018; Harms, Michie and Näätänen, 2016). The deviant and standard stimuli can differ in various dimensions, such as carrier frequency, intensity, and duration (Picton *et al.*, 2000). Studies with human participants showed that the mismatch response could be elicited not only by deviations from a regular stimulus train but by any violation of established expectations or prediction, including abstract rules (Garrido *et al.*, 2009). Although studies showed that attention to the deviant could exaggerate the response (Näätänen *et al.*, 1993; Sussman, Ritter and Vaughan, 1998; Garrido *et al.*, 2009), the mismatch response phenomenon persists even in the absence of attention or in situations of impaired consciousness, i.e., minimal consciousness state and vegetative state (Shelley *et al.*, 1991; Erlbeck *et al.*, 2017). Thus, it is believed that the mismatch response is an electrophysiological manifestation of a pre-attentive process of repetitive, predictable stimuli (such as *standard* stimuli), which provides perceptual saliency to sounds that deviate from that expectation, thus carrying important information (Escera *et al.*, 1998, 2003; Carbajal and Malmierca, 2018).

Following the predictive coding theory mentioned in Section 1.3, the mismatch response represents a consequence of "violation" of established rules based on previous experience. Briefly, it has been suggested that when a standard stimulus is repeatedly presented, this leads to a sensory memory trace and a resultant prediction about what the upcoming stimulus will be (Wacongne, Changeux and Dehaene, 2012; Lieder, Daunizeau, *et al.*, 2013; Lieder, Stephan, *et al.*, 2013; Parras *et al.*, 2017). Consequently, if the upcoming stimulus meets the expectations of the prediction, the neural response to this stimulus is attenuated, referred to as *repetition suppression*. In contrast, if the actual stimulus differs from the expectation, an exaggerated neural response (i.e., a *prediction error*) is elicited.

Studies on humans show that the underlying network involved in the generation of the mismatch response is complex and involves multiple higher-order cortical regions. For example, clinical studies revealed significant mismatch response deficits in patients with frontal cortex lesions (Alho *et al.*, 1994). Furthermore, numerous studies on the mismatch response demonstrated the involvement of cortical regions, such as the auditory cortex, prefrontal cortex, and insula (Woldorff and Hillyard, 1991; Alho, 1995; Marco-Pallarés, Grau and Ruffini, 2005; Shiramatsu, Kanzaki and Takahashi, 2013; Takahashi *et al.*, 2013; Camalier *et al.*, 2019), but also subcortical regions (e.g., amygdala) (Camalier *et al.*, 2019). Adding to these clinical findings, a recent electrophysiological study in rodents recorded the single-unit mismatch responses from successive regions in the lemniscal and non-lemniscal auditory pathway, and found that the *prediction error* response increased along the hierarchy, such that the most robust *prediction error* was evident at the level of the non-lemniscal auditory cortex (Parras *et al.*, 2017). Based on these findings, the authors suggested that the non-lemniscal auditory pathway may play a role in higher-order processing of sensory information (Carbajal and Malmierca, 2018). Although it is well established that the prefrontal cortex exerts top-down modulation on the sensory cortices (see above sections), preclinical studies have not used rodent models to

investigate the direct role of the mPFC in the generation of mismatch response recorded from the auditory cortex.

1.6 Behavioural approaches to study auditory processing, perception, and cognitive abilities

1.6.1 Acoustic Startle Response

It is possible to behaviourally assess auditory processing along the brainstem using the acoustic startle response (ASR). The ASR is a rapid motoric response following an unexpected and intense acoustic stimulus. This pre-attentive sensorimotor action is highly conserved across evolution and has been observed in a variety of species, including invertebrates, rodents, non-human primates as well as humans (Valls-Solé *et al.*, 1995; Koch, 1999; Davis *et al.*, 2008; Fewtrell and McCauley, 2012; Paz *et al.*, 2019). The startle response can be elicited by a sudden acoustic stimulus at a sound level of 80 dB SPL or above (Koch, 1999). The ASR represents a protective response and includes reactions such as stiffening of the neck musculature, eyelid closure, limb flexion, and facilitation of a flight response (Gogan, 1970; Koch and Schnitzler, 1997; Koch, 1999). The primary neurophysiological pathway underlying the acoustic startle response has been well-studied and is believed to be confined to brainstem circuitry. Briefly, the acoustic information about the startling stimulus is transduced into an electrical signal by the sensory hair cells of the inner ear, which are innervated by spiral ganglion neurons that project to the cochlear root in rodents, or to the cochlear nucleus in humans. The cochlear root projects to the caudal pontine reticular nucleus (PnC), where it synapses on giant neurons, which directly synapse on motoneurons within the spinal cord to elicit the motoric response.

The acoustic startle response is a dynamic process subjected to both attenuations, e.g., habituation and prepulse inhibition, and enhancement, e.g., sensitization and prepulse facilitation. It is thought that the attenuation of the startle response, through both habituation and prepulse inhibition, serves to reduce the cognitive load of redundant

sensory information, (Koch and Schnitzler, 1997). Short-term habituation is an example of such sensory filtering that manifests as a gradual decrease in startle magnitude to a repeated startling stimulus. It has been proposed that the habituation process can be regarded as a form of learning in which the repeated stimulus does not carry any significant information. Thus, the organism ceases to respond (Geyer *et al.*, 1990; Kirshenbaum, Chabot and Gibney, 2019; Hermann *et al.*, 2020). The neural mechanism underlying this short-term habituation is still not fully resolved; however, it is suspected to occur directly within the startle pathway, as studies showed rats exhibiting intact short-term habituation following chronic decerebration (Leaton, Cassella and Borszcz, 1985). It is thought that the repeated activation of the synapses within the primary startle pathway results in synaptic depression due to a reduced amount of released presynaptic neurotransmitters or by decreased sensitivity of postsynaptic receptors, or possibly by a combination of both (Leaton, Cassella and Borszcz, 1985; Zaman *et al.*, 2017).

Another pre-attentive process suggested to reduce the cognitive burden of redundant sensory information is prepulse inhibition (PPI). Prepulse inhibition was first described by Sechenov in 1863 and manifested as a decrease in the startling response due to non-startling prepulse stimulus before the presentation of the startling stimulus compared to a response elicited by the startling stimulus alone (Peak, 1939; Hoffman and Fleshler, 1963; Geyer *et al.*, 1990; Fulcher *et al.*, 2020). Studies have shown that this response is present in various vertebrate species, including mammals, implying its vital importance for animal survival (Koch, 1999; Burgess and Granato, 2007b, 2007a; Neumeister, Szabo and Preuss, 2008; Valsamis and Schmid, 2011). Unlike habituation, prepulse inhibition occurs already at the first trial. It reflects a direct gating of the motor response, in which the processing of the prepulse stimulus inhibits the processing of the startle stimulus, resulting in attenuation of the motor response. This sensorimotor gating process is thought to prevent distractive interference during concurrent neural activation, thereby acting as a protective mechanism preventing sensory information from overloading the higher-order cortical regions and preserving the brain's limited attentional capacity (Koch

and Schnitzler, 1997; Swerdlow, Braff and Geyer, 2016). Studies show that prepulse inhibition can be observed in rats following the removal of the cortex (Davis and Gendelman, 1977; Fox, 1979; Li and Frost, 2000) as well as in humans during sleep (Silverstein, Graham and Calloway, 1980; Wu *et al.*, 1990; Fendt, Li and Yeomans, 2001). Based on these findings, it has been suggested that the neural circuits mediating prepulse inhibition must reside within the brainstem, where they impinge upon the primary startle pathway. According to this view, the acoustic stimulus information is transmitted from the cochlear root neurons to the inferior and superior colliculi and ultimately to the pedunculopontine tegmental nucleus (PPT). In turn, the PPT sends inhibitory projections to the caudal pontine reticular nucleus (PnC), which results in decreased activation of the giant motor neurons, ultimately manifesting as a decreased motor response (Fendt, Li and Yeomans, 2001). Adding to this long-standing theory, a more recent study proposed that there might be an additional "fast" circuit mediating the prepulse inhibition within the brainstem in which the information from the cochlear nucleus is transmitted to the ventral nucleus of the trapezoid body, which inhibits the cochlear root nucleus, decreasing its excitatory effect on the caudal pontine reticular nucleus ultimately leading to decreased activation of giant motor neurons and reduced motor response (Gómez-Nieto *et al.*, 2014).

1.6.2 Operant conditioning-based tasks

Operant conditioning-based tasks are a widely used method to investigate various cognitive and perceptual phenomena in humans, non-human primates, rodents, and other species (Staddon and Cerutti, 2003; Kirsch *et al.*, 2004). Operant conditioning-based tasks were first designed by EL Thorndike's, based on his Law of Effect (1905) which states that behaviour tends to be repeated (i.e., strengthened) when reinforced. In contrast, the lack of reinforcement leads to extinguishing behaviour (i.e., weakened) (Skinner, 2019). In such a task, a subject (e.g., rat) is typically placed in a testing chamber, where it is exposed to carefully controlled stimuli and can make one or two repeatable responses, such as pressing a lever or poking its nose in a feeding trough. In the case of appetitive

operant conditioning, an association between the stimuli and the desired choice can be established through positive reinforcement, whereby the animal is rewarded for its correct choice (e.g., food pellet delivery) (Delamater and Holland, 2008).

Executive functions are essential for normal behaviour and are mediated by cortical networks involving regions within the prefrontal cortex, thalamus and striatum (Ragozzino, Detrick and Kesner, 1999; Stefani and Moghaddam, 2005; Floresco *et al.*, 2006; Block *et al.*, 2007; Ghods-Sharifi, Haluk and Floresco, 2008; Brady and Floresco, 2015). One of the widely used assessment approaches of executive functions in rats is a set of automated operant conditioning-based lever pressing tasks, in which they learn to press a correct lever associated with a specific rule through positive reinforcement with sugar pellets (Floresco, Zhang and Enomoto, 2009). In the following section, I will describe how operant conditioning-based lever pressing tasks are used to assess cognitive functions such as: stimulus-response habit learning via visual-cue discrimination, attentional set-shifting, and reversal learning.

During a visual-cue discrimination task, animals are tested for their ability to learn a simple rule, such as pressing a lever associated with an illuminated visual-cue stimulus light, through positive reinforcement in the form of a sugar pellet for each correct response (i.e., stimulus-response habit learning). Attentional set-shifting requires an animal to abandon an initially learned rule (e.g., press the lever under the illuminated cue light) when the task is unexpectedly changed to a response discrimination task (e.g., only the left lever is correct, regardless of the cue light). This cognitive flexibility, in which the animal abandons the original rule within the visual modality ("follow the light") and acquires a new rule within egocentric modality ("left lever"), is called set-shifting, as the animal needed to switch its attention from one rule (set) to another.

Reversal learning is a cognitive flexibility skill related to set-shifting, but it requires an animal to abandon the previous rule and acquire a new one within the same modality. For example, the animal must abandon the previously learned egocentric rule (e.g., "always

left") and learn an opposite rule (e.g., "always right") (Floresco *et al.*, 2006; Block *et al.*, 2007; Floresco, Zhang and Enomoto, 2009; Brady and Floresco, 2015). Taken together, this series of operant conditioning-based lever tasks provides a fully automated examination of various executive functions, with minimal interference of an experimenter (Block *et al.*, 2007).

This battery of lever-pressing operant-conditioning tasks allows investigators to assess the functional consequences of changes that may have occurred in various brain regions. For instance, studies in rodents have shown that the ability to learn the visual-cue discrimination task is disrupted following insult to the dorsolateral striatum (McDonald *et al.*, 2007; Delotterie *et al.*, 2015). By comparison, inactivation or damage to the mPFC does not affect rats initial learning of the visual-cue discrimination task or reversal learning, but it appears to impair set-shifting (Ragozzino, Detrick and Kesner, 1999; Floresco *et al.*, 2006; Floresco, Block and Tse, 2008). Finally, inactivation of the orbitofrontal cortex, similar to insults to the mPFC does not seem to affect the animals' ability to acquire the original rule but results in impaired reversal-learning and intact set-shifting (Ghods-Sharifi *et al.*, 2008). The dissociable behavioural results of these studies suggest that various cortical and subcortical circuits mediate executive functions.

The lever-pressing operant-conditioning tasks, as described above, have been used in numerous preclinical models to study cognitive abilities in relation to Alzheimer's disease, schizophrenia, alcoholism, depression, and stroke (Sullivan, Rosenbloom and Pfefferbaum, 2000; Leeson *et al.*, 2009; McKirdy *et al.*, 2009; Cumming, Marshall and Lazar, 2013; Snyder, 2013). Moreover, animal models have been used to investigate the molecular, cellular and circuit basis of goal-directed learning and executive function (Floresco *et al.*, 2006; Desai, Allman and Rajakumar, 2017, 2018; Szkudlarek *et al.*, 2019).

1.6.3 Spatial learning and reference memory

For several decades, researchers have used rodent models and specialized behavioural tasks to understand the brain regions and mechanisms underlying spatial learning and

reference memory. For example, the Morris water maze test was introduced almost 40 years ago (Morris, 1984) and, since then, has become one of the most popular laboratory tools in behavioural neuroscience to assess spatial learning and reference memory in rodents. Unlike operant conditioning-based tasks, the Morris water maze test does not rely on positive or negative reinforcement but relies on the innate aversion of rodents to water and their strong motivation to find a solid ground (Morris, 1984; Brandeis, Brandys and Yehuda, 1989; Vorhees and Williams, 2006). The set-up of the Morris water maze test consists of a large circular tank filled with opaque water in which a small escape platform is hidden slightly below the surface, and visually discriminable landmarks placed around the periphery that were visible to the swimming rats (Morris, 1984; Brandeis, Brandys and Yehuda, 1989; Vorhees and Williams, 2006). Although there are many variations to the basic protocol depending on the specific research question being asked, at its core, the Morris water maze test consists of a *learning session* (with a variable number of trials) in which rats are repeatedly placed into the water in the tank where they must use visual cues to learn (and remember) the location of a hidden platform in order to escape the water. During a separate *probe session*, the platform is removed, and the rats' reference memory can be assessed using a variety of metrics associated with the timing and swim path relative to the prior location of the platform (Morris, 1984; Brandeis, Brandys and Yehuda, 1989; Vorhees and Williams, 2006).

Numerous studies have confirmed the essential role of sub-regions within the hippocampus for the spatial learning aspects of the Morris water maze. For example, hippocampal-lesioned rats show impaired acquisition of hidden, but not visible platform location during the learning trials (Brandeis, Brandys and Yehuda, 1989; Benhamou and Poucet, 1995; Bures *et al.*, 1997; Silva *et al.*, 1998; Poucet, Save and Lenck-Santini, 2000), as well as the impaired performance of a subsequent probe trial (Logue, Paylor and Wehner, 1997; Cho, Friedman and Silva, 1998; Clark, Broadbent and Squire, 2005). The severity of these deficits appears to be related to the volume of damaged hippocampal tissue, with lesions in the dorsal part of the hippocampus being more debilitating than

ventral lesions (Moser, Moser and Andersen, 1993; Moser *et al.*, 1995). Despite its essential role in spatial learning and reference memory, the hippocampus is not the only brain region contributing to performance on the Morris water maze. Disruption of inputs to the perforant pathway, as well as lesions to the entorhinal cortex, striatum, basal forebrain (Riekkinen, Sirvio and Riekkinen, 1990; Compton *et al.*, 1995), cerebellum (Petrosini, Molinari and Dell'Anna, 1996), and amygdala (Decker, Curzon and Brioni, 1995; Roozendaal and McGaugh, 1997a, 1997b; Spanis *et al.*, 1999), can also disrupt performance on this task.

Due to its reliability and the general consistency of results across labs (D'Hooge and De Deyn, 2001), the Morris water maze is also frequently used to study cognitive impairments correlated with various conditions, including AIDS dementia complex (Avgeropoulos *et al.*, 1998; D'Hooge *et al.*, 1999; Iida *et al.*, 1999), traumatic brain injury (Loane *et al.*, 2009; Budinich *et al.*, 2013; Brabazon *et al.*, 2017), neuroinflammation (Levit *et al.*, 2017, 2019), and many others (for review see: D'Hooge and De Deyn, 2001; Paterno, Folweiler and Cohen, 2017).

1.7 Methods to study the functions of cortical regions

At present, there are multiple ways in which researchers can approach studying the function of various cortical regions. For example, animal studies provide us with the opportunity to manipulate specific brain regions to study their function. One of the most popular approaches to assessing the functional role of a particular cortical region is its temporary or permanent inactivation. Although current advances in technology provide us with various options (e.g., inactivation by temporary cooling of the cortical region; applying electrical stimulation; optogenetic and chemogenetic strategies for neuronal activation or silencing), pharmacological approaches remain widely used. The following section briefly describes the pharmacological agent, muscimol, as well as its use in past neurophysiological and behavioural studies, given that it was used in the present thesis to inactivate the mPFC.

1.7.1 Pharmacological inactivation with muscimol

Muscimol is [(5-aminomethyl)-isoxazol-3-ol] is a psychoactive substance present in the mushroom *Amanita muscaria* (Akk *et al.*, 2020). This potent GABA$_A$ receptor (GABA$_A$R) agonist acts via the transmitter binding site and can activate all of the GABA$_A$R subtypes (Beaumont *et al.*, 1978; Deng, Ransom and Olsen, 1986; Smith and Olsen, 1994). Thus, muscimol is commonly used to temporarily reduce neural activation within the affected cortical region (DeFeudis, 1980; Edeline *et al.*, 2002; Benkherouf *et al.*, 2019). Indeed, local infusions of muscimol within the rodent mPFC have been widely used in various investigations. For example, studies showed that inactivation of the mPFC with muscimol increased impulsivity (Pezze, Marshall and Cassaday, 2020), impaired timing precision (Buhusi *et al.*, 2018) and enhanced the extinction of conditioned fear (Akirav, Raizel and Maroun, 2006). With respect to the dosing regime of muscimol, a past study reported that behavioural effects could be elicited at concentrations as low as 4 nM/0.5 µL (Shah, Sjovold and Treit, 2004); however, it is not uncommon for behavioural studies to use higher concentrations, e.g., 0.5 mM or 1.0 mM (Buhusi *et al.*, 2018; Pezze, Marshall and Cassaday, 2020).

1.8 Overview of the thesis

1.8.1. Medial Prefrontal Cortex Plasticity and Cognitive-Behavioural Deficits Following Noise-Induced Hearing Loss (Chapter 2).

Rationale and objectives: Excessive noise exposure is a leading cause of sensorineural hearing loss worldwide. Moreover, preclinical studies have shown that damaging effects of loud noise are not limited to auditory deficits and can affect other brain regions such as the hippocampus, striatum, cerebellum, mPFC (Cui *et al.*, 2012, 2015; Frenzilli *et al.*, 2017). Behavioural studies have shown that noise-exposed animals exhibit impaired hippocampal-dependent spatial learning and memory as assessed by the Morris water maze; however, it was unknown whether noise exposure affects non-hippocampal

cognitive functions as well as neurophysiological responses within the mPFC and its functional connectivity with the auditory cortex.

Experimental approach: To investigate the noise-induced plasticity within the mPFC and its functional connectivity with the auditory cortex, spontaneous neural oscillation and the 40-Hz auditory steady-state response were recorded using chronically implanted electrodes. The effects of noise exposure on non-hippocampal cognitive performance were determined using lever-pressing stimuli-response learning tasks (i.e., visual cue discrimination) and cognitive flexibility (i.e., set-shifting and reversal learning), whereas noise-induced hippocampal deficits in spatial learning and reference memory were assessed using the Morris water maze.

1.8.2 The Effects of Noise-induced Hearing Loss on Sounds Detection (Chapter 3)

Rationale and objectives: A study in normal-hearing ferrets reported that sound detection in background noise elicits functional connectivity between auditory cortex and prefrontal cortex (Fritz *et al.*, 2010), whereas the experiments in Chapter 2 showed a loss of functional connectivity between the auditory cortex and mPFC following noise-induced permanent hearing loss (Wieczerzak *et al.*, 2020). Although a recent study on rats showed that a noise-induced temporary threshold shift resulted in a decreased ability to hear in noise using a modified prepulse inhibition test (Lobarinas, Spankovich and Le Prell, 2017), the effect of noise-induced permanent hearing loss on detecting sound in the quiet and noisy background has not been investigated comprehensively in a preclinical model.

Experimental approach: Before investigating the perceptual consequences of noise-induced hearing loss, I designed and validated a novel 2-AFC behavioural paradigm for rodents that assessed their ability to detect sound in quiet and background noise, while also allowing for an assessment of impulsive behaviour. After establishing the task, I investigated the effects of permanent noise-induced hearing loss on sound discrimination and impulsivity in quiet and background noise. Lastly, to address the possibility that the

noise-induced tinnitus could have interfered with performance in the sound detection, the rats' ability to detect sounds in quiet was tested following common tinnitus inducers—either a brief exposure to a high-intensity sound (12 kHz tone) or pharmacologically induced through systemic injection of sodium salicylate.

1.8.3 The Effects of Medial Prefrontal Cortex Inactivation on Auditory Processing and Perception (Chapter 4)

Rationale and objectives: The role of the prefrontal cortex in auditory perception and processing is not fully understood. That said, it has been suggested that the prefrontal cortex might play a significant role in auditory attention, especially during the sound detection in background noise (Fritz *et al.,* 2010), whereas some lesion studies suggest it might be involved in pre-attentive sensorimotor gating, as evident in decreased prepulse inhibition (Koch and Bubser, 1994; Lacroix *et al.*, 2000; Uehara *et al.*, 2007). Although a clinical study reported an increased auditory response in patients with prefrontal cortex lesions (Knight *et al.*, 1999), the direct effects of mPFC inactivation on sound detection, sound-evoked responses and spontaneous gamma oscillations within the auditory cortex have not been studied in animal models. Furthermore, despite the theorized involvement of higher-order cortical areas in mismatch response, the role of the mPFC has not been addressed.

Experimental approach: Using a rat model, the mPFC contribution to auditory processing and perception was investigated in a variety of behavioural and electrophysiological experiments. To inactivate the mPFC, the same pharmacological treatment was used in each experimental series; muscimol, a potent $GABA_A$ receptor agonist, was administered directly into the mPFC via chronically-implanted infusion cannulae. Sound detection in quiet and in background noise was assessed using the task developed in Chapter 3. Brainstem-mediated auditory processing was assessed through the behavioural measures of the acoustic startle response and its modulation, including short-term habituation (i.e., sensory filtering) and prepulse inhibition (i.e., sensorimotor gating). In addition to this

behavioural testing, the effects of mPFC inactivation and its potential contribution to central gain enhancement within the auditory cortex were assessed through electrophysiological measures of the initial sound-evoked response (N18). Moreover, the electrophysiological correlates of perceptual abilities were assessed by measuring inter-trial coherence to the 40-Hz auditory steady-state response, spontaneous gamma oscillations, and the mismatch response.

1.9 References

Aitkin, L. (1986) *The Auditory Midbrain: Structure and Function in the Central Auditory Pathway*. Springer Science & Business Media.

Akirav, I., Raizel, H. and Maroun, M. (2006) 'Enhancement of conditioned fear extinction by infusion of the GABAA agonist muscimol into the rat prefrontal cortex and amygdala', *European Journal of Neuroscience*, 23(3), pp. 758–764. doi: https://doi.org/10.1111/j.1460-9568.2006.04603.x.

Akk, G. *et al.* (2020) 'Enhancement of Muscimol Binding and Gating by Allosteric Modulators of the GABAA Receptor: Relating Occupancy to State Functions', *Molecular Pharmacology*, 98(4), pp. 303–313. doi: 10.1124/molpharm.120.000066.

Alexander, G. E., Newman, J. D. and Symmes, D. (1976) 'Convergence of prefrontal and acoustic inputs upon neurons in the superior temporal gyrus of the awake squirrel monkey', *Brain Research*, 116(2), pp. 334–338. doi: 10.1016/0006-8993(76)90913-6.

Alho, K. *et al.* (1994) 'Lesions of frontal cortex diminish the auditory mismatch negativity', *Electroencephalography and Clinical Neurophysiology*, 91(5), pp. 353–362. doi: 10.1016/0013-4694(94)00173-1.

Alho, K. (1995) 'Cerebral Generators of Mismatch Negativity (MMN) and Its Magnetic Counterpart (MMNm) Elicited by Sound Changes', *Ear and Hearing*, 16(1), pp. 38–51.

Alvarado, J. C. *et al.* (2012) 'Normal variations in the morphology of auditory brainstem response (ABR) waveforms: a study in wistar rats', *Neuroscience Research*, 73(4), pp. 302–311. doi: 10.1016/j.neures.2012.05.001.

An, K. *et al.* (2018) 'Altered Gamma Oscillations during Motor Control in Children with Autism Spectrum Disorder', *Journal of Neuroscience*, 38(36), pp. 7878–7886. doi: 10.1523/JNEUROSCI.1229-18.2018.

Anderson, L. A., Christianson, G. B. and Linden, J. F. (2009) 'Stimulus-Specific Adaptation Occurs in the Auditory Thalamus', *Journal of Neuroscience*, 29(22), pp. 7359–7363. doi: 10.1523/JNEUROSCI.0793-09.2009.

Anderson, L. A. and Linden, J. F. (2011) 'Physiological differences between histologically defined subdivisions in the mouse auditory thalamus', *Hearing Research*, 274(1), pp. 48–60. doi: 10.1016/j.heares.2010.12.016.

Atagün, M. İ. (2016) 'Brain oscillations in bipolar disorder and lithium-induced changes', *Neuropsychiatric Disease and Treatment*, 12, pp. 589–601. doi: 10.2147/NDT.S100597.

Atiani, S. *et al.* (2009) 'Task Difficulty and Performance Induce Diverse Adaptive Patterns in Gain and Shape of Primary Auditory Cortical Receptive Fields', *Neuron*, 61(3), pp. 467–480. doi: 10.1016/j.neuron.2008.12.027.

Auerbach, B. D., Rodrigues, P. V. and Salvi, R. J. (2014) 'Central Gain Control in Tinnitus and Hyperacusis', *Frontiers in Neurology*, 5. doi: 10.3389/fneur.2014.00206.

Avgeropoulos, N. *et al.* (1998) 'SCID Mice With HIV Encephalitis Develop Behavioral Abnormalities', *JAIDS Journal of Acquired Immune Deficiency Syndromes*, 18(1), pp. 13–20.

Baccus, S. A. (2006) 'From a Whisper to a Roar: Adaptation to the Mean and Variance of Naturalistic Sounds', *Neuron*, 51(6), pp. 682–684. doi: 10.1016/j.neuron.2006.09.007.

Baradits, M. *et al.* (2019) 'Alterations in resting-state gamma activity in patients with schizophrenia: a high-density EEG study', *European Archives of Psychiatry and Clinical Neuroscience*, 269(4), pp. 429–437. doi: 10.1007/s00406-018-0889-z.

Başar, E. *et al.* (2001) 'Gamma, alpha, delta, and theta oscillations govern cognitive processes', *International Journal of Psychophysiology*, 39(2), pp. 241–248. doi: 10.1016/S0167-8760(00)00145-8.

Başar, E. *et al.* (2016) 'What does the broken brain say to the neuroscientist? Oscillations and connectivity in schizophrenia, Alzheimer's disease, and bipolar disorder', *International Journal of Psychophysiology*, 103, pp. 135–148. doi: 10.1016/j.ijpsycho.2015.02.004.

Beaumont, K. *et al.* (1978) 'Muscimol binding in rat brain: Association with synaptic GABA receptors', *Brain Research*, 148(1), pp. 153–162. doi: 10.1016/0006-8993(78)90385-2.

Benhamou, S. and Poucet, B. (1995) 'A comparative analysis of spatial memory processes', *Behavioural Processes*, 35(1), pp. 113–126. doi: 10.1016/0376-6357(95)00060-7.

Benkherouf, A. Y. *et al.* (2019) 'Extrasynaptic δ-GABAA receptors are high-affinity muscimol receptors', *Journal of Neurochemistry*, 149(1), pp. 41–53. doi: https://doi.org/10.1111/jnc.14646.

Block, A. E. *et al.* (2007) 'Thalamic-prefrontal cortical-ventral striatal circuitry mediates dissociable components of strategy set shifting', *Cerebral Cortex (New York, N.Y.: 1991)*, 17(7), pp. 1625–1636. doi: 10.1093/cercor/bhl073.

Boly, M. *et al.* (2011) 'Preserved Feedforward But Impaired Top-Down Processes in the Vegetative State', *Science*, 332(6031), pp. 858–862. doi: 10.1126/science.1202043.

Brabazon, F. *et al.* (2017) 'Intranasal insulin treatment of an experimental model of moderate traumatic brain injury', *Journal of Cerebral Blood Flow & Metabolism*, 37(9), pp. 3203–3218. doi: 10.1177/0271678X16685106.

Brady, A. M. and Floresco, S. B. (2015) 'Operant Procedures for Assessing Behavioral Flexibility in Rats', *JoVE (Journal of Visualized Experiments)*, (96), p. e52387. doi: 10.3791/52387.

Brandeis, R., Brandys, Y. and Yehuda, S. (1989) 'The Use of the Morris Water Maze in the Study of Memory and Learning', *International Journal of Neuroscience*, 48(1–2), pp. 29–69. doi: 10.3109/00207458909002151.

Brenner, C. A. *et al.* (2009) 'Steady State Responses: Electrophysiological Assessment of Sensory Function in Schizophrenia', *Schizophrenia Bulletin*, 35(6), pp. 1065–1077. doi: 10.1093/schbul/sbp091.

Brown, V. J. and Bowman, E. M. (2002) 'Rodent models of prefrontal cortical function', *Trends in Neurosciences*, 25(7), pp. 340–343. doi: 10.1016/S0166-2236(02)02164-1.

Browne, C. J., Morley, J. W. and Parsons, C. H. (2012) 'Tracking the Expression of Excitatory and Inhibitory Neurotransmission-Related Proteins and Neuroplasticity Markers after Noise Induced Hearing Loss', *PLOS ONE*, 7(3), p. e33272. doi: 10.1371/journal.pone.0033272.

Budinich, C. S. *et al.* (2013) 'Short and long-term motor and behavioral effects of diazoxide and dimethyl sulfoxide administration in the mouse after traumatic brain injury', *Pharmacology Biochemistry and Behavior*, 108, pp. 66–73. doi: 10.1016/j.pbb.2013.04.001.

Buhusi, C. V. *et al.* (2018) 'Inactivation of the Medial-Prefrontal Cortex Impairs Interval Timing Precision, but Not Timing Accuracy or Scalar Timing in a Peak-Interval Procedure in Rats', *Frontiers in Integrative Neuroscience*, 12. doi: 10.3389/fnint.2018.00020.

Bures, J. *et al.* (1997) 'Place cells and place navigation', *Proceedings of the National Academy of Sciences*, 94(1), pp. 343–350. doi: 10.1073/pnas.94.1.343.

Burgess, H. A. and Granato, M. (2007a) 'Modulation of locomotor activity in larval zebrafish during light adaptation', *Journal of Experimental Biology*, 210(14), pp. 2526–2539. doi: 10.1242/jeb.003939.

Burgess, H. A. and Granato, M. (2007b) 'Sensorimotor Gating in Larval Zebrafish', *Journal of Neuroscience*, 27(18), pp. 4984–4994. doi: 10.1523/JNEUROSCI.0615-07.2007.

Buzsaki, G. (2006) *Rhythms of the Brain*. Oxford University Press.

Buzsáki, G. and Wang, X.-J. (2012) 'Mechanisms of Gamma Oscillations', *Annual Review of Neuroscience*, 35(1), pp. 203–225. doi: 10.1146/annurev-neuro-062111-150444.

Camalier, C. R. *et al.* (2019) 'A Comparison of Auditory Oddball Responses in Dorsolateral Prefrontal Cortex, Basolateral Amygdala, and Auditory Cortex of Macaque', *Journal of Cognitive Neuroscience*, 31(7), pp. 1054–1064. doi: 10.1162/jocn_a_01387.

Canali, P. *et al.* (2017) 'Abnormal brain oscillations persist after recovery from bipolar depression', *European Psychiatry*, 41(1), pp. 10–15. doi: 10.1016/j.eurpsy.2016.10.005.

Cant, N. B. and Oliver, D. L. (2018) 'Overview of Auditory Projection Pathways and Intrinsic Microcircuits', in Oliver, D. L. et al. (eds) *The Mammalian Auditory Pathways: Synaptic Organization and Microcircuits*. Cham: Springer International Publishing (Springer Handbook of Auditory Research), pp. 7–39. doi: 10.1007/978-3-319-71798-2_2.

Carbajal, G. V. and Malmierca, M. S. (2018) 'The Neuronal Basis of Predictive Coding Along the Auditory Pathway: From the Subcortical Roots to Cortical Deviance Detection', *Trends in Hearing*, 22, p. 2331216518784822. doi: 10.1177/2331216518784822.

Cardin, J. A. *et al.* (2009) 'Driving fast-spiking cells induces gamma rhythm and controls sensory responses', *Nature*, 459(7247), pp. 663–667. doi: 10.1038/nature08002.

Cardin, J. A. (2016) 'Snapshots of the Brain in Action: Local Circuit Operations through the Lens of γ Oscillations', *Journal of Neuroscience*, 36(41), pp. 10496–10504. doi: 10.1523/JNEUROSCI.1021-16.2016.

Cervera-Paz, F. J., Saldaña, E. and Manrique, M. (2007) 'A Model for Auditory Brain Stem Implants: Bilateral Surgical Deafferentation of the Cochlear Nuclei in the Macaque Monkey', *Ear and Hearing*, 28(3), pp. 424–433. doi: 10.1097/AUD.0b013e31804793d9.

Chen, G.-D. *et al.* (2013) 'Salicylate-induced cochlear impairments, cortical hyperactivity and re-tuning, and tinnitus', *Hearing Research*, 295, pp. 100–113. doi: 10.1016/j.heares.2012.11.016.

Chen, T.-J. and Chen, S.-S. (1991) 'Generator study of brainstem auditory evoked potentials by a radiofrequency lesion method in rats', *Experimental Brain Research*, 85(3). doi: 10.1007/BF00231737.

Cheng, L. *et al.* (2011) 'Moderate noise induced cognition impairment of mice and its underlying mechanisms', *Physiology & Behavior*, 104(5), pp. 981–988. doi: 10.1016/j.physbeh.2011.06.018.

Chiappa, K. H., Gladstone, K. J. and Young, R. R. (1979) 'Brain Stem Auditory Evoked Responses: Studies of Waveform Variations in 50 Normal Human Subjects', *Archives of Neurology*, 36(2), pp. 81–87. doi: 10.1001/archneur.1979.00500380051005.

Cho, Y. H., Friedman, E. and Silva, A. J. (1998) 'Ibotenate lesions of the hippocampus impair spatial learning but not contextual fear conditioning in mice', *Behavioural Brain Research*, 98(1), pp. 77–87. doi: 10.1016/S0166-4328(98)00054-0.

Clark, R. E., Broadbent, N. J. and Squire, L. R. (2005) 'Impaired remote spatial memory after hippocampal lesions despite extensive training beginning early in life', *Hippocampus*, 15(3), pp. 340–346. doi: https://doi.org/10.1002/hipo.20076.

Compton, D. M. *et al.* (1995) 'Spatial and non-spatial learning in the rat following lesions to the nucleus locus coeruleus', *Neuroreport: An International Journal for the Rapid Communication of Research in Neuroscience*, 7(1), pp. 177–182. doi: 10.1097/00001756-199512000-00043.

Cui, B. *et al.* (2012) 'Chronic noise exposure causes persistence of tau hyperphosphorylation and formation of NFT tau in the rat hippocampus and

prefrontal cortex', *Experimental Neurology*, 238(2), pp. 122–129. doi: 10.1016/j.expneurol.2012.08.028.

Cui, B. *et al.* (2015) 'Chronic Noise Exposure Acts Cumulatively to Exacerbate Alzheimer's Disease-Like Amyloid-β Pathology and Neuroinflammation in the Rat Hippocampus', *Scientific Reports*, 5(1), p. 12943. doi: 10.1038/srep12943.

Cui, B., Wu, M. and She, X. (2009) 'Effects of Chronic Noise Exposure on Spatial Learning and Memory of Rats in Relation to Neurotransmitters and NMDAR2B Alteration in the Hippocampus', *Journal of Occupational Health*, advpub, pp. 0902160059–0902160059. doi: 10.1539/joh.L8084.

Cumming, T. B., Marshall, R. S. and Lazar, R. M. (2013) 'Stroke, cognitive deficits, and rehabilitation: still an incomplete picture', *International Journal of Stroke: Official Journal of the International Stroke Society*, 8(1), pp. 38–45. doi: 10.1111/j.1747-4949.2012.00972.x.

Davis, M. *et al.* (2008) 'Acoustic startle reflex in rhesus monkeys: A review', *Reviews in the Neurosciences*, 19(2–3), pp. 171–185. doi: 10.1515/REVNEURO.2008.19.2-3.171.

Davis, M. and Gendelman, P. M. (1977) 'Plasticity of the acoustic startle response in the acutely decerebrate rat', *Journal of Comparative and Physiological Psychology*, 91(3), pp. 549–563. doi: 10.1037/h0077345.

Dean, I. *et al.* (2008) 'Rapid Neural Adaptation to Sound Level Statistics', *Journal of Neuroscience*, 28(25), pp. 6430–6438. doi: 10.1523/JNEUROSCI.0470-08.2008.

Dean, I., Harper, N. S. and McAlpine, D. (2005) 'Neural population coding of sound level adapts to stimulus statistics', *Nature Neuroscience*, 8(12), pp. 1684–1689. doi: 10.1038/nn1541.

Decker, M. W., Curzon, P. and Brioni, J. D. (1995) 'Influence of Separate and Combined Septal and Amygdala Lesions on Memory, Acoustic Startle, Anxiety, and Locomotor Activity in Rats', *Neurobiology of Learning and Memory*, 64(2), pp. 156–168. doi: 10.1006/nlme.1995.1055.

DeFeudis, F. V. (1980) 'Physiological and behavioral studies with muscimol', *Neurochemical Research*, 5(10), pp. 1047–1068. doi: 10.1007/BF00966163.

Delamater, A. R. and Holland, P. C. (2008) 'The influence of CS-US interval on several different indices of learning in appetitive conditioning', *Journal of Experimental Psychology: Animal Behavior Processes*, 34(2), pp. 202–222. doi: 10.1037/0097-7403.34.2.202.

Delotterie, D. F. *et al.* (2015) 'Touchscreen tasks in mice to demonstrate differences between hippocampal and striatal functions', *Neurobiology of Learning and Memory*, 120, pp. 16–27. doi: 10.1016/j.nlm.2015.02.007.

Deng, L., Ransom, R. W. and Olsen, R. W. (1986) '[3H]Muscimol photolabels the γ-aminobutyric acid receptor binding site on a peptide subunit distinct from that labeled with benzodiazepines', *Biochemical and Biophysical Research Communications*, 138(3), pp. 1308–1314. doi: 10.1016/S0006-291X(86)80425-9.

Desai, S. J., Allman, B. L. and Rajakumar, N. (2017) 'Combination of behaviorally sub-effective doses of glutamate NMDA and dopamine D1 receptor antagonists impairs executive function', *Behavioural Brain Research*, 323, pp. 24–31. doi: 10.1016/j.bbr.2017.01.030.

Desai, S. J., Allman, B. L. and Rajakumar, N. (2018) 'Infusions of Nerve Growth Factor Into the Developing Frontal Cortex Leads to Deficits in Behavioral Flexibility and Increased Perseverance', *Schizophrenia Bulletin*, 44(5), pp. 1081–1090. doi: 10.1093/schbul/sbx159.

D'Hooge, R. *et al.* (1999) 'Age-related behavioural deficits in transgenic mice expressing the HIV-1 coat protein gp120', *European Journal of Neuroscience*, 11(12), pp. 4398–4402. doi: https://doi.org/10.1046/j.1460-9568.1999.00857.x.

D'Hooge, R. and De Deyn, P. P. (2001) 'Applications of the Morris water maze in the study of learning and memory', *Brain Research Reviews*, 36(1), pp. 60–90. doi: 10.1016/S0165-0173(01)00067-4.

Dias, R., Robbins, T. W. and Roberts, A. C. (1996) 'Primate analogue of the Wisconsin card sorting test: Effects of excitotoxic lesions of the prefrontal cortex in the marmoset', *Behavioral Neuroscience*, 110(5), pp. 872–886. doi: 10.1037/0735-7044.110.5.872.

Dong, S. *et al.* (2010) 'Acoustic trauma evokes hyperactivity and changes in gene expression in guinea-pig auditory brainstem', *European Journal of Neuroscience*, 31(9), pp. 1616–1628. doi: https://doi.org/10.1111/j.1460-9568.2010.07183.x.

Edeline, J.-M. (1999) 'Learning-induced physiological plasticity in the thalamo-cortical sensory systems: a critical evaluation of receptive field plasticity, map changes and their potential mechanisms', *Progress in Neurobiology*, 57(2), pp. 165–224. doi: 10.1016/S0301-0082(98)00042-2.

Edeline, J.-M. *et al.* (2002) 'Muscimol Diffusion after Intracerebral Microinjections: A Reevaluation Based on Electrophysiological and Autoradiographic

Quantifications', *Neurobiology of Learning and Memory*, 78(1), pp. 100–124. doi: 10.1006/nlme.2001.4035.

Edgar, J. C. *et al.* (2016) 'Translating Adult Electrophysiology Findings to Younger Patient Populations: Difficulty Measuring 40-Hz Auditory Steady-State Responses in Typically Developing Children and Children with Autism Spectrum Disorder', *Developmental Neuroscience*, 38(1), pp. 1–14. doi: 10.1159/000441943.

Edinger, H. M., Siegel, A. and Troiano, R. (1975) 'Effect of stimulation of prefrontal cortex and amygdala on diencephalic neurons', *Brain Research*, 97(1), pp. 17–31. doi: 10.1016/0006-8993(75)90911-7.

Erlbeck, H. *et al.* (2017) 'Basic discriminative and semantic processing in patients in the vegetative and minimally conscious state', *International Journal of Psychophysiology*, 113, pp. 8–16. doi: 10.1016/j.ijpsycho.2016.12.012.

Escera, C. *et al.* (1998) 'Neural Mechanisms of Involuntary Attention to Acoustic Novelty and Change', *Journal of Cognitive Neuroscience*, 10(5), pp. 590–604. doi: 10.1162/089892998562997.

Escera, C. *et al.* (2003) 'Attention capture by auditory significant stimuli: semantic analysis follows attention switching', *European Journal of Neuroscience*, 18(8), pp. 2408–2412. doi: https://doi.org/10.1046/j.1460-9568.2003.02937.x.

Fendt, M., Li, L. and Yeomans, J. S. (2001) 'Brain stem circuits mediating prepulse inhibition of the startle reflex', *Psychopharmacology*, 156(2), pp. 216–224. doi: 10.1007/s002130100794.

Fewtrell, J. L. and McCauley, R. D. (2012) 'Impact of air gun noise on the behaviour of marine fish and squid', *Marine Pollution Bulletin*, 64(5), pp. 984–993. doi: 10.1016/j.marpolbul.2012.02.009.

Floresco, S. B. *et al.* (2006) 'Multiple dopamine receptor subtypes in the medial prefrontal cortex of the rat regulate set-shifting', *Neuropsychopharmacology: Official Publication of the American College of Neuropsychopharmacology*, 31(2), pp. 297–309. doi: 10.1038/sj.npp.1300825.

Floresco, S. B., Block, A. E. and Tse, M. T. L. (2008) 'Inactivation of the medial prefrontal cortex of the rat impairs strategy set-shifting, but not reversal learning, using a novel, automated procedure', *Behavioural Brain Research*, 190(1), pp. 85–96. doi: 10.1016/j.bbr.2008.02.008.

Floresco, S. B., Zhang, Y. and Enomoto, T. (2009) 'Neural circuits subserving behavioral flexibility and their relevance to schizophrenia', *Behavioural Brain Research*, 204(2), pp. 396–409. doi: 10.1016/j.bbr.2008.12.001.

Fox, J. E. (1979) 'Habituation and prestimulus inhibition of the auditory startle reflex in decerebrate rats', *Physiology & Behavior*, 23(2), pp. 291–297. doi: 10.1016/0031-9384(79)90370-6.

Freeman, W. J. (2003) 'Neurodynamic Models of Brain in Psychiatry', *Neuropsychopharmacology*, 28(1), pp. S54–S63. doi: 10.1038/sj.npp.1300147.

Frenzilli, G. *et al.* (2017) 'Loud Noise Exposure Produces DNA, Neurotransmitter and Morphological Damage within Specific Brain Areas', *Frontiers in Neuroanatomy*, 11. doi: 10.3389/fnana.2017.00049.

Friston, K. (2010) 'The free-energy principle: a unified brain theory?', *Nature Reviews Neuroscience*, 11(2), pp. 127–138. doi: 10.1038/nrn2787.

Fritz, J. B. *et al.* (2010) 'Adaptive, behaviorally gated, persistent encoding of task-relevant auditory information in ferret frontal cortex', *Nature Neuroscience*, 13(8), pp. 1011–1019. doi: 10.1038/nn.2598.

Fritz, J. B., Elhilali, M. and Shamma, S. A. (2007) 'Adaptive Changes in Cortical Receptive Fields Induced by Attention to Complex Sounds', *Journal of Neurophysiology*, 98(4), pp. 2337–2346. doi: 10.1152/jn.00552.2007.

Fulcher, N. *et al.* (2020) 'Deciphering midbrain mechanisms underlying prepulse inhibition of startle', *Progress in Neurobiology*, 185, p. 101734. doi: 10.1016/j.pneurobio.2019.101734.

Gandal, M. J. *et al.* (2010) 'Validating γ Oscillations and Delayed Auditory Responses as Translational Biomarkers of Autism', *Biological Psychiatry*, 68(12), pp. 1100–1106. doi: 10.1016/j.biopsych.2010.09.031.

Garrido, M. I. *et al.* (2009) 'The mismatch negativity: A review of underlying mechanisms', *Clinical Neurophysiology*, 120(3), pp. 453–463. doi: 10.1016/j.clinph.2008.11.029.

Geyer, M. A. *et al.* (1990) 'Startle response models of sensorimotor gating and habituation deficits in schizophrenia', *Brain Research Bulletin*, 25(3), pp. 485–498. doi: 10.1016/0361-9230(90)90241-Q.

Ghods-Sharifi, S., Haluk, D. M. and Floresco, S. B. (2008) 'Differential effects of inactivation of the orbitofrontal cortex on strategy set-shifting and reversal learning', *Neurobiology of Learning and Memory*, 89(4), pp. 567–573. doi: 10.1016/j.nlm.2007.10.007.

Gogan, P. (1970) 'The startle and orienting reactions in man. A study of their characteristics and habituation', *Brain Research*, 18(1), pp. 117–135. doi: 10.1016/0006-8993(70)90460-9.

Gómez-Nieto, R. *et al.* (2014) 'Origin and function of short-latency inputs to the neural substrates underlying the acoustic startle reflex', *Frontiers in Neuroscience*, 8. doi: 10.3389/fnins.2014.00216.

Gong, N. *et al.* (2008) 'The aspirin metabolite salicylate enhances neuronal excitation in rat hippocampal CA1 area through reducing GABAergic inhibition', *Neuropharmacology*, 54(2), pp. 454–463. doi: 10.1016/j.neuropharm.2007.10.017.

Harms, L. *et al.* (2014) 'Mismatch Negativity (MMN) in Freely-Moving Rats with Several Experimental Controls', *PLOS ONE*, 9(10), p. e110892. doi: 10.1371/journal.pone.0110892.

Harms, L. *et al.* (2018) 'Late deviance detection in rats is reduced, while early deviance detection is augmented by the NMDA receptor antagonist MK-801', *Schizophrenia Research*, 191, pp. 43–50. doi: 10.1016/j.schres.2017.03.042.

Harms, L., Michie, P. T. and Näätänen, R. (2016) 'Criteria for determining whether mismatch responses exist in animal models: Focus on rodents', *Biological Psychology*, 116, pp. 28–35. doi: 10.1016/j.biopsycho.2015.07.006.

Hermann, B. *et al.* (2020) 'Habituation of auditory startle reflex is a new sign of minimally conscious state', *Brain*, 143(7), pp. 2154–2172. doi: 10.1093/brain/awaa159.

Hoffman, H. S. and Fleshler, M. (1963) 'Startle Reaction: Modification by Background Acoustic Stimulation', *Science*, 141(3584), pp. 928–930. doi: 10.1126/science.141.3584.928.

Hu, B. (2003) 'Functional organization of lemniscal and nonlemniscal auditory thalamus', *Experimental Brain Research*, 153(4), pp. 543–549. doi: 10.1007/s00221-003-1611-5.

Hume, D. (2003) *A Treatise of Human Nature*. Courier Corporation.

Iida, R. *et al.* (1999) 'Characterization of learning and memory deficits in C57BL/6 mice infected with LP-BM5, a murine model of AIDS', *Journal of Neuroimmunology*, 95(1), pp. 65–72. doi: 10.1016/S0165-5728(98)00259-8.

Joliot, M., Ribary, U. and Llinás, R. (1994) 'Human oscillatory brain activity near 40 Hz coexists with cognitive temporal binding', *Proceedings of the National Academy of Sciences*, 91(24), pp. 11748–11751. doi: 10.1073/pnas.91.24.11748.

Joos, K. *et al.* (2014) 'From sensation to percept: The neural signature of auditory event-related potentials', *Neuroscience & Biobehavioral Reviews*, 42, pp. 148–156. doi: 10.1016/j.neubiorev.2014.02.009.

Karakaş, S. and Barry, R. J. (2017) 'A brief historical perspective on the advent of brain oscillations in the biological and psychological disciplines', *Neuroscience & Biobehavioral Reviews*, 75, pp. 335–347. doi: 10.1016/j.neubiorev.2016.12.009.

Kim, S. *et al.* (2019) 'Cortical volume and 40-Hz auditory-steady-state responses in patients with schizophrenia and healthy controls', *NeuroImage: Clinical*, 22, p. 101732. doi: 10.1016/j.nicl.2019.101732.

Kirsch, I. *et al.* (2004) 'The role of cognition in classical and operant conditioning', *Journal of Clinical Psychology*, 60(4), pp. 369–392. doi: https://doi.org/10.1002/jclp.10251.

Kirshenbaum, A. P., Chabot, E. and Gibney, N. (2019) 'Startle, pre-pulse sensitization, and habituation in zebrafish', *Journal of Neuroscience Methods*, 313, pp. 54–59. doi: 10.1016/j.jneumeth.2018.12.017.

Klimesch, W., Sauseng, P. and Hanslmayr, S. (2007) 'EEG alpha oscillations: The inhibition–timing hypothesis', *Brain Research Reviews*, 53(1), pp. 63–88. doi: 10.1016/j.brainresrev.2006.06.003.

Knight, R. T. *et al.* (1999) 'Prefrontal cortex regulates inhibition and excitation in distributed neural networks', *Acta Psychologica*, 101(2), pp. 159–178. doi: 10.1016/S0001-6918(99)00004-9.

Knill, D. C. and Pouget, A. (2004) 'The Bayesian brain: the role of uncertainty in neural coding and computation', *Trends in Neurosciences*, 27(12), pp. 712–719. doi: 10.1016/j.tins.2004.10.007.

Koch, M. (1999) 'The neurobiology of startle', *Progress in Neurobiology*, 59(2), pp. 107–128. doi: 10.1016/S0301-0082(98)00098-7.

Koch, M. and Bubser, M. (1994) 'Deficient Sensorimotor Gating After 6-Hydroxydopamine Lesion of the Rat medial Prefrontal Cortex is Reversed by Haloperidol', *European Journal of Neuroscience*, 6(12), pp. 1837–1845. doi: https://doi.org/10.1111/j.1460-9568.1994.tb00576.x.

Koch, M. and Schnitzler, H.-U. (1997) 'The acoustic startle response in rats—circuits mediating evocation, inhibition and potentiation', *Behavioural Brain Research*, 89(1), pp. 35–49. doi: 10.1016/S0166-4328(97)02296-1.

Komura, Y. *et al.* (2001) 'Retrospective and prospective coding for predicted reward in the sensory thalamus', *Nature*, 412(6846), pp. 546–549. doi: 10.1038/35087595.

Komura, Y. *et al.* (2005) 'Auditory thalamus integrates visual inputs into behavioral gains', *Nature Neuroscience*, 8(9), pp. 1203–1209. doi: 10.1038/nn1528.

Kraus, K. S. *et al.* (2010) 'Noise trauma impairs neurogenesis in the rat hippocampus', *Neuroscience*, 167(4), pp. 1216–1226. doi: 10.1016/j.neuroscience.2010.02.071.

Kraus, N. *et al.* (1994) 'Nonprimary auditory thalamic representation of acoustic change', *Journal of Neurophysiology*. doi: 10.1152/jn.1994.72.3.1270.

Kujawa, S. G. and Liberman, M. C. (2006) 'Acceleration of Age-Related Hearing Loss by Early Noise Exposure: Evidence of a Misspent Youth', *Journal of Neuroscience*, 26(7), pp. 2115–2123. doi: 10.1523/JNEUROSCI.4985-05.2006.

Kujawa, S. G. and Liberman, M. C. (2009) 'Adding Insult to Injury: Cochlear Nerve Degeneration after "Temporary" Noise-Induced Hearing Loss', *Journal of Neuroscience*, 29(45), pp. 14077–14085. doi: 10.1523/JNEUROSCI.2845-09.2009.

Lacroix, L. *et al.* (2000) 'The effects of ibotenic acid lesions of the medial and lateral prefrontal cortex on latent inhibition, prepulse inhibition and amphetamine-induced hyperlocomotion', *Neuroscience*, 97(3), pp. 459–468. doi: 10.1016/S0306-4522(00)00013-0.

Langguth, B. *et al.* (2012) 'Neuroimaging and Neuromodulation: Complementary Approaches for Identifying the Neuronal Correlates of Tinnitus', *Frontiers in Systems Neuroscience*, 6. doi: 10.3389/fnsys.2012.00015.

Laubach, M. *et al.* (2018) 'What, If Anything, Is Rodent Prefrontal Cortex?', *eNeuro*, 5(5). doi: 10.1523/ENEURO.0315-18.2018.

Leaton, R. N., Cassella, J. V. and Borszcz, G. S. (1985) 'Short-term and long-term habituation of the acoustic startle response in chronic decerebrate rats', *Behavioral Neuroscience*, 99(5), pp. 901–912. doi: 10.1037/0735-7044.99.5.901.

Leeson, V. C. *et al.* (2009) 'Discrimination learning, reversal, and set-shifting in first-episode schizophrenia: stability over six years and specific associations with medication type and disorganization syndrome', *Biological Psychiatry*, 66(6), pp. 586–593. doi: 10.1016/j.biopsych.2009.05.016.

Levit, A. *et al.* (2017) 'Behavioural inflexibility in a comorbid rat model of striatal ischemic injury and mutant hAPP overexpression', *Behavioural Brain Research*, 333, pp. 267–275. doi: 10.1016/j.bbr.2017.07.006.

Levit, A. *et al.* (2019) 'Impaired behavioural flexibility related to white matter microgliosis in the TgAPP21 rat model of Alzheimer disease', *Brain, Behavior, and Immunity*, 80, pp. 25–34. doi: 10.1016/j.bbi.2019.02.013.

Li, L. and Frost, B. J. (2000) 'Azimuthal directional sensitivity of prepulse inhibition of the pinna startle reflex in decerebrate rats', *Brain Research Bulletin*, 51(1), pp. 95–100. doi: 10.1016/S0361-9230(99)00215-4.

Liberman, M. C. and Dodds, L. W. (1984) 'Single-neuron labeling and chronic cochlear pathology. III. Stereocilia damage and alterations of threshold tuning curves', *Hearing Research*, 16(1), pp. 55–74. doi: 10.1016/0378-5955(84)90025-X.

Lieder, F., Stephan, K. E., *et al.* (2013) 'A Neurocomputational Model of the Mismatch Negativity', *PLOS Computational Biology*, 9(11), p. e1003288. doi: 10.1371/journal.pcbi.1003288.

Lieder, F., Daunizeau, J., *et al.* (2013) 'Modelling Trial-by-Trial Changes in the Mismatch Negativity', *PLOS Computational Biology*, 9(2), p. e1002911. doi: 10.1371/journal.pcbi.1002911.

Liu, L. *et al.* (2016) 'Noise induced hearing loss impairs spatial learning/memory and hippocampal neurogenesis in mice', *Scientific Reports*, 6(1), p. 20374. doi: 10.1038/srep20374.

Liu, L. *et al.* (2018) 'Hippocampal Mechanisms Underlying Impairment in Spatial Learning Long After Establishment of Noise-Induced Hearing Loss in CBA Mice', *Frontiers in Systems Neuroscience*, 12. doi: 10.3389/fnsys.2018.00035.

Loane, D. J. *et al.* (2009) 'Amyloid precursor protein secretases as therapeutic targets for traumatic brain injury', *Nature Medicine*, 15(4), pp. 377–379. doi: 10.1038/nm.1940.

Lobarinas, E., Spankovich, C. and Le Prell, C. G. (2017) 'Evidence of "hidden hearing loss" following noise exposures that produce robust TTS and ABR wave-I amplitude reductions', *Hearing Research*, 349, pp. 155–163. doi: 10.1016/j.heares.2016.12.009.

Logue, S. F., Paylor, R. and Wehner, J. M. (1997) 'Hippocampal lesions cause learning deficits in inbred mice in the Morris water maze and conditioned-fear task', *Behavioral Neuroscience*, 111(1), pp. 104–113. doi: 10.1037/0735-7044.111.1.104.

Loo, E. van der *et al.* (2009) 'Tinnitus Intensity Dependent Gamma Oscillations of the Contralateral Auditory Cortex', *PLOS ONE*, 4(10), p. e7396. doi: 10.1371/journal.pone.0007396.

Lu, J. *et al.* (2011) 'GABAergic neural activity involved in salicylate-induced auditory cortex gain enhancement', *Neuroscience*, 189, pp. 187–198. doi: 10.1016/j.neuroscience.2011.04.073.

Malmierca, M. S. and Ryugo, D. K. (2011) 'Descending Connections of Auditory Cortex to the Midbrain and Brain Stem', in Winer, J. A. and Schreiner, C. E. (eds) *The Auditory Cortex*. Boston, MA: Springer US, pp. 189–208. doi: 10.1007/978-1-4419-0074-6_9.

Marco-Pallarés, J., Grau, C. and Ruffini, G. (2005) 'Combined ICA-LORETA analysis of mismatch negativity', *NeuroImage*, 25(2), pp. 471–477. doi: 10.1016/j.neuroimage.2004.11.028.

McDonald, R. J. *et al.* (2007) 'A complex associative structure formed in the mammalian brain during acquisition of a simple visual discrimination task: Dorsolateral striatum, amygdala, and hippocampus', *Hippocampus*, 17(9), pp. 759–774. doi: https://doi.org/10.1002/hipo.20333.

McKirdy, J. *et al.* (2009) 'Set shifting and reversal learning in patients with bipolar disorder or schizophrenia', *Psychological Medicine*, 39(8), pp. 1289–1293. doi: 10.1017/S0033291708004935.

Merleau-Ponty, M. (no date) *Phenomenology of Perception*. Available at: http://books.google.com/books?id=tOCZPO6EFQAC&dq=phenomenology of perception&source=gbs_navlinks_s.

Miller, E. K. and Cohen, J. D. (2001) 'An Integrative Theory of Prefrontal Cortex Function', *Annual Review of Neuroscience*, 24(1), pp. 167–202. doi: 10.1146/annurev.neuro.24.1.167.

MILNER, B. (1963) 'Effects of Different Brain Lesions on Card Sorting: The Role of the Frontal Lobes', *Archives of Neurology*, 9(1), pp. 90–100. doi: 10.1001/archneur.1963.00460070100010.

Moller, A. R. (2003) *Sensory Systems: Anatomy, Physiology and Pathophysiology*. Gulf Professional Publishing.

Montez, T. *et al.* (2009) 'Altered temporal correlations in parietal alpha and prefrontal theta oscillations in early-stage Alzheimer disease', *Proceedings of the National Academy of Sciences*, 106(5), pp. 1614–1619. doi: 10.1073/pnas.0811699106.

Moore, A. K. and Wehr, M. (2013) 'Parvalbumin-Expressing Inhibitory Interneurons in Auditory Cortex Are Well-Tuned for Frequency', *Journal of Neuroscience*, 33(34), pp. 13713–13723. doi: 10.1523/JNEUROSCI.0663-13.2013.

Morris, R. (1984) 'Developments of a water-maze procedure for studying spatial learning in the rat', *Journal of Neuroscience Methods*, 11(1), pp. 47–60. doi: 10.1016/0165-0270(84)90007-4.

Moser, E., Moser, M. B. and Andersen, P. (1993) 'Spatial learning impairment parallels the magnitude of dorsal hippocampal lesions, but is hardly present following ventral lesions', *Journal of Neuroscience*, 13(9), pp. 3916–3925. doi: 10.1523/JNEUROSCI.13-09-03916.1993.

Moser, M. B. *et al.* (1995) 'Spatial learning with a minislab in the dorsal hippocampus', *Proceedings of the National Academy of Sciences*, 92(21), pp. 9697–9701. doi: 10.1073/pnas.92.21.9697.

Näätänen, R. *et al.* (1993) 'Attention and mismatch negativity', *Psychophysiology*, 30(5), pp. 436–450. doi: https://doi.org/10.1111/j.1469-8986.1993.tb02067.x.

Näätänen, R. *et al.* (2001) '"Primitive intelligence" in the auditory cortex', *Trends in Neurosciences*, 24(5), pp. 283–288. doi: 10.1016/S0166-2236(00)01790-2.

Näätänen, R., Jacobsen, T. and Winkler, I. (2005) 'Memory-based or afferent processes in mismatch negativity (MMN): A review of the evidence', *Psychophysiology*, 42(1), pp. 25–32. doi: https://doi.org/10.1111/j.1469-8986.2005.00256.x.

Nagel, K. I. and Doupe, A. J. (2006) 'Temporal Processing and Adaptation in the Songbird Auditory Forebrain', *Neuron*, 51(6), pp. 845–859. doi: 10.1016/j.neuron.2006.08.030.

Neumeister, H., Szabo, T. M. and Preuss, T. (2008) 'Behavioral and Physiological Characterization of Sensorimotor Gating in the Goldfish Startle Response', *Journal of Neurophysiology*, 99(3), pp. 1493–1502. doi: 10.1152/jn.00959.2007.

Ono, Y. *et al.* (2020) 'Auditory steady-state response at 20 Hz and 40 Hz in young typically developing children and children with autism spectrum disorder', *Psychiatry and Clinical Neurosciences*, 74(6), pp. 354–361. doi: https://doi.org/10.1111/pcn.12998.

Osipova, D. *et al.* (2005) 'Altered generation of spontaneous oscillations in Alzheimer's disease', *NeuroImage*, 27(4), pp. 835–841. doi: 10.1016/j.neuroimage.2005.05.011.

Owen, A. M. *et al.* (1991) 'Extra-dimensional versus intra-dimensional set shifting performance following frontal lobe excisions, temporal lobe excisions or amygdalo-hippocampectomy in man', *Neuropsychologia*, 29(10), pp. 993–1006. doi: 10.1016/0028-3932(91)90063-E.

Özerdem, A. *et al.* (2010) 'Disturbance in long distance gamma coherence in bipolar disorder', *Progress in Neuro-Psychopharmacology and Biological Psychiatry*, 34(6), pp. 861–865. doi: 10.1016/j.pnpbp.2010.04.001.

Paavilainen, P. *et al.* (2001) 'Preattentive extraction of abstract feature conjunctions from auditory stimulation as reflected by the mismatch negativity (MMN)', *Psychophysiology*, 38(2), pp. 359–365. doi: https://doi.org/10.1111/1469-8986.3820359.

Palop, J. J. and Mucke, L. (2016) 'Network abnormalities and interneuron dysfunction in Alzheimer disease', *Nature Reviews Neuroscience*, 17(12), pp. 777–792. doi: 10.1038/nrn.2016.141.

Parkkonen, L., Fujiki, N. and Mäkelä, J. P. (2009) 'Sources of auditory brainstem responses revisited: Contribution by magnetoencephalography', *Human Brain Mapping*, 30(6), pp. 1772–1782. doi: https://doi.org/10.1002/hbm.20788.

Parras, G. G. *et al.* (2017) 'Neurons along the auditory pathway exhibit a hierarchical organization of prediction error', *Nature Communications*, 8(1), p. 2148. doi: 10.1038/s41467-017-02038-6.

Paterno, R., Folweiler, K. A. and Cohen, A. S. (2017) 'Pathophysiology and Treatment of Memory Dysfunction after Traumatic Brain Injury', *Current neurology and neuroscience reports*, 17(7), p. 52. doi: 10.1007/s11910-017-0762-x.

Paz, A. *et al.* (2019) 'Evolution of the acoustic startle response of Mexican cavefish', *bioRxiv*, p. 809665. doi: 10.1101/809665.

Peak, H. (1939) 'Time order error in successive judgments and in reflexes. I. Inhibition of the judgment and the reflex', *Journal of Experimental Psychology*, 25(6), pp. 535–565. doi: 10.1037/h0063056.

Petrosini, L., Molinari, M. and Dell'Anna, M. E. (1996) 'Cerebellar Contribution to Spatial Event Processing: Morris Water Maze and T-maze', *European Journal of Neuroscience*, 8(9), pp. 1882–1896. doi: https://doi.org/10.1111/j.1460-9568.1996.tb01332.x.

Pezze, M. A., Marshall, H. J. and Cassaday, H. J. (2020) 'Muscimol-induced inactivation of the anterior cingulate cortex does not impair trace fear conditioning in the rat',

Journal of Psychopharmacology, 34(12), pp. 1457–1460. doi: 10.1177/0269881120965914.

Pickles, J. (2013) *An Introduction to the Physiology of Hearing: Fourth Edition*, *An Introduction to the Physiology of Hearing*. Brill. Available at: https://brill.com/view/title/24209 (Accessed: 15 April 2021).

Picton, T. W. *et al.* (2000) 'Mismatch Negativity: Different Water in the Same River', *Audiology and Neurotology*, 5(3–4), pp. 111–139. doi: 10.1159/000013875.

Picton, T. W. *et al.* (2003) 'Human auditory steady-state responses: Respuestas auditivas de estado estable en humanos', *International Journal of Audiology*, 42(4), pp. 177–219. doi: 10.3109/14992020309101316.

Plack, C. J. (2018) *The Sense of Hearing*. Routledge.

Popelar, J. *et al.* (2008) 'Comparison of noise-induced changes of auditory brainstem and middle latency response amplitudes in rats', *Hearing Research*, 245(1), pp. 82–91. doi: 10.1016/j.heares.2008.09.002.

Popelář, J., Syka, J. and Berndt, H. (1987) 'Effect of noise on auditory evoked responses in awake guina pigs', *Hearing Research*, 26(3), pp. 239–247. doi: 10.1016/0378-5955(87)90060-8.

Poucet, B., Save, E. and Lenck-Santini, pierre-pascal (2000) 'Sensory and Memory Properties of Hippocampal Place Cells', *Reviews in the neurosciences*, 11, pp. 95–111. doi: 10.1515/REVNEURO.2000.11.2-3.95.

R. Henry, K. (1979) 'Differential changes of auditory nerve and brain stem short latency evoked potentials in the laboratory mouse', *Electroencephalography and Clinical Neurophysiology*, 46(4), pp. 452–459. doi: 10.1016/0013-4694(79)90146-9.

Rabinowitz, N. C. *et al.* (2011) 'Contrast Gain Control in Auditory Cortex', *Neuron*, 70(6), pp. 1178–1191. doi: 10.1016/j.neuron.2011.04.030.

Ragozzino, M. E., Detrick, S. and Kesner, R. P. (1999) 'Involvement of the prelimbic-infralimbic areas of the rodent prefrontal cortex in behavioral flexibility for place and response learning', *The Journal of Neuroscience: The Official Journal of the Society for Neuroscience*, 19(11), pp. 4585–4594.

Reichmuth, C. *et al.* (2007) 'Measurement and Response Characteristics of Auditory Brainstem Responses in Pinnipeds', *Aquatic Mammals*, 33(1), pp. 132–150. doi: 10.1578/AM.33.1.2007.132.

Riekkinen, P., Sirvio¨, J. and Riekkinen, P. (1990) 'Interaction between raphe dorsalis and nucleus basalis magnocellularis in spatial learning', *Brain Research*, 527(2), pp. 342–345. doi: 10.1016/0006-8993(90)91156-B.

Robertson, M. M. *et al.* (2019) 'EEG power spectral slope differs by ADHD status and stimulant medication exposure in early childhood', *Journal of Neurophysiology*, 122(6), pp. 2427–2437. doi: 10.1152/jn.00388.2019.

Robinson, B. L. and McAlpine, D. (2009) 'Gain control mechanisms in the auditory pathway', *Current Opinion in Neurobiology*, 19(4), pp. 402–407. doi: 10.1016/j.conb.2009.07.006.

Ronconi, L. *et al.* (2020) 'Altered neural oscillations and connectivity in the beta band underlie detail-oriented visual processing in autism', *NeuroImage: Clinical*, 28, p. 102484. doi: 10.1016/j.nicl.2020.102484.

Roozendaal, B. and McGaugh, J. L. (1997a) 'Basolateral Amygdala Lesions Block the Memory-enhancing Effect of Glucocorticoid Administration in the Dorsal Hippocampus of Rats', *European Journal of Neuroscience*, 9(1), pp. 76–83. doi: https://doi.org/10.1111/j.1460-9568.1997.tb01355.x.

Roozendaal, B. and McGaugh, J. L. (1997b) 'Glucocorticoid Receptor Agonist and Antagonist Administration into the Basolateral but Not Central Amygdala Modulates Memory Storage', *Neurobiology of Learning and Memory*, 67(2), pp. 176–179. doi: 10.1006/nlme.1996.3765.

Ryan, A. F. *et al.* (2016) 'Temporary and Permanent Noise-induced Threshold Shifts: A Review of Basic and Clinical Observations', *Otology & Neurotology*, 37(8), p. e271. doi: 10.1097/MAO.0000000000001071.

Salvi, R. J. *et al.* (1990) 'Enhanced evoked response amplitudes in the inferior colliculus of the chinchilla following acoustic trauma', *Hearing Research*, 50(1), pp. 245–257. doi: 10.1016/0378-5955(90)90049-U.

Salvi, R. J., Hamernik, R. P. and Henderson, D. (1978) 'Discharge patterns in the cochlear nucleus of the chinchilla following noise induced asymptotic threshold shift', *Experimental Brain Research*, 32(3), pp. 301–320. doi: 10.1007/BF00238704.

Schormans, A. L., Typlt, M. and Allman, B. L. (2019) 'Adult-Onset Hearing Impairment Induces Layer-Specific Cortical Reorganization: Evidence of Crossmodal Plasticity and Central Gain Enhancement', *Cerebral Cortex*, 29(5), pp. 1875–1888. doi: 10.1093/cercor/bhy067.

Seymour, R. A. *et al.* (2020) 'Reduced auditory steady state responses in autism spectrum disorder', *Molecular Autism*, 11(1), p. 56. doi: 10.1186/s13229-020-00357-y.

Shah, A. A., Sjovold, T. and Treit, D. (2004) 'Inactivation of the medial prefrontal cortex with the GABAA receptor agonist muscimol increases open-arm activity in the elevated plus-maze and attenuates shock-probe burying in rats', *Brain Research*, 1028(1), pp. 112–115. doi: 10.1016/j.brainres.2004.08.061.

Shelley, A. M. *et al.* (1991) 'Mismatch negativity: An index of a preattentive processing deficit in schizophrenia', *Biological Psychiatry*, 30(10), pp. 1059–1062. doi: 10.1016/0006-3223(91)90126-7.

Shephard, E. *et al.* (2019) 'Oscillatory neural networks underlying resting-state, attentional control and social cognition task conditions in children with ASD, ADHD and ASD+ADHD', *Cortex*, 117, pp. 96–110. doi: 10.1016/j.cortex.2019.03.005.

Sheppard, A. *et al.* (2014) 'Review of salicylate-induced hearing loss, neurotoxicity, tinnitus and neuropathophysiology', *Acta Otorhinolaryngologica Italica*, 34(2), pp. 79–93.

Shiramatsu, T. I., Kanzaki, R. and Takahashi, H. (2013) 'Cortical Mapping of Mismatch Negativity with Deviance Detection Property in Rat', *PLOS ONE*, 8(12), p. e82663. doi: 10.1371/journal.pone.0082663.

Silva, A. J. *et al.* (1998) 'Molecular, Cellular, and Neuroanatomical Substrates of Place Learning', *Neurobiology of Learning and Memory*, 70(1), pp. 44–61. doi: 10.1006/nlme.1998.3837.

Silverstein, L. D., Graham, F. K. and Calloway, J. M. (1980) 'Preconditioning and excitability of the human orbicularis oculi reflex as a function of state', *Electroencephalography and Clinical Neurophysiology*, 48(4), pp. 406–417. doi: 10.1016/0013-4694(80)90133-9.

Simpson, G. V. *et al.* (1985) 'Altered peripheral and brainstem auditory function in aged rats', *Brain Research*, 348(1), pp. 28–35. doi: 10.1016/0006-8993(85)90355-5.

Skinner, B. F. (2019) *The Behavior of Organisms: An Experimental Analysis*. B. F. Skinner Foundation.

Skinner, J. E. (1984) 'Central Gating Mechanisms That Regulate Event-Related Potentials and Behavior', in Elbert, T. et al. (eds) *Self-Regulation of the Brain and Behavior*. Berlin, Heidelberg: Springer, pp. 42–55. doi: 10.1007/978-3-642-69379-3_4.

Smith, G. B. and Olsen, R. W. (1994) 'Identification of a [3H]muscimol photoaffinity substrate in the bovine gamma-aminobutyric acidA receptor alpha subunit.',

Journal of Biological Chemistry, 269(32), pp. 20380–20387. doi: 10.1016/S0021-9258(17)32003-3.

Snyder, H. R. (2013) 'Major depressive disorder is associated with broad impairments on neuropsychological measures of executive function: a meta-analysis and review', *Psychological Bulletin*, 139(1), pp. 81–132. doi: 10.1037/a0028727.

Sohal, V. S. *et al.* (2009) 'Parvalbumin neurons and gamma rhythms enhance cortical circuit performance', *Nature*, 459(7247), pp. 698–702. doi: 10.1038/nature07991.

Sohal, V. S. (2016) 'How Close Are We to Understanding What (if Anything) γ Oscillations Do in Cortical Circuits?', *Journal of Neuroscience*, 36(41), pp. 10489–10495. doi: 10.1523/JNEUROSCI.0990-16.2016.

Spanis, C. W. *et al.* (1999) 'Excitotoxic basolateral amygdala lesions potentiate the memory impairment effect of muscimol injected into the medial septal area', *Brain Research*, 816(2), pp. 329–336. doi: 10.1016/S0006-8993(98)01104-4.

Staddon, J. E. R. and Cerutti, D. T. (2003) 'Operant Conditioning', *Annual Review of Psychology*, 54(1), pp. 115–144. doi: 10.1146/annurev.psych.54.101601.145124.

Stefani, M. R. and Moghaddam, B. (2005) 'Systemic and prefrontal cortical NMDA receptor blockade differentially affect discrimination learning and set-shift ability in rats', *Behavioral Neuroscience*, 119(2), pp. 420–428. doi: 10.1037/0735-7044.119.2.420.

Sullivan, E. V., Rosenbloom, M. J. and Pfefferbaum, A. (2000) 'Pattern of motor and cognitive deficits in detoxified alcoholic men', *Alcoholism, Clinical and Experimental Research*, 24(5), pp. 611–621.

Sun, W. *et al.* (2008) 'Noise exposure–induced enhancement of auditory cortex response and changes in gene expression', *Neuroscience*, 156(2), pp. 374–380. doi: 10.1016/j.neuroscience.2008.07.040.

Sun, W. *et al.* (2012) 'Noise exposure enhances auditory cortex responses related to hyperacusis behavior', *Brain Research*, 1485, pp. 108–116. doi: 10.1016/j.brainres.2012.02.008.

Sussman, E., Ritter, W. and Vaughan, H. G. (1998) 'Attention affects the organization of auditory input associated with the mismatch negativity system', *Brain Research*, 789(1), pp. 130–138. doi: 10.1016/S0006-8993(97)01443-1.

Swerdlow, N. R., Braff, D. L. and Geyer, M. A. (2016) 'Sensorimotor gating of the startle reflex: what we said 25 years ago, what has happened since then, and what comes

next', *Journal of Psychopharmacology*, 30(11), pp. 1072–1081. doi: 10.1177/0269881116661075.

Syka, J. and Rybalko, N. (2000) 'Threshold shifts and enhancement of cortical evoked responses after noise exposure in rats', *Hearing Research*, 139(1), pp. 59–68. doi: 10.1016/S0378-5955(99)00175-6.

Syka, J., Rybalko, N. and Popelář, J. (1994) 'Enhancement of the auditory cortex evoked responses in awake guinea pigs after noise exposure', *Hearing Research*, 78(2), pp. 158–168. doi: 10.1016/0378-5955(94)90021-3.

Szkudlarek, H. J. *et al.* (2019) 'Δ -9-Tetrahydrocannabinol and Cannabidiol produce dissociable effects on prefrontal cortical executive function and regulation of affective behaviors', *Neuropsychopharmacology*, 44(4), pp. 817–825. doi: 10.1038/s41386-018-0282-7.

Takahashi, H. *et al.* (2013) 'Neural substrates of normal and impaired preattentive sensory discrimination in large cohorts of nonpsychiatric subjects and schizophrenia patients as indexed by MMN and P3a change detection responses', *NeuroImage*, 66, pp. 594–603. doi: 10.1016/j.neuroimage.2012.09.074.

Thuné, H., Recasens, M. and Uhlhaas, P. J. (2016) 'The 40-Hz Auditory Steady-State Response in Patients With Schizophrenia: A Meta-analysis', *JAMA Psychiatry*, 73(11), pp. 1145–1153. doi: 10.1001/jamapsychiatry.2016.2619.

Uehara, T. *et al.* (2007) 'Effect of prefrontal cortex inactivation on behavioral and neurochemical abnormalities in rats with excitotoxic lesions of the entorhinal cortex', *Synapse*, 61(6), pp. 391–400. doi: https://doi.org/10.1002/syn.20383.

Uhlhaas, P. J. *et al.* (2008) 'The Role of Oscillations and Synchrony in Cortical Networks and Their Putative Relevance for the Pathophysiology of Schizophrenia', *Schizophrenia Bulletin*, 34(5), pp. 927–943. doi: 10.1093/schbul/sbn062.

Uhlhaas, P. J. *et al.* (2010) 'Neural synchrony and the development of cortical networks', *Trends in Cognitive Sciences*, 14(2), pp. 72–80. doi: 10.1016/j.tics.2009.12.002.

Uhlhaas, P. J. and Singer, W. (2010) 'Abnormal neural oscillations and synchrony in schizophrenia', *Nature Reviews Neuroscience*, 11(2), pp. 100–113. doi: 10.1038/nrn2774.

Valls-Solé, J. *et al.* (1995) 'Reaction time and acoustic startle in normal human subjects', *Neuroscience Letters*, 195(2), pp. 97–100. doi: 10.1016/0304-3940(94)11790-P.

Valsamis, B. and Schmid, S. (2011) 'Habituation and Prepulse Inhibition of Acoustic Startle in Rodents', *JoVE (Journal of Visualized Experiments)*, (55), p. e3446. doi: 10.3791/3446.

Vorhees, C. V. and Williams, M. T. (2006) 'Morris water maze: procedures for assessing spatial and related forms of learning and memory', *Nature Protocols*, 1(2), pp. 848–858. doi: 10.1038/nprot.2006.116.

Wacongne, C., Changeux, J.-P. and Dehaene, S. (2012) 'A Neuronal Model of Predictive Coding Accounting for the Mismatch Negativity', *Journal of Neuroscience*, 32(11), pp. 3665–3678. doi: 10.1523/JNEUROSCI.5003-11.2012.

Wang, H.-T. *et al.* (2006) 'Sodium salicylate reduces inhibitory postsynaptic currents in neurons of rat auditory cortex', *Hearing Research*, 215(1), pp. 77–83. doi: 10.1016/j.heares.2006.03.004.

Wang, J., Ding, D. and Salvi, R. J. (2002) 'Functional reorganization in chinchilla inferior colliculus associated with chronic and acute cochlear damage', *Hearing Research*, 168(1), pp. 238–249. doi: 10.1016/S0378-5955(02)00360-X.

Wang, Y., Hirose, K. and Liberman, M. C. (2002) 'Dynamics of Noise-Induced Cellular Injury and Repair in the Mouse Cochlea', *Journal of the Association for Research in Otolaryngology*, 3(3), pp. 248–268. doi: 10.1007/s101620020028.

Watkins, P. V. and Barbour, D. L. (2008) 'Specialized neuronal adaptation for preserving input sensitivity', *Nature Neuroscience*, 11(11), pp. 1259–1261. doi: 10.1038/nn.2201.

Weisz, N. *et al.* (2011) 'Alpha Rhythms in Audition: Cognitive and Clinical Perspectives', *Frontiers in Psychology*, 2. doi: 10.3389/fpsyg.2011.00073.

Wen, B. *et al.* (2012) 'Time course of dynamic range adaptation in the auditory nerve', *Journal of Neurophysiology*, 108(1), pp. 69–82. doi: 10.1152/jn.00055.2012.

Wieczerzak, K. B. *et al.* (2020) 'Differential Plasticity in Auditory and Prefrontal Cortices, and Cognitive-Behavioral Deficits Following Noise-Induced Hearing Loss', *Neuroscience*. doi: 10.1016/j.neuroscience.2020.11.019.

Willmore, B. D. B., Cooke, J. E. and King, A. J. (2014) 'Hearing in noisy environments: noise invariance and contrast gain control', *The Journal of Physiology*, 592(16), pp. 3371–3381. doi: https://doi.org/10.1113/jphysiol.2014.274886.

Willott, J. F. and Lu, S. M. (1982) 'Noise-induced hearing loss can alter neural coding and increase excitability in the central nervous system', *Science*, 216(4552), pp. 1331–1334. doi: 10.1126/science.7079767.

Woldorff, M. G. and Hillyard, S. A. (1991) 'Modulation of early auditory processing during selective listening to rapidly presented tones', *Electroencephalography and Clinical Neurophysiology*, 79(3), pp. 170–191. doi: 10.1016/0013-4694(91)90136-R.

Wu, M.-F. *et al.* (1990) 'Lesions producing REM sleep without atonia disinhibit the acoustic startle reflex without affecting prepulse inhibition', *Brain Research*, 528(2), pp. 330–334. doi: 10.1016/0006-8993(90)91677-9.

Yang, G. *et al.* (2007) 'Salicylate induced tinnitus: Behavioral measures and neural activity in auditory cortex of awake rats', *Hearing Research*, 226(1), pp. 244–253. doi: 10.1016/j.heares.2006.06.013.

Yin, P., Fritz, J. B. and Shamma, S. A. (2014) 'Rapid Spectrotemporal Plasticity in Primary Auditory Cortex during Behavior', *Journal of Neuroscience*, 34(12), pp. 4396–4408. doi: 10.1523/JNEUROSCI.2799-13.2014.

Zaman, T. *et al.* (2017) 'BK Channels Mediate Synaptic Plasticity Underlying Habituation in Rats', *Journal of Neuroscience*, 37(17), pp. 4540–4551. doi: 10.1523/JNEUROSCI.3699-16.2017.

Zamorano, F. *et al.* (2020) 'Lateral Prefrontal Theta Oscillations Reflect Proactive Cognitive Control Impairment in Males With Attention Deficit Hyperactivity Disorder', *Frontiers in Systems Neuroscience*, 14. doi: 10.3389/fnsys.2020.00037.

Zilany, M. S. A. *et al.* (2009) 'A phenomenological model of the synapse between the inner hair cell and auditory nerve: Long-term adaptation with power-law dynamics', *The Journal of the Acoustical Society of America*, 126(5), pp. 2390–2412. doi: 10.1121/1.3238250.

Chapter 2

2. Medial Prefrontal Cortex Plasticity and Cognitive-Behavioural Deficits Following Noise-Induced Hearing Loss.

2.1 Introduction

Excessive exposure to loud noise is a major cause of hearing loss worldwide (Wilson *et al.*, 2017). In the U.S., it is estimated that 10 million adults live with hearing loss caused by noise exposure (Carroll *et al.*, 2017), and each year, ~22 million workers are exposed to hazardous noise sufficient to cause hearing damage (Tak, Davis and Calvert, 2009). Adding to the negative consequences of hearing loss itself, there is mounting evidence that noise exposure also represents a significant public health risk due to its non-auditory effects, such as sleep disturbance, increased occurrence of cardiovascular disease and hypertension, as well as impaired cognitive performance in children, including memory deficits (Basner *et al.*, 2014).

In addition to episodic long-term memory deficits (Rönnberg *et al.*, 2011; Rönnberg *et al.*, 2014), systematic meta-analyses (Taljaard *et al.*, 2016) have also identified that individuals with hearing loss are at increased risk of impairments in executive function; a constellation of intellectual abilities which include working memory, inhibition, attention and cognitive flexibility (i.e., the ability to adopt a new approach when a previously-learned strategy ceases to be effective). At present, however, the effects of noise exposure on brain regions subserving executive function (e.g., prefrontal cortex) are not well understood. In fact, to our knowledge, no preclinical studies have investigated noise-induced neural plasticity in the prefrontal cortex, or the extent to which noise exposure affects behavioural performance on tasks requiring executive function.

In the days following noise exposure, the central auditory system can undergo considerable neural plasticity, evident in electrophysiological recordings from noise-

exposed animals. Triggered by the loss of afferent activity from the noise-damaged cochlea, successive relay nuclei along the auditory pathway compensate by increasing neural sensitivity, which ultimately manifests at the level of the auditory cortex as an amplification of sound-evoked responses (i.e., central gain enhancement) (Popelář, Syka and Berndt, 1987; Syka, Rybalko and Popelář, 1994; Syka and Rybalko, 2000; Popelar *et al.*, 2008; Sun *et al.*, 2008; Schormans, Typlt and Allman, 2019). Although it has been theorized that central gain enhancement represents a neural correlate for such audiologic complaints as tinnitus and hyperacusis (Gu *et al.*, 2010; Noreña, 2011; Schaette and McAlpine, 2011; Auerbach, Rodrigues and Salvi, 2014) *cf.* (Rüttiger *et al.*, 2013; Möhrle *et al.*, 2019; Sedley, 2019), brain regions outside of the auditory pathway have also been implicated in these clinical conditions (Schlee *et al.*, 2008; Rauschecker, Leaver and Mühlau, 2010; Leaver *et al.*, 2011; Han *et al.*, 2018). Therefore, it is important to consider whether higher-order cortical areas, such as the prefrontal cortex, exhibit neural hyper-excitability similar to the auditory cortex, or if noise-induced plasticity manifests differentially outside of the auditory pathway. Moreover, it would also be worthwhile to determine the effect of noise exposure on the functional connectivity between the auditory cortex and prefrontal cortex. The 40-Hz auditory steady-state response (ASSR) can be used to assess the capacity of neurons to sustain a synchronized response to rapidly-presented acoustic stimuli, and ultimately represents a useful tool for investigating the functional connectivity between various brain regions (Shahriari *et al.*, 2016). Although no preclinical studies have used the 40-Hz ASSR to determine the effect of noise-induced plasticity on the functional connectivity between the auditory cortex and prefrontal cortex, it is reasonable to predict that it may be altered post-noise exposure, as subjects with long-term hearing loss were found to have hyper-coupling between these brain regions during resting-state neuroimaging (Luan *et al.*, 2019).

To date, the long-term effects of noise exposure on cognitive function in animal models has largely focused on characterizing hippocampal dependent behavioural performance. In the weeks and months following noise exposure, rodents consistently demonstrate

impaired spatial learning and memory performance as assessed with the Morris water maze; deficits that have been linked to changes within the hippocampus including impaired neurogenesis (Kraus *et al.*, 2010), neuroinflammation (Cui *et al.*, 2015), tau hyper-phosphorylation and the formation of neurofibrillary tangles (Cui *et al.*, 2012). Apart from these hippocampal dependent effects, the long-term effects of noise exposure on other cognitive domains such as executive function have been unexplored in animal studies. Importantly, using operant conditioning lever-pressing tasks, rodents can be screened for executive functions such as cognitive flexibility that rely heavily on the medial prefrontal cortex (mPFC). Investigating the effects of noise exposure on these behavioural tasks could provide insight into the mechanisms underlying the epidemiological link between hearing loss and executive dysfunction.

The series of experiments on adult rats presented in this chapter, provide a more complete understanding of the neural plasticity that occurs within and beyond the auditory pathway in the days following noise exposure, and whether noise-induced hearing loss results in long-term impairments in executive function. Using chronically-implanted electrodes in awake rats, this study investigated noise-induced plasticity in the auditory cortex and mPFC in the days following noise exposure via metrics associated with spontaneous neural oscillations and the 40-Hz auditory steady-state response (ASSR). Furthermore, the effects of noise exposure on cognitive-behavioural performance were investigated using lever-pressing tasks to assess cognitive flexibility (i.e., set-shifting and reversal learning), as well as the Morris water maze to assess spatial learning and reference memory. Overall, the present study has characterized the differential neural plasticity that occurs in the auditory pathway compared to the mPFC post-noise exposure, and the behavioural experiments have identified the varying degrees of susceptibility of non-auditory, cognitive tasks of learning, memory and executive function to noise exposure.

2.2 Materials and Methods

2.2.1 Animals and Experimental Design

Adult male Sprague Dawley rats were used in this study. To assess noise-induced neural plasticity, a within-subjects design was used in a cohort of rats (n = 10) that underwent electrophysiological recordings in the auditory and mPFC before, as well as 2- and 7-days post exposure **(Figure 2.1A)**. In a separate cohort of rats that underwent cognitive-behavioural testing, training commenced 30 days after exposure, and a between-subjects design was used to compare the performance of a group of noise-exposed rats (n = 11) to that of a separate group of sham-exposed rats (n = 11) **(Figure 2.1B)**.
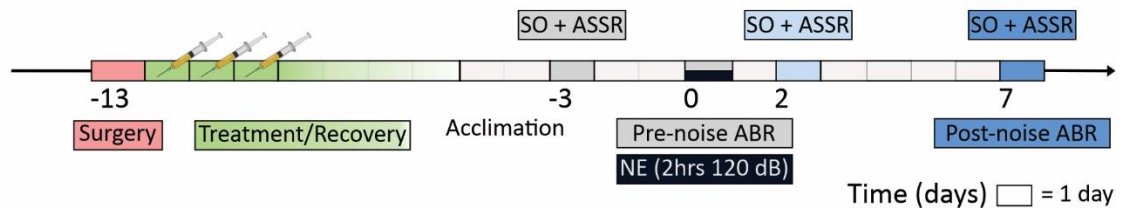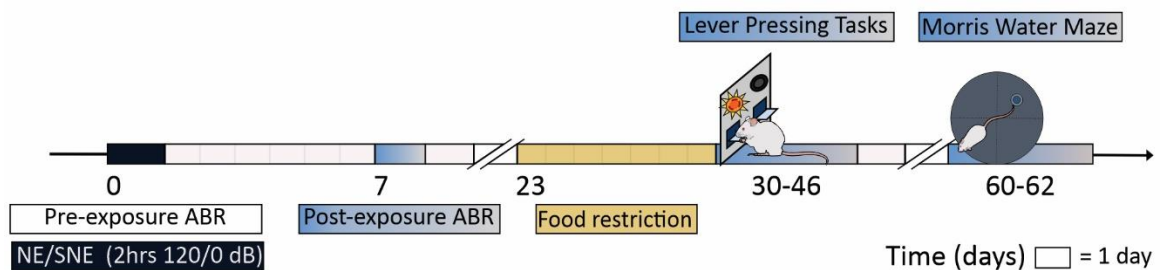
Figure 2.1 Experimental timelines. *(A) Experimental timeline of the first experimental series indicating the time points of spontaneous oscillation (SO) auditory steady-state response (ASSR) and auditory brainstem response (ABR) recordings with respect to the noise exposure (NE). (B) Experimental timeline of the second experimental series indicating the time points of lever-pressing tasks, Morris water maze test and auditory brainstem response (ABR) recordings with respect to the noise exposure (NE).*

All rats were housed in a temperature-controlled room with a 12 h light-dark cycle, and they were provided food and water *ad libitum* unless otherwise stated. All experimental

procedures were approved by the University of Western Ontario Animal Use Subcommittee and were in accordance with the guidelines established by the Canadian Council on Animal Care.

2.2.2 Hearing Testing and Noise Exposure

Hearing sensitivity was determined using an auditory brainstem response (ABR) protocol (Schormans, Typlt and Allman, 2019). Rats were anesthetized with ketamine (80 mg/kg; i.p.) and xylazine (5 mg/kg; i.p.), placed in a double-walled sound-attenuating chamber, and maintained at a body temperature of ~37 °C using a homeothermic heating pad (507220F; Harvard Apparatus, Holliston, MA). Subdermal electrodes (27 gauge; Rochester Electro-Medical, Lutz, FL) were positioned with the reference electrode over the right mastoid process, the ground electrode on the mid-back, and the active electrode located at either the vertex of the scalp (for rats used in the cognitive behavioural experiments) or the left mastoid process when the vertex position was obstructed in rats with chronically-implanted cortical electrodes. ABR testing included the presentation of click (0.1 ms) and tonal stimuli (4 and 20 kHz; 5 ms duration and 1 ms rise/fall time) generated by a Tucker-Davis Technologies (TDT, Alachua, FL) RZ6 processor at 100 kHz sampling rate, and delivered by a magnetic speaker (MF1; TDT) positioned 5 cm from the animal's right ear. The left ear was occluded with a custom foam earplug. The sound-evoked responses were acquired using a low-impedance headstage (RA4L1; TDT), preamplified and digitized using an RA16SD Medusa preamp (TDT) and sent to an RZ6 processor via a fiber optic cable. The sound level of the acoustic stimuli for ABRs (as well as the subsequent noise exposure) were calibrated with custom Matlab software (The Mathworks, Natick, MA) using a ¼-inch microphone (2530; Larson Davis, Depew, NY) and preamplifier (2221; Larson Davis). Each stimulus type was presented 1000 times (21 times/s) at decreasing intensities from 90 dB sound pressure level (SPL) in 10 dB steps. Near the threshold, the steps were reduced to 5 dB to ensure an accurate determination of the hearing threshold using the criteria of just noticeable deflection of the averaged electrical activity within the 10-ms time window (Popelar *et al.*, 2008; Schormans, Typlt and Allman, 2019).

Additionally, to characterize the impact of the noise exposure on the auditory nerve, the amplitude of wave I evoked by the click stimulus at 80 dB SPL was recorded (Schormans, Typlt and Allman, 2019).

Noise and sham exposures were carried out under anesthesia (ketamine: 80 mg/kg i.p; xylazine: 5 mg/kg, i.p.; supplemental i.m. doses, as needed). A homeothermic heating pad was used to maintain body temperature at ~37 °C for the duration of the procedure. Using TDT software and hardware (RPvdsEx; RZ6 processor), a broadband noise (0.8 – 20 kHz) was delivered bilaterally for two hours at 120 dB SPL through a super tweeter (T90A; Fostex, Tokyo, Japan) placed 10 cm in front of the anesthetized rat. This noise exposure protocol was chosen because it was previously shown to induce permanent changes in auditory processing at the level of the cochlea, brainstem and auditory cortex (Schormans, Typlt and Allman, 2019). Sham exposed rats underwent the same treatment as noise-exposed rats; however, the speaker was turned off.

2.2.3 Noise-Induced Cortical Plasticity: Event-Related Potential, 40-Hz Auditory Steady-State Responses and Spontaneous Oscillations

To investigate the nature and extent of noise-induced plasticity in the auditory cortex and mPFC, spontaneous oscillations and sound-evoked activity (i.e., event-related potentials and 40-Hz ASSR) were recorded from chronically-implanted electrodes in awake rats (n = 10) before as well as 2 days and 7 days after noise exposure. In preparation for the implantation of the chronic electrodes, the rats were anesthetized with isoflurane (4% induction; 2% maintenance) and fixed into a stereotaxic frame with blunt ear bars. Body temperature was maintained at ~37 °C using a homeothermic heating pad. A midline incision was made in the scalp, allowing for the fascia and the left temporalis muscle to be removed. Epidural screw electrodes (E363-20; PlasticsOne Inc., Roanoke, VA, USA) were implanted over the left auditory cortex (4.3 mm caudal to bregma and 4.5 mm ventral to the dorsal surface of the skull), and over the cerebellum (2.0 mm caudal to lambda and 2.0 mm lateral to the midline), which served as the reference/ground

electrode (Paxinos and Watson, 2006). For the recordings from the mPFC, an indwelling electrode (stainless steel; outer diameter: 0.41mm) was implanted (3.7 mm anterior to bregma; 0.8 mm left of midline; 2.5 mm ventral to the dorsal surface of the skull) (Paxinos and Watson, 2006). As such, this electrode targeted the mPFC in rats, which includes the anterior cingulate, prelimbic and infralimbic regions, but not the more laterally-located orbitofrontal cortex (Laubach *et al.*, 2018) **(Figure 2.2)**. The connector pins from the three electrodes were fed into a pedestal (MS363; PlasticsOne Inc.), which was secured to the skull with dental cement. The scalp wound was sutured using standard techniques. Following the surgery, the rats were monitored until they became ambulatory. Rats were administered Metacam (1 mg/kg, subcutaneously) and Baytril (10 mg/kg, subcutaneously) for the next three days, and their body mass, appearance, and behaviour were closely monitored for seven days.
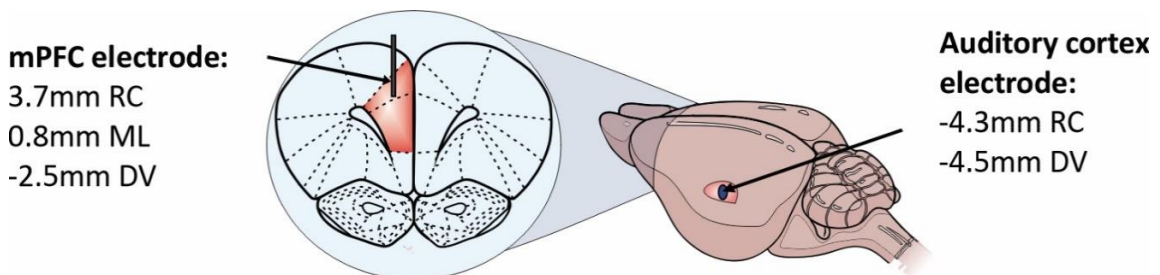
Figure 2.2 Electrode placement with respect to the bregma. *RC indicates rostral-caudal direction with positive numbers indicating location rostral to bregma and negative numbers caudal to bregma. ML indicates the medial-lateral directions with positive numbers indicating left to the midline. DV indicates dorsal - ventral directions, with negative numbers indicating the location below the surface of the skull.*

Once the rats had fully recovered from their implant surgery, initial (pre-noise) cortical recordings were performed in a custom chamber (43 × 23 × 23 cm), which was housed in a sound-attenuating box. The recording chamber was equipped with a house light, and a speaker (FT17H; Fostex) mounted on the ceiling. The rat's electrode pedestal was connected to a commutator (SL6C-SB; PlasticsOne Inc.) via a tether (363-363; PlasticsOne Inc.) that was long enough to allow unrestricted movements inside the recording chamber. The commutator was connected via a cable (363-441-6; PlasticsOne Inc.) to a

RA4LI low-impedance headstage (TDT), which was then connected to an RZ6 processor (TDT) via a fiber optic cable.

Guided by previous studies that investigated auditory steady-state responses in normal-hearing rats (Vohs *et al.*, 2010, 2012; Sivarao *et al.*, 2013, 2016; Sullivan *et al.*, 2015), the present electrophysiological protocol included 150 trials of a 40-Hz stimulus train. Using an RZ6 processor, each of the 40-Hz stimulus trains lasted a total duration of 500 ms, and consisted of 20 repetitive noise bursts (1-45 kHz; 80 dB SPL; 10 ms duration; 0.1 ms rise/fall time; 25 ms inter-stimulus interval). Ultimately, because the 40-Hz stimulus trains were each separated by 5 s of silence, this protocol allowed for the collection of both spontaneous oscillations and sound-evoked activity (i.e., the event-related potential to the first stimulus of each train, as well as the 40-Hz ASSR) (see **Figure 2.3** for the protocol overview).

During the recording session, the delivery of the 40-Hz stimulus trains and the acquisition of the local field potential (LFP) signal were controlled through custom Matlab protocols. The LFP signal was digitized at a 1017.25 Hz sampling rate, and band-pass filtered between 0.5 and 300 Hz. For each of the 150 trials, the LFP signal was first subjected to a range-based artifact rejection (Spencer *et al.*, 2008, 2009; Spencer, 2012; Sullivan *et al.*, 2015), where the trial was removed from further analysis if its amplitude range exceeded two-thirds of the LFP amplitude range of the entire recording block. For each accepted trial, the event-related potential (ERP) in response to the first noise burst of the 40-Hz stimulus train was collected from the auditory and prefrontal cortices. The peak amplitude of the N18 response (i.e., first negative peak at ~18 ms after stimulus onset) was measured from the auditory cortex, whereas the P30 response (i.e., positive peak at ~30 ms after stimulus onset) was measured from the mPFC.

A

Protocol overview

Spontaneous Activity   40Hz ASSR

Trial Start   Trial End

Onset   Offset

- 4   0   0.5   1.5

Time (s)   ☐ = 0.5s

B

Time Domain

Event Related Potential

C

Time-Frequency Decomposition

Frequency Power Spectrum   Inter-Trial Coherence   Phase-Locking Value
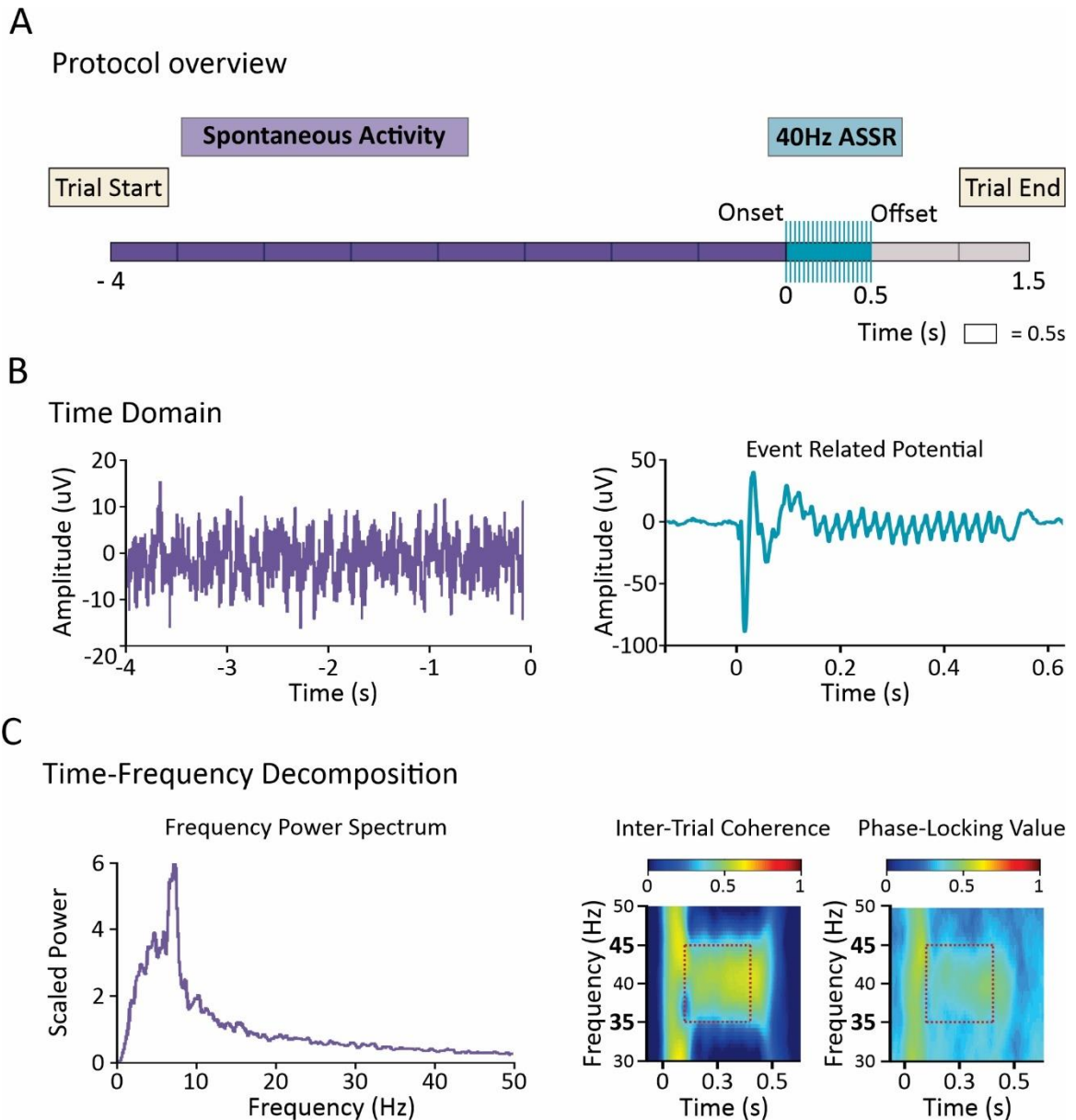
Figure 2.3. Overview of the electrophysiological protocol to obtain both spontaneous oscillations, event-related potentials and 40-Hz auditory steady-state responses: **(A)** *A graphical representation of a single trial of the electrophysiological protocol.* **(B)** *Representative examples of the LFP signal collected from auditory cortex within the time domain. The spontaneous oscillations are indicated in purple. The teal trace shows the event-related potential recorded within the auditory cortex.* **(C)** *In purple: normalized frequency power spectrum resulting from the Fast-Fourier transformation of the spontaneous oscillation recorded within the auditory cortex. The heat maps on the right show an example of the ITC recorded from the auditory cortex, and the phase-locking value between the auditory cortex and mPFC. The dashed red square (35-45 Hz; 100-400 ms), indicates the area that was used to obtain the ITC and phase-locking values for statistical analysis.*

57

To assess the ability of the auditory and prefrontal cortices to synchronize with rapidly-presented acoustic stimuli, the inter-trial coherence (ITC) of the 40-Hz ASSR was calculated for both cortices (Roach and Mathalon, 2008; Brenner *et al.*, 2009). Each accepted trial of the recorded LFP was subjected to time-frequency decomposition via the *'ft_freqanalysis'* function in the FieldTrip toolbox (Oostenveld *et al.*, 2010) With this function, the '*mtmconvol*' method was used, which performed a time-frequency analysis on the time-series data (i.e., the LFP values comprising the accepted trial) using the conventional Hann window taper. A complex value, containing the phase information from the LFP values, was created for each frequency of interest (i.e., $0 - 50$ Hz in 0.5 Hz steps) from the beginning to the end of the trial (i.e., from $0 - 5500$ ms) using a 200 ms window centered on 1 ms steps. The resulting complex values for each trial were divided by their magnitude and then averaged across trials (Roach and Mathalon, 2008), yielding a value between zero and one (with one reflecting maximum phase coherence). Consistent with previous studies (Spencer *et al.*, 2008, 2009; Vohs *et al.*, 2010, 2012), the calculated ITC values were then baseline-corrected; a process that is important for revealing changes in this measurement that may not be evident from the raw values (Roach and Mathalon, 2008). A mean ITC baseline value was calculated within -400 ms to -100 ms time window with respect to stimulus onset at each frequency of interest (i.e., $0 - 50$ Hz in 0.5 Hz steps). These mean ITC baseline values were then subtracted from all ITC values from $0 - 5500$ ms of corresponding frequencies to yield the baseline-corrected ITC values. For both cortical regions, baseline corrected ITC values for each day (pre-noise; 2 days post-noise; 7 days post-noise) are shown as group averaged spectrograms plotted as frequency (30 Hz $-$ 50 Hz) × time (-500 $-$ 1000 ms with respect to stimulus onset) × magnitude of ITC (values ranging from $0 - 1$). These baseline-corrected values were further quantified by calculating each rat's mean ITC between $100 - 400$ ms post-stimulus onset and $35 - 45$ Hz, thereby incorporating the maximum region of the evoked response, and then averaged across rats to yield group averaged ITC values.

To evaluate the effect of noise exposure on the functional connectivity between the auditory cortex and mPFC, the synchrony of their LFPs was calculated through a measure of the phase-locking value (Lachaux *et al.*, 1999; Mormann *et al.*, 2000; Shahriari *et al.*, 2016). Whereas the ITC calculations determine the consistency of the phase across trials within a given brain region, the phase-locking value measures the extent to which the phase is consistent between two brain regions over multiple trials. The phases of the signal from the auditory cortex and mPFC were extracted as described above, and the phase angle difference between the two signals was calculated, separately for each trial, and then averaged across the trials. This yielded a value between zero (no phase synchrony) and one (full phase synchrony). The calculated phase-locking values were then baseline-corrected similarly to the ITC calculations. The phase-locking values between the auditory cortex and mPFC were obtained pre-noise exposure, as well as 2 and 7 days post-noise, and displayed as group average spectrograms plotted as frequency (30 – 50 Hz) × time (-500 – 1000 ms with respect to stimulus onset) × magnitude of phase-locking values (ranging from 0 – 1). The baseline-corrected values were further quantified by calculating each rat's mean phase-locking value between 100 – 400 ms post-stimulus onset in the range from 35 – 45 Hz, to incorporate the maximum region of the evoked response, and then averaged across the rats to yield a group averaged phase-locking value.

To examine spontaneous oscillations in the auditory cortex and mPFC, LFP amplitudes between -4000 – 0 ms relative to the onset of the 40-Hz stimulus train from each trial were subjected to time-frequency decomposition via Fast - Fourier Transformation (FFT) that utilized the Hann window taper. Power was calculated as the squared magnitude of the complex numbers resulting from the FFT. To account for variability in the spontaneous LFP signal strength between the individual rats, each rat's 0.5 – 50 Hz power spectrum was normalized by dividing it by its overall mean power, thereby yielding a scaled power; a method used in previous studies (Weisz *et al.*, 2005, 2011; Weisz, Dohrmann and Elbert, 2007). The scaled power was calculated independently for each of the days (pre-noise; 2 days post-noise; 7 days post-noise) and brain regions (auditory cortex; mPFC). Finally, the

scaled power was computed within four frequency bins of interest (delta, 2-4 Hz; theta, 4-8 Hz; alpha, 8-12; and gamma, 30-50 Hz), which were then averaged across rats for each of the days.

Once the ERPs, 40-Hz ASSR, and spontaneous oscillations were collected at the initial time point (pre-noise), the rats were later anesthetized, and their hearing was assessed. Immediately following the ABR, the rats were noise-exposed, as described above. The electrophysiological protocol was repeated 2 days and 7 days after the noise exposure. Finally, a post-noise ABR was collected to assess the level of permanent hearing damage. Prior to emerging from anesthesia, the rats were exsanguinated via transcardial perfusion of 0.9% saline (300 mL), 0.1 M phosphate buffer (PB; 400 mL), and 4% paraformaldehyde (PFA; 400 mL). To ensure the accurate placement of the indwelling electrode in the mPFC, the brains were harvested and prepared for histological analysis. First, the brains were post-fixed in 4% PFA for at least 24 h, and stored in 30% sucrose/PB solution for cryoprotection for at least 72 h. Using a freezing microtome (HM 430/34; Thermo Scientific, Waltham, MA), the brains were cut into 50 µm coronal sections. Following Nissl staining with thionin, the coronal sections were imaged using an Axio Vert A1 inverted microscope (Carl Zeiss Microscopy GmbH). In all rats, the indwelling electrode was confirmed to have targeted the mPFC based on a stereotaxic atlas (Paxinos and Watson, 2006).

2.2.4 Cognitive-Behavioural Testing and Noise Exposure

To determine the effect of noise-induced hearing loss on cognitive flexibility (i.e., set-shifting and reversal learning), groups of sham (n = 11) and noise-exposed rats (n = 11) were tested using protocols associated with a series of lever-pressing tasks, including visual-cue discrimination, response discrimination, and reversed-response discrimination (Floresco, Block and Tse, 2008; Desai, Allman and Rajakumar, 2017, 2018; Levit *et al.*, 2017). These same groups of rats were then tested using the Morris water maze (Roof Robin L. *et al.*, 2001; Levit *et al.*, 2019) to assess the effect of noise exposure on spatial

learning and reference memory. Before any cognitive-behavioural training, the rats were anesthetized, and an ABR protocol was performed to assess initial hearing, followed by either noise exposure or sham exposure (as described above). In order for the rats to ultimately perform the lever-pressing tasks, they first underwent basic training procedures, which commenced 30 days after the noise (or sham) exposure. One week preceding the first training session, the rats were placed on food restriction so that they approached 85% of their free-feeding body mass. This food restriction was carefully monitored and persisted for the duration of the lever-pressing testing.

The lever-pressing tasks were performed in an operant conditioning apparatus, which included a modular acrylic test chamber (30.5 × 24 × 21 cm), housed in a sound-attenuating box. The test chamber had two cue lights, each located above a retractable lever that was positioned on either side of a central pellet receptacle. A house light was located on the opposite wall of the chamber. A customized computer software program (MED-PC IV, Med-Associates) controlled the operation of the test chamber.

During the acclimation and initial training sessions, rats were conditioned to press the lever that was randomly extended into the chamber within a 10-s response window to receive a sucrose pellet (45 mg; Bio-Serv, Frenchtown, NJ) in the center receptacle. Failure to press the extended lever resulted in its retraction, no pellet delivery, and the turning off of the house light. Once rats reached the performance criterion (i.e., less than 5 omissions over 90 consecutive trials), their preference for a given lever was determined. As described in detail previously (Floresco, Block and Tse, 2008), over a series of trials, both levers were simultaneously extended, and depending on the number of times the rat pressed each lever, it was determined whether the rat preferred the left or right lever (i.e., its side bias). This information was later used for the response discrimination task, where the lever opposite to the rat's side bias was to be considered the correct lever **(Figure 2.4A)**.
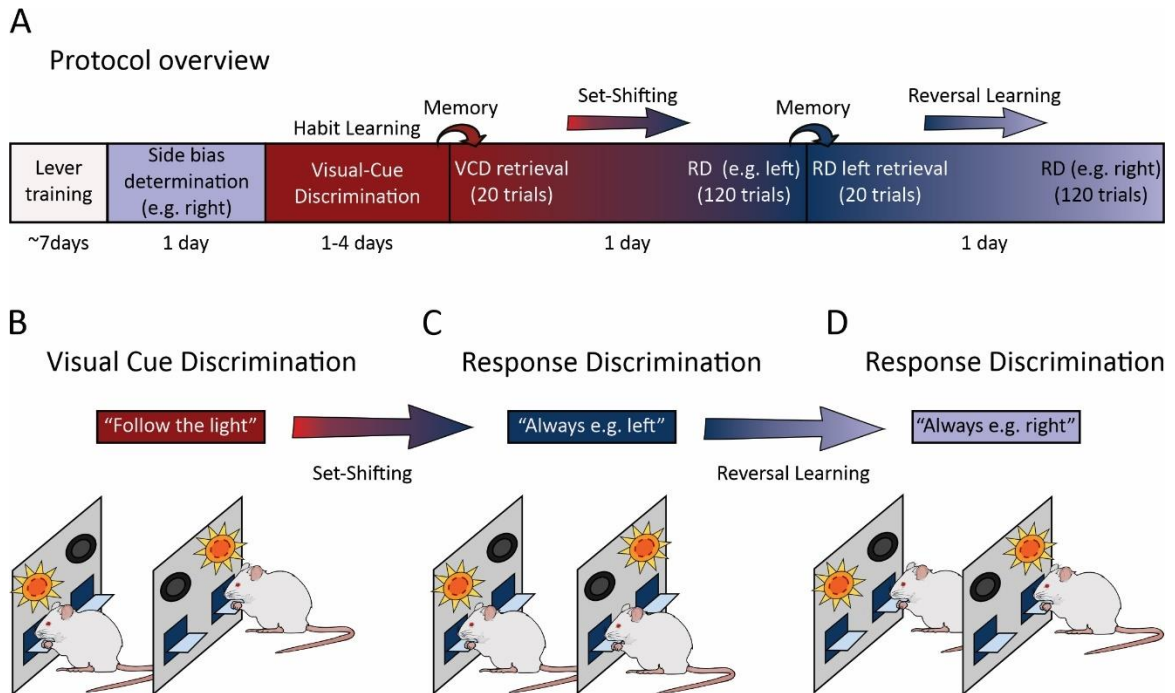
Figure 2.4 Overview of the lever-pressing cognitive task. A) *The lever-pressing task protocol. Prior to starting the protocol, rats were acclimatized to the behavioural boxes. The duration of each stage is indicated below the timeline. The cognitive abilities tested during each of the stages is indicated above the protocol timeline.* **(B-D)** *Graphical representation of the visual-cue discrimination, and two of the response discrimination tasks used in this experiment. The rules (e.g., "follow the light") are indicated on the boxes above the diagrams.*

On the day following side bias determination, rats performed a visual-cue discrimination task that required them to learn to press the lever associated with an illuminated cue light; an example of stimulus-response habit learning. In a given trial, a cue light was pseudo-randomly illuminated, followed 3 seconds later by the extension of both levers; the rat needed to press the lever located below the cue light within a 10-s response window to receive a sucrose pellet. Performance during the visual-cue discrimination task served to teach the rats the initial rule (set): press the lever located below the illuminated cue light. Ultimately, each rat's performance was scored by tallying the number of incorrect lever presses committed over 100 trials of the visual-cue discrimination task **(Figure 2.4B)**.

On the day after completing the visual-cue discrimination task, rats were subjected to 20 visual-cue discrimination trials to determine their memory retrieval of the initial set

formation (i.e., follow the cue light). Starting on the 21st trial, the protocol was switched to a response discrimination task for 120 trials, in which the rats had to "set-shift" (a form of cognitive flexibility reliant on the mPFC) and now respond to a new rule: press the lever opposite to their side bias during every trial regardless of the location of the cue light. Again, each trial began with the pseudo-random illumination of a cue light, followed 3 s later by the extension of both levers. A correct lever press within the 10-s response window resulted in the delivery of a sucrose pellet. Ultimately, to quantify the rat's ability to set-shift, its performance in the response discrimination task was scored by tallying the number of incorrect lever presses committed over the 120 trials **(Figure 2.4C)**.

In addition to assessing set-shifting, I also investigated how reversal learning (another form of cognitive flexibility reliant on the orbitofrontal cortex) was affected by noise exposure. One day following the response discrimination task, the rats performed 20 trials under the same protocol conditions, as this would allow for a determination of their memory retrieval (e.g., always press the left lever, regardless of the cue light). Then, to assess the rat's ability for reversal learning, the protocol was switched so that for the next 120 trials, the opposite (e.g., right) lever was now always correct, regardless of the location of the cue light. Performance in this reversed-response discrimination task was scored by tallying the number of incorrect lever presses committed over the 120 trials **(Figure 2.4D)**.

Following the completion of the lever-pressing tasks, the sham- and noise-exposed rats were no longer food restricted. Three weeks later, the effect of noise exposure on spatial learning and reference memory was assessed using protocols associated with the Morris water maze (Roof *et al.*, 2001; Levit *et al.*, 2019). A circular tank (144 cm diameter) was filled with water at room temperature (22-23 °C) that was dyed with black non-toxic acrylic paint. Within the testing room, cue signs were placed on the north (green cross), west (black square) and south (white triangle) walls **(Figure 2.5A)**. To acclimate the rats, they were placed in the corner of the testing room while in their home cage for 7 h on the day before testing, and 1 h on the day of testing. Ultimately, during the learning session,

the rats underwent 6 trials, each separated by 1 h **(Figure 2.5B)**. A trial started with the rat being placed in the water facing the tank wall in the south-west quadrant. The trial continued until the rat swam and found the hidden platform (12 cm diameter; 3 cm below the surface of the water), which was positioned in the north-east quadrant. If the rat did not find the platform within the 90-s maximum trial duration, it was cued to the platform by the experimenter, and allowed to rest on the platform for 30 s to observe its location with respect to the cue signs. Throughout testing, the rats were tracked with ANYmaze software (v4.70, Stoelting Company) using a webcam (C525, Logitech) mounted on the ceiling above the tank. During the learning session, each rat's time to the platform and swimming speed were recorded.

Twenty-four hours after the 6th trial of the learning session, the rats performed a probe test, in which the submerged platform was removed from the tank. The rats were again placed in the water facing the tank wall in the south-west quadrant, but because there was no platform, the rats were allowed to swim for the full 90 s. The rat's ability to recall the location of the platform was assessed by recording the time required to first enter the platform zone (27 cm diameter). The rats' swimming speed, as well as the time spent in the target quadrant and the perimeter of the pool were also tabulated **(Figure 2.5C)**.

One hour after the completion of the probe test, a final protocol was conducted to investigate the possibility of differences in visual acuity and/or swim speed confounding the performance of the shams versus noise-exposed rats during the learning session or probe test. In total, each rat performed eight visually-cued trials, wherein the cue signs on the walls were removed, and the location of the platform was now indicated using a marker (flag) positioned directly above the surface of the water. For each of these eight visually-cued trials, the marked platform was positioned in one of four possible locations, and the rats were placed into the tank at one of two different starting locations. The trials that were performed with the same platform location occurred back-to-back, without a rest interval. In contrast, a 1-h interval separated the trials when the platform was moved to a new location **(Figure 2.5D)**. ANYmaze software was used to track each rat's swimming

speed, and the elapsed time to reach the marked platform. For each platform location, the time it took for each rat to reach the platform from both starting locations was summed, and ultimately averaged across all the rats.

A

Morris Water Maze

B

Spatial Learning

C

Reference Memory

D

Cued Trials
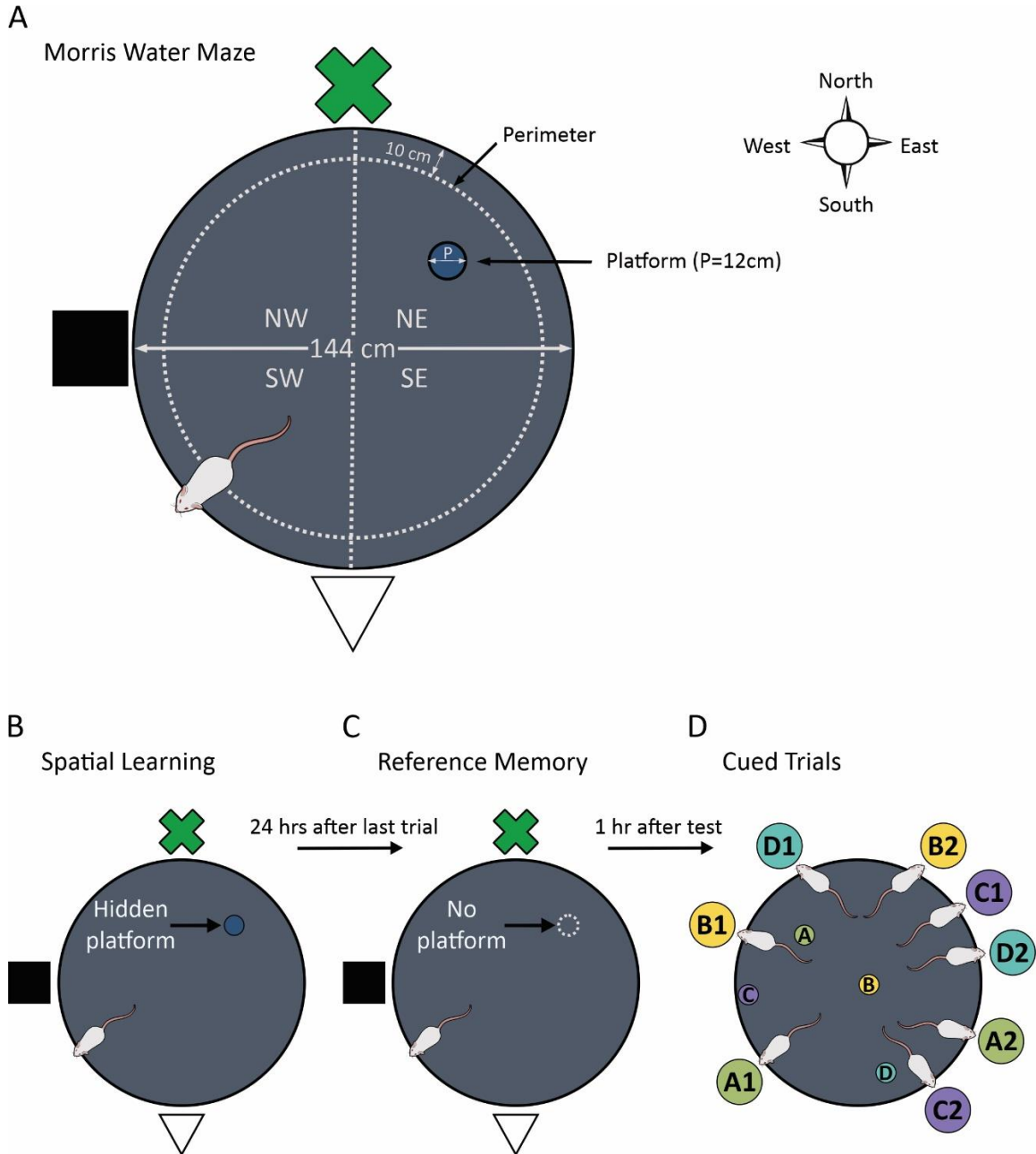
Figure 2.5 Overview of the Morris water maze testing apparatus and protocol. **(A)** *Schematics representing the MWM set-up are shown, with the quadrants named in reference to the green cross as "North".* **(B-D)** *Schematics representing the three stages of testing using the MWM: spatial learning, reference memory and cued trials.*

2.2.5 Data Presentation and Statistics

Statistical analyses were conducted using GraphPad Prism or SPSS (Version 20, IBM Corp.), and included one-way, two-way or three-way repeated measures analysis of variance (ANOVA), as well as paired or unpaired (Welch's) t-tests, all depending on the comparison of interest. In cases when the data distributions failed to pass the Shapiro-Wilk normality test, a Wilcoxon matched-paired signed-rank test was performed for paired comparisons, whereas the Mann-Whitney U test was used to compare unpaired groups. *Post hoc* paired-samples t-tests with a Bonferroni-corrected significance level were used to compare differences in the group means in the case of a significant interaction. The following sections provide a summary of the various statistical tests performed in each of the experimental series.

2.2.5.1 Hearing Sensitivity & Noise Exposure

To compare ABR thresholds before and after noise exposure in rats undergoing electrophysiological recordings, a two-way repeated measures ANOVA was performed for day (pre-noise; 7 days post-noise) × stimulus type (click; 4 kHz tone; 20 kHz tone). Furthermore, the severity of the hearing trauma was also assessed by comparing the magnitude of the wave I amplitude before and after noise exposure. As the wave I amplitude pre-noise was not normally distributed, a Wilcoxon matched-pairs signed-rank test was used for comparison to the wave I amplitude 7-days post-noise. For both the sham and noise exposed rats that underwent behavioural testing, ABR thresholds were first compared using a three-way repeated measures ANOVA, considering day (pre-noise; post-noise) × stimulus type (click; 4 kHz tone; 20 kHz tone) × group (sham; noise-exposed). As a significant interaction was found between day and group, separate two-way repeated measures ANOVAs were then performed to assess the effects of the sham or noise exposure on the thresholds for click, 4 kHz and 20 kHz tones. To compare wave I amplitudes before and after noise exposure in the behavioural cohort of rats, a two-way

repeated measures ANOVA was performed for day (pre-noise; 7 days post-noise) × group (sham; noise-exposed).

2.2.5.2 Noise-Induced Cortical Plasticity

The effect of noise exposure on the sound-evoked ERPs recorded from the auditory cortex (N18) and mPFC (P30) were assessed with separate one-way repeated measures ANOVAs (pre-noise; 2 days post-noise; 7 days post-noise). A two-way repeated measures ANOVA for brain regions (auditory cortex; mPFC) × day (pre-noise; 2 days post-noise; 7 days post-noise) was used to investigate how noise exposure affected ITC in response to 40-Hz sound stimulation. Moreover, the effect of noise exposure on the functional connectivity between the auditory cortex and mPFC was determined by performing a one-way repeated measures ANOVA on the phase-locking values recorded before (pre-noise) and after noise exposure (2 days post-noise; 7 days post-noise). Finally, to investigate the effects of noise exposure on spontaneous neural oscillations, a three-way repeated-measures ANOVA was performed on the scaled power recorded in the different brain regions (auditory cortex; mPFC) × various frequency bins (delta, 2-4 Hz; theta, 4-8 Hz; alpha, 8-12; and gamma, 30-50 Hz) × day (pre-noise; 2 days post-noise; 7 days post-noise).

2.2.5.3 Cognitive-Behavioural Testing & Noise Exposure

To determine the effect of noise exposure on cognitive function using a series of lever-pressing tasks, unpaired Welch's t-tests or Mann-Whitney U tests were used to compare the performance of sham versus noise-exposed rats. To investigate the effect of noise exposure on the rats' timed performance to locate the hidden platform during the spatial learning trials on the Morris water maze, a two-way repeated measures ANOVA was performed for trial number (2; 3; 4; 5; 6) × exposure (sham rats; noise rats). Similarly, a two-way repeated measures ANOVA was used to compare the sham versus noise-exposed rats' swim speeds over these learning trials. Performance during the visually-cued trials of the Morris water maze was assessed using separate two-way repeated measures ANOVAs

for the time to reach the cued platform (starting location × exposure), and swim speed (starting location × exposure).

2.2.5.4 Correlational Analyses

To quantify the relationship between the degree of hearing loss and various electrophysiological metrics (i.e., ERP, ITC, and PLV) or behavioural metrics (i.e., lever-pressing and Morris water maze performance), ABR threshold shifts for the click stimulus were plotted against each metric and Pearson's correlation coefficients (R^2) were determined.

2.3 Results

2.3.1 Central gain enhancement was evident in the auditory cortex, but not in the mPFC, following noise exposure.

Seven days following the noise exposure, rats used in the electrophysiological experiments showed a significant increase in their hearing thresholds to the click stimulus (pre-noise: 34.5 ± 0.9 dB SPL vs. 7 days post-noise: 51.5 ± 3.0 dB SPL, $p_{Bonf} < 0.01$), 4 kHz stimulus (pre-noise: 28.5 ± 1.1 dB SPL vs. 7 days post-noise: 51.5 ± 3.1 dB SPL, $p_{Bonf} < 0.01$), and 20 kHz stimulus (pre-noise: 28.0 ± 1.5 dB SPL vs. 7 days post-noise: 54.0 ± 4.3 dB SPL, $p_{Bonf} < 0.01$) (**Figure 2.6A**). In addition to determining the ABR threshold, the amplitude of the first positive wave of the ABR trace (wave I) in response to the 80 dB SPL click stimulus was used to assess the level of noise-induced damage to the cochlear hair cell afferents (Kujawa and Liberman, 2009). Compared to the pre-noise results, the noise exposure caused a significant reduction (65%) of the wave I amplitude measured 7 days later (p < 0.01; **Figure 2.6B**).
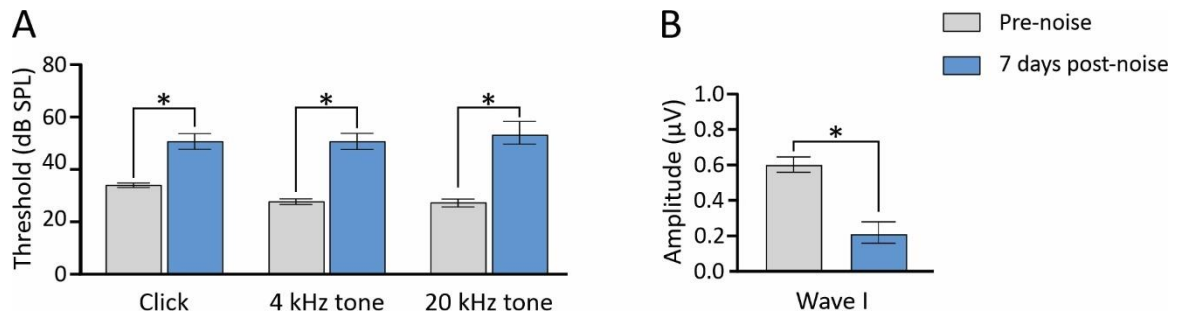
Figure 2.6 Hearing loss following noise exposure in rats used for electrophysiological recordings
(A) *The auditory brainstem response (ABR) protocol revealed a significant elevation of hearing thresholds for the click, 4 kHz, and 20 kHz stimuli compared to the pre-noise exposure threshold.* ***(B)*** *Noise exposure also significantly reduced the wave I amplitude 7 days after noise exposure as compared to the initial (pre-noise) recordings. Data represent group mean ± SEM; n = 10 rats; *p < 0.01.*

Despite this hearing impairment, event-related potentials (ERPs) recorded from the auditory cortex (N18) were increased at both 2 days ($p_{Bonf} < 0.01$) and 7 days ($p_{Bonf} < 0.05$) after noise exposure compared to the pre-noise recordings (**Figure 2.7A** and **2.7B**). In contrast, ERPs recorded from the mPFC (P30) of the same rats were not significantly increased post-noise exposure ($F_{(1.442, 12.98)} = 2.52$, p= 0.129; **Figure 2.7C** and **2.7D**). Taken together, these findings reveal that the extent of noise-induced central gain enhancement observed in the auditory pathway failed to manifest at the higher-level, mPFC. The detailed results of the statistical analysis are presented in the **table 2.1**.
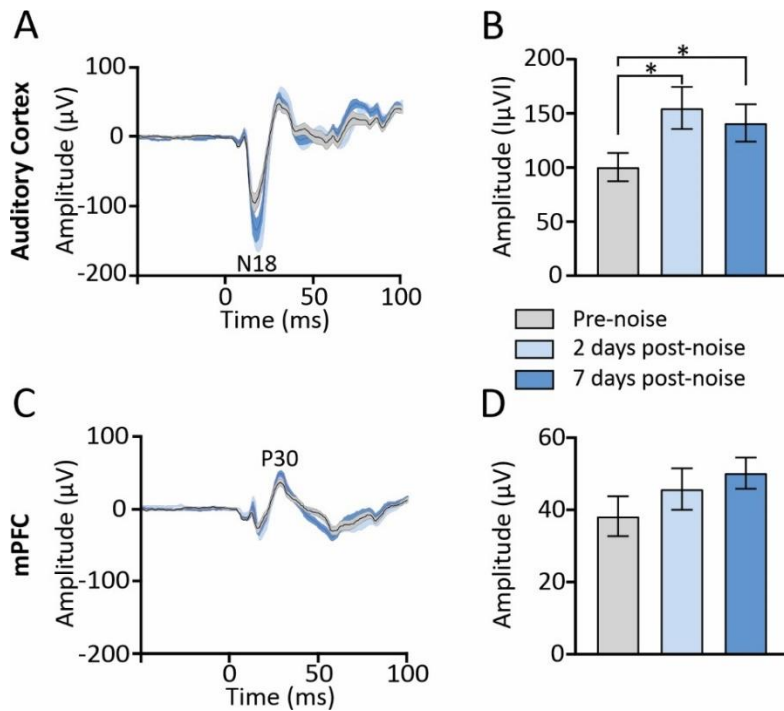
Figure 2.7 Sound-evoked responses in the auditory cortex, but not mPFC, were increased following noise exposure. (A, C) The group mean ERP trace (shading indicates SEM) in response to an 80 dB SPL stimulus recorded from the auditory cortex *(A)* and mPFC *(C)* before (pre-noise: grey) and after noise exposure (2 days post-noise: light blue; 7 days post-noise: dark blue). *(B)* The peak amplitude of the N18 response in the auditory cortex was significantly increased post-noise compared to the initial recordings (*p_{Bonf} < 0.05), indicative of central gain enhancement. *(D)* The peak amplitude of the P30 response recorded from the mPFC did not differ across days. Data represent group mean ± SEM; n = 10 rats;

2.3.2 Noise exposure impaired inter-trial coherence of the 40-Hz auditory steady-state response in the mPFC, but not auditory cortex

To further examine the effect of noise exposure on sound-evoked cortical activity, the pre-noise 40-Hz ASSR was compared to that recorded at 2 days and 7 days post-noise. Again, the results showed differential plasticity in the two cortical regions (two-way repeated measures ANOVA; significant interaction of brain region × day, $F_{(2, 18)}$ = 7.046, p< 0.006), which was characterized by a lack of change in ITC of the 40-Hz ASSR in the auditory cortex (**Figure 2.8A and 2.8B**), and a significant decrease in ITC in the mPFC at 2 days (p_{Bonf} < 0.0005) and 7 days (p_{Bonf} < 0.002) after noise exposure compared to the initial recordings (**Figure 2.7C and 2.7D**). Further statistical details are presented in the **table 2.1**.
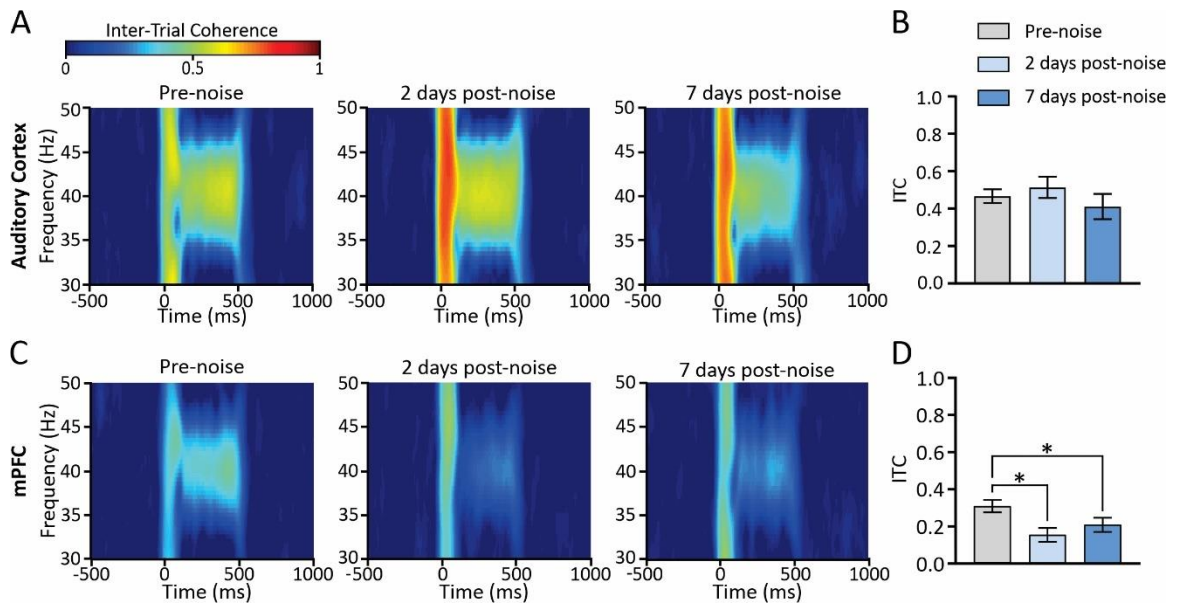
Figure 2.8 Inter-trial coherence of the 40-Hz auditory steady-state responses was decreased in the mPFC, but not auditory cortex, following noise exposure. (A, C) The heat maps plot the group average of the inter-trial coherence (ITC) of the 40-Hz auditory steady-state response from the auditory cortex *(A)* and mPFC *(C)* before (pre-noise) and after noise exposure (2- and 7-days post-noise). *(B)* The group average magnitude of ITC (35 − 45 Hz within 100 − 400 ms after stimulus onset) revealed no significant differences in the auditory cortex before and after noise exposure. *(D)* In contrast, compared to the pre-noise recordings, ITC in the mPFC was significantly reduced in the days after noise exposure (*$p_{Bonf} < 0.002$). Data in bar graphs represents group mean ± SEM; n = 10 rats

Ultimately, this differential plasticity underscored a loss of functional connectivity between the auditory and prefrontal cortices, as the phase-locking value between the cortical regions was lower at both 2 days ($p_{Bonf} < 0.005$) and 7 days ($p_{Bonf} < 0.01$) after noise exposure (**Figure 2.9**). Combined with the ERP data (**Figure 2.7**), these 40-Hz ASSR results confirm that the nature and extent of plasticity induced by the noise exposure differed between the auditory cortex and mPFC (**Table 2.1**)
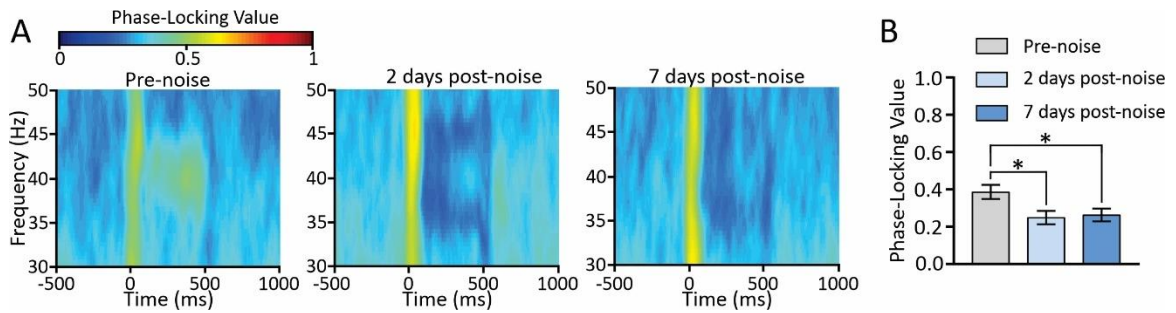
Figure 2.9 Decreased functional connectivity between the auditory cortex and mPFC following noise exposure. (A) *The heat maps plot the group average of the phase-locking value between the auditory cortex and mPFC, which was determine from the 40 – Hz auditory steady-state response recorded before (pre-noise) and after noise exposure (2- and 7-days post-noise).* ***(B)*** *Compared to the pre-noise recordings, the group average magnitude of the phase-locking value (35 – 45 Hz within 100 – 400 ms after stimulus onset) was significantly decreased in the days following noise exposure (*p_{Bonf} < 0.01). Data in bar graphs represents group mean ± SEM; n = 10 rats*

2.3.3 Spontaneous cortical oscillations were unaffected by noise exposure.

To investigate the effect of noise exposure on spontaneous oscillations in the auditory and prefrontal cortices, the scaled power of the LFP signal from each cortical region was calculated within four frequency bins of interest (delta, 2-4 Hz; theta, 4-8 Hz; alpha, 8-12; and gamma, 30-50 Hz). Not surprisingly, an initial three-way repeated measures ANOVA revealed a significant three-way interaction ($p < 0.001$) for brain region (auditory cortex vs. mPFC) × time (pre- vs. 2 days post-noise vs. 7 days post-noise) × frequency (delta vs. theta vs. alpha vs. gamma). However, subsequent two-way repeated measures ANOVAs of each cortical area failed to reveal either a significant main effect of time (auditory cortex: $p = 0.932$; mPFC: $p = 0.407$) or significant interactions (auditory cortex: $p = 0.244$; mPFC: $p = 0.127$). Thus, unlike the sound-evoked activity (i.e., ERPs, **Figure 2.7** and 40-Hz ASSR, **Figure 2.8**, noise exposure did not cause a differential effect on spontaneous oscillations in the auditory cortex and mPFC (**Figure 2.10**). For more detail of statistical results see **table 2.1**.
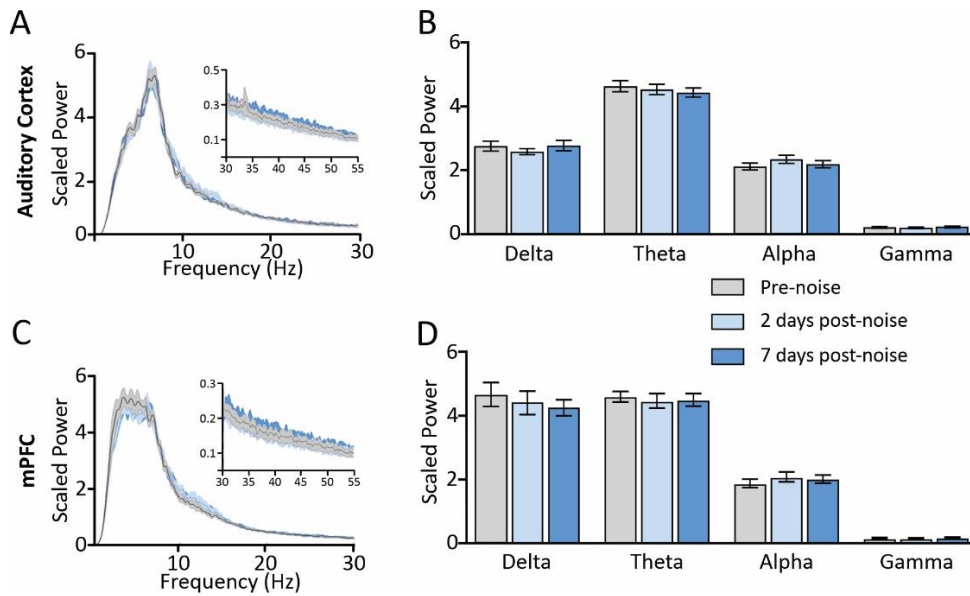
Figure 2.10 Noise exposure did not affect spontaneous oscillations in the auditory cortex and mPFC. (A, C) *The group mean profiles of scaled power 9shading indicates SEM) of spontaneous oscillations at 0-30 Hz (main graph) and 30-55 Hz (inset) recorded from the auditory cortex **(A)** and mPFC **(C)** before (pre-noise: grey) and after noise exposure (2-days post-noise: light blue; 7-days post-noise: dark blue). **(B, D)** The scaled power of the spontaneous oscillations in the auditory cortex and mPFC are plotted over time for each of the frequency bins. Ultimately, noise exposure did not alter the scaled power in any of the frequency bins in the auditory cortex or mPFC. Data in bar graphs represents group mean ± SEM; n = 10 rats*

Normality Data	p-value	Test	Main effects/ Comparisons	p-value	F-value/ t-value
Figure 2.6 Hearing assessment: Study 1—Experimental Series 1A					
Figure 2.6 A. Click stimulus ABR threshold (n=10)					
		2-way RM-ANOVA	Time (pre, 7-d post) *	<0.01	$F_{(1.0, 9.0)} = 57.74$
			Stimulus (click, 4 kHz, 20 kHz)	0.18	$F_{(1.84, 16.58)} = 11.94$
			Interaction (time x stimulus) *	0.03	$F_{(1.43, 12.90)} = 7.24$
Pre[#]	<0.01	Wilcoxon matched-	Click stimulus	<0.01	
7-d post	0.19	pairs signed-rank	Pre vs. 7-d post*		
Pre[#]	0.01	Wilcoxon matched-	4 kHz tone stimulus	<0.01	
7-d post	0.50	pairs signed-rank	Pre vs. 7-d post*		
Pre	0.25	Paired sample,	20 kHz tone stimulus	<0.01	$t = 6.09; DF = 9$
7-d post	0.34	2-tailed t-test	Pre vs. 7-d post*		
Figure 2.6 Wave I amplitude (n=10)					
Pre	0.26	Paired sample,	Wave I amplitude	<0.01	$t = 5.76; DF = 9$
7-d post	0.44	2-tailed t-test	Pre vs. 7-d post*		
Figure 2.7 Initial Sound-Evoked Response					
		2-way RM-ANOVA	Region (auditory cortex, mPFC) *	<0.001	$F_{(1,9)} = 28.38$
			Time (pre, 2-d post, 7-d post) *	0.002	$F_{(2,18)} = 8.84$
			Interaction (region x time) *	<0.001	$F_{(2,18)} = 14.14$
Figure 2.7 A, B. Auditory Cortex N18					
		1-way RM-ANOVA	Time (pre, 2-d, 7-d post) *	0.002	$F_{(1.60,14.41)} = 11.7$
		Post hoc	pre vs. 2-days post*	0.006[B]	$t = 4.05; DF = 9$
		Post hoc	pre vs. 7-days post*	0.02[B]	$t = 3.21; DF = 9$
Figure 2.7 C, D. mPFC P30					
		1-way RM-ANOVA	Time (pre, 2- d,7-d post)	0.13	$F_{(1.44,12.98)} = 2.52$
Figure 2.8 Inter-Trial Coherence					
		2-way RM-ANOVA	Region (auditory cortex, mPFC) *	0.003	$F_{(1,9)} = 15.61$
			Time (pre, 2-d post, 7-d post) *	0.042	$F_{(2,18)} = 3.81$
			Interaction (region x time) *	0.005	$F_{(2,18)} = 7.04$
Figure 2.8 A, B. Auditory Cortex					
		1-way RM-ANOVA	Time (pre, 2-d,7-d post)	0.18	$F_{(1.74, 15.68)} = 1.93$
Figure 2.8 C, D. mPFC					
		1-way RM-ANOVA	Time (pre, 2-d, 7-d post) *	<0.001	$F_{(1.85,16.64)} = 22.63$
		Post hoc	Pre vs. 2-d post *	<0.001[B]	$t = 6.55; DF = 9$
		Post hoc	Pre vs. 7-d post *	0.001[B]	$t = 5.01; DF = 9$
Figure 2.9 Phase-Locking Value					
		1-way RM-ANOVA	Time (pre, 2-d, 7-d post) *	<0.001	$F_{(1.54, 13.85)} = 16.78$
		Post hoc	Pre vs. 2-d post *	0.002[B]	$t = 4.78; DF = 9$
		Post hoc	Pre vs. 7-d post *	0.005[B]	$t = 4.10; DF = 9$
Figure 2.10 Spontaneous Oscillations					
		3-way RM-ANOVA	Region (auditory cortex, mPFC) *	0.001	$F_{(1,9)} = 20.55$
			Time (pre, 2-d, 7-d post)	0.24	$F_{(2,18)} = 1.55$
			Freq. (delta, theta, alpha, gamma) *	<0.001	$F_{(1.82,16.38)} = 241.0$
			Interaction (region x time)	>0.99	$F_{(2,18)} = 0.39$
			Interaction (region x freq.) *	0.001	$F_{(1.91,10.72)} = 17.08$
			Interaction (time x freq.)	0.35	$F_{(6,54)} = 1.14$
			Interaction (region x time x freq.)	0.10	$F_{(6,54)} = 1.86$

Table 2.1 Summary of the statistical tests performed in the electrophysiological experiments
[B]*Bonferroni corrected p-value; * statistical significance; # violated normal distribution as assessed by the Shapiro-Wilk test for normal distribution; Pre: before noise exposure; 2-d post: 2-days post-noise exposure; 7-d post: 7-days post-noise exposure; Freq. – frequency*

2.3.4 Cognitive flexibility appeared unaffected by noise exposure despite initial impairments in the visual-cue discrimination task.

Initial hearing thresholds in sham and noise-exposed rats used in the cognitive-behavioural testing did not differ for the click, 4 kHz or 20 kHz stimulus (**Figure 2.11A**). Moreover, as expected, the sham rats did not show any change in their ABR thresholds or wave I amplitude over time. In contrast, the noise-exposed rats showed a significant elevation in their click (pre-noise: 27.7 ± 0.8 dB SPL vs. post-noise: 39.1 ± 1.8 dB SPL, $p_{Bonf} < 0.001$), 4 kHz (pre-noise: 25.5 ± 0.8 dB SPL vs. post-noise: 42.3 ± 2.0 dB SPL, $p_{Bonf} < 0.001$) and 20 kHz (pre-noise: 20.9 ± 0.9 dB SPL vs. post-noise: 38.2 ± 3.0 dB SPL, $p_{Bonf} = 0.001$) thresholds post-exposure (**Figure 2.11A**), as well as a significant reduction (61%) in wave I amplitude (p< 0.01; **Figure 2.11B**); findings consistent with the hearing loss induced in the cohort of noise-exposed rats used in the electrophysiological experiments in the present study. For more details on statistical results see **table 2.2**.
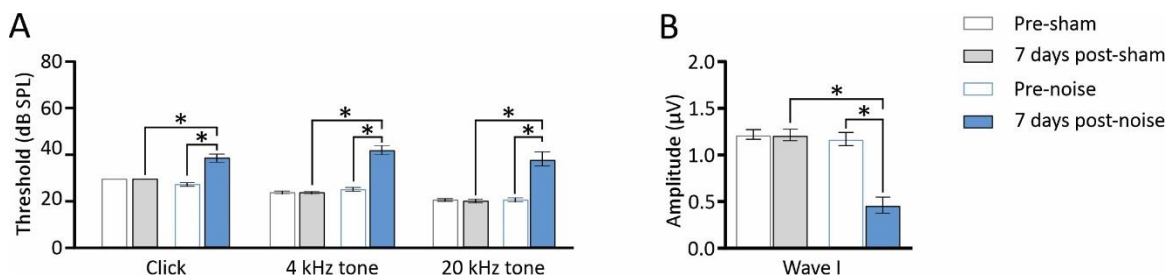
Figure 2.11 Hearing loss following noise exposure in rats used for cognitive-behavioural testing. (A) The auditory brainstem response (ABR) protocol revealed a significant elevation of hearing thresholds for the click, 4 kHz, and 20 kHz stimuli for noise-exposed rats (*p < 0.01), but not for sham exposed rats. (B) Noise-exposed rats also had a significant reduction in wave I amplitude post-noise exposure (*p < 0.01), with no change in wave I amplitude observed following sham exposure. Data represent group mean ± SEM; n = 10 rats

To determine the effect of noise exposure on cognitive flexibility, a series of lever-pressing tasks was performed over consecutive days. As shown in **Figure 2.12**, compared to the shams (n=11), the noise-exposed rats (n=11) committed a greater number of errors during the 100 trials of the visual-cue discrimination task (Welch's t-test, p< 0.001; **Figure 2.12B**). This initial impairment, however, did not carry over to a statistically significant deficit during the 20 trials of the visual-cue retrieval task performed 24 h later (Welch's t-test,

p=0.20; **Figure 2.12C**). When the rule (set) of the visual-cue discrimination task was shifted from "follow the light" to "always press one lever, e.g., left" during the response discrimination task (**Figure 2.12D**), the noise-exposed rats appeared to demonstrate a similar ability as the shams to perform the set-shift, having committed an equivalent number of errors over 120 trials (Welch's t-test, p=0.92; **Figure 2.12E**). Twenty-four hours later, the noise-exposed rats seemed to adequately recall the rule of the previous task, as they committed a similar number of errors as the sham rats during the 20 trials of response discrimination retrieval task (Mann-Whitney U test, U = 41.0, p= 0.21; **Figure 2.12F**). Finally, during the reversed-response discrimination task (**Figure 2.12G**), no difference was found in the number of errors committed by noise-exposed rats compared to the shams (Welch's t-test, p = 0.84; **Figure 2.12H**), which suggests that noise exposure did not impair reversal learning. The detailed statistical results are presented in **Table 2.2**.
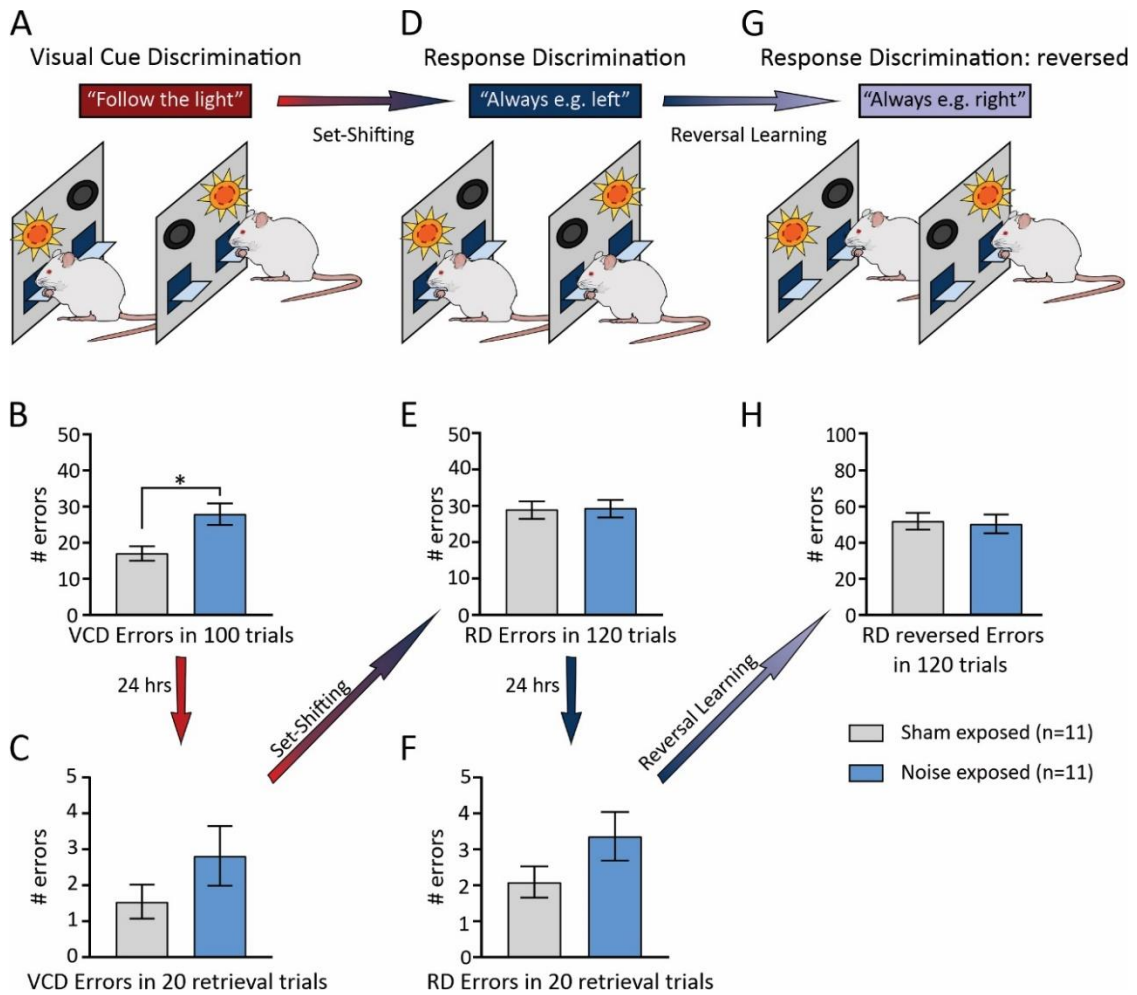
Figure 2.12 Noise exposure impaired visual-cue discrimination but did not affect cognitive flexibility as measured by set-shifting and reversal learning. (A) *During the visual-cue discrimination (VCD) task, rats learned to press the lever located beneath the pseudo-randomly illuminated cue light.* ***(B)*** *Compared to the sham (grey), the noise-exposed rats (blue) committed significantly more errors during the acquisition of the visual-cue rule; findings consistent with impaired stimulus-response habit learning.* ***(C)*** *The noise-exposed rats also trended toward a greater number of errors during the VCD retrieval task performed 24 hrs later; however, these data did not reach statistical significance.* ***(D)*** *Immediately following the VCD retrieval trials, the task shifted to a response discrimination (RD), in which the rats had to learn that the side opposite to their side-bias (e.g., left) was now the correct response regardless of the cue light.* ***(E)*** *Noise exposure did not appear to affect the rat's ability to set-shift, as the shams and noise-exposed rats committed a similar number of errors during the RD task***.** ***(F)*** *Similar to the VCD retrieval trials, there was a trend for the noise-exposed rats to perform more errors than the shams during the retrieval trials performed 24 hrs after the RD task, yet the results were not statistically significant.* ***(G)*** *Immediately following the RD retrieval trials, the rules of the task were reversed such that the rats had to learn to press the opposite lever (e.g., right).* ***(H)*** *During the reversed-RD task, the noise-exposed rats committed a similar number of errors as the shams; findings which suggest that the rats' reversal learning was not impaired following noise exposure. Data represent group mean ± SEM; n= 11 rats; *p < 0.05*

2.3.5 Noise exposure impaired spatial learning and reference memory in the Morris water maze

Three weeks after the lever-pressing tasks were completed, spatial learning and reference memory were assessed using protocols associated with the Morris water maze. As shown in **Figure 2.13B,** the noise-exposed rats took significantly longer time to find the hidden platform during the first learning trial (Mann-Whitney U test, U=30.0, p< 0.05). Furthermore, the noise-exposed rats demonstrated learning deficits as evidenced by the significantly increased time to the platform during the third learning trial ($p_{Bonf} < 0.05$, **Figure 2.13C**) as well as by a longer cumulative time to the platform during learning trials 2 − 6 (Welch's t-test, p< 0.05; **Figure 2.13D**), despite similar swimming speeds (**Figure 2.13E**). Furthermore, the noise-exposed rats showed a deficit in spatial reference memory as seen in the longer time to the first entry to the platform zone during the probe test which occurred 24 h after the initial learning trials (Mann-Whitney U test, U=20.5, p< 0.01; **Figure 2.13G**), without differences in swimming speed (**Figure 2.13J**). Although their memory of the precise location of the platform was impaired, over the 90-s duration of the probe test, the noise-exposed rats spent an equivalent amount of time as the shams in the quadrant where the hidden platform had been located (**Figure 2.13H**) and in the perimeter of the pool (**Figure 2.13I**), all while swimming at similar speeds (**Figure 2.13J**). Finally, when cued to the platform location with a visual marker, the noise-exposed rats reached the platform in times that were consistent with the shams (**Figure 2.13L-N**), thereby confirming that the impaired performance of noise-exposed rats during the hidden platform and probe trials was not due to a deficit in visual acuity. See **table 2.2**. for more detailed statistical results.
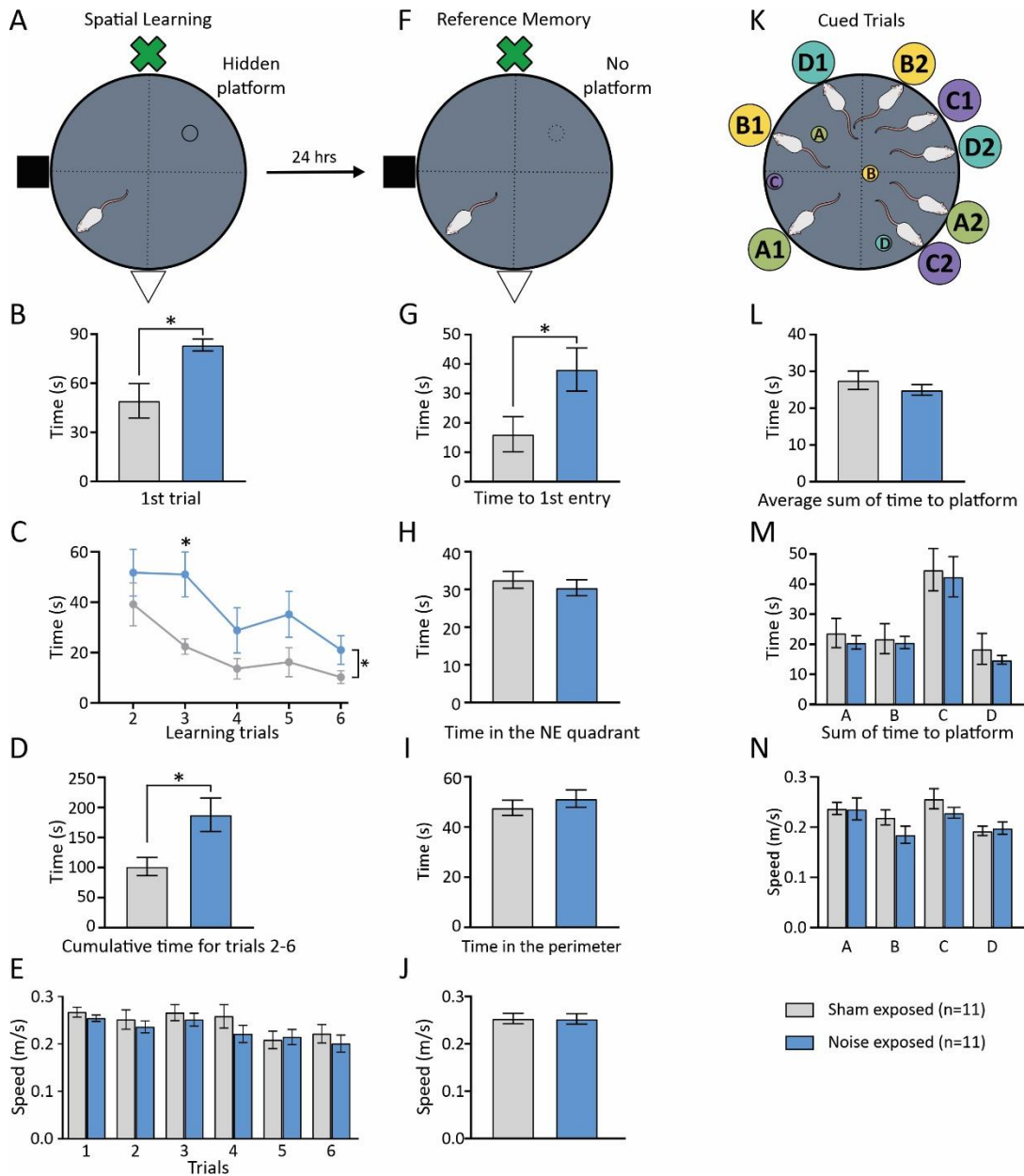
Figure 2.13 Impaired spatial learning and reference memory following noise exposure. (A) *During the first day of testing in the Morris water maze, the rats performed 6 trials which required them to swim to the hidden platform by relying on visual cues on the lab walls. **(B** and **C)** The noise-exposed rats took longer than the shams to locate the hidden platform on the first trial and took longer to complete the third learning trial. **(D** and **E)** The noise-exposed rats had a longer cumulative time to reach the platform during learning trials 2-6 than the shams, but this was not due to differences in swim speeds. **(F)** Twenty-four hours after the learning trials, the rats performed the 90-s probe test, in which the hidden platform was removed. **(G)** Compared to the shams, the noise-exposed rats had a delayed time to their first entry to the platform zone, indicative of a deficit in spatial reference memory. **(H-J)** The noise-exposed rats and shams showed consistent performance on the time spent in the platform quadrant and perimeter of the pool, and*

*they swam at similar speeds during the 90-s probe test. **(K)** In the final series, the external cues on the walls were removed, and the rats were placed at varying start locations (A1,2; B1,2; C1,2; D1,2) so they could swim to a novel platform location marked with a visual-cue flag (A-D). **(L)** For each cued platform location (e.g. A), the sum of the time it took for the rats to reach the platform from the two start locations (A1 + A2) was calculated, and then averaged for the four platform locations. **(M** and **N)** Overall, the time to platform was not different between the noise-exposed rats and shams during the visually cued trials, and they swam similar speeds. Data represent group mean ± SEM; n= 11 rats; *p_{Bonf} < 0.05*

Data	Normality p-value	Test	Main effects/ Comparisons	p-value	F-value/ t-vale
Figure 2.11 Hearing assessment: Cognitive-behavioural group					
Figure 2.11 A. Click stimulus ABR threshold					
		3-way ANOVA	Stimulus (click, 4 kHz, 20 kHz) *	<0.001	$F_{(2,40)} = 66.35$
			Exposure (noise, sham) *	<0.001	$F_{(1,20)} = 47.23$
			Time (pre, 7-d post) *	<0.001	$F_{(1,20)} = 52.47$
			Interaction (stimulus x exposure) *	<0.001	$F_{(2,40)} = 17.92$
			Interaction (stimulus x time)	0.1	$F_{(2,40)} = 2.44$
			Interaction (exposure x time) *	<0.001	$F_{(1,20)} = 54.61$
			Interaction (stim. x exp. x time) *	<0.001	$F_{(2,40)} = 2.91$
		Post hoc	Click pre-sham vs. post-sham	>0.999[B]	t = 0.0 DF = 60
		Post hoc	4 kHz pre-sham vs. post-sham	>0.999 [B]	t = 0.0 DF = 60
		Post hoc	20 kHz pre-Sham vs. post-sham	>0.999 [B]	t = 0.24 DF = 60
		Post hoc	Click pre-noise vs. post-noise *	<0.001 [B]	t = 6.07; DF = 60
		Post hoc	4 kHz pre-noise vs. post-noise *	<0.001 [B]	t = 8.99; DF = 60
		Post hoc	20 kHz pre-noise vs. post-noise *	<0.001 [B]	t = 9.23; DF = 60
		Post hoc	Click pre-sham vs. pre-noise	>0.999 [B]	t = 1.24; DF = 120
		Post hoc	4 kHz pre-sham vs. pre-noise	>0.999 [B]	t = 0.75; DF = 120
		Post hoc	20 kHz pre-sham vs. pre-noise	>0.999 [B]	t = 0; DF = 120
		Post hoc	Click post-sham vs. post-noise *	<0.001 [B]	t = 4.98; DF = 120
		Post hoc	4 kHz post-sham vs. post-noise *	<0.001 [B]	t = 9.96; DF = 120
		Post hoc	20 kHz post-sham vs. post-noise *	<0.001 [B]	t = 9.71; DF = 120
Figure 2.11 B. Wave I Amplitude					
		2-way MANOVA	Time (pre, 7-d post) *	<0.001	$F_{(1,20)} = 75.10$
			Exposure (noise, sham) *	<0.001	$F_{(1,20)} = 20.38$
			Interaction (time x exposure) *	<0.001	$F_{(1,20)} = 72.82$
Pre-sham	0.55	Welch's t-test two-tailed	Sham exposure pre vs. 7-d post	0.947	t = 0.07; DF = 20
Post-sham	0.86				
Pre-noise#	0.02	Mann Whitney; two- tailed	Noise exposure pre vs. 7-d post *	<0.001	
Post-noise	0.42				
Figure 2.12 Lever-pressing tasks					
Figure 2.12 B. Visual-Cue Discrimination (learning)					
Sham	0.79	Welch's t-test two-tailed	Visual Cue Discrimination sham exposed vs. noise exposed *	<0.01	t = 3.04; DF = 17.51
Noise	0.10				
Figure 2.12 C. Visual-Cue Discrimination retrieval					
Sham	0.051	Welch's t-test two-tailed	VCD retrieval sham exposed vs. noise exposed	0.20	t = 1.33; DF = 15.91
Noise	0.065				
Figure 2.12 E. Response Discrimination					
Sham	0.806	Welch's t-test two-tailed	Response Discrimination sham exposed vs. noise exposed	0.92	t = 1.11; DF = 20
Noise	0.918				
Figure 2.12 F. Response Discrimination retrieval					
Sham	0.333	Mann Whitney; two- tailed	RD retrieval sham exposed vs. noise exposed	0.21	
Noise#	0.01				
Figure 2.12 H. Reversed Response Discrimination					

Sham	0.077	Welch's t-test	Reversed RD	0.84	t = 0.21; DF =19.71
Noise	0.488	two-tailed	sham exposed vs. noise exposed		

Figure 2.13 Morris water maze					
Figure 2.13 B. Time to 1st trial					
Sham[#]	0.027	Mann Whitney;	Time to platform (1st trial)	0.03	
Noise[#]	<0.001	two- tailed	Sham exposed vs. Noise exposed *		
Figure 2.13 C. Time to platform trials 2-6					
			Trials (2-6) *	<0.01	$F_{(2.5,50.86)}$ = 7.79
		2-way MANOVA	Exposure (sham, noise) *	0.01	$F_{(1,20)}$ = 7.44
			Interaction (trials, exposure)	0.62	$F_{(4,80)}$ = 0.67
		Post hoc	Trial 2: sham vs noise	>0.99[B]	t = 1.0; DF = 19.86
		Post hoc	Trial 3: sham vs noise *	0.049[B]	t = 3.0; DF = 12.35
		Post hoc	Trial 4: sham vs noise	0.72[B]	t = 1.54; DF=13.88
		Post hoc	Trial 5: sham vs noise	0.48[B]	t = 1.76; DF=16.91
		Post hoc	Trial 6: sham vs noise	0.53[B]	t = 1.73; DF=13.92
Figure 2.13 D. Cumulative time to platform (sum of trials 2-6)					
Sham	0.141	Welch's t-test	Cumulative time to platform (2-6)	0.01	t = 2.73; DF = 15.41
Noise	0.084	two-tailed	Sham vs. noise *		
Figure 2.13 E. Average swimming speed (first day)					
			Trial (1-6) *	<0.01	$F_{(3.7,74.07)}$ = 7.58
		2-way MANOVA	Exposure (sham, noise)	0.42	$F_{(1,20)}$ = 0.69
			Interaction (trial x exposure)	0.58	$F_{(5,100)}$ = 0.76
Figure 2.13 G. Time to first entry to the platform zone (probe trial)					
Sham[#]	<0.001	Mann Whitney;	Time to platform (1st. entry)	<0.01	
Noise	0.294	two-tailed	sham vs. noise *		
Figure 2.13 H. Time spent in the North-East quadrant					
Sham	0.462	Welch's t-test	Time spent in NE quadrant probe	0.51	t = 0.67; DF= 19.93
Noise	0.257	two-tailed	sham vs. noise		
Figure 2.13 I. Time spent in the perimeter (probe trial)					
Sham	0.467	Welch's t-test	Time spent in perimeter probe	0.44	t = 0.79; DF= 19.63
Noise	0.705	two-tailed	sham vs. noise		
Figure 2.13 J. Average swimming speed (probe trial)					
Sham	0.832	Welch's t-test	Average speed during probe	0.95	t = 0.06; DF = 19.98
Noise	0.506	two-tailed	sham vs. noise		
Figure 2.13 L. Average time to platform (cued trials)					
Sham	0.556	Welch's t-test	Average time to platform (cued)	0.38	t = 0.06; DF = 19.98
Noise	0.121	two-tailed	sham vs. noise		
Figure 2.13 M. Time to platform (cued trials)					
			Platform location (A-D) *	<0.01	$F_{(3,30)}$ = 13.21
		2-way MANOVA	Exposure (sham, noise)	0.48	$F_{(1,10)}$ = 0.54
			Interaction (location x exposure)	>0.99	$F_{(3,30)}$ = 0.021
Figure 2.11 N. Average speed (cued trials)					
			Platform Location (A-D) *	<0.01	$F_{(3,30)}$ = 6.72
		2-way MANOVA	Exposure (Sham, Noise)	0.24	$F_{(1,10)}$ = 1.52
			Interaction (Location x Exposure)	0.35	$F_{(3,30)}$ = 1.23

Table 2.2 Summary of the statistical tests performed in the behavioural experiments [B] *Bonferroni corrected p-value; * statistical significance; # violated normal distribution as assessed by the Shapiro-Wilk test for normal distribution; Pre-noise: before noise exposure; Post-noise: 7 days post-noise exposure; Pre-sham: pre-sham exposure; Post-sham: 7 days post-sham exposure*

2.3.6 The degree of hearing loss did not correlate with neural plasticity or cognitive-behavioural performance following noise exposure.

Pearson's correlation analyses were performed to determine whether the degree of hearing loss following noise exposure was correlated with metrics obtained from the electrophysiological or cognitive behavioural analyses (**Table 2.3**). No significant correlations were observed between the click stimulus ABR threshold shift and any of the electrophysiological measures, which included the event-related potential (ERP) and inter-trial coherence (ITC) recorded from the auditory cortex or mPFC, and the phase-locking value (PLV), at either the 2 day or 7 day time point post-noise exposure. Similarly, no significant correlations were observed between the click stimulus ABR threshold shift and any of the cognitive behavioural metrics obtained from the lever-pressing and Morris water maze tasks.

MEASURE	R^2- VALUE	P-VALUE
EVENT RELATED POTENTIAL		
Auditory cortex ERP (percent change) 2 days	0.009	0.791
Auditory cortex ERP (percent change) 7 days	0.001	0.945
mPFC ERP (percent change) 2 days	0.026	0.655
mPFC ERP (percent change) 7 days	0.063	0.483
AUDITORY STEADY-STATE RESPONSE		
Auditory cortex ITC, 2 days post	0.020	0.694
Auditory cortex ITC, 7 days post	0.080	0.423
mPFC ITC, 2 days post	0.002	0.895
mPFC ITC, 7 days post	0.040	0.556
Phase-locking value 2 days	0.167	0.241
Phase-locking value 7 days	0.020	0.715
LEVER PRESSING COGNITIVE TASKS		
Visual cue discrimination errors	0.010	0.732
Visual cue discrimination retrieval errors	0.120	0.300
Response discrimination errors	0.130	0.281
Response discrimination retrieval errors	0.280	0.090
Response discrimination reversal learning errors	0.030	0.607
MORRIS WATER MAZE		
Cumulative time to platform on learning trials	0.050	0.493
Time to platform on probe trial	0.060	0.455

Table 2.3 *Pearson's R^2 and corresponding p values for correlations of ABR click stimulus threshold shifts to ERP, ASSR, and cognitive task metrics. No significant correlations were found between the degree of hearing loss and any of the electrophysiological or behvaioural metrics*

2.4 Discussion

The present study included a novel series of electrophysiological and behavioural experiments on adult rats to determine (1) if noise-induced plasticity that occurs in the auditory cortex also manifests at the level of the mPFC; a higher-order brain region that processes auditory information and subserves executive function, and (2) whether the cognitive impairments caused by noise exposure extend beyond hippocampal-dependent spatial learning/memory tasks to include deficits in executive function.

2.4.1 Differential Plasticity Within and Beyond the Auditory Pathway

As expected, the chosen noise exposure caused a permanent shift in hearing thresholds, as well as an enhancement of sound-evoked activity in the auditory pathway. Indeed, despite a significant reduction in the afferent drive from the cochlea evidenced by a significantly reduced wave I amplitude of the ABR, the amplitude of the sound-evoked ERP recorded from the auditory cortex was significantly increased (41%) in the week following noise exposure. These results were not surprising given that central gain enhancement in the auditory cortex has been reported in numerous electrophysiological studies on animals with hearing loss (Popelář, Syka and Berndt, 1987; Syka, Rybalko and Popelář, 1994; Syka and Rybalko, 2000; Popelar *et al.*, 2008; Sun *et al.*, 2008; Schormans, Typlt and Allman, 2019). It was, however, a novel observation that the mPFC did not show significantly enhanced responses to acoustic stimulation in the week following the noise exposure. Although it has been shown that this higher-order brain region receives projections from the hyperresponsive auditory cortex, these connections were rather sparse (Eden, Lamme and Uylings, 1992).

Previous studies have investigated the effect of noise exposure on sound-evoked activity outside of the auditory pathway, including the amygdala and the multisensory cortex. Although compensation was observed in the rat lateral amygdala post-noise exposure (as measured by the relative changes of the amygdalar response compared to the cochlear output), the absolute amplitude of the sound-evoked responses to high-intensity stimuli

was reduced (Radziwon *et al.*, 2019). Moreover, our earlier work (Schormans, Typlt and Allman, 2017, 2019) showed that noise exposure caused sound-evoked responses to suprathreshold stimuli to be significantly reduced in the rat audiovisual cortex; a brain region responsible for integrating multisensory information via its extensive reciprocal connections with the auditory and visual cortices (Laramée and Boire, 2015). To date, a variety of mechanisms have been suggested to underlie central gain enhancement within the auditory pathway, including homeostatic plasticity and an imbalance in excitatory and inhibitory neurotransmission (Noreña, 2011; Auerbach, Rodrigues and Salvi, 2014; Salvi *et al.*, 2017). At this time, it is unclear if such cellular/molecular changes are largely absent in brain regions outside of the auditory pathway (e.g., mPFC; amygdala; audiovisual cortex), or whether competing mechanisms are instead responsible for actively dampening the hyper-excitability to acoustic stimulation.

In addition to regional differences in the extent of central gain enhancement, we also observed differential plasticity in the auditory versus prefrontal cortices using metrics of sensory-evoked oscillations gleaned from the 40-Hz ASSR. For example, inter-trial coherence (ITC), which assesses the ability of a given brain region to synchronize to the repetitive acoustic stimulus over multiple trials, was significantly reduced in the mPFC, despite no change in the auditory cortex. Furthermore, by comparing the synchrony of the LFPs in the auditory cortex and mPFC using the phase-locking value, we found a noise-induced reduction in the extent that the phase of the entrained response could be maintained between the two brain regions over multiple trials; findings which suggest that the noise exposure disrupted the functional connectivity between the auditory and prefrontal cortices. In contrast, a recent neuroimaging study on humans with long-term hearing loss reported a higher coupling between auditory areas and the dorsolateral prefrontal cortex (Luan *et al.*, 2019), the putative homologue to the rodent mPFC. Perhaps these disparate results are due to the difference in the duration of hearing loss between the two studies (i.e., long-term hearing loss vs. acute noise-induced hearing loss), or methodological differences, as the neuroimaging study assessed functional connectivity

during resting-state conditions, as opposed to when sounds were passively delivered to the subjects, like in the present study.

It is important to note that although the 40-Hz ASSR has been used in humans and preclinical models to probe for altered auditory processing associated with tinnitus (Schlee *et al.*, 2008; Hayes *et al.*, 2020) as well as neuropsychiatric conditions (e.g., schizophrenia (Spencer *et al.*, 2008, 2009; Vohs *et al.*, 2010, 2012; Spencer, 2012; Shahriari *et al.*, 2016)) and dementia (e.g., Alzheimer's disease (Ribary *et al.*, 1991; van Deursen *et al.*, 2011)), to our knowledge, the present study represents a novel approach of using the 40-Hz ASSR to assess disruption of the functional connectivity between the auditory and prefrontal cortices following noise exposure. Currently, the mechanism(s) responsible for the decrease in ITC in the mPFC post-noise exposure, as well as the reduced phase-locking value between the auditory cortex and mPFC remain elusive. That said, it is reasonable to speculate that noise-induced changes in glutamate signalling may contribute to the impaired 40-Hz ASSR, as antagonism of the N-methyl-D-aspartate receptor (NMDAR), an ionotropic glutamate receptor involved in synaptic plasticity, augments the ITC in normal-hearing rats (Sivarao *et al.*, 2013; Sullivan *et al.*, 2015), and noise exposure is known to reduce the expression of the NMDAR subunit, NR2B, in another non-auditory brain region, the hippocampus (Cui, Wu and She, 2009). Alternatively, given that noise exposure can cause pathology in the prefrontal cortex reminiscent of Alzheimer's disease (e.g., hyper-phosphorylation of the microtubule-associated protein, tau, as well as the formation of pathological neurofibrillary tangles) (Cui *et al.*, 2012), it is also possible that such pathology contributed to the loss of functional connectivity between the prefrontal and auditory cortices observed in the present study. More work is needed to investigate this possibility, however, as previous clinical studies have shown conflicting results of either a decrease (Ribary *et al.*, 1991) or an increase (van Deursen *et al.*, 2011) of the 40-Hz ASSR in patients with Alzheimer's disease versus healthy elderly subjects.

Given the contribution of the thalamus to spontaneous oscillations at the level of the cortex (Llinás *et al.*, 2005), one could predict that subcortical plasticity in the auditory pathway post-noise exposure would manifest as altered spontaneous, rhythmic activity in the cortex. However, there was no effect of noise-induced hearing loss on the spontaneous oscillations recorded from either the auditory or prefrontal cortices in the days following noise exposure, despite differential effects observed in sound-evoked responses (i.e., ERPs; ITC). In support of the present findings, a recent study from our lab also found no effect of noise-induced hearing loss on spontaneous oscillations; in this case, when the recordings were made immediately following the noise exposure, at a time corresponding to the presence of tinnitus (Hayes *et al.*, 2020). Taken together, these results emphasize that the differential nature of noise-induced plasticity is not restricted to the effects between brain regions that process auditory input, but also that within a given region, aspects of its neuronal activity (spontaneous vs. evoked) can be distinctly affected by noise-induced hearing loss.

2.4.2 Susceptibility of Learning, Memory and Executive Function to Noise-Induced Deficits

As expected, Morris water maze test revealed a significant impairment in hippocampal-dependent spatial learning and reference memory in the noise-exposed versus sham rats, consistent with previous reports on noise-exposed rodents (Cui, Wu and She, 2009; Cheng *et al.*, 2011; Liu *et al.*, 2016, 2018). These cognitive impairments manifested in a delay to learn the location of the hidden platform, as well as a deficit in recalling its location 24 h later. Various noise-induced changes within the hippocampus could contribute to the deficits in spatial learning and reference memory, including suppression of neurogenesis (Kraus *et al.*, 2010), abnormal place cell activity (Goble, Møller and Thompson, 2009), altered glutamate signalling (Cui, Wu and She, 2009), neuroinflammation (Cui *et al.*, 2015), as well as tau hyper-phosphorylation and neurofibrillary tangles (Cui *et al.*, 2012). At present, however, it remains intriguing why the hippocampus appears to be particularly vulnerable to noise exposure.

Motivated by the reports of meta-analyses indicating a relationship between hearing loss and deficits in executive function (Taljaard *et al.*, 2015), the current study carried out a novel investigation of the effect of noise exposure on cognitive flexibility, an executive function which requires subjects to abandon a previously learned behavioural strategy once it is no longer correct and adopt a newly rewarding strategy. The presented study, investigated cognitive flexibility using lever-pressing tasks of set-shifting and reversal learning that have proven effective for screening rat models associated with schizophrenia (Desai, Allman and Rajakumar, 2017, 2018) and dementia (Levit *et al.*, 2017, 2019). Overall, there was no apparent deficits in either set-shifting or reversal learning as assessed by the errors committed during the response discrimination task or reversed-response discrimination task, respectively. However, find that the noise-exposed rats showed a significant impairment in the visual-cue discrimination task; the prerequisite step preformed 24 h prior to set-shifting (**see Figure 2.12**). As the visual-cue discrimination task is considered an example of stimulus-response habit learning, the impaired performance may have occurred due to noise-induced changes in the striatum, as this brain region, as opposed to the mPFC and hippocampus, has been heavily implicated in stimulus-response habit learning (McDonald *et al.*, 2007; Floresco, Block and Tse, 2008; Delotterie *et al.*, 2015). To date, previous studies that investigated the effect of noise exposure on the striatum have focused on changes in the neurotransmitter systems that are believed to be associated with the acute/chronic stress of the exposure itself, rather than plasticity induced by the resultant hearing loss. Collectively, these studies have shown that noise exposure increases striatal levels of glutamate and dopamine, as well as serotonergic turnover, while at the same time, reducing GABA and acetylcholine levels (Sembulingam, Sembulingam and Namasivayam, 1996; Samson *et al.*, 2006; Kazi and Oommen, 2014); findings which could result in an imbalance of excitatory/inhibitory neurotransmission in the striatum, along with disruptions to neuromodulation associated with the altered monoamine levels. Given that the aforementioned neurotransmitters have been implicated in various striatal-dependent learning tasks (Lovinger, 2010), it is

difficult to speculate which particular mechanism(s) may contribute to the impaired stimulus-response habit learning observed in the present study.

In light of the disparate results we observed between the visual-cue discrimination task and subsequent response discrimination tasks, it is worth noting that one of the inherent challenges of assessing cognitive flexibility is the potential confound of impaired learning of the initial rule (e.g., choose the lever under the cue light), as this would be expected to influence the ease at which subjects are then able to abandon this rule and shift to a new strategy (e.g., always choose the left lever, regardless of the light). Indeed, because the noise-exposed rats showed difficulty in learning the initial rule **(Figure 2.12B)** as well as a tendency to not remember it as well **(Figure 2.12C)**, perhaps this contributed to their apparent ability to abandon this rule and demonstrate equivalent set-shifting ability as the sham rats **(Figure 2.12E)**. Similar issues with interpreting set-shifting results have been reported following pharmacological manipulations that disrupted initial-rule learning (Floresco, Zhang and Enomoto, 2009). That said, in the present study, it is still reasonable to conclude that noise exposure did not impair reversal learning, as the noise-exposed and sham rats demonstrated equivalent abilities to both learn the response discrimination rule **(Figure 2.12E),** and then perform the reversed-response discrimination task **(Figure 2.12H).** Given that reversal learning is dependent on the orbitofrontal cortex (McAlonan and Brown, 2003; Ghods-Sharifi, Haluk and Floresco, 2008; Floresco, Zhang and Enomoto, 2009), it appears that this brain region is spared from noise-induced disruption.

2.5 References

Auerbach, B. D., Rodrigues, P. V. and Salvi, R. J. (2014) 'Central Gain Control in Tinnitus and Hyperacusis', *Frontiers in Neurology*, 5. doi: 10.3389/fneur.2014.00206.

Basner, M. *et al.* (2014) 'Auditory and non-auditory effects of noise on health', *The Lancet*, 383(9925), pp. 1325–1332. doi: 10.1016/S0140-6736(13)61613-X.

Brenner, C. A. *et al.* (2009) 'Steady State Responses: Electrophysiological Assessment of Sensory Function in Schizophrenia', *Schizophrenia Bulletin*, 35(6), pp. 1065–1077. doi: 10.1093/schbul/sbp091.

Carroll, Y. I. *et al.* (2017) 'Vital Signs: Noise-Induced Hearing Loss Among Adults — United States 2011–2012', *MMWR. Morbidity and Mortality Weekly Report*, 66(5), pp. 139–144. doi: 10.15585/mmwr.mm6605e3.

Cheng, L. *et al.* (2011) 'Moderate noise induced cognition impairment of mice and its underlying mechanisms', *Physiology & Behavior*, 104(5), pp. 981–988. doi: 10.1016/j.physbeh.2011.06.018.

Cui, B. *et al.* (2012) 'Chronic noise exposure causes persistence of tau hyperphosphorylation and formation of NFT tau in the rat hippocampus and prefrontal cortex', *Experimental Neurology*, 238(2), pp. 122–129. doi: 10.1016/j.expneurol.2012.08.028.

Cui, B. *et al.* (2015) 'Chronic Noise Exposure Acts Cumulatively to Exacerbate Alzheimer's Disease-Like Amyloid-β Pathology and Neuroinflammation in the Rat Hippocampus', *Scientific Reports*, 5(1), p. 12943. doi: 10.1038/srep12943.

Cui, B., Wu, M. and She, X. (2009) 'Effects of Chronic Noise Exposure on Spatial Learning and Memory of Rats in Relation to Neurotransmitters and NMDAR2B Alteration in the Hippocampus', *Journal of Occupational Health*, advpub, pp. 0902160059–0902160059. doi: 10.1539/joh.L8084.

Desai, S. J., Allman, B. L. and Rajakumar, N. (2017) 'Combination of behaviorally sub-effective doses of glutamate NMDA and dopamine D1 receptor antagonists impairs executive function', *Behavioural Brain Research*, 323, pp. 24–31. doi: 10.1016/j.bbr.2017.01.030.

Desai, S. J., Allman, B. L. and Rajakumar, N. (2018) 'Infusions of Nerve Growth Factor Into the Developing Frontal Cortex Leads to Deficits in Behavioral Flexibility and Increased Perseverance', *Schizophrenia Bulletin*, 44(5), pp. 1081–1090. doi: 10.1093/schbul/sbx159.

van Deursen, J. A. *et al.* (2011) '40-Hz steady state response in Alzheimer's disease and mild cognitive impairment', *Neurobiology of Aging*, 32(1), pp. 24–30. doi: 10.1016/j.neurobiolaging.2009.01.002.

Eden, C. G. van, Lamme, V. a. F. and Uylings, H. B. M. (1992) 'Heterotopic Cortical Afferents to the Medial Prefrontal Cortex in the Rat. A Combined Retrograde and Anterograde Tracer Study', *European Journal of Neuroscience*, 4(1), pp. 77–97. doi: https://doi.org/10.1111/j.1460-9568.1992.tb00111.x.

Floresco, S. B., Block, A. E. and Tse, M. T. L. (2008) 'Inactivation of the medial prefrontal cortex of the rat impairs strategy set-shifting, but not reversal learning, using a novel, automated procedure', *Behavioural Brain Research*, 190(1), pp. 85–96. doi: 10.1016/j.bbr.2008.02.008.

Floresco, S. B., Zhang, Y. and Enomoto, T. (2009) 'Neural circuits subserving behavioral flexibility and their relevance to schizophrenia', *Behavioural Brain Research*, 204(2), pp. 396–409. doi: 10.1016/j.bbr.2008.12.001.

Ghods-Sharifi, S., Haluk, D. M. and Floresco, S. B. (2008) 'Differential effects of inactivation of the orbitofrontal cortex on strategy set-shifting and reversal learning', *Neurobiology of Learning and Memory*, 89(4), pp. 567–573. doi: 10.1016/j.nlm.2007.10.007.

Goble, T. J., Møller, A. R. and Thompson, L. T. (2009) 'Acute high-intensity sound exposure alters responses of place cells in hippocampus', *Hearing Research*, 253(1), pp. 52–59. doi: 10.1016/j.heares.2009.03.002.

Gu, J. W. *et al.* (2010) 'Tinnitus, Diminished Sound-Level Tolerance, and Elevated Auditory Activity in Humans With Clinically Normal Hearing Sensitivity', *Journal of Neurophysiology*, 104(6), pp. 3361–3370. doi: 10.1152/jn.00226.2010.

Han, J. J. *et al.* (2018) 'Increased parietal circuit-breaker activity in delta frequency band and abnormal delta/theta band connectivity in salience network in hyperacusis subjects', *PLOS ONE*, 13(1), p. e0191858. doi: 10.1371/journal.pone.0191858.

Hayes, S. H. *et al.* (2020) 'Uncovering the contribution of enhanced central gain and altered cortical oscillations to tinnitus generation', *Progress in Neurobiology*, p. 101893. doi: 10.1016/j.pneurobio.2020.101893.

Kazi, A. I. and Oommen, A. (2014) 'Chronic noise stress-induced alterations of glutamate and gamma-aminobutyric acid and their metabolism in the rat brain', *Noise and Health*, 16(73), p. 343. doi: 10.4103/1463-1741.144394.

Kraus, K. S. *et al.* (2010) 'Noise trauma impairs neurogenesis in the rat hippocampus', *Neuroscience*, 167(4), pp. 1216–1226. doi: 10.1016/j.neuroscience.2010.02.071.

Kujawa, S. G. and Liberman, M. C. (2009) 'Adding Insult to Injury: Cochlear Nerve Degeneration after "Temporary" Noise-Induced Hearing Loss', *Journal of Neuroscience*, 29(45), pp. 14077–14085. doi: 10.1523/JNEUROSCI.2845-09.2009.

Lachaux, J.-P. *et al.* (1999) 'Measuring phase synchrony in brain signals', *Human Brain Mapping*, 8(4), pp. 194–208. doi: https://doi.org/10.1002/(SICI)1097-0193(1999)8:4<194::AID-HBM4>3.0.CO;2-C.

Laramée, M.-E. and Boire, D. (2015) 'Visual cortical areas of the mouse: comparison of parcellation and network structure with primates', *Frontiers in Neural Circuits*, 8. doi: 10.3389/fncir.2014.00149.

Laubach, M. *et al.* (2018) 'What, If Anything, Is Rodent Prefrontal Cortex?', *eNeuro*, 5(5). doi: 10.1523/ENEURO.0315-18.2018.

Leaver, A. M. *et al.* (2011) 'Dysregulation of Limbic and Auditory Networks in Tinnitus', *Neuron*, 69(1), pp. 33–43. doi: 10.1016/j.neuron.2010.12.002.

Levit, A. *et al.* (2017) 'Behavioural inflexibility in a comorbid rat model of striatal ischemic injury and mutant hAPP overexpression', *Behavioural Brain Research*, 333, pp. 267–275. doi: 10.1016/j.bbr.2017.07.006.

Levit, A. *et al.* (2019) 'Impaired behavioural flexibility related to white matter microgliosis in the TgAPP21 rat model of Alzheimer disease', *Brain, Behavior, and Immunity*, 80, pp. 25–34. doi: 10.1016/j.bbi.2019.02.013.

Liu, L. *et al.* (2016) 'Noise induced hearing loss impairs spatial learning/memory and hippocampal neurogenesis in mice', *Scientific Reports*, 6(1), p. 20374. doi: 10.1038/srep20374.

Liu, L. *et al.* (2018) 'Hippocampal Mechanisms Underlying Impairment in Spatial Learning Long After Establishment of Noise-Induced Hearing Loss in CBA Mice', *Frontiers in Systems Neuroscience*, 12. doi: 10.3389/fnsys.2018.00035.

Llinás, R. *et al.* (2005) 'Rhythmic and dysrhythmic thalamocortical dynamics: GABA systems and the edge effect', *Trends in Neurosciences*, 28(6), pp. 325–333. doi: 10.1016/j.tins.2005.04.006.

Lovinger, D. M. (2010) 'Neurotransmitter roles in synaptic modulation, plasticity and learning in the dorsal striatum', *Neuropharmacology*, 58(7), pp. 951–961. doi: 10.1016/j.neuropharm.2010.01.008.

Luan, Y. *et al.* (2019) 'Prefrontal-Temporal Pathway Mediates the Cross-Modal and Cognitive Reorganization in Sensorineural Hearing Loss With or Without Tinnitus: A Multimodal MRI Study', *Frontiers in Neuroscience*, 13. doi: 10.3389/fnins.2019.00222.

McAlonan, K. and Brown, V. J. (2003) 'Orbital prefrontal cortex mediates reversal learning and not attentional set shifting in the rat', *Behavioural Brain Research*, 146(1), pp. 97–103. doi: 10.1016/j.bbr.2003.09.019.

Möhrle, D. *et al.* (2019) 'Enhanced Central Neural Gain Compensates Acoustic Trauma-induced Cochlear Impairment, but Unlikely Correlates with Tinnitus and

Hyperacusis', *Neuroscience*, 407, pp. 146–169. doi: 10.1016/j.neuroscience.2018.12.038.

Mormann, F. *et al.* (2000) 'Mean phase coherence as a measure for phase synchronization and its application to the EEG of epilepsy patients', *Physica D: Nonlinear Phenomena*, 144(3), pp. 358–369. doi: 10.1016/S0167-2789(00)00087-7.

Noreña, A. J. (2011) 'An integrative model of tinnitus based on a central gain controlling neural sensitivity', *Neuroscience & Biobehavioral Reviews*, 35(5), pp. 1089–1109. doi: 10.1016/j.neubiorev.2010.11.003.

Oostenveld, R. *et al.* (2010) *FieldTrip: Open Source Software for Advanced Analysis of MEG, EEG, and Invasive Electrophysiological Data*, *Computational Intelligence and Neuroscience*. Hindawi. doi: https://doi.org/10.1155/2011/156869.

Paxinos, G. and Watson, C. (2006) *The Rat Brain in Stereotaxic Coordinates: Hard Cover Edition*. Elsevier.

Popelar, J. *et al.* (2008) 'Comparison of noise-induced changes of auditory brainstem and middle latency response amplitudes in rats', *Hearing Research*, 245(1), pp. 82–91. doi: 10.1016/j.heares.2008.09.002.

Popelář, J., Syka, J. and Berndt, H. (1987) 'Effect of noise on auditory evoked responses in awake guina pigs', *Hearing Research*, 26(3), pp. 239–247. doi: 10.1016/0378-5955(87)90060-8.

Radziwon, K. *et al.* (2019) 'Noise-Induced loudness recruitment and hyperacusis: Insufficient central gain in auditory cortex and amygdala', *Neuroscience*, 422, pp. 212–227. doi: 10.1016/j.neuroscience.2019.09.010.

Rauschecker, J. P., Leaver, A. M. and Mühlau, M. (2010) 'Tuning Out the Noise: Limbic-Auditory Interactions in Tinnitus', *Neuron*, 66(6), pp. 819–826. doi: 10.1016/j.neuron.2010.04.032.

Ribary, U. *et al.* (1991) 'Magnetic field tomography of coherent thalamocortical 40-Hz oscillations in humans', *Proceedings of the National Academy of Sciences*, 88(24), pp. 11037–11041. doi: 10.1073/pnas.88.24.11037.

Roach, B. J. and Mathalon, D. H. (2008) 'Event-Related EEG Time-Frequency Analysis: An Overview of Measures and An Analysis of Early Gamma Band Phase Locking in Schizophrenia', *Schizophrenia Bulletin*, 34(5), pp. 907–926. doi: 10.1093/schbul/sbn093.

Rönnberg, J. *et al.* (2014) 'The effect of functional hearing loss and age on long- and short-term visuospatial memory: evidence from the UK biobank resource', *Frontiers in Aging Neuroscience*, 6. doi: 10.3389/fnagi.2014.00326.

Rönnberg Jerker *et al.* (2011) 'Hearing Loss Is Negatively Related to Episodic and Semantic Long-Term Memory but Not to Short-Term Memory', *Journal of Speech, Language, and Hearing Research*, 54(2), pp. 705–726. doi: 10.1044/1092-4388(2010/09-0088).

Roof Robin L. *et al.* (2001) 'A Comparison of Long-Term Functional Outcome After 2 Middle Cerebral Artery Occlusion Models in Rats', *Stroke*, 32(11), pp. 2648–2657. doi: 10.1161/hs1101.097397.

Rüttiger, L. *et al.* (2013) 'The Reduced Cochlear Output and the Failure to Adapt the Central Auditory Response Causes Tinnitus in Noise Exposed Rats', *PLOS ONE*, 8(3), p. e57247. doi: 10.1371/journal.pone.0057247.

Salvi, R. *et al.* (2017) 'Inner Hair Cell Loss Disrupts Hearing and Cochlear Function Leading to Sensory Deprivation and Enhanced Central Auditory Gain', *Frontiers in Neuroscience*, 10. doi: 10.3389/fnins.2016.00621.

Samson, J. *et al.* (2006) 'Biogenic amine changes in brain regions and attenuating action of Ocimum sanctumin noise exposure', *Pharmacology Biochemistry and Behavior*, 83(1), pp. 67–75. doi: 10.1016/j.pbb.2005.12.008.

Schaette, R. and McAlpine, D. (2011) 'Tinnitus with a Normal Audiogram: Physiological Evidence for Hidden Hearing Loss and Computational Model', *Journal of Neuroscience*, 31(38), pp. 13452–13457. doi: 10.1523/JNEUROSCI.2156-11.2011.

Schlee, W. *et al.* (2008) 'Using Auditory Steady State Responses to Outline the Functional Connectivity in the Tinnitus Brain', *PLOS ONE*, 3(11), p. e3720. doi: 10.1371/journal.pone.0003720.

Schormans, A. L., Typlt, M. and Allman, B. L. (2017) 'Crossmodal plasticity in auditory, visual and multisensory cortical areas following noise-induced hearing loss in adulthood', *Hearing Research*, 343, pp. 92–107. doi: 10.1016/j.heares.2016.06.017.

Schormans, A. L., Typlt, M. and Allman, B. L. (2019) 'Adult-Onset Hearing Impairment Induces Layer-Specific Cortical Reorganization: Evidence of Crossmodal Plasticity and Central Gain Enhancement', *Cerebral Cortex*, 29(5), pp. 1875–1888. doi: 10.1093/cercor/bhy067.

Sedley, W. (2019) 'Tinnitus: Does Gain Explain?', *Neuroscience*, 407, pp. 213–228. doi: 10.1016/j.neuroscience.2019.01.027.

Sembulingam, K., Sembulingam, P. and Namasivayam, A. (1996) 'Effect of Acute Noise Stress on Cholinergic Neurotransmitter in Corpus Striatum of Albino Rats', *Pharmacy and Pharmacology Communications*, 2(5), pp. 241–242. doi: https://doi.org/10.1111/j.2042-7158.1996.tb00602.x.

Shahriari, Y. *et al.* (2016) 'Impaired auditory evoked potentials and oscillations in frontal and auditory cortex of a schizophrenia mouse model', *The World Journal of Biological Psychiatry*, 17(6), pp. 439–448. doi: 10.3109/15622975.2015.1112036.

Sivarao, D. V. *et al.* (2013) 'MK-801 disrupts and nicotine augments 40 Hz auditory steady state responses in the auditory cortex of the urethane-anesthetized rat', *Neuropharmacology*, 73, pp. 1–9. doi: 10.1016/j.neuropharm.2013.05.006.

Sivarao, D. V. *et al.* (2016) '40 Hz Auditory Steady-State Response Is a Pharmacodynamic Biomarker for Cortical NMDA Receptors', *Neuropsychopharmacology*, 41(9), pp. 2232–2240. doi: 10.1038/npp.2016.17.

Spencer, K. M. *et al.* (2008) 'Sensory-Evoked Gamma Oscillations in Chronic Schizophrenia', *Biological Psychiatry*, 63(8), pp. 744–747. doi: 10.1016/j.biopsych.2007.10.017.

Spencer, K. M. *et al.* (2009) 'Left auditory cortex gamma synchronization and auditory hallucination symptoms in schizophrenia', *BMC Neuroscience*, 10(1), p. 85. doi: 10.1186/1471-2202-10-85.

Spencer, K. M. (2012) 'Baseline gamma power during auditory steady-state stimulation in schizophrenia', *Frontiers in Human Neuroscience*, 5. doi: 10.3389/fnhum.2011.00190.

Sullivan, E. M. *et al.* (2015) 'Effects of NMDA and GABA-A Receptor Antagonism on Auditory Steady-State Synchronization in Awake Behaving Rats', *International Journal of Neuropsychopharmacology*, 18(7). doi: 10.1093/ijnp/pyu118.

Sun, W. *et al.* (2008) 'Noise exposure–induced enhancement of auditory cortex response and changes in gene expression', *Neuroscience*, 156(2), pp. 374–380. doi: 10.1016/j.neuroscience.2008.07.040.

Syka, J. and Rybalko, N. (2000) 'Threshold shifts and enhancement of cortical evoked responses after noise exposure in rats', *Hearing Research*, 139(1), pp. 59–68. doi: 10.1016/S0378-5955(99)00175-6.

Syka, J., Rybalko, N. and Popelář, J. (1994) 'Enhancement of the auditory cortex evoked responses in awake guinea pigs after noise exposure', *Hearing Research*, 78(2), pp. 158–168. doi: 10.1016/0378-5955(94)90021-3.

Tak, S., Davis, R. R. and Calvert, G. M. (2009) 'Exposure to hazardous workplace noise and use of hearing protection devices among US workers—NHANES, 1999–2004', *American Journal of Industrial Medicine*, 52(5), pp. 358–371. doi: https://doi.org/10.1002/ajim.20690.

Taljaard, D. S. *et al.* (2016) 'The relationship between hearing impairment and cognitive function: a meta-analysis in adults', *Clinical Otolaryngology*, 41(6), pp. 718–729. doi: https://doi.org/10.1111/coa.12607.

Vohs, J. L. *et al.* (2010) 'GABAergic modulation of the 40 Hz auditory steady-state response in a rat model of schizophrenia', *International Journal of Neuropsychopharmacology*, 13(4), pp. 487–497. doi: 10.1017/S1461145709990307.

Vohs, J. L. *et al.* (2012) 'Auditory steady state responses in a schizophrenia rat model probed by excitatory/inhibitory receptor manipulation', *International Journal of Psychophysiology*, 86(2), pp. 136–142. doi: 10.1016/j.ijpsycho.2012.04.002.

Weisz, N. *et al.* (2005) 'Tinnitus Perception and Distress Is Related to Abnormal Spontaneous Brain Activity as Measured by Magnetoencephalography', *PLOS Medicine*, 2(6), p. e153. doi: 10.1371/journal.pmed.0020153.

Weisz, N. *et al.* (2011) 'Alpha Rhythms in Audition: Cognitive and Clinical Perspectives', *Frontiers in Psychology*, 2. doi: 10.3389/fpsyg.2011.00073.

Weisz, N., Dohrmann, K. and Elbert, T. (2007) 'The relevance of spontaneous activity for the coding of the tinnitus sensation', in Langguth, B. et al. (eds) *Progress in Brain Research*. Elsevier (Tinnitus: Pathophysiology and Treatment), pp. 61–70. doi: 10.1016/S0079-6123(07)66006-3.

Wilson, B. S. *et al.* (2017) 'Global hearing health care: new findings and perspectives', *The Lancet*, 390(10111), pp. 2503–2515. doi: 10.1016/S0140-6736(17)31073-5.

Chapter 3

3. The Effects of Noise-Induced Hearing Loss on Sound Detection in Background Noise

3.1 Introduction

Hearing impairment is a highly prevalent neurological problem, affecting ~16% of adults in the USA (Agrawal, Platz and Niparko, 2008). Consistent with non-invasive human studies, preclinical research using animal models has revealed that noise-induced hearing loss causes considerable neural plasticity throughout the peripheral and central auditory pathway (e.g., Popelář, Syka and Berndt, 1987; Syka, Rybalko and Popelář, 1994; Popelar *et al.*, 2008; Salvi *et al.*, 2017). Furthermore, the previous study described in Chapter 2 of this thesis revealed that noise exposure leads to plasticity within the medial prefrontal cortex (mPFC), evident as a decreased ability to entrain to sound-evoked gamma oscillations. Furthermore, that investigation also showed significantly decreased functional connectivity between the auditory cortex and mPFC following noise exposure (Wieczerzak *et al.*, 2020). At present, however, the behavioural consequences of this noise-induced plasticity are not fully understood.

In considering the normal relationship between neural activity in the auditory cortex and higher-order brain regions, a previous study by Fritz and colleagues (Fritz *et al.*, 2010)) in ferrets reported that during an auditory detection task there was a strong functional connectivity between the auditory cortex and regions of their frontal cortex which corresponded to the primate dorsolateral prefrontal cortex (Duque and McCormick, 2010) and rodent mPFC (Seamans, Lapish and Durstewitz, 2008). Additional studies by these authors have also shown that the ability to hear in noise depends on higher-order attentional functions (Fritz, Elhilali and Shamma, 2007; Atiani *et al.*, 2009; Yin, Fritz and Shamma, 2014). Despite growing interest in studying the neural basis of deficits in hearing in noise, we still lack a complete understanding of how an auditory insult, such as hearing

loss induced by loud noise exposure, affects the ability to hear in a noisy background environment. A recent study by Lobarinas and colleagues (Lobarinas, Spankovich and Le Prell, 2017) investigated the ability of rats to detect sounds in noisy backgrounds following a loud noise exposure that resulted in a temporary shift in hearing thresholds. In contrast, the effects of permanent noise-induced hearing loss on sound detection in background noise and on auditory attention have not been studied comprehensively. Ultimately, given the fact that noise exposure is known to disrupt the functional connectivity between the auditory cortex and mPFC (Wieczerzak *et al.*, 2020), and these brain regions are suggested to be involved in sound detection tasks (include references), it is worthwhile to investigate the effects of noise-induced hearing loss on sound detection in conditions that require increased attention, such as background noise.

The present study first established a new operant-based two-alternative forced-choice (2AFC) sound detection task for rats, and then validated its sensitivity to increasing background noise levels. Next, using a noise exposure paradigm that has been shown to not only induce permanent hearing loss (Schormans, Typlt and Allman, 2017, 2019) but also cause a significant decrease of functional connectivity between auditory cortex and mPFC (Chapter 2; (Wieczerzak *et al.*, 2020), the effect of this auditory insult on sound detection was assessed in both quiet and noisy background environments. More specifically, before and after noise-induced hearing loss, the rats' sound detection ability was measured using the signal detection metric *d'-score* (O'mahony, 1992; Stanislaw and Todorov, 1999), which depends on detecting the target sound as well correctly rejecting the distractors. Furthermore, as a complementary performance measure to the *d'-score*, the rats' *impulsivity* was assessed by measuring the number of nose-pokes that they made before they successfully held their nose in the center port long enough (2-3 sec) to initiate a trial. Previous studies have shown that this is an effective assessment of impulsivity, a form of attentional measure that depends on the mPFC (Adriani *et al.*, 2003; Economidou *et al.*, 2009; Doremus-Fitzwater, Barreto, and Spear, 2012). Thus, the rats' *d'-score* and impulsivity measurements provided a useful tools to assess whether changes in

performance post-noise exposure were due to the rat's overall inability to hear the acoustic stimuli or an attentional deficit.

When considering the effect of noise exposure on behavioural task performance, it is important to acknowledge that, in addition to hearing loss, the noise-exposed subjects could also be experiencing tinnitus, i.e., sound perception in the absence of a physical stimulus (Eggermont and Roberts, 2004; Roberts *et al.*, 2010). As an example of tinnitus affecting auditory processing, a past study on humans reported that tinnitus impaired the subjects' ability for gap detection in background noise, as assessed by the acoustic startle response's prepulse inhibition (Fournier and Hébert, 2013). Similarly, animal models of tinnitus induced either by sodium salicylate (Turner and Parrish, 2008) or noise exposure (Turner *et al.*, 2006) also reported a decreased prepulse inhibition of the gap detection paradigm. Although these studies might provide a model to assess the presence of tinnitus, via impaired prepulse inhibition induced by the presence of a silent gap in a background noise, the nature of the testing paradigm is not able to reveal anything about auditory perceptual abilities. Interestingly, while some clinical research suggests that tinnitus affects auditory perception in individuals with otherwise normal hearing (Ch, Jain and Sahoo, 2014), in contrast, a recent study concluded that the presence of tinnitus itself does not affect sound detection ability (Zeng, Richardson and Turner, 2020). Given these disparate results, the present study considered the possibility that the rats' performance following noise-induced hearing loss could perhaps be affected by the concurrent presence of tinnitus. To assess this possibility, a separate experimental series was conducted in which the rats' performance on the sound detection task was tested following two commonly used tinnitus inducers: high dose of sodium salicylate (Yang *et al.*, 2007; Stolzberg *et al.*, 2013; Jiang *et al.*, 2017) and 15-min exposure to a loud tone (Hayes *et al.*, 2020).

Ultimately, this novel 2AFC sound detection task revealed that auditory insults such as noise-induced hearing loss or tinnitus do not necessarily lead to sound detection deficits. Furthermore, although the rats' impulsivity was not significantly increased following the

noise exposure when the effect was assessed at the level of the whole cohort of tested rats, there was a significant correlation between the degree of hearing loss and the increased number of nose pokes required to initiate the trial, providing a rationale for future studies investigating the effects of noise exposure on attention.

3.2 Material and Methods

3.2.1 Animals

Adult Sprague Dawley rats (Charles River Laboratories Inc., Wilmington, MA, USA) were used in three experimental series, as described below. All rats were ~75 days old upon the beginning of the handling protocol and ~90 days old at the beginning of the behavioural training. Rats were food restricted so that they approached 85% of free-feeding body mass at the beginning of training to encourage exploration in the behavioural boxes. The food restriction was maintained throughout testing, and the rats' body mass and well-being were monitored daily. All procedures were approved by the University of Western Ontario Animal Care and use Committee and were per guidelines established by the Canadian Council of Animal Care.

3.2.2 Experimental Design

In all three experimental series described in this chapter, a within-subject design was used, whereby each rat was tested in control and experimental conditions. The details about the experimental designs for each of the series are described below.

3.2.2.1 Development of sound detection task in background noise

In the first series, rats (n = 16) were used to develop and optimize a novel sound detection test that was sensitive to the increasing level of background noise. Overall, a variety of acoustic stimuli were used throughout the training and testing protocols associated with the sound detection task. The specific details about each of these sound stimuli can be found below in section *3.2.2.2 Acoustic Stimuli*, and **Figures 3.3** and **3.4** show representative waveforms. Following an extensive training regime that lasted until the

animals could detect the *steady* sound from three different *other (Oth-A, Oth-B, Oth-C) training* stimuli with > 90% accuracy, successive test sessions commenced. First, rats were tested on three separate testing protocols (*test-I, test-II, test-III*), which included the training *steady* and *other (Oth-C)* sounds and one new *unknown (UN-I, UN-II or UN-III)* stimulus. The fourth testing protocol (*test*) included the training sounds (*steady, Oth-C*) and all three *unknown (UN-I, UN-II, UN-III)* stimuli. After confirmation that performance was consistent regardless of whether only one or all three *unknown testing* stimuli were presented and the training *Oth-C* and *steady* sounds within a test session, the subsequent test sessions included the testing protocol *test*. In the next step, the sound detection was examined using *test* protocol, now presented in a continuous noisy background environment. (**Figure 3.1 A**).
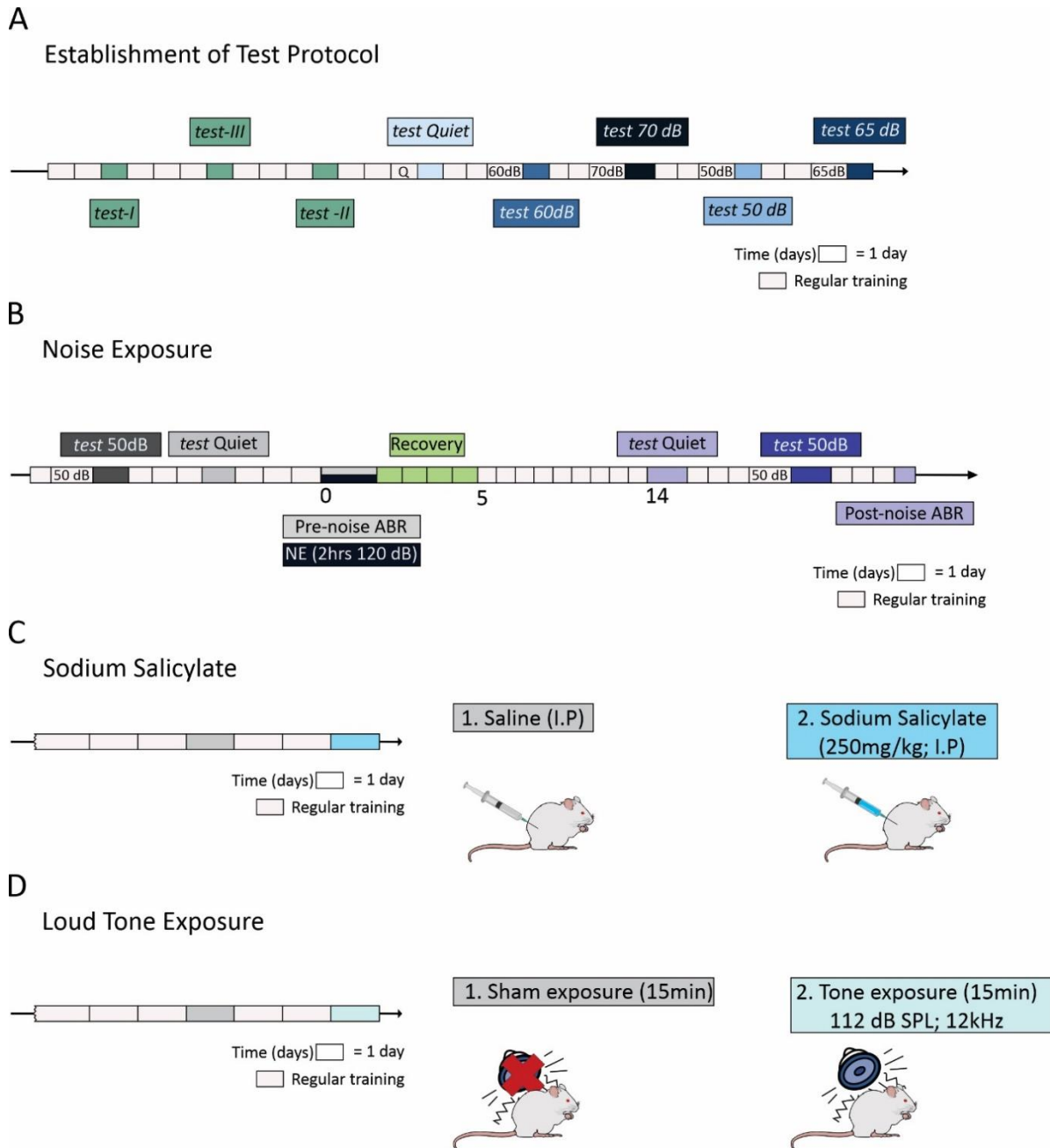
Figure 3.1 Experimental timelines. *Timelines for the three experimental series performed in this study (A) Establishment and validation of the sound detection task's testing protocol. In green are the days in which the test protocols included only one of the unknown sounds (corresponding: UN-I, UN-II, UN-III). The days marked in different shades of blue indicate the test protocol in which all three unknown sounds were presented. The background conditions are indicated on the timeline (n = 16) (B) The experimental timeline for investigating noise exposure effects on sound detection in quiet and in 50-dB SPL background noise. Grey shades indicate the test performed before noise exposure, and purple refers to the post-noise testing (n = 11). (C and D) The effects of two common tinnitus inducers: sodium salicylate (C, blue) and 15-min loud tone exposure (D, teal) on the sound detection task performed in quiet background conditions.*

3.2.2.2 The effects of noise exposure on sound detection in background noise

The second experimental series investigated the effects of permanent noise-induced hearing loss on sound detection performance in quiet and background noise. A group of previously trained rats (n=11) performed the sound detection task (testing protocol *test*) in both quiet and 50 dB SPL background noise, before and in the days after noise exposure. The first testing session commenced two weeks (on the 14th day) following the noise exposure. Consistent with a previous study in our lab that investigated noise-induced plasticity in audiovisual perception (Schormans, Typlt, and Allman, 2017), the successive test sessions were separated by four days training. Before the test session in 50 dB background noise, the rats were trained using the standard training protocol with that background noise (**Figure 3.1B**). The final ABR protocol was performed upon completion of the behavioural testing to assess the degree of noise-induced hearing loss. The order of background conditions in the pre-test and post-test sessions was pseudo-randomized to avoid any confounding effects.

3.2.2.3 The effects of tinnitus on sound detection

Finally, experimental series 3 was performed to assure that the results of the experimental series 2 were not affected by the possible presence of tinnitus. Two separate groups of previously trained rats were used to test the effects of two common tinnitus inducers: 1) 250 mg/kg injection of sodium salicylate (n = 8) and 2) 15-min exposure to a loud tonal stimulus (n = 8), and their performance was compared to their respective control conditions **(Figure 3.1C, D).**

3.2.3 Sound Detection Task

3.2.3.1 Behavioural Apparatus

Behavioural training and testing were performed in a standard modular test chamber (ENV-008CT), Med Associates Inc., St. Albans, VT) that was housed within a sound-attenuating box (29" W by 23.5" H by 23.5" D, Med Associates Inc., St. Albans, VT). The

front wall of the behavioural chamber included a center port with two stainless steel feeder troughs positioned on either side, each fitted with an infrared (IR) beam used to detect nose-pokes. Each feeder trough was attached to a food pellet dispenser located behind the behavioural chamber. A house light was located on the back wall to illuminate the chamber, and a white light-emitting diode (LED) was located directly above the center nose-poke, which served as a GO cue during behavioural training and testing **(Figure 3.2)**. Auditory stimulus delivery, nose-poke responses, and positive/negative reinforcement were controlled using custom behavioural protocols (EPsych Toolbox, dstolz.github.io/epsych/) running in MATLAB (MathWorks, Nattick, MA, USA) and interfaced with real-time processing hardware RZ6; Tucker-Davis Technologies (TDT), Alachua, FL, USA).
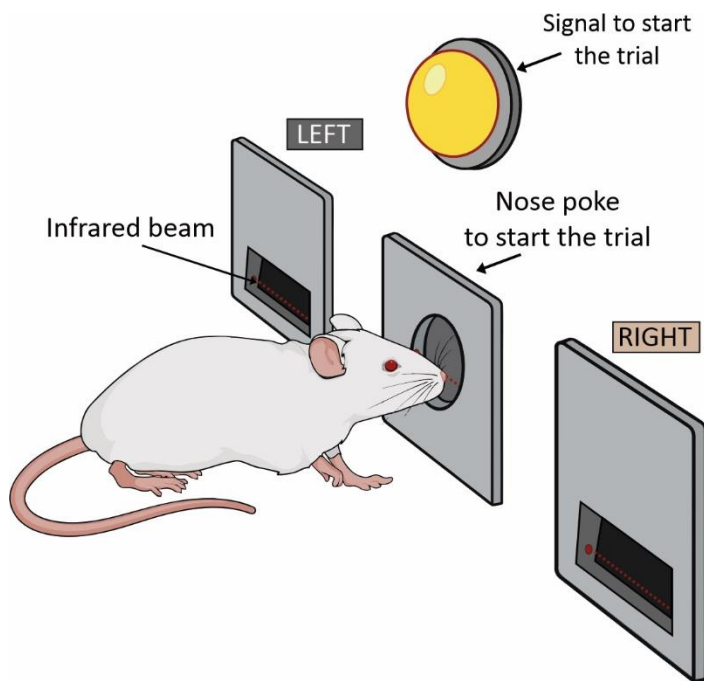
Figure 3.2 Behavioural apparatus

3.2.3.2 Acoustic Stimuli and Background Noise

The acoustic stimuli were programmed to play from a speaker (FT28D; Fostex, Tokyo, Japan) mounted on the roof of the behavioural chamber. There were four training stimuli: *steady* and three *other (Oth-A, Oth-B, Oth-C).* Furthermore, there were also three

unknown (UN-I, UN-II, UN-III) testing stimuli. The *steady* sound **(Figure 3.3D)** was an unmodulated narrowband noise (NBN; 1/8th octave band, the center frequency at 16 kHz). The training *other* and the *unknown* testing sounds used the same NBN as a carrier signal (*carrier)*. They were modified using a sinusoidal modulating function at the frequency of 19 Hz (*modulator)* and different magnitude of amplitude of the carrier (AC) and constant amplitude of the modulation signal (AM = 1), following equation 3.1, except for the *Oth-A,* modulated with the modulation signal AM = 0.5, amplitude modulation, thus with index *m = 0.5* **(Figure 3.3A).**

Equation 3.1: General sinusoidal amplitude modulation of a signal

$$stimulus = AC + AM \, (modulator)(carrier)$$

To better describe the modulation of the signal, the modulating index was calculated as the ratio of the amplitudes between the modulating signal and the carrier (equation 3.2)

Equation 3.2 Modulation index *m*

$$m = \frac{AM}{AC}$$

Thus, ultimately the modulation of the training *other* and testing *unknown* sounds can be described by equation 3.3, where AC indicates the amplitude of the carrier, and *m* stands for the modulation index.

Equation 3.3 Sinusoidal amplitude modulation equation

$$stimulus = AC[\,1 + \, m(modulator)(carrier)]$$

The *Oth-B* consisted of the NBN carrier signal with the amplitude *AC = 0.75* and the modulation index *m = 1.33* **(Figure 3.3B)**. Like the previous other sounds, the *Oth-C* was an NBN modulated with the modulating signal with the amplitude AM = 1 at the 19 Hz rate. This time, the carrier signal's amplitude was 0.5; thus, the sound was ultimately amplitude overmodulated with the modulating index m= 2 **(Figure 3.3C).** The unknown

testing sound *UN-I* was the NBN with amplitude AC = 0.025 and amplitude modulated by a sinusoidal modifying signal with the amplitude AM = 1 at the rate of 19 Hz. Thus, resulting in an overmodulated signal with a modifying index *m = 40*. **(Figure 3.4A)**. The *UN-II* testing sound had the carrier amplitude AC = 0.1, resulting in the modulation index *m = 10* **(Figure 3.4B).** The unknown testing stimulus *UN-III* **(Figure 3.4C)** had the amplitude of the carrier AC = 0.2, leading to an amplitude overmodulated signal with the modulation index *m = 5*
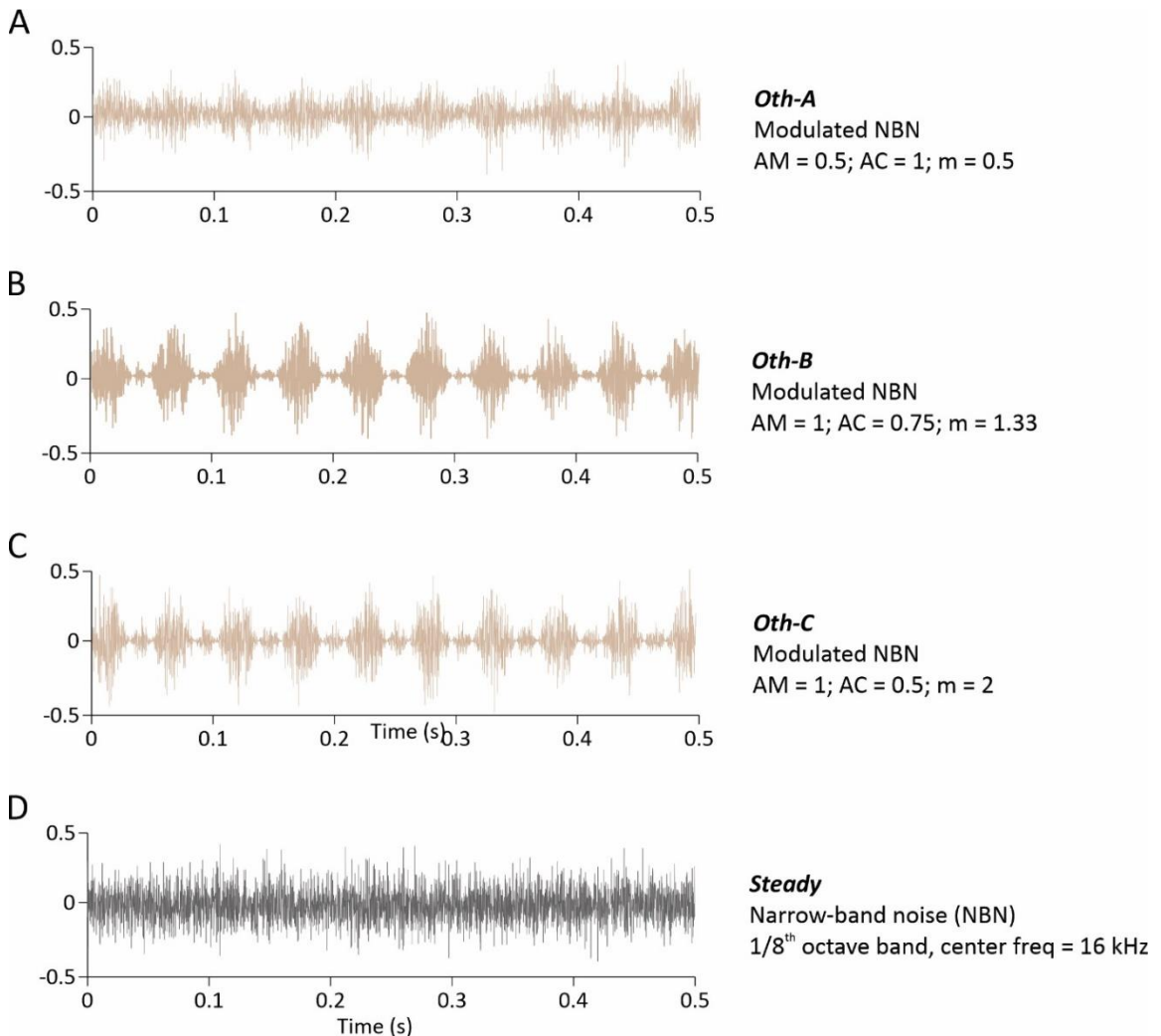
Figure 3.3 Training Acoustic stimuli (A-C) *Other training stimuli used throughout the training regime. All of them used the narrowband noise as a carrier and were modulated as indicated in the figure. Oth-C (C) sound was also used during the testing protocols. (D) Steady target stimulus (narrowband noise; 1/8th octave band, the center frequency at 16 kHz). Steady target sound was used in training and the testing protocol.*

A

0.5
0
-0.5
0   0.1   0.2   0.3   0.4   0.5
Time (s)

UN-I
Modulated NBN
AM = 1; AC = 0.025; m = 40

B

0.5
0
-0.5
0   0.1   0.2Time (s)0.3   0.4   0.5

UN-II
Modulated NBN
AM = 1; AC = 0.1; m = 10

C

0.5
0
-0.5
0   0.1   0.2   0.3   0.4   0.5
Time (s)

UN-III
Modulated NBN
AM = 1; AC = 0.2; m = 5

D

UN-I   UN-I
Test-I

E

UN-I   UN-III   UN-II   UN-I   UN-II   UN-III   UN-II
Test
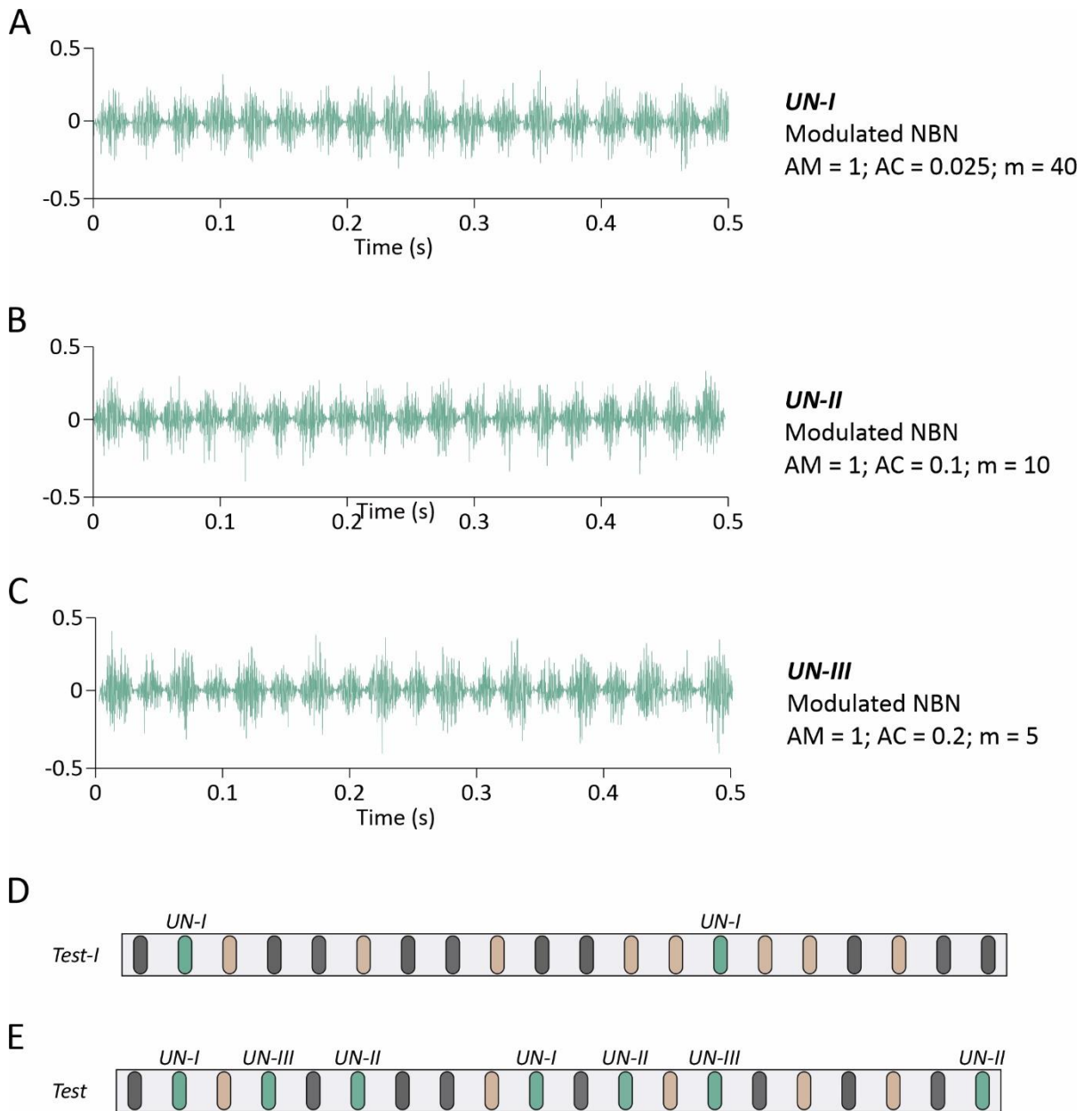
Figure 3.4 Unknown testing stimuli (A-C) Unknown (UN I-III) testing stimuli used in testing protocols used NBN noise as the carrier with modulations as indicated in the figure. *(D)* An example of a test-I protocol that used only one unknown testing stimulus (UN-I). Test-II and test-III were similar with regards that only used one unknown stimulus, i.e., test-II included UN-II and test-III used UN-III stimulus only. During those protocols, the steady sound was in 50% of trials (grey), Oth-C (beige) 40% and the respective unknown (green) stimulus in 10% of the trials. *(E)* An example of the test protocol that used all three unknown stimuli. In this test protocol, the steady sound (grey) was presented in 40% of the trials, Oth-C (beige) in 30% and each of the unknown (green) in 10% of trials (i.e., of all trials, 30% were unknown sounds). The order of the stimuli was pseudo-randomized.

All the acoustic stimuli were calibrated using TDT software and hardware (RPvdsEX, RZ6 module; TDT) to ~75 dB SPL using a ¼" microphone (2530, Larson-Davis, Depew, NY, USA) and preamplifier (2221, Larson Davis). The background sound (broadband noise; BBN 1-32 Hz) used to create a noisy environment was played from a speaker mounted on the wall opposite to the feeder troughs, and it was calibrated to the appropriate level (50, 60, 65, 70 dB SPL) using the method described above.

3.2.3.3 Training regiment and protocols

Rats were trained 30 min per day, six days per week. Regardless of the training stage and subsequent testing, the general features of the sound detection task remained the same. For a given trial, the acoustic stimulus (e.g., *steady*) was played continuously from the overhead speaker, and it was only after the rat elected to nose-poke the center port (detected by interrupting an infrared beam) that the actual trial could commence. In this case, the rat needed to poke/hold its nose in the center port for a specific amount of time (duration dependent on training stage; see **Table 3.1**), and upon being presented a single light flash as a GO cue, the rat then made its choice to nose-poke into either the left or right feeder trough. Upon crossing the infrared beam in a feeder trough, the acoustic stimulus was pseudo-randomly changed, and the rat was again allowed to nose-poke the center port to initiate the subsequent trial at its own pace. It is significant to note that a critical feature of this task is that the acoustic stimuli that the rat was exposed to were not presented as discrete sounds; instead, there was always an acoustic stimulus (e.g., *steady*, *other,* or *unknown*) presented from the overhead speaker. Thus, during sessions, when background noise was presented from the speaker at the back of the chamber, it competed with the actual acoustic stimulus.

Protocol	Left stimulus	Right stimulus	Delay	Duration	Food provided
Handling	N/A	N/A	N/A	1 week	ab libitum
Food restriction	N/A	N/A	N/A	1 week	
Phase 1A		Oth-A	500 ms	3-4 days	
Phase 2A	Steady NBN	Oth-A	2000-3000 ms	2-3 weeks	4g/100g
Phase 2B		Oth-B		1-2 weeks	
Phase 2C		Oth-C		1-2 weeks	

Table 3.1 *Overview of the training protocols used for the amplitude-modulation discrimination task*. *Rats were trained using successive protocols to introduce them to each type of stimulus slowly. Typically, 3 to 4 months were required for rats to complete training, which was considered as maintaining a >90% hit rate over consecutive training days.*

Initial training sessions (Phase 1A) required rats to insert their noses (*nose-poke*) into the center port to trigger a GO cue (LED flash). Upon removing its nose from the center port, the rat was immediately reinforced with a food pellet (Bio-Serv, Frenchtown, NJ, USA) dropped into the appropriate feeder trough associated with the acoustic stimulus playing from the overhead speaker. The left feeder trough for the *steady* stimulus and the right feeder trough for the *Oth-A* sound stimulus. If the animal then nose-poked the correct feeder trough within 5 seconds of the initial pellet delivery (detected by the trough IR beam's interruption), it was given a second food pellet reward to reinforce the stimulus association further. During a 30-minute training session, trial type (*steady* or *Oth-A*) was distributed evenly and presented in a randomized order. When rats became more proficient at the task, the cue delay (time required to trigger the GO cue) was gradually increased from 100 to 500 ms.

Upon learning to frequently nose poke the center port (typically after 3 to 4 days), rats were then trained on a new protocol (Phase 2A) where the initial pellet reinforcement was removed, and pellet delivery was provided only if the rat poked its nose in the correct feeder trough in response to a given auditory stimulus. Rats received 100% reward rates, and incorrect responses were punished with a 15-s timeout, during which the subsequent trial could not be initiated. Furthermore, as the rats became more proficient at the task, the cue delay was slowly increased from 500 to 3000 ms. Rats remained on Phase 2A until

they could correctly associate feeder troughs with the given auditory stimuli with >90% accuracy for at least three consecutive days (typically after two weeks).

Once rats could correctly distinguish *steady* sound from the *Oth-A*, a new protocol (Phase 2B) was introduced. In this protocol, rats had trained to nose poke the left trough for *steady* as before and the right trough for a new *Oth-B* stimulus. After reaching >90% accuracy for at least three consecutive days on this protocol, rats were introduced to the final training protocol (Phase 2C). The rats continue to train to detect the *steady* sound (associated with the left feeder), but this time from *Oth-C* sound. Ultimately, at the end of the training, the rats learned to detect the *steady* sound associated with the left feeder trough from *other* training sounds associated with the right feeder trough.

3.2.3.4 Optimizing testing protocol.

Once rats achieved >90% accuracy on the final training protocol, a series of test sessions occurred. First rats were tested on three separate testing protocols (test-I; test-II; test-III) in a pseudo-randomized order. Each of those tests included the *steady* sound (50% of trials), training *Oth-C* sound (40% of trials), and only one of the three *unknown* test stimuli *(UN-I, UN-II, UN-III)* (10% of trials) as follow: test-I included UN-I; test-II protocol UN-II; and test-III included UN-III **(Figure 3.4D)**. There were at least two days of regular training (*steady* vs. *Oth-C*) separating the test sessions.

After rats were tested on those three testing protocols; a new testing protocol (referred to as *test)* was introduced that included training sounds: *steady* (40% of trials) and the *Oth-C* (30% of trials), as well as all three *unknown* sounds (each 10% of trials) **(Figure 3.4E)**. In all testing protocols, the rats received a food award upon correct response to the *steady* (left) and the *Oth-C* (right) sounds. The rats' responses during the *unknown* trials (i.e., *UN – I, UN-II and UN-III*) were rewarded regardless of choice.

Following confirmation that the *test* protocol yielded the same accuracy of the responses as the *test-I, -II and -III* protocols (as assessed by the *d'-score*; see below for details), the

protocol's sensitivity to background noise was assessed. To that end, rats were tested with the *test* protocol in quiet, 50-, 60-, 65-, and 70-dB SPL background noise (i.e., considering the stimulus always played at 75 dB SPL, the signal-to-noise ratios were respectively: 25-, 15- 10-and 5-dB). Recall that the background noise was presented from a secondary speaker to compete with the actual acoustic stimuli that the rat attempted to identify. The testing order was pseudo-randomized, and the test sessions were separated by at least two training days. Additionally, one day before the test session, the rats performed the regular training protocol with the same level of background noise that was to be used in the subsequent test session.

3.2.3.5 Data Analysis

To assess the rats' ability to detect the *steady* sound, the detection index, i.e., *d'-score* based on the signal detection theory, was calculated (O'mahony, 1992; Stanislaw and Todorov, 1999). Here, a *hit* was defined as the response to the left during the trials where the *steady* sound was played, and the *false alarm* was the response to the left during the trials where the *unknown* sounds were played **(Table 3.2).** Thus, the *d'-score* was calculated as a difference between the distribution of the probabilities of *hits* and *false alarms,* expressed as Z-score equivalents using the inverse cumulative normal distributions. The *d'-score* formula is presented below in equation 3.4 (Stanislaw and Todorov, 1999):

Equation 3.4 Simplified *d'-score* equation

$$d' - score = Z(Hit\ rate) - Z(False\ Alarm\ Rate)$$

Thus, in this case, the *d'-score* reflects the rats' ability to detect the *steady* sound, independently of their response bias (O'mahony, 1992; Stanislaw and Todorov, 1999). Ultimately, the rat's performance depended on it detecting the *steady* and correctly rejecting the *unknown* sounds.

Stimulus/Response	Left feeder	Right Feeder
Steady	Hit	Miss
Unknown (UN-I, UN-II, UN-III)	False Alarm	Correct rejection

Table 3.2 *Response definition in the sound detection task*

Furthermore, to assess the attentional abilities of the rat, the average number of nose pokes required to initiate the *steady* and the *unknown* trials were calculated, as it has been previously shown to be a reliable metric of impulsivity (Adriani *et al.*, 2003; Economidou *et al.*, 2009; Doremus-Fitzwater, Barreto, and Spear, 2012).

3.2.4 Hearing Assessment with Auditory Brainstem Response

Consistent with a previously established protocol in our lab (Schormans, Typlt, and Allman, 2017), hearing sensitivity was assessed with the auditory brainstem response (ABR), which was performed in a double-walled sound-attenuating chamber (MDL 6060 ENV, Whisper Room Inc, Knoxville, TN). Rats were anesthetized with ketamine (80 mg/kg; IP) and xylazine (5 mg/kg; IP), and subdermal electrodes (27 gauge; Rochester Electro-Medical, Lutz, FL) were positioned at the vertex, over the right mastoid, and on the back. Throughout the hearing assessment procedure, body temperature was maintained at ~37 °C using a homeothermic heating pad (507220F; Harvard Apparatus, Kent, UK).

Auditory stimuli consisting of a click (0.1 ms) and 2 tones (4 kHz and 20 kHz; 5 ms duration and 1 ms rise/fall time) were generated using Tucker-Davis Technologies RZ6 processing module sampled at 100 kHz (TDT, Alachua, FL). The auditory stimuli were delivered by a speaker (MF1; TDT) positioned 5 cm from the animal's right ear while the left ear was occluded with a custom foam earplug. All stimuli were presented 1000 times (21 times/s) at decreasing intensities from 90 to 10 dB sound pressure level (SPL). Near the threshold, successive steps were decreased to 5 dB SPL, and each sound level was presented twice to determine the ABR threshold using the criteria of just noticeable deflection of the averaged electrical activity within the 10-ms time window (Popelar *et al.*, 2008). Sound stimuli used for the ABR, noise exposure, and electrophysiological recordings were calibrated with custom MATLAB software (The Mathworks, Natick, MA) using a ¼-inch

microphone (2530; Larson Davis, Depew, NY) and preamplifier (2221; Larson Davis). The auditory-evoked activity was collected using a low-impedance headstage (RA4L1; TDT), then preamplified and digitized (RA16SD Medusa preamp; TDT) sent to an RZ6 processing module via a fibre optic cable.

3.2.5 Noise Exposure

Rats were bilaterally exposed to broadband noise (0.8–20 kHz) for 2 hours at 120 dB SPL while under ketamine (80 mg/kg; IP) and xylazine (5 mg/kg; IP), and body temperature was maintained at ~37 °C using a homeothermic heating pad. This broadband noise exposure protocol was chosen because it was found to be effective at inducing a permanent threshold shift as assessed using the ABR (Popelar *et al.*, 2008; Schormans, Typlt, and Allman, 2017, 2019) as well as leading to decreased functional connectivity between the auditory and medial prefrontal cortex (Wieczerzak *et al.*, 2020). The broadband noise was generated with TDT software (RPvdsEx) and hardware (RZ6) and delivered by a super tweeter (T90A; Fostex, Tokyo, Japan) which was placed 10 cm in front of the rat.

3.2.6 Tinnitus Induction

3.2.6.1 Sodium Salicylate Treatment

Rats were first tested on the sound detection task following saline treatment (1 ml IP; equivalent volume to the sodium salicylate treatment). After two days of the regular training, rats were tested again, but this time following the treatment with a high sodium salicylate dose (250 mg/kg, IP; Sigma-Aldrich, St. Louis, MO, USA). In both sessions, the testing began two hours after the injection. This dosing and timing were chosen based on findings of peak electrophysiological and tinnitus-related behavioural effects resulting from sodium salicylate administration in rodents (Yang *et al.*, 2007; Stolzberg *et al.*, 2013; Jiang *et al.*, 2017).

3.2.6.2 Exposure to 15-minute Loud Tonal Stimulus

Rats were first tested following a sham exposure (i.e., placed in the sound-attenuating chamber, but no sound was presented from the speaker). After two regular training days, rats were again tested, following brief exposure to a loud tonal stimulus. The rats were placed inside a sound-attenuating chamber (ENV-022MD; Med Associates, Inc.), which included a standard rat home cage equipped with a ceiling-mounted speaker (T90 A Horn Tweeter, Fostex). For the sham treatment, the rats remained inside the sound-attenuating chamber for 15 min in the absence of acoustic stimuli. For the loud sound exposure, rats were subjected to a 12 kHz tone presented at 112 dB SPL for 15 min. The intensity of the tonal stimulus was calibrated as described in previous sections. The loud tonal exposure parameters were chosen based on previous work from our lab, which demonstrated that this protocol invariably caused behavioural evidence of tinnitus in adult Sprague Dawley rats (Hayes *et al.*, 2020). In the present experiments, rats that received either the sham or loud tonal exposure began their testing session 10 min after removal from the sound-attenuating chamber.

3.2.7 Data Presentation and Statistics

Statistical analyses were performed using GraphPad Prism and included one-way and two-way repeated-measures analysis of variance (RM-ANOVA) and Pearson's correlation analysis. Post hoc paired-samples t-tests with Bonferroni-corrected significance level were used to compare differences in the group means in the case of significant effects or interactions. In the data sets where the normality was validated, the group was compared using Wilcoxon matched-pairs signed-rank test. The data figures were generated in GraphPad Prism and edited for aesthetic purposes using CorelDRAW Graphics Suite 2020. The methods figures containing the acoustic stimulus samples were generated using MatLab and edited in CorelDRAW Graphics Suite 2020.

3.3 Results

3.3.1 The type and the number of unknown sounds in the test protocol did not affect the ability to detect the steady stimulus.

This experimental series was designed to establish an optimal testing protocol in which the animal was required to detect the previously learned *steady* sound (**Figure 3.3D**) from the three *unknown* sounds (*UN-I, UN-II, UN-III;* **Figure 3.4A-C**). Two-way RM-ANOVA for *unknown* stimulus type (*UN-I, UN-II, UN-III*) x testing protocol type (*test-I, test-II, test-III, test*) failed to reveal a significant effect of the type of the *unknown* sound ($F_{(1.54, 23.08)}$ = 0.35; p = 0.65) or the testing protocol ($F_{(1.0, 15.0)}$ = 0.79; p = 0.39) on the ability to detect the *steady* sound **(Figure 3.5A)**. Furthermore, as shown in a separate two-way RM-ANOVA, the rats' impulsivity, measured as an average number of nose pokes required to initiate a trial, was also not affected by the stimulus type ($F_{(1.34, 20.05)}$ = 1.49; p = 0.24) nor the testing protocol ($F_{(1.00, 15.0)}$ = 0.59; p = 0.45) **(Figure 3.5B).** Therefore, in the following experiments, it was decided to use the testing protocol *test,* which used the training *steady* and *Oth-C* sounds and all the three *unknown (UN-I, UN-II, UN-III)* sounds. The details of the statistical results are presented in **Table 3.3**.
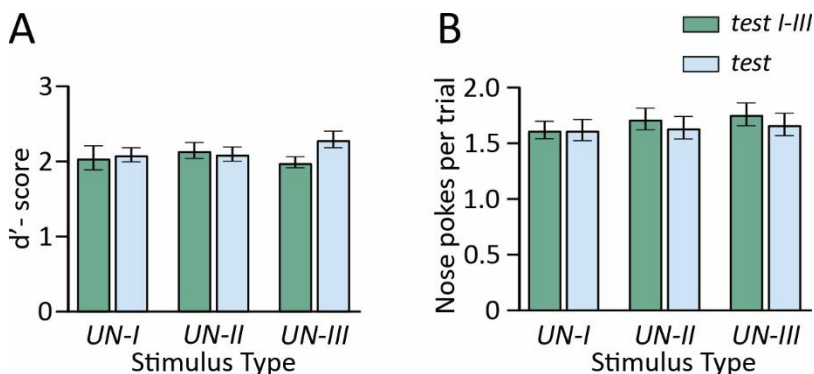
Figure 3.5 The unknown test sound type and the test protocol type did not affect the rats' performance. (A) *The rats detected the steady sound with equal accuracy, no matter whether they were presented with one or many unknown test sounds.* ***(B)*** *On average, the rats made the same number of nose pokes per trial for all protocol types. Data represent group mean ± SEM; n= 16 rats.*

3.3.2 Steady sound detection was affected by increases in background noise.

To assess whether the sound detection task was sensitive to environmental challenges, rats were tested under various noisy background conditions. As expected, a one-way RM-ANOVA revealed a significant effect of the background noise on the *d'-score* ($F_{(2.49, 37.41)}$ = 33.40; $p < 0.001$). Furthermore, Bonferroni corrected post-hoc analysis revealed that when the background noise was 50 or 60 dB SPL, the rats could detect the *steady* sound with the same accuracy as in quiet background conditions (**see Table 3.3**). However, their performance was significantly worsened with 65 dB SPL background noise as compared with the quiet conditions (quiet: 2.15 ± 0.09 vs. 65 dB SPL: 1.45 ± 0.09; p_{Bonf} < 0.01). Upon increasing the intensity of the background noise to 70 dB SPL, the rat's performance declined further (quiet: 2.15 ± 0.09 vs. 70-dB SPL: 0.99 ± 0.12; $p_{Bonf} < 0.01$) (**Figure 3.6A; Table 3.3**). Additional one-way RM-ANOVA failed to reveal a significant effect of the increasing background noise on the average number of nose-pokes required to initiate a trial ($F_{(2.81, 42.13)}$ = 0.90; $p = 0.44$) (**Figure 3.6B**). Thus, it is reasonable to conclude that their poor performance in 65 and 70 dB SPL background noise was not a result of increased impulsivity. Together, these findings suggest that the newly designed *steady* sound detection task represents an effective method for studying auditory detection in background noise and could prove useful in investigating the consequences of hearing loss on listening in quiet versus noisy environments. The detailed results of the statistical analysis are presented in **Table 3.3.**

A

B
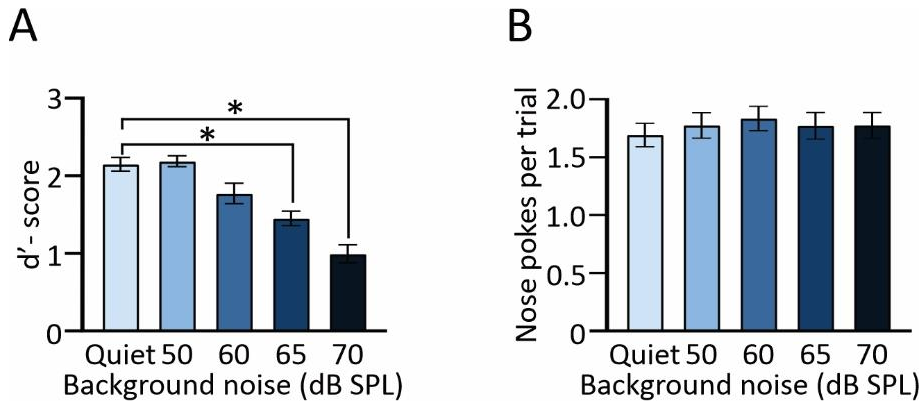
Figure 3.6 Elevated background noise worsened performance on the sound detection task but did not alter impulsivity. (A) *The group average of the combined d'-score for steady sound performed in various background noise conditions from quiet to 70 dB SPL revealed that rats' performance significantly decreased with the 65 dB SPL background noise but not with 50 or 60 dB SPL.* **(B)** *The background noise did not affect rats' impulsivity as judged by the number of nose-pokes required to initiate a trial. Data in bar graphs represent group mean ± SEM; n = 16; *p_{Bonf} < 0.05.*

TEST	Main effects/ Comparison	p-value	F-value/t-value; DF
Figure 3.5 Establishing the testing protocol			
Figure 3.5 A. d'-score			
	Stimulus type (*UN-I, UN-II, UN-III*)	0.65	$F_{(1.54, 23.08)} = 0.35$
2-way RM-ANOVA	Testing protocol (*test-I, test-II, test-III, test*)	0.39	$F_{(1.00, 15.00)} = 0.79$
	Interaction (stimulus type x testing protocol)	0.16	$F_{(1.66, 24.90)} = 2.05$
Figure 3.5 B. Impulsivity			
	Stimulus type (*UN-I, UN-II, UN-III*)	0.24	$F_{(1.34, 20.05)} = 1.49$
2-way RM-ANOVA	Testing protocol (*test-I, test-II, test-III, test*)	0.45	$F_{(1.00, 15.00)} = 0.59$
	Interaction (stimulus type x testing protocol)	0.56	$F_{(1.6, 17.36)} = 0.56$
Figure 3.6 The effects of background noise on the sound detection task			
Figure 3.6 A. d'-score			
1-way RM-ANOVA	Background noise (Quiet, 50-70 dB SPL) *	< 0.001	$F_{(2.49, 37.41)} = 33.40$
Post hoc	*d'-score* Quiet vs. 50 dB SPL	> 0.99 [B]	t = 0.36; DF = 15
Post hoc	*d'-score* Quiet vs. 60 dB SPL	0.11 [B]	t = 2.43; DF = 15
Post hoc	*d'-score* Quiet vs. 65 dB SPL *	<0.001 [B]	t = 5.26; DF = 15
Post hoc	*d'-score* Quiet vs. 70 dB SPL *	<0.001 [B]	t = 6.85; DF = 15
Figure 3.6 B. Impulsivity			
1-way RM-ANOVA	Background noise (Quiet, 50-70 dB SPL)	0.44	$F_{(2.81, 42.13)} = 0.90$

Table 3.3 *Summary of the statistical tests performed in the experimental series establishing the test protocol for the sound detection task. [B] Bonferroni corrected p-value; * statistical significance.*

3.3.3 Noise-induced deficits in *steady* sound detection were correlated with the degree of hearing loss.

Consistent with the rats tested in a previous study (**Chapter 2**), the chosen noise exposure (0.8-20 kHz at 120 dB SPL for two hours) led to a permanent hearing loss, as evident in the ABR recordings. A two-way RM-ANOVA for time (pre-noise vs. post-noise exposure) x stimulus (click, 4 kHz, 20 kHz) showed a significant effect of noise exposure ($F_{(1, 10)}$ = 27.40; $p < 0.01$), as well as stimulus type ($F_{(1.52, 15.25)}$ = 6.87; $p = 0.01$). Furthermore, this analysis also showed a significant interaction between the time (pre-noise vs. post-noise exposure) and stimulus type ($F_{(1.96, 19.60)}$ = 5.02; $p = 0.01$), indicating that the noise exposure affected the hearing threshold for those stimuli differently. Consequently, additional statistical analysis, separate for each stimulus, was performed. The Shapiro-Wilk test for normality revealed that the data set representing the hearing threshold for click stimulus pre-noise exposure was not normally distributed ($p = 0.02$). Thus, to compare the pre-noise vs. post-noise click stimulus hearing threshold, a Wilcoxon-matched pair signed-rank test was performed, which revealed that hearing threshold was significantly increased following noise exposure (click stimulus threshold pre-noise 29.55 ± 1.25 dB SPL vs. post-noise 42.27 ± 2.06 dB SPL; $p < 0.01$). The paired sample two-tailed t-test revealed that the hearing threshold post-noise exposure for the 4 kHz stimulus was also significantly increased as compared to the pre-noise conditions (pre-noise: 21.82 ± 1.55 dB SPL vs. post-noise: 43.18 ± 2.96 dB SPL; $p < 0.01$). Finally, the Wilcoxon-matched pairs signed-rank test for the 20 kHz tonal stimulus also revealed a significantly increased hearing threshold following noise exposure (pre-noise: 19.09 ± 0.91 dB SPL vs. post-noise: 41.36 ± 4.58 dB SPL; $p < 0.01$) (**Figure 3.7A**). Furthermore, a paired sample two-tailed t-test revealed that the amplitude of the wave I elicited by the click stimulus at 80 dB SPL was significantly decreased as compared to pre-noise condition (pre-noise: 1.17 ± 0.05 µV vs. post-noise: 0.33 ± 0.08 µV; $p < 0.0001$) (**Figure 3.7B**, **Table 3.5**).
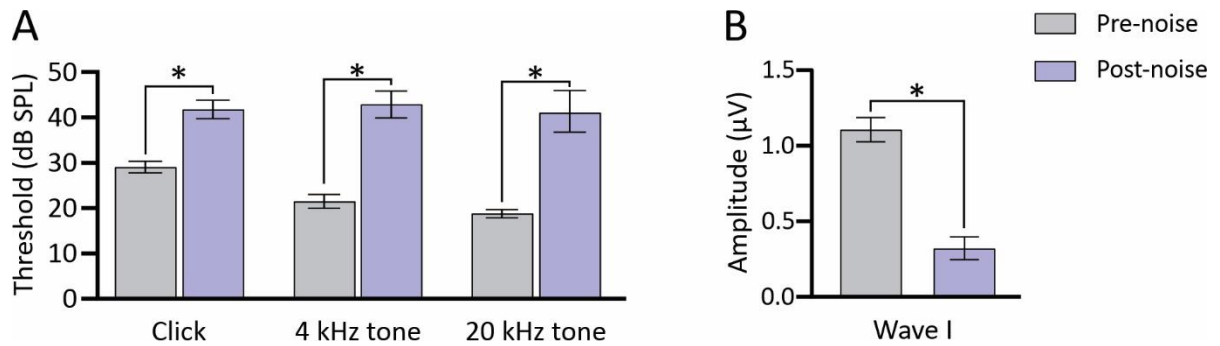
Figure 3.7 Hearing assessment. (A) *The auditory brainstem responses (ABR) protocol revealed a significant threshold shift in response to click, 4 kHz tone, and 20 kHz tone stimuli following the noise exposure.* ***(B)*** *The wave I amplitude was also significantly reduced post-noise, as compared to pre-noise conditions. Data represent group mean ± SEM; n= 11 rats; *p_{Bonf}< 0.001.*

The effects of noise exposure on the ability to detect *steady* sound in quiet and in a noisy background were assessed by a two-way RM-ANOVA for time (pre-noise; post-noise) x background conditions (quiet; 50 dB SPL). The results revealed a significant effect of the noise exposure on the ability to detect the *steady* sound as measured by the d'-score ($F_{(1,10)}$ = 5.02; p = 0.049). Bonferroni corrected post hoc analysis found that the d'-score was significantly decreased in both in quiet (pre-noise: 2.32 ± 0.16 vs. post-noise: 1.72 ± 0.30; p_{Bonf} = 0.01) and in 50 dB SPL background noise (pre-noise: 2.03 ± 0.14 vs. post-noise: 1.50 ± 0.25; p_{Bonf} = 0.02) (**Figure 3.8A, Table 3.5**). Furthermore, Pearson's correlation test revealed that the rats' performance was significantly correlated with the degree of hearing loss as indicated by the threshold shift to the click stimulus in quiet (R^2 = 0.577; p < 0.01) (**Figure 3.8B**) as well as in 50 dB SPL background noise (R^2 = 0.495; p = 0.02) (**Figure 3.8C**) (**Table 3.4**).
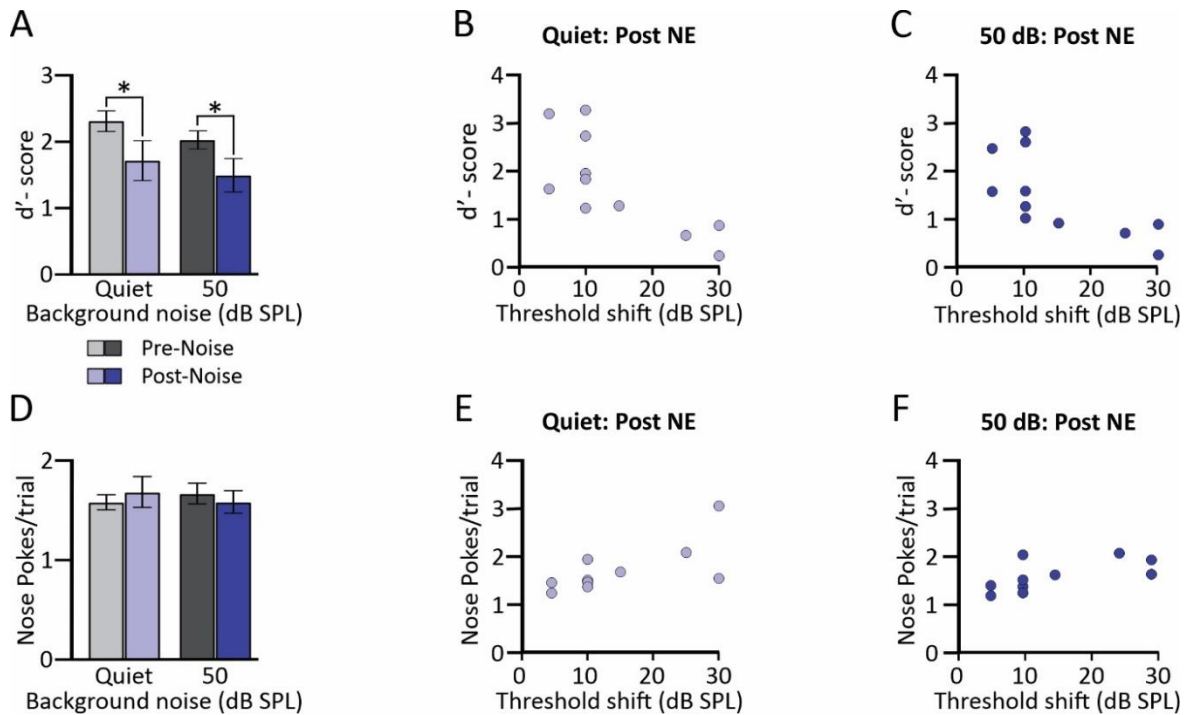
Figure 3.8 Noise-induced hearing loss was correlated with decreased performance on the sound detection task and increased impulsivity in quiet and in 50 dB SPL background noise. (A) The group average of d'-score revealed that rats' ability to detect steady sound was significantly decreased in quiet and in 50 dB SPL background. (B and C) The correlation analysis between the click stimulus threshold shift and d'-score in quiet (B) and 50 dB SPL (C) revealed that task performance was significantly correlated with the degree of hearing loss. (D) The group average of nose pokes required to initiate a trial was not affected by the noise-induced hearing loss in quiet or 50 dB SPL background noise; however, (E and F) correlation analysis revealed a significance in quiet (E) and background noise (F). Data in bar graphs represent group mean ± SEM; n = 11; *p_{Bonf} < 0.05. NE= noise exposure.

To investigate the possibility that performance during sound detection task decreased due to attentional deficits, the effects of noise exposure on impulsivity were investigated by measuring the number of nose-pokes required to initiate a trial. A two-way RM-ANOVA for time (pre-noise; post-noise) x background conditions (quiet; 50 dB SPL) failed to reveal a significant effect of the noise exposure ($F_{(1, 10)}$ = 0.01; p = 0.90) **(Figure 3.8D).** Interestingly, despite this lack of the significant effect of the noise exposure on the impulsivity when assessed for the whole cohort of rats, a Pearson's correlation test revealed that the rats' degree of hearing loss was significantly correlated to their

impulsivity in the quiet condition (R^2 = 0.470; p = 0.019) **(Figure 3.8 E)** as well as in the 50

dB SPL background noise (R^2 = 0.405; p = 0.035) **(Figure 3.8 F) (Table 3.4)**.

Measurement	R^2	p-value
d'-score: Quiet	0.5770	0.0067
d'-score: 50 dB SPL background noise	0.4945	0.0158
Nose pokes/ trial: Quiet	0.4702	0.0198
Nose pokes/trial: 50 dB SPL background noise	0.4046	0.0354

Table 3.4 *Performance during the sound detection task was correlated with the degree of hearing loss (n=11 rats).*

3.3.4 Hearing loss does not necessarily result in impaired sound detection in quiet or in noisy background conditions.

To further investigate the effect of noise-induced hearing loss on the ability to detect

steady sound in quiet and in background conditions, the rats with mild hearing loss, i.e.,

exhibiting a threshold shift of ≤15 dB (n = 8), were separated from the rats that showed a

more severe hearing loss, i.e., a threshold shift of at least 25 dB (n = 3). Despite a

significantly decreased ABR wave I amplitude to an 80 dB SPL click stimulus as revealed by

the paired sample two-tailed t-test (pre-noise: 1.15 ± 0.06 vs. post-noise: 0.41 ± 0.09;

p_{Bonf} < 0.01) (**Figure 3.9A**) in the mild hearing loss group, the noise exposure did not affect

these rats' ability to detect *steady* sound in quiet nor in 50-dB SPL background noise

conditions (**Figure 3.9B**). Furthermore, their impulsivity was also not affected

(**Figure 3.9C**). Although the small size did not allow for statistical analyses in the rats with

the more severe hearing loss (n=3), their data indicate significant damage to their

cochleae (**Figure 3.9D**) and a worsened ability to detect the *steady* stimuli

(Figure 3.9E and F). Collectively, these results identify that, although noise exposure could

impair auditory detection if the level of peripheral damage was extensive, noise-induced

hearing loss *per se* was not necessarily sufficient to impair the rats' ability to detect *steady*

sounds in either a quiet or noisy background. The details of the statistical tests performed

in this experimental series are shown in **Table 3.5**.

Mild hearing loss < 25dB SPL threshold shift (n = 8)
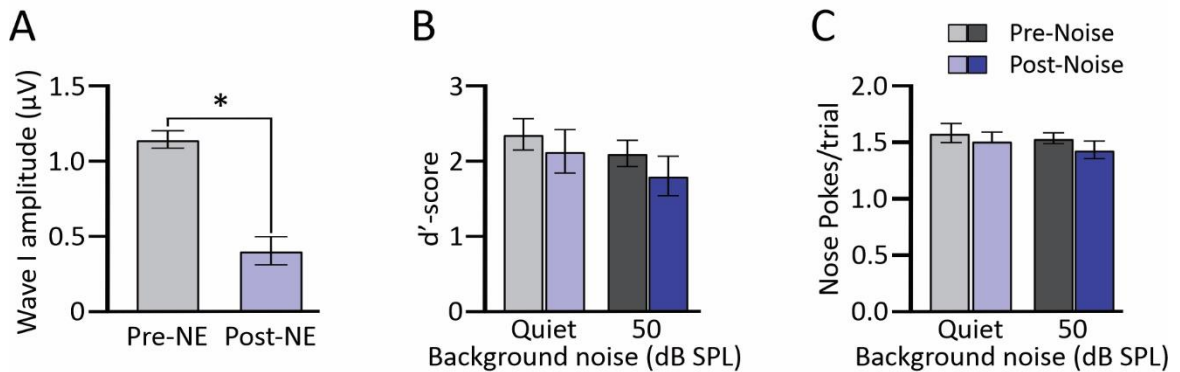
Severe hearing loss >/= 25dB SPL threshold shift (n = 3)
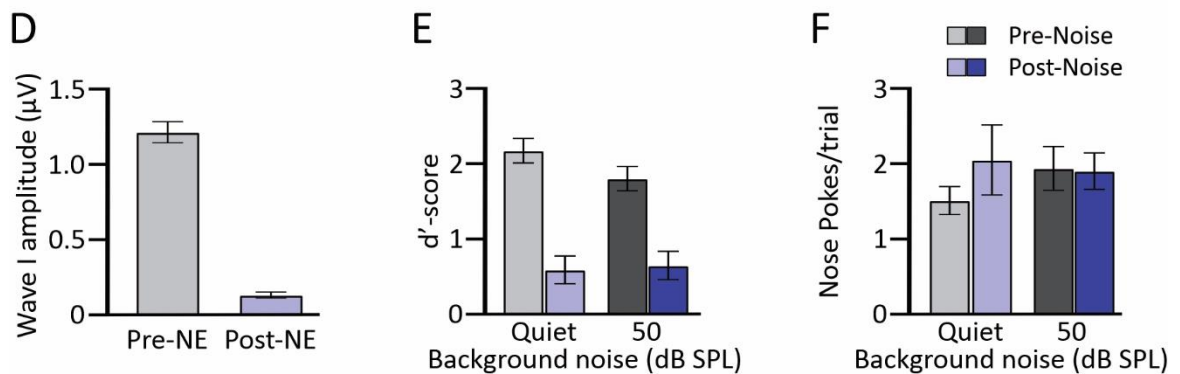
Figure 3.9 Rats with mild hearing loss did not show a decreased ability to detect steady sound in quiet or 50 dB background noise. (A) The group average of the wave I amplitude in rats with mild hearing loss (n=8) was significantly decreased (*p$_{Bonf}$ < 0.05), indicative of significant damage to the peripheral auditory pathway. (B) The rats with mild hearing loss (n=8) showed no change in their post-noise exposure performance on the steady sound detection task, as revealed by the group average of the d'-score. (C) Similarly, the rats' impulsivity was not affected following noise exposure (n=8). (D) For the rats with more severe hearing loss (n=3), their group average wave I amplitude was significantly reduced, indicating extensive peripheral damage. (E) Unlike the rats with mild hearing loss (n=8), rats with more severe hearing loss (n=3) showed impaired task performance in both the quiet and noisy background conditions, as well as a trend for increased impulsivity (F). However, due to the low sample size (n=3), it was not prudent to perform statistical analyses on the data collected from these rats (D-F). Data in all bar graphs represent group mean ± SEM.

Normality Data	p-value	Test	Main effects/ Comparison	p-value	F-/ t-
Figure 3.7 Hearing assessment					
Figure 3.7 A. Click stimulus ABR threshold (n=11)					
		2-way RM-ANOVA	Time (pre-noise, post-noise) *	<0.01	$F_{(1, 10)} = 27.40$
			Stimulus (click, 4 kHz, 20 kHz) *	0.01	$F_{(1.52, 15.25)} = 6.87$
			Interaction (time x stimulus) *	0.01	$F_{(1.96, 19.60)} = 5.02$
Pre [#]	0.02	Wilcoxon matched-	Click Stimulus	<0.01	
Post	0.73	pairs signed-rank	pre-noise vs. post-noise *		
Pre	0.054	Paired sample,	4 kHz tone stimulus	<0.01	t = 5.43; DF = 10
Post	0.12	two-tailed t-test	pre-noise vs. post-noise *		
Pre [#]	<0.01	Wilcoxon matched-	20 kHz tone stimulus	<0.01	
Post	0.058	pairs signed-rank	pre-noise vs. post-noise *		
Figure 3.7 B. Wave I amplitude (n=11)					
Pre	0.53	Paired sample,	Wave I Amplitude	<0.01	t = 11; DF = 10
Post	0.28	two-tailed t-test	pre-noise vs. post-noise *		
Figure 3.8 The effects of noise exposure on the sound detection task performance					
Figure 3.8 A. Performance (d'-score) (n=11)					
		2-way RM-ANOVA	Time (pre-noise, post-noise) *	0.049	$F_{(1, 10)} = 5.02$
			Background noise (Quiet, 50 dB SPL) *	0.045	$F_{(1, 10)} = 5.24$
			Interaction (time x background)	0.800	$F_{(1, 10)} = 0.07$
		Post-hoc	*d'-score* Quie*t* dB SPL (pre- vs. post-noise)*	0.01 [B]	t = 3.44; DF = 10
		Post-hoc	*d'-score* 50 dB SPL pre-vs. post-noise *	0.02 [B]	t = 3.08; DF = 10
Figure 3.8 D Impulsivity (nose pokes/trial) (n=11)					
		2-way RM-ANOVA	Time (pre-noise, post-noise)	0.90	$F_{(1, 10)} = 0.01$
			Background noise (Quiet, 50 dB SPL)	0.89	$F_{(1, 10)} = 0.02$
			Interaction (time x background)	0.27	$F_{(1, 10)} = 1.37$
Figure 3.9 The effects of mild hearing loss on the sound detection task performance					
Figure 3.9 A. Wave I amplitude in mild hearing loss group (n=8)					
Pre	0.43	Paired sample,	Wave I in mild hearing loss	<0.01	t = 9.50; DF = 7
Post	0.71	two-tailed t-test	pre-noise vs. post noise *		
Figure 3.9 B. Performance in mild hearing loss group (n=8)					
		2-way ANOVA	Time (pre-noise, post-noise)	0.35	$F_{(1, 7)} = 0.98$
			Background noise (Quiet, 50 dB SPL)	0.09	$F_{(1, 7)} = 3.94$
			Interaction (time x background)	0.82	$F_{(1, 7)} = 0.06$
Figure 3.9 C. Impulsivity in mild hearing loss group (n=8)					
		2-way ANOVA	Time (pre-noise, post-noise)	0.22	$F_{(1, 7)} = 1.79$
			Background (Quiet, 50 dB SPL)	0.11	$F_{(1, 7)} = 3.28$
			Interaction (time x background)	0.81	$F_{(1, 7)} = 0.06$

Table 3.5 *Summary of the statistical tests performed in the experimental series investigating sound detection ability following noise exposure [B] Bonferroni corrected p-value; * statistical significance; [#] violated normal distribution as assessed by the Shapiro-Wilk test for normal distribution; Pre: before noise-exposure; Post: after noise exposure.*

3.3.5 The presence of tinnitus was not sufficient to disrupt performance in the sound detection task in a quiet background.

This experimental series aimed to address the possibility that the decreased performance on the sound detection task following noise exposure could be affected by the presence of tinnitus. A paired sample two-tailed t-test revealed a significantly decreased ability to detect *steady* sound following the treatment with sodium salicylate (250mg/kg; IP) (saline: 2.09 ± 0.19 vs. SS: 1.25 ± 0.19; p = 0.03) **(Figure 3.10 A)** without affecting the impulsivity **(Figure 3.10 B; Table 3.6).**
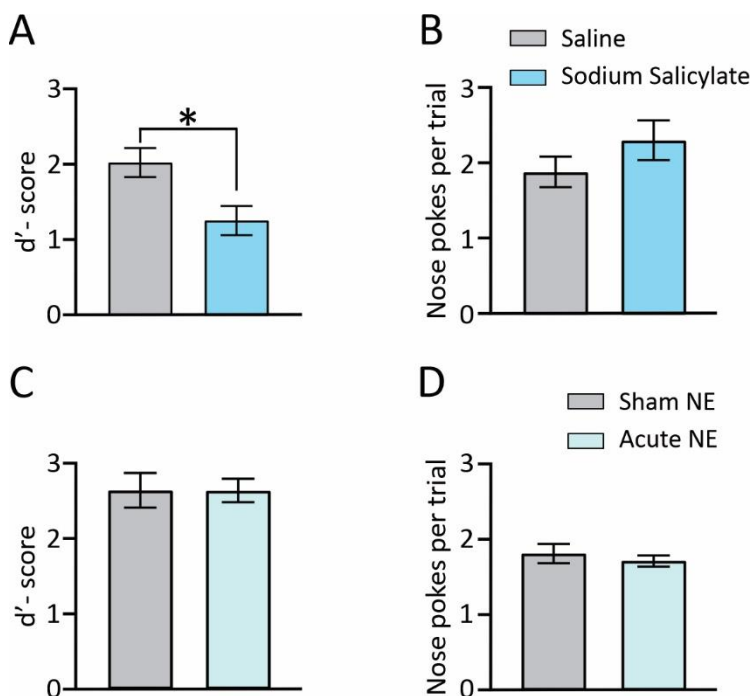
Figure 3.10 Sodium salicylate treatment, but not exposure to a loud tonal stimulus decreased performance on the steady sound detection task. (A) *As measured by their d'-score, the rats' performance decreased significantly (*p = 0.03) following sodium salicylate treatment (blue) as compared to the saline condition (grey).* ***(C)*** *In contrast, 15-minute exposure to a loud tonal stimulus (12 kHz tone at 112 dB SPL) did not affect task performance (teal) as compared to the sham condition (grey).* ***(B*** *and* ***D)*** *Neither the SS treatment (B) nor tone exposure (D) leads to significant changes in the rats' impulsivity. Data represent group mean ± SEM; n = 8 in each group*

Systemic treatment of sodium salicylate affects auditory processing and perception in ways beyond inducing tinnitus (Douek, Dodson and Bannister, 1983; Shehata, Brownell and Dieler, 1991; Wei, Ding and Salvi, 2010; Ciganović *et al.*, 2018; Zhang *et al.*, 2020), and

also disrupts other brain functions (Gong *et al.*, 2008; Azimi *et al.*, 2012; Chen, Manohar and Salvi, 2012). Thus, to investigate whether the presence of tinnitus was indeed sufficient to cause impaired performance on the sound detection task, a separate group of rats was subjected to a 15-min exposure of a loud tonal stimulus (112 dB SPL; 12 kHz); a protocol that was shown previously in our lab to invariably induce tinnitus (Hayes et al., 2020). Interestingly, neither the rats' ability to detect the *steady* stimulus (**Figure 3.10C**) nor their impulsivity (**Figure 3.10D**) was affected by the tone exposure. Taken together, the results of this experiment indicate that the presence of tinnitus was not sufficient to affect performance on the sound detection task. The detailed results of the statistical analysis performed in this experimental series are presented in **Table 3.6.**

Normality test Data	p-value	Test	Comparison	p-value	t-value; DF
Figure 3.10					
Figure 3.10 A. The effect of sodium salicylate on the sound detection task					
Saline	0.87	Paired sample,	*d'-score*	0.03	t = 2.75; DF = 7
SS	0.99	two-tailed t-test	*Saline vs. Sodium Salicylate* *		
Figure 3.10 B. Impulsivity following sodium salicylate treatment					
Saline	0.07	Wilcoxon matched-pairs	Nose Pokes	0.19	
SS [#]	0.04	signed-rank	Saline vs. Sodium Salicylate		
Figure 3.10 C. The effect of 15-min exposure to a loud tonal stimulus on the sound detection task					
Sham	0.55	Paired sample,	*d'-score*	0.99	t = 0.01; DF = 7
Noise	0.41	two-tailed t-test	Sham vs. Loud Tone		
Figure 3.10 D. Impulsivity following 15-min exposure to a loud tonal stimulus					
Sham	0.71	Paired sample,	Nose Pokes	0.47	t = 0.75; DF = 7
Noise	0.95	two-tailed t-test	Sham vs. Loud Tone		

Table 3.6 *Summary of the statistical tests performed during the investigation of tinnitus effects on sound detection.* [#] *Violated normal distribution as assessed by the Shapiro-Wilk test for normality;* *Statistical significance*

3.4 Discussion

Overall, the present study successfully established a novel sound detection task sensitive to increasing levels of background noise. Furthermore, this study investigated the effects of permanent noise-induced hearing loss on sound detection ability in background noise. The data revealed that although the degree of hearing loss was significantly correlated with the sound detection accuracy, mild hearing loss (5-15 dB threshold shift) did not

necessarily lead to significant deficits in performance. This study also showed that the presence of tinnitus was not sufficient to affect performance on this task. Finally, although the degree of hearing loss was significantly correlated with the increased impulsivity, the comparison between the group averages failed to reach significance, and as such, whether there are effects of noise exposure on impulsivity and attention warrant further investigation.

3.4.1 Increased background noise decreased performance on the sound detection task

As expected, the novel sound detection task established in this study proved to be sensitive to the increasing level of background noise. Interestingly, although rats' performance measured by the *d'-score* was significantly decreased with the background noise above 65 dB SPL (i.e., 10 dB signal-to-noise ratio), their impulsivity, as assessed by the number of nose-pokes per trial, was not affected. These results indicate that the observed effect reflected rats' inability to distinguish between the target *steady* sound and the *other* distractors in background noise rather than an attentional deficit.

3.4.2 Noise-induced hearing loss was correlated with but did not necessarily lead to poor performance on the sound detection task

The degree of noise-induced hearing loss was correlated with the accuracy of the sound detection measured by the *d'-score* for both quiet and 50 dB SPL background conditions. Although the total group average significantly worsened performance in quiet and background conditions, these effects disappeared after excluding the three animals exhibiting the more severe hearing loss (i.e. ≥ 25 dB threshold shift). Thus, these results suggest that despite significant hearing impairment as evident by the threshold shift and reduced ABR wave I amplitude, rats with the mild hearing loss could still accurately detect the sounds used in the task, even in background noise. The present findings contrast a previous study on rats investigating cochlear trauma on auditory processing in noisy environments. In 2017, Lobarinas and colleagues found that rats with noise-induced

cochlear synaptopathy (i.e., defined by the authors as a reduced wave I amplitude, despite normal hearing thresholds post-exposure) exhibited a decreased ability to hear in noise (Lobarinas, Spankovich and Le Prell, 2017). The discrepancy between this past study and the current investigation may originate from the different approaches used to assess the rats' ability to hear in noise. While the experiments described in this thesis evaluated the ability to detect sound in noise through a conditioning-based two-alternative forced-choice task, the study by Lobarinas et al. (2017) assessed the ability to hear a stimulus in background noise through a modified sensorimotor gating protocol. Briefly, in the presence of constant background noise, the narrowband noise burst served as a prepulse to a startling tactile stimulus elicited by an air puff. The magnitude of prepulse inhibition was used to assess the rats' ability to hear the target stimulus. Consequently, the decreased level of startle response attenuation was indicative of impaired ability to hear in noise (Lobarinas, Spankovich and Le Prell, 2017). Thus, unlike the operant conditioning-based behavioural task described in this thesis, the modified prepulse inhibition of the startle response is based on a pre-attentive response to a sensory stimulus. Adding to the perceptual differences between the two tasks, another possible explanation for the disparate results between the present experiments and the study by Lobarinas et al. (2017) might be the level of task difficulty. The signal-to-noise ratio used in the present study was 25 dB. In contrast, Lobarinas et al. (2017) found a significant performance deficit in the 20 dB signal-to-noise ratio conditions, a more challenging listening condition than was investigated in the present experiments.

3.4.3 Noise-induced hearing loss was correlated with increased impulsivity

The noise exposure used in this study has been shown to induce significant plasticity within the mPFC as well as a loss of functional connectivity between the auditory cortex and mPFC (Chapter 2, (Wieczerzak *et al.*, 2020)). Furthermore, animal studies have shown that both of these brain regions are engaged in auditory tasks, especially in scenarios requiring increased attention, e.g., background noise (Fritz, Elhilali and Shamma, 2007; Atiani *et al.*, 2009; Fritz *et al.*, 2010). Therefore, it was possible that the noise exposure

might result in an attentional impairment, and consequently sound detection deficits, that were independent of the degree of hearing loss. As mentioned above, however, the rats' detection accuracy was significantly correlated with their hearing loss, indicating that primary sensory processing deficits, rather than solely changes at the level of the mPFC, contributed to their task performance. In line with this conclusion, at the level of the whole cohort of rats, noise exposure did not cause a significant change in the rats' impulsivity—a behavioural effect which is known to depend on mPFC activity (Murphy *et al.*, 2012; Feja and Koch, 2014). That said, there was a significant correlation between the degree of hearing loss and increased impulsivity during the detection task. This association could perhaps imply that rats with a more severe hearing loss exhibited some attentional deficits. If confirmed, this finding would be in line with clinical studies reporting that long-term exposure to noise leads to impaired attention control and increased distractibility (Kujala *et al.*, 2004). Ultimately, given that we found that degree of hearing loss was correlated to impulsivity, yet not all of the noise-exposed rats showed increased impulsivity, future studies are warranted to investigate whether it was simply the magnitude of peripheral damage that contributed to the increased impulsivity, or if noise exposure also causes neural plasticity in higher-order cortical regions that directly contributes to attentional deficits.

3.4.4 Tinnitus and sound detection

In the present study, the possible confounding effects of tinnitus on sound detection were studied using sodium salicylate and a brief exposure to a loud sound; two well-known tinnitus inducers (Yang *et al.*, 2007; Turner Jeremy G. and Parrish Jennifer, 2008; Hayes *et al.*, 2020). The results were conflicting, as the systemic injection of sodium salicylate led to a decrease in the rats' ability to perform sound detection, whereas exposure to a loud sound did not impair task performance. These data suggest that the presence of tinnitus itself does not necessarily interfere with the ability to detect sounds in an otherwise quiet environment. Consistent with these findings are recent observations from a clinical study indicating that when controlled for other factors such as hearing loss, age, and stimulus

variables, the presence of tinnitus itself does not interfere with auditory perception (Zeng, Richardson and Turner, 2020).

Why did the task performance results differ between exposure to sodium salicylate versus loud sound? Although both sodium salicylate and exposure to loud sounds are known to induce tinnitus, they likely have differential mechanisms, contributing to a different set of perceptual deficits beyond phantom auditory perception. The detrimental effects of sodium salicylate on the auditory systems have been extensively studied. For example, the consequences of a high dose of sodium salicylate extend beyond merely inducing tinnitus and include ototoxic effects on sensory hair cells within the cochlea that ultimately lead to peripheral hearing loss (Douek, Dodson and Bannister, 1983; Shehata, Brownell and Dieler, 1991; Wei, Ding and Salvi, 2010; Ciganović *et al.*, 2018; Zhang *et al.*, 2020). It is also important to note that due to the systemic administration of the sodium salicylate, it is impossible to conclude that this experiment's behavioural effects originated solely from dysfunction in the auditory system. Sodium salicylate also affects brain regions outside of the auditory pathway, such as the amygdala, striatum, hippocampus, dorsal raphe nucleus (Gong *et al.*, 2008; Azimi *et al.*, 2012; Chen, Manohar and Salvi, 2012). Considering the specific effects of sodium salicylate in the cochlea, i.e., blocking outer hair cell electromotility (Shehata, Brownell and Dieler, 1991; Ciganović *et al.*, 2018) as well as its broad actions on neurons throughout various brain regions (Gong *et al.*, 2008; Su *et al.*, 2009), it is not unreasonable to suggest that the deficits in sound detection observed in the present study were independent of the presence of tinnitus. Indeed, while both the chosen sound exposure and sodium salicylate dose were shown previously in our lab to induce tinnitus (Hayes *et al.*, 2020), the mechanisms contributing to the phantom perception induced in both cases might be fundamentally different. It is possible that this mechanistic difference contributed to the negative effect of sodium salicylate, but not intense sound exposure, on sound detection ability.

3.5 References

Adriani, W. *et al.* (2003) 'The spontaneously hypertensive-rat as an animal model of ADHD: evidence for impulsive and non-impulsive subpopulations', *Neuroscience & Biobehavioral Reviews*, 27(7), pp. 639–651. doi: 10.1016/j.neubiorev.2003.08.007.

Agrawal, Y., Platz, E. A. and Niparko, J. K. (2008) 'Prevalence of hearing loss and differences by demographic characteristics among US adults: data from the National Health and Nutrition Examination Survey, 1999-2004', *Archives of Internal Medicine*, 168(14), pp. 1522–1530. doi: 10.1001/archinte.168.14.1522.

Atiani, S. *et al.* (2009) 'Task Difficulty and Performance Induce Diverse Adaptive Patterns in Gain and Shape of Primary Auditory Cortical Receptive Fields', *Neuron*, 61(3), pp. 467–480. doi: 10.1016/j.neuron.2008.12.027.

Azimi, L. *et al.* (2012) 'Effects of Peripheral and Intra-hippocampal Administration of Sodium Salicylate on Spatial Learning and Memory of Rats', *Iranian Journal of Basic Medical Sciences*, 15(2), pp. 709–718.

Carroll, Y. I. *et al.* (2017) 'Vital Signs: Noise-Induced Hearing Loss Among Adults — United States 2011–2012', *MMWR. Morbidity and Mortality Weekly Report*, 66(5), pp. 139–144. doi: 10.15585/mmwr.mm6605e3.

Ch, Jain, N. and Sahoo, J. P. (2014) 'The effect of tinnitus on some psychoacoustical abilities in individuals with normal hearing sensitivity', *The International Tinnitus Journal*, 19(1), pp. 28–35.

Chen, G.-D., Manohar, S. and Salvi, R. (2012) 'Amygdala hyperactivity and tonotopic shift after salicylate exposure', *Brain Research*, 1485, pp. 63–76. doi: 10.1016/j.brainres.2012.03.016.

Ciganović, N. *et al.* (2018) 'Static length changes of cochlear outer hair cells can tune low-frequency hearing', *PLOS Computational Biology*, 14(1), p. e1005936. doi: 10.1371/journal.pcbi.1005936.

Doremus-Fitzwater, T. L., Barreto, M. and Spear, L. P. (2012) 'Age-related differences in impulsivity among adolescent and adult Sprague-Dawley rats', *Behavioral Neuroscience*, 126(5), pp. 735–741. doi: 10.1037/a0029697.

Douek, E. E., Dodson, H. C. and Bannister, L. H. (1983) 'The effects of sodium salicylate on the cochlea of guinea pigs', *The Journal of Laryngology & Otology*, 97(9), pp. 793–799. doi: 10.1017/S0022215100095025.

Duque, A. and McCormick, D. A. (2010) 'Circuit-based Localization of Ferret Prefrontal Cortex', *Cerebral Cortex*, 20(5), pp. 1020–1036. doi: 10.1093/cercor/bhp164.

Economidou, D. *et al.* (2009) 'High Impulsivity Predicts Relapse to Cocaine-Seeking After Punishment-Induced Abstinence', *Biological Psychiatry*, 65(10), pp. 851–856. doi: 10.1016/j.biopsych.2008.12.008.

Eggermont, J. J. and Roberts, L. E. (2004) 'The neuroscience of tinnitus', *Trends in Neurosciences*, 27(11), pp. 676–682. doi: 10.1016/j.tins.2004.08.010.

Feja, M. and Koch, M. (2014) 'Ventral medial prefrontal cortex inactivation impairs impulse control but does not affect delay-discounting in rats', *Behavioural Brain Research*, 264, pp. 230–239. doi: 10.1016/j.bbr.2014.02.013.

Fournier, P. and Hébert, S. (2013) 'Gap detection deficits in humans with tinnitus as assessed with the acoustic startle paradigm: Does tinnitus fill in the gap?', *Hearing Research*, 295, pp. 16–23. doi: 10.1016/j.heares.2012.05.011.

Fritz, J. B. *et al.* (2010) 'Adaptive, behaviorally gated, persistent encoding of task-relevant auditory information in ferret frontal cortex', *Nature Neuroscience*, 13(8), pp. 1011–1019. doi: 10.1038/nn.2598.

Fritz, J. B., Elhilali, M. and Shamma, S. A. (2007) 'Adaptive Changes in Cortical Receptive Fields Induced by Attention to Complex Sounds', *Journal of Neurophysiology*, 98(4), pp. 2337–2346. doi: 10.1152/jn.00552.2007.

Gong, N. *et al.* (2008) 'The aspirin metabolite salicylate enhances neuronal excitation in rat hippocampal CA1 area through reducing GABAergic inhibition', *Neuropharmacology*, 54(2), pp. 454–463. doi: 10.1016/j.neuropharm.2007.10.017.

Hayes, S. H. *et al.* (2020) 'Uncovering the contribution of enhanced central gain and altered cortical oscillations to tinnitus generation', *Progress in Neurobiology*, p. 101893. doi: 10.1016/j.pneurobio.2020.101893.

Jiang, C. *et al.* (2017) 'Plastic changes along auditory pathway during salicylate-induced ototoxicity: Hyperactivity and CF shifts', *Hearing Research*, 347, pp. 28–40. doi: 10.1016/j.heares.2016.10.021.

Kujala, T. *et al.* (2004) 'Long-term exposure to noise impairs cortical sound processing and attention control', *Psychophysiology*, 41(6), pp. 875–881. doi: https://doi.org/10.1111/j.1469-8986.2004.00244.x.

Lobarinas, E., Spankovich, C. and Le Prell, C. G. (2017) 'Evidence of "hidden hearing loss" following noise exposures that produce robust TTS and ABR wave-I amplitude

reductions', *Hearing Research*, 349, pp. 155–163. doi: 10.1016/j.heares.2016.12.009.

Murphy, E. R. *et al.* (2012) 'Impulsive behaviour induced by both NMDA receptor antagonism and GABAA receptor activation in rat ventromedial prefrontal cortex', *Psychopharmacology*, 219(2), pp. 401–410. doi: 10.1007/s00213-011-2572-1.

O'mahony, M. (1992) 'Understanding Discrimination Tests: A User-Friendly Treatment of Response Bias, Rating and Ranking R-Index Tests and Their Relationship to Signal Detection', *Journal of Sensory Studies*, 7(1), pp. 1–47. doi: https://doi.org/10.1111/j.1745-459X.1992.tb00519.x.

Popelar, J. *et al.* (2008) 'Comparison of noise-induced changes of auditory brainstem and middle latency response amplitudes in rats', *Hearing Research*, 245(1), pp. 82–91. doi: 10.1016/j.heares.2008.09.002.

Popelář, J., Syka, J. and Berndt, H. (1987) 'Effect of noise on auditory evoked responses in awake guina pigs', *Hearing Research*, 26(3), pp. 239–247. doi: 10.1016/0378-5955(87)90060-8.

Roberts, L. E. *et al.* (2010) 'Ringing Ears: The Neuroscience of Tinnitus', *Journal of Neuroscience*, 30(45), pp. 14972–14979. doi: 10.1523/JNEUROSCI.4028-10.2010.

Salvi, R. *et al.* (2017) 'Inner Hair Cell Loss Disrupts Hearing and Cochlear Function Leading to Sensory Deprivation and Enhanced Central Auditory Gain', *Frontiers in Neuroscience*, 10. doi: 10.3389/fnins.2016.00621.

Schormans, A. L., Typlt, M. and Allman, B. L. (2017) 'Crossmodal plasticity in auditory, visual and multisensory cortical areas following noise-induced hearing loss in adulthood', *Hearing Research*, 343, pp. 92–107. doi: 10.1016/j.heares.2016.06.017.

Schormans, A. L., Typlt, M. and Allman, B. L. (2019) 'Adult-Onset Hearing Impairment Induces Layer-Specific Cortical Reorganization: Evidence of Crossmodal Plasticity and Central Gain Enhancement', *Cerebral Cortex*, 29(5), pp. 1875–1888. doi: 10.1093/cercor/bhy067.

Seamans, J. K., Lapish, C. C. and Durstewitz, D. (2008) 'Comparing the prefrontal cortex of rats and primates: Insights from electrophysiology', *Neurotoxicity Research*, 14(2), pp. 249–262. doi: 10.1007/BF03033814.

Shehata, W. E., Brownell, W. E. and Dieler, R. (1991) 'Effects of Salicylate on Shape, Electromotility and Membrane Characteristics of Isolated Outer Hair Cells from

Guinea Pig Cochlea', *Acta Oto-Laryngologica*, 111(4), pp. 707–718. doi: 10.3109/00016489109138403.

Stanislaw, H. and Todorov, N. (1999) 'Calculation of signal detection theory measures', *Behavior Research Methods, Instruments, & Computers*, 31(1), pp. 137–149. doi: 10.3758/BF03207704.

Stolzberg, D. *et al.* (2013) 'A novel behavioral assay for the assessment of acute tinnitus in rats optimized for simultaneous recording of oscillatory neural activity', *Journal of Neuroscience Methods*, 219(2), pp. 224–232. doi: 10.1016/j.jneumeth.2013.07.021.

Su, Y.-Y. *et al.* (2009) 'Differential effects of sodium salicylate on current-evoked firing of pyramidal neurons and fast-spiking interneurons in slices of rat auditory cortex', *Hearing Research*, 253(1), pp. 60–66. doi: 10.1016/j.heares.2009.03.007.

Syka, J., Rybalko, N. and Popelář, J. (1994) 'Enhancement of the auditory cortex evoked responses in awake guinea pigs after noise exposure', *Hearing Research*, 78(2), pp. 158–168. doi: 10.1016/0378-5955(94)90021-3.

Tak, S., Davis, R. R. and Calvert, G. M. (2009) 'Exposure to hazardous workplace noise and use of hearing protection devices among US workers—NHANES, 1999–2004', *American Journal of Industrial Medicine*, 52(5), pp. 358–371. doi: https://doi.org/10.1002/ajim.20690.

Turner, J. *et al.* (2006) 'Gap detection deficits in rats with tinnitus: A potential novel screening tool.', *Behavioral Neuroscience*, 120(1), pp. 188–195. doi: https://doi.org/10.1037/0735-7044.120.1.188.

Turner Jeremy G. and Parrish Jennifer (2008) 'Gap Detection Methods for Assessing Salicylate-Induced Tinnitus and Hyperacusis in Rats', *American Journal of Audiology*, 17(2), pp. S185–S192. doi: 10.1044/1059-0889(2008/08-0006).

Wei, L., Ding, D. and Salvi, R. (2010) 'Salicylate-induced degeneration of cochlea spiral ganglion neurons-apoptosis signaling', *Neuroscience*, 168(1), pp. 288–299. doi: 10.1016/j.neuroscience.2010.03.015.

Wieczerzak, K. B. *et al.* (2020) 'Differential Plasticity in Auditory and Prefrontal Cortices, and Cognitive-Behavioral Deficits Following Noise-Induced Hearing Loss', *Neuroscience*. doi: 10.1016/j.neuroscience.2020.11.019.

Yang, G. *et al.* (2007)' Salicylate induced tinnitus: Behavioral measures and neural activity in auditory cortex of awake rats', *Hearing Research*, 226(1), pp. 244–253. doi: 10.1016/j.heares.2006.06.013.

Yin, P., Fritz, J. B. and Shamma, S. A. (2014) 'Rapid Spectrotemporal Plasticity in Primary Auditory Cortex during Behavior', *Journal of Neuroscience*, 34(12), pp. 4396–4408. doi: 10.1523/JNEUROSCI.2799-13.2014.

Zeng, F.-G., Richardson, M. and Turner, K. (2020) 'Tinnitus Does Not Interfere with Auditory and Speech Perception', *Journal of Neuroscience*, 40(31), pp. 6007–6017. doi: 10.1523/JNEUROSCI.0396-20.2020.

Zhang, W. *et al.* (2020) *Loss of Cochlear Ribbon Synapse Is a Critical Contributor to Chronic Salicylate Sodium Treatment-Induced Tinnitus without Change Hearing Threshold*, *Neural Plasticity*. Hindawi. doi: https://doi.org/10.1155/2020/3949161.

Chapter 4

4. The Effects of Medial Prefrontal Cortex Inactivation on Auditory Processing and Perception

4.1. Introduction

The prefrontal cortex plays an essential role in many higher executive functions, including working memory, attention, decision-making, and emotion (Groenewegen and Uylings, 2000; Miller and Cohen, 2001; Dalley, Cardinal and Robbins, 2004; Wise, 2008). Furthermore, consistent with its suggested role in top-down modulation, numerous past studies have indicated that the prefrontal cortex can significantly influence sensory processing and perception (Shimamura, 2000; Miller and Cohen, 2001; Bizley and Cohen, 2013). For example, the prefrontal cortex is crucial for inhibiting distracting information, such as background noise during an auditory working memory task, as patients with prefrontal lesions show an impaired ability to focus attention on task-relevant stimuli (Knight *et al.*, 1981; Woods and Knight, 1986; Damasio and Anderson, 2003). Furthermore, clinical studies also showed an increased sound-evoked response in patients with prefrontal lesions (Knight *et al.*, 1999). That said, the extent that top-down modulation from the prefrontal cortex affects resting state activity in the auditory cortex is not well understood, and it is unclear if other passively recorded, sound-evoked activity from the auditory cortex, such as the 40-Hz auditory steady-state response or mismatch response to oddball stimuli, are affected by disruptions to the prefrontal cortex. It is possible that the top-down modulation of auditory processing may not be restricted to tasks requiring perception or decision-making, as animal studies report conflicting results of the involvement of prefrontal cortex in the pre-attentive sound processing, such as sensorimotor gating of the acoustic startle response (Davis and Gendelman, 1977; Fox, 1979; Koch and Bubser, 1994; Lacroix *et al.*, 2000; Uehara *et al.*, 2007). Overall, to address these gaps in knowledge, the goal of the current study was to conduct a comprehensive investigation into the nature and extent that the medial prefrontal cortex (mPFC)

influences auditory processing and perception in a rat model through examining the effects of pharmacological inactivation of the mPFC (via muscimol) on: 1) sound detection in quiet and in background noise; 2) acoustic startle response and its modulation; and 3) the neurophysiological activity within the auditory cortex via metrics associated with spontaneous gamma oscillations, 40-Hz auditory steady-state response and mismatch response. Additional rationale for each of these experimental series are outlined in the following paragraphs.

Animal studies have revealed that the ability to detect sounds in noise depends not only on the way neurons adapt to the stimulus statistics but also on the level of attention to the task (Fritz, Elhilali and Shamma, 2007; Atiani *et al.*, 2009; Yin, Fritz and Shamma, 2014). In line with those behavioural reports, recordings from the primary cortical neurons within the auditory cortex of ferrets trained to discriminate tones in background noise show that the gain and shape of those neurons' spectrotemporal receptive field changed within minutes of commencing the task in background noise, perhaps improving the perceptual discrimination. As this change was correlated with the ferret's task performance requiring attention to the stimulus, it was concluded that the transient neural adaptation enhanced the contrast between the target stimuli and the background noise, indicating the effect of attention and the possible role of higher-order cortical regions in discriminating sounds in noise (Atiani *et al.*, 2009). Another study in ferrets has shown that during an auditory attention task, the auditory cortex and frontal cortex areas (corresponding to primate's dorsolateral prefrontal cortex (Duque and McCormick, 2010) thus homologous to the rodent mPFC (Seamans, Lapish and Durstewitz, 2008)), establish functional connectivity (Fritz *et al.*, 2010). Furthermore, a study in rats trained to respond to a target sound within other sounds, showed that the activity within the mPFC encoded the selection rule (Rodgers and DeWeese, 2014). Moreover, the same study also revealed that electrical disruption of the mPFC, significantly impaired performance on this task, further indicating a significant role of the mPFC in auditory selective attention (Rodgers

and DeWeese, 2014). That said, how an inactivation of the mPFC would affect sound detection in quiet and noisy background conditions has not been studied.

The neural basis of acoustic startle response has been extensively studied, with crucial structures identified within the brainstem circuitry (Koch and Schnitzler, 1997; Koch, 1999). The attenuation of the startle response upon repeated presentation of the same stimulus, i.e., *short-term habituation*, is considered a result of synaptic depression due to repeated stimulation (Fox, 1979; Leaton, Cassella and Borszcz, 1985; Zaman *et al.*, 2017). In line with these views is evidence from studies showing intact short-term habituation following decerebration and prefrontal lesions (Leaton, Cassella and Borszcz, 1985). Although these studies confirm that the prefrontal cortex and higher-order cortical regions are not *necessary* for short-term habituation to occur, they do not rule out that these brain regions influence short-term habituation via top-down modulatory effects (Koch, 1999). Furthermore, although the leading theory stands that neural circuits mediating the prepulse inhibition reside within the brainstem, studies show conflicting results. Although decerebration studies (Davis and Gendelman, 1977; Fox, 1979; Li and Frost, 2000) show no effect on prepulse inhibition; others report that the extensive inactivation of the prefrontal cortex significantly disrupted prepulse inhibition (Koch and Bubser, 1994; Lacroix *et al.*, 2000; Uehara *et al.*, 2007).

Numerous studies have reported noise-induced central gain enhancement (i.e., increased sound-evoked responses) throughout the auditory pathway, particularly the auditory cortex (Salvi *et al.*, 2017; Möhrle *et al.*, 2019; Hayes *et al.*, 2020); however, the underlying mechanisms are still not fully understood. Research has focused little on the role of higher-level brain regions, such as the prefrontal cortex, in contributing to central gain enhancement at the auditory cortex level. For example, the prefrontal cortex is known to exert inhibitory output to multiple cortical and subcortical regions (Edinger, Siegel and Troiano, 1975; Alexander, Newman and Symmes, 1976), and it has been shown to gate input to primary sensory cortices (Skinner, 1984). Moreover, clinical studies have revealed that patients with unilateral prefrontal lesions exhibit increased sound-evoked responses.

These results indicate that the prefrontal cortex exerts early inhibitory modulation of input to the primary auditory cortex in humans (Knight et al., 1999). It provides support for further investigating whether altered activity in the prefrontal cortex could indeed contribute to central gain enhancement in the auditory cortex.

Alterations to prefrontal cortex function are thought to play a crucial role in the etiology of schizophrenia (Selemon, 2001; Weinberger *et al.*, 2001; Cannon *et al.*, 2005). Interestingly, clinical studies show altered gamma oscillations in patients with schizophrenia, including the spontaneous (e.g., Cho and Lewis, 2015; Hirano *et al.*, 2015; Grent-'t-Jong *et al.*, 2018, Baradits *et al.*, 2019; for review: Uhlhaas and Singer, 2010; Gonzalez-Burgos,) as well as sound-evoked gamma oscillation measured via the metrics of 40-Hz auditory steady-state response (Thuné, Recasens and Uhlhaas, 2016; Kim *et al.*, 2019; for review: Tada *et al.*, 2020). To date, however, the contribution of the prefrontal cortex to neurophysiological responses in the auditory cortex has not been studied in detail. Furthermore, despite theorized and empirical evidence of higher-order brain regions' involvement in generating the mismatch response (Alho *et al.*, 1994; Alho, 1995; Carbajal and Malmierca, 2018), the contribution of the prefrontal cortex is still relatively unknown. Interestingly, a clinical study reported a decrease in mismatch response in patients with prefrontal lesions, which was also correlated with a decreased performance in detecting between the standard and deviant stimulus (Alho *et al.*, 1994). Together, these findings indicate that the prefrontal cortex might play an essential role in generating the mismatch response, allowing for detection of deviance from the repetitive standard stimuli. That said, this hypothesis has not been extensively studied and has not yet been confirmed in an animal model.

Overall, the current study presents a series of experiments on adult rats that examined behavioural and neurophysiological aspects of the auditory perception and processing following the pharmacological inactivation of the mPFC through a local infusion of muscimol. More specifically, using a chronically implanted bilateral cannulae, this study examined the effects of local mPFC infusions of muscimol on sound detection in a quiet

and noisy background, as well as on features of the acoustic startle response (i.e., acoustic reactivity, sensory filtering and sensorimotor gating). Additionally, using a chronically implanted electrode, neurophysiological responses in the auditory cortex were examined via metrics associated with spontaneous gamma oscillation, the 40-Hz auditory steady-state response, and mismatch response following the same pharmacological intervention. Ultimately, this study revealed sound detection deficits following the mPFC inactivation, which were exaggerated by background noise, and correlated with increased impulsivity. Furthermore, although the initial sound-evoked response in the auditory cortex was unaffected by muscimol infusion in mPFC, the higher-order auditory processing was disrupted, as evident by the diminished deviant response effect in the late-latency response to the oddball stimulus. Finally, although the inactivation of the mPFC did not affect the ability of the auditory cortex to entrain to sound-evoked gamma oscillations, the spontaneous gamma oscillations were significantly decreased.

4.2 Materials and Methods

4.2.1 Animals and Experimental Design

Adult male Sprague Dawley rats (Charles River Laboratories Inc., Wilmington, MA, USA, ~90 days old) were used in three experimental series to investigate the role of the mPFC in auditory processing and perception. A within-subject design was used throughout the entire study, in which electrophysiological and behavioural measures were compared in the same animals after bilaterally infusing into mPFC various pharmacological treatments: (1) artificial cerebrospinal fluid (aCSF); (2) 0.5 mM and (3) 1.0 mM muscimol. The first experimental series (n = 8 rats) assessed the role of mPFC in sound detection in quiet and in background noise **(Figure 4.1A)**. The second experimental series used a group of rats (n = 14) to investigate the effect of inactivation of the mPFC on brainstem-mediated acoustic reactivity, sensory filtering, and sensorimotor gating **(Figure 4.1B)**. Using chronically implanted electrodes, the last experimental series (n = 13) investigated the effects of mPFC inactivation on (1) spontaneous gamma oscillation activity within the auditory

cortex; (2) the ability of neurons in the auditory cortex to entrain to the acoustically induced gamma frequency (40-Hz ASSR); and (3) mismatch responses to oddball stimulation paradigms **(Figure 4.1C)**. All behavioural and electrophysiological procedures were approved by the University of Western Ontario Animal Care and use Committee and were per guidelines established by the Canadian Council of Animal Care.
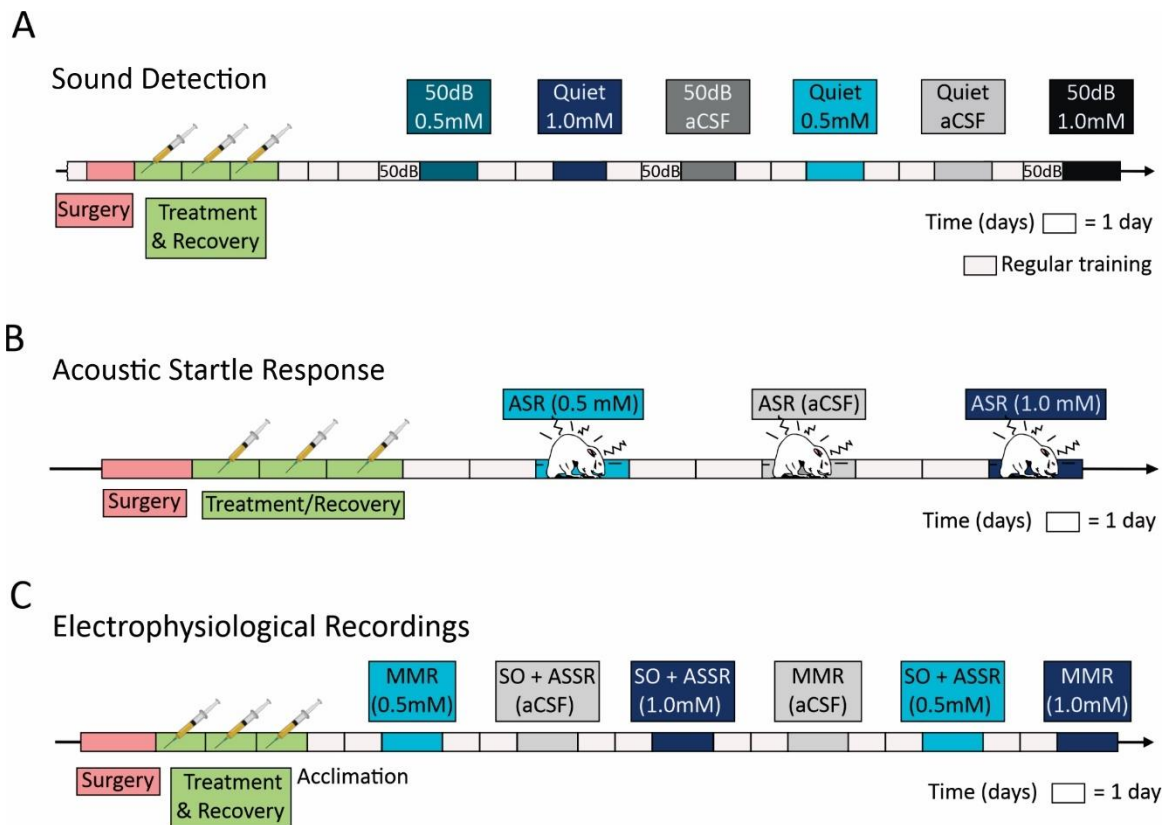
Figure 4.1 Experimental timelines. *Examples of timelines for the three experimental series performed in this study investigating the effects of medial prefrontal cortex inactivation on **(A)** sound detection in quiet and in 50 dB SPL background noise, **(B)** acoustic startle response and **(C)** electrophysiological recordings. In all three studies, the order of treatments was pseudo-randomized between the animals.*

4.2.2 Surgery Procedures

Rats were anesthetized with isoflurane (induction: 4%; maintenance: 2%), and body temperature was maintained at 37°C using a homeothermic heating pad (507220F; Harvard Apparatus) throughout the procedure. Subcutaneous injection of meloxicam (1 mg/kg) was administered before surgery. Once a surgical plane of anesthesia was

achieved, rats were placed in a stereotaxic frame with blunt ear bars, and a midline incision was made in the scalp, and the dorsal aspect of the skull was cleaned with a scalpel blade. After small burr holes were drilled in the skull, stainless-steel bilateral guide cannulae (62069; outer diameter: 0.41 mm; length: 3.5 mm; RWD Life Science Inc. San Diego, CA, USA) was implanted to target the anterior cingulate of the medial prefrontal cortex (3.7 mm rostral to bregma; 0.8 mm lateral from midline; 2.5 mm ventral from the surface of the skull **(Figure 4.2)**). This guide cannula was secured to the skull using dental cement and bone screws as anchors. A dummy cannula (62169; RWD Life Science Inc. San Diego, CA, USA) was placed into the guide cannula to prevent blockage.

Furthermore, the rats undergoing the electrophysiological experiments were additionally implanted with epidural screw electrodes (E363-20; PlasticsOne Inc., Roanoke, VA, USA) over the left auditory cortex (4.3 mm caudal to bregma and 4.5 mm ventral to the dorsal surface of the skull), and over the cerebellum (2.0 mm caudal to lambda and 2.0 mm lateral to the midline), which served as the reference/ground electrode (Paxinos and Watson, 2006). The connector pins from the electrodes were fed into a pedestal (MS363; PlasticsOne Inc.) secured to the skull with dental cement. The scalp wound was sutured using standard techniques. Following the surgery, the rats were monitored until they became ambulatory. Rats were administered Metacam (1 mg/kg, subcutaneously) and Baytril (10 mg/kg, subcutaneously) for the next three days, and their body mass and appearance were closely monitored for seven days.

3.7mm RC
0.8mm ML
-2.5mm DV (end of the guide cannula)
-4.0mm DV (end of the infusion cannula)
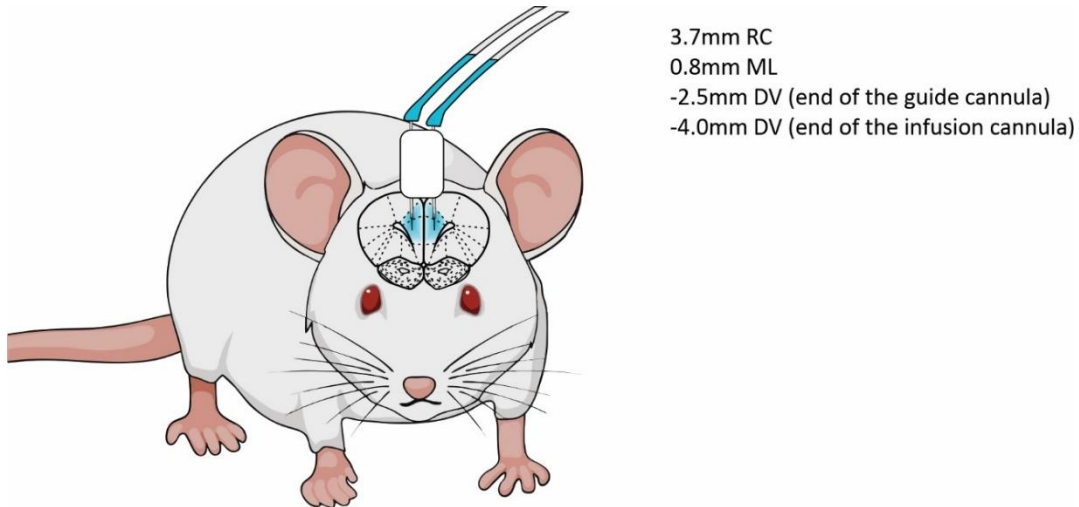
Figure 4.2 Placement of the guide and infusion cannulae. *The guide cannula was targeted to end within the anterior cingulate of the medial prefrontal cortex. The infusion cannula extended 1.5 mm below the guide cannula; thus, its tip targeted the prelimbic area. Considering the spread of the drug diffusion, the treatment was targeted to the rat medial prefrontal cortex, which includes the anterior cingulate, prelimbic and infralimbic areas.*

4.2.3 Muscimol Infusions into the Medial Prefrontal Cortex

Muscimol was delivered locally through the infusion cannula (62269; outer diameter: 0.21 mm; length: 4.5 mm; RWD life Science Inc. San Diego, CA, USA), which was inserted into the previously implanted guide cannula and extended 1.5 mm beyond its end, i.e., ending 4.0 mm below the skull, thus targeting the prelimbic area of the mPFC. Thus, considering the drug's diffusion within the brain tissue, the entire mPFC (i.e., anterior cingulate, prelimbic and infralimbic area) was likely affected **(Figure 4.2)**. The muscimol concentration used in this study was prepared from a stock solution (4.0 mM) on the day of the experiments. As needed, an aliquot was thawed to room temperature and diluted with aCSF to the proper concentration. Micro infusions of the drug were performed in awake animals. On a testing day, a given rat received a bilateral infusion of either aCSF (0.5 µL/side), a low dose of muscimol (0.5 mM; 0.5 µL/side) or a high dose of muscimol (1.0 mM; 0.5 µL/side) before beginning the test session. Both sides of the brain were infused simultaneously using a micro-infusion pump and Hamilton syringes paired to the infusion cannula via Teflon tubing. Infusions were made over 5 min (0.1 µL/min), and the

infusion cannula was then left in place for an additional 1 min to allow adequate diffusion of the drug into the targeted area. In each experimental series, the test session commenced 20 min following the end of the infusion.

4.2.4 Sound Detection

4.2.4.1 Behavioural Apparatus

The behavioural apparatus consisted of a standard modular test chamber (ENV-008CT; Med Associates Inc., St. Albans, Vt, USA) housed in a sound-attenuating box (29" x 23.5" x 23.5"; Med Associates Inc.). The front wall of the behavioural chamber included a center port with two stainless steel feeder troughs positioned on either side, each fitted with an infrared (IR) beam used to detect nose-pokes. Each feeder trough was attached to a food pellet dispenser located behind the behavioural chamber. A house light was located on the back wall to illuminate the chamber, and the white light-emitting diode (LED) was located directly above the center nose-poke, which served as a GO cue during behavioural training and testing. Auditory stimulus delivery, nose-poke responses, and positive/negative reinforcement were controlled using custom behavioural protocols (EPsych Toolbox, dstolz.github.io/epsych/) running in MATLAB (MathWorks, Nattick, MA, USA) and interfaced with real-time processing hardware RZ6; Tucker-Davis Technologies (TDT), Alachua, FL, USA).

4.2.4.2 Acoustic Stimuli and Background Noise

The acoustic stimuli were programmed to play from a speaker (FT28D; Fostex, Tokyo, Japan) mounted on the roof of the behavioural chamber. The *steady stimulus* **(Figure 4.3.A)** was an unmodulated narrow-band noise (NBN; 1/8th octave band, the center frequency at 16 kHz). The training (i.e., *other* and *steady*) and the *unknown* test sounds (i.e., *UN-I, UN-II and UN-III*) used the same NBN as a carrier signal (*carrier*). They were modified using a sinusoidal modulating function at the frequency of 19 Hz (*modulator*) with varying the amplitude of the carrier (AC) and constant amplitude of the modulating

142

signal (AM = 1), thus varying degrees of modulating index *m* as described by the equation 4.1.

Equation 4.1: Amplitude modulation of a sound

$$stimulus = AC[\,1 + \, m(modulator)(carrier)]$$

The amplitude of the carrier (AC) in the training *other* stimulus was equal to the amplitude of the NBN (i.e., AC = 0.5) **(Figure 4.3B)**. Since the modulator's amplitude was constant (AM = 1), it resulted in an amplitude overmodulated sound with a modulation index *m* = 2 (i.e., the AM was twice as large as the AC). The carrier amplitude in the *UN-I* stimulus **(Figure 4.3C)** was 0.025, resulting in a signal with an overall amplitude modulation index *m = 40*. The carrier amplitude in the *UN-II* sound was 0.1 leading to the modulation index *m = 10* **(Figure 4.3D)**, and in the *UN-III* stimulus **(Figure 4.3E)**, the carrier's amplitude was 0.2 leading to an amplitude overmodulated signal with the modulation index *m = 5*.

The background sound used to create a noisy environment was a broadband noise (BBN; 1-32 kHz), and it was played from a speaker mounted on the wall opposite to the feeder troughs. The sounds were calibrated using TDT software and hardware (RPvdsEX, RZ6 module; TDT) using ¼" microphone (2530, Larson-Davis, Depew NY, USA) and preamplifier (2221, Larson Davis). The acoustic stimuli were calibrated to 75 dB SPL, while the background noise to 50 dB SPL.
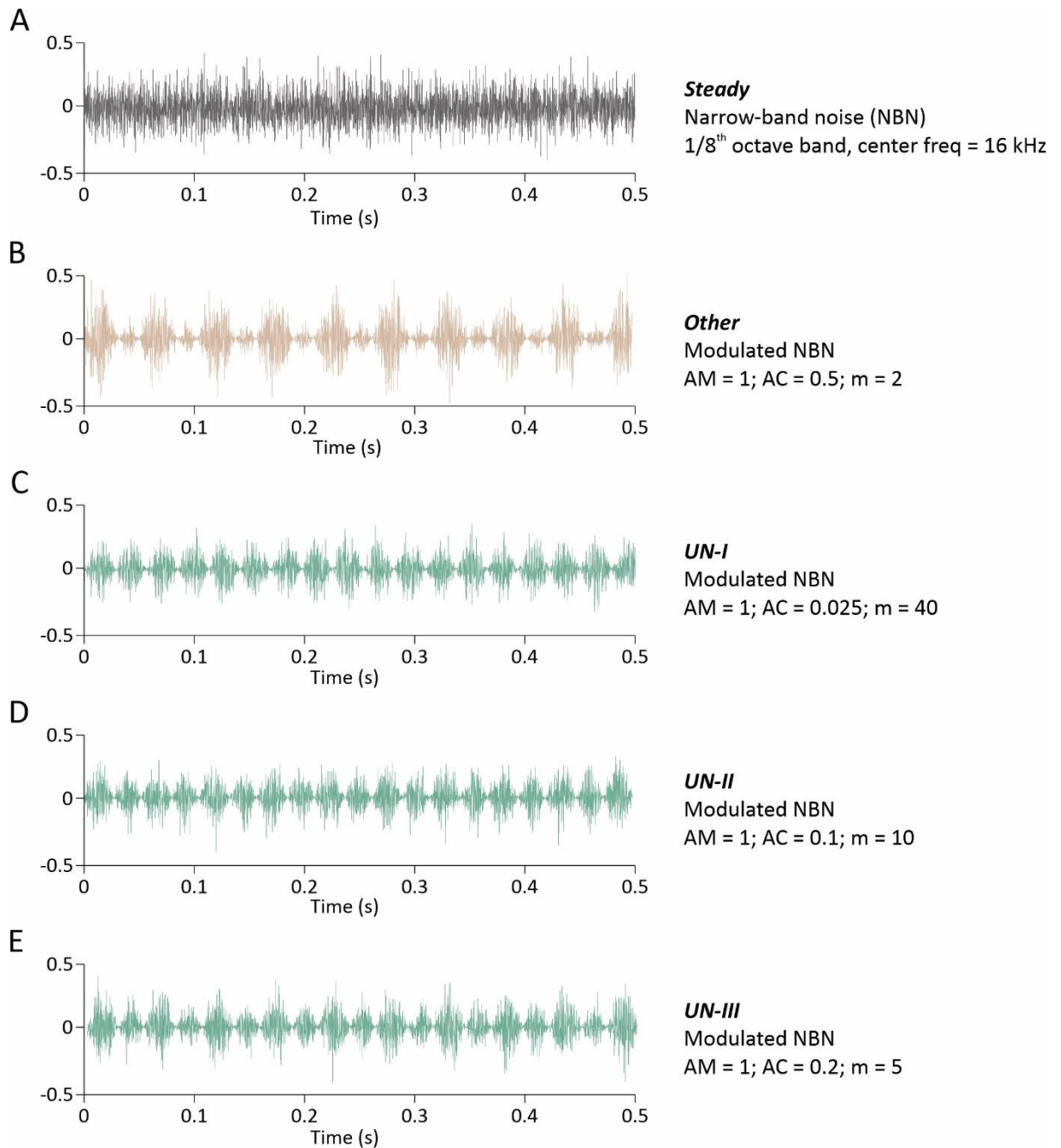
Figure 4.3 Acoustic stimuli used in the sound detection task. (A) *Steady stimulus (grey; narrow-band noise; 1/8ᵗʰ octave band, the center frequency at 16 kHz) was used in training and the testing protocol. It served as the carrier signal for the modulated sounds.* **(B)** *Other training stimulus (beige) was an amplitude overmodulated NBN with the carrier amplitude of AC = 0.5, modulating amplitude AM = 1 and modulating index m = 2, used in training and the testing protocols.* **(C-E)** *Testing stimuli (UN-I, UN-II and UN-III; green) were only used in the testing protocol and consisted of amplitude overmodulated NBN with the amplitude of the modulator AM =1 and carrier amplitude of* **(C)** *AC = 0.025 and modulating index m = 40;* **(D)** *AC = 0.1 and modulating index m = 10; and* **(E)** *AC = 0.2 and modulating index m = 5.*

4.2.4.3 Training and Testing Protocols

Rats were trained 30 min per day, six days per week to ultimately detect the *steady* stimulus (narrow-band noise) and respond by going to the left feeder, from the *other* training stimulus and respond by going to the right feeder (for details regarding the training see Chapter 3). For a given trial, the acoustic stimulus (e.g., *steady*) was played continuously from the overhead speaker, and it was only after the rat elected to nose-poke the center port (detected by interrupting an infrared beam) and hold its nose in the center port for 2-3 sec, that the trial could commence. Upon being presented with a single light flash as a GO cue, the rat then made its choice to nose-poke into either the left or right feeder trough. Upon crossing the infrared beam in a feeder trough, the acoustic stimulus was pseudo-randomly changed, and the rat was again allowed to nose-poke the center port to initiate the subsequent trial at its own pace. The training protocol consisted of 200-250 trials, which were either *steady* or *other* stimulus presented in pseudo-randomized order with the probability of 50%, and they were rewarded only upon the correct response. During the testing protocol, the rats performed 200- 250 trials, and they were presented with the *steady* stimulus (40%; rewarded only upon the correct choice), *other* stimulus (30%; rewarded only upon the correct response) and three types of *unknown* testing stimuli *(UN-I, UN-II and UN-III)* (total 30%; rewarded regardless of the response).

4.2.4.4 Data analysis

As described in detail in the previous study (see Chapter 3), to assess the ability of the rats to detect the *steady* sound in quiet and in background noise, the *d'-score* was calculated for the *steady* sound, by taking the responses to the left during the *steady* as the correct response (i.e., "hit"). A *false alarm* was defined as the response to the left during the trials that played the *unknown* testing stimuli. The assumption was that if the rats were able to detect the *steady* sound correctly, they would choose to go to the right feeder (i.e., the

one associated with "*other* training stimulus) during the trials when the three- *unknown* test stimuli played. (Equation 4.2)

Equation 4.2: *d'-score*

$$d' - score = Z(Hit\ rate) - Z(False\ Alarm\ Rate)$$

Furthermore, in addition to the *d'-score*, assessing the accuracy of rats' performance, the effects of the medial prefrontal cortex on impulsivity was measured by comparing the number of nose-pokes required to initiate a trial (Adriani *et al.*, 2003; Economidou *et al.*, 2009; Doremus-Fitzwater, Barreto and Spear, 2012).

4.2.5 Acoustic Startle Response and Its Modulation

4.2.5.1 Apparatus

Following recovery from the infusion cannula implantation, the effect of mPFC inhibition on acoustic reactivity and its modulation was assessed in sound-attenuating startle boxes (LE116; Panlab) using the StartFear system and software module (PACKWIN-CSST, PACKWIN version 2.0; Panlab). Before the testing session, rats were handled and acclimated to the startle boxes over three 10-min rounds within two days. Only background noise (60 dB SPL, white noise) was presented to the animals during these acclimation sessions. The rats were placed into an acoustically transparent plastic tube that restricted locomotion and they were set on a weight-transducing platform in the sound-attenuating chamber.

4.2.5.2 Protocol

A protocol was designed that allowed for simultaneous assessment of three features associated with the brainstem-mediated acoustic startle response (i.e., acoustic reactivity, sensory filtering and sensorimotor gating). The paradigm started with the acclimation

block (5 min), during which time only the background white noise of 60 dB SPL was presented. This background noise was played throughout the entire protocol to mask any noise from the outside of the testing box that could disturb the animal's behaviour. Following the acclimation, the experimental protocol commenced. The first block consisted of 10 consecutive pulses at 110 dB SPL (20 ms white noise burst with 5 ms rise/fall time) separated by 15-20 s, which tested the rats' sensory filtering through the short-term habituation effect. After a 9 min pause block (background white noise of 60 dB SPL was continuously played), the final block's stimuli were played. This block consisted of a series of startle stimuli of increasing intensity from 70 to 110 dB SPL in 5 dB SPL steps (20 ms white noise with 5 ms rise/fall time). Each stimulus was presented ten times in pseudo-random order with a pseudo-randomly varying inter-trial interval between 15-20 s. Additionally, ten trials randomly distributed among the entire block assessed the rats' sensorimotor gating. In these trials, the startle stimulus (*pulse;* presented at 110dB SPL) was preceded by a brief, non-startling stimulus (*prepulse;* presented at 70 dB SPL), delivered 30 ms before the startling pulse.

4.2.5.3 Sensory Filtering

Sensory filtering was assessed based on the habituation block that consisted of 10 consecutive pulses at 110 dB SPL. To investigate the extent of short-term habituation following inactivation of the mPFC the average acoustic startle response (ASR) of the last two trials (*ωASR;* i.e., trials 9 and 10) was compared to the average ASR elicited by the first two trials (*αASR;* i.e. trials 1 and 2) within each of the treatments. Furthermore, the *habituation score* was calculated as the average of the last two trials (*ωASR*) relative to the average of the first two trials (*αASR*) (see equation 4.3 below) (Scott *et al.*, 2018).

Equation 4.3: Habituation Score

$$Habituation\ Score = \left(\frac{\omega\ ASR}{\alpha\ ASR}\right) * 100\%$$

4.2.5.4 Acoustic Reactivity

The average startle response to the stimuli presented at each of the intensities was calculated across the rats for each treatment condition (i.e., aCSF, 0.5 and 1.0 mM muscimol). Furthermore, the relative startle response (*normalized ASR$_t$*) elicited at each sound level (t) was calculated, where for each animal, the average ASR at each sound level (*ASR$_t$*) was expressed as the percentage of the max ASR (Equation 4.4).

Equation 4.4: Normalized Acoustic Startle Response

$$Normalized\ ASR_t = \left(\frac{ASR_t}{ASR_{max}}\right) * 100\%$$

4.2.5.5 Sensorimotor Gating

The effect of mPFC inactivation on sensorimotor gating were assessed by measuring the amount that each rat's startle response was attenuated when the startle-eliciting stimulus (pulse) was preceded by a brief, non-startling stimulus (prepulse). The relative attenuation of the ASR (i.e., percentage of prepulse inhibition, % PPI) was calculated as shown in equation 4.5. The ASR$_{base}$ indicates the startle response to the pulse alone, while the ASR$_{PP}$ indicates the startle response to a pulse preceded by a prepulse (Scott *et al.*, 2018; Fulcher *et al.*, 2020).

Equation 4.5: % Prepulse Inhibition

$$\%\ PPI = \left(1 - \left(\frac{ASR_{PP}}{ASR_{base}}\right)\right) * 100\%$$

4.2.6 Electrophysiological Recordings

4.2.6.1 Recording Apparatus

The electrophysiological recordings were performed in a standard (9" L x 17" D x 9" H) rat home cage ("recording cage") placed in a sound-attenuating box equipped with a house

light that remained on at all times and a webcam (LifeCam Cinema HD; Microsoft) for monitoring the animal during the experimental sessions. Sounds were generated using the TDT RZ6 processing module, sampled at 100 kHz, and delivered via a loudspeaker (FT17H Horn Super Tweeter; Fostex) placed at the center of the ceiling. For the recording sessions, the rat's electrode pedestal was connected to a commutator (SL6C-SB; PlasticsOne Inc.) via a headstage cable (363-363; PlasticsOne Inc.) that was long enough to allow unrestricted movements inside the cage. The commutator was connected via a cable (363-441-6; Plasticsone Inc.) to a RA4LI low impedance headstage (TDT). The LFP signal was digitized at a 1017.25-Hz sampling rate and band-pass filtered between 0.5 and 300 Hz using the RA4SD Medusa preamp (TDT), which was connected to an RZ6 processor (TDT) via fibre optic cable. The acoustic stimulus delivery and the LFP signal acquisition were controlled through custom Matlab protocols.

4.2.6.2 Auditory Steady-State Response and Spontaneous Oscillation

Protocol

The stimulus paradigm used in this study was the same as described previously (Chapter 2) and was designed based on previous studies that investigated the auditory steady-state response (ASSR) recorded from various brain regions in normal-hearing rodents (Vohs *et al.*, 2010, 2012; Sivarao *et al.*, 2013; Sullivan, Timi, Elliot Hong, *et al.*, 2015). Briefly, each of the 150 trials included three epochs: (1) 4 s quiet period; (2) 0.5 s of 40 Hz stimulus train, consisting of 20 repetitive noise burst (1-45 kHz; 80 dB SPL; 10 ms duration; 0.1 ms rise/fall time; 25 ms inter-stimulus interval); (3) 1 s quiet period **(Figure 4.4)**.
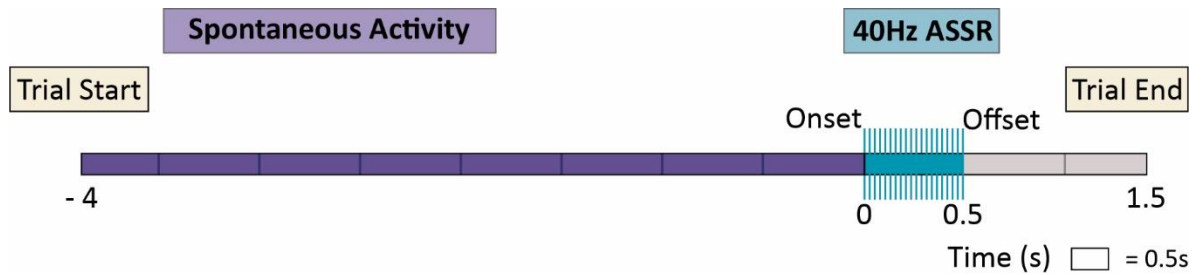
Figure 4.4 Auditory Steady-State Response and Spontaneous Oscillation Protocol Overview. *The trial started with 4 seconds of silence before the onset of the 20 click stimuli presented at the 80 dB SPL over 0.5 s (i.e., 40 Hz), allowing assessment of spontaneous oscillation, in addition to initial sound-evoked response (N18) and auditory-steady state response metrics (inter-trial coherence and evoked power).*

Data analysis

Data analysis was performed using custom Matlab scripts and functions from the FieldTrip toolbox (Oostenveld *et al.*, 2010). At first, the LFP signal from each of 150 trials was subjected to a range-based artifact rejection (Spencer *et al.*, 2009; Spencer, 2012; Sullivan, Timi, Hong, *et al.*, 2015), where the trial was removed from the further analysis if its amplitude range exceeded two-thirds of the LFP amplitude range of the entire recording block. To investigate the effect of mPFC inactivation on sound-evoked response in the auditory cortex, the event-related potential (ERP) in response to the first noise burst of the 40-Hz stimulus train was collected. The negative peak amplitude at ~18 ms from the onset of the stimulus (i.e., N18) was measured.

To investigate the effect of mPFC inactivation on the auditory cortex's ability to entrain to the sound-evoked gamma oscillations at 40 Hz, each accepted trail was subjected to time-frequency decomposition via the '*ft_freqanalysis*' function in the FieldTrip toolbox, using the multi-taper-method convolution ("*mtmconvol*") and the Hanning window taper. Next, a complex value containing the magnitude and phase information was calculated for the frequencies of interest (0-50 Hz in 0.5 Hz steps) from the onset of the stimulus to the end of the trial (0 - 5.5 s) using a 200 ms window centred on 1 ms steps. The resulting complex values for each trial were then used to calculate the inter-trial coherence (ITC).

The effects of the mPFC inactivation on auditory cortex spontaneous gamma oscillations were assessed by extracting the LFP signal from -4 to 0s relative to the stimulus and subjecting it to time-frequency decomposition via Fast-Fourier Transformation (FFT) using Hanning window taper. To account for variability in LFP signal strength between the individual rats, each rat's power spectrum was normalized by its mean power, thus converting the power spectrum units to scaled power, a normalization method used in previous studies (Weisz *et al.*, 2005; Weisz, Dohrmann and Elbert, 2007). For each of the three conditions, scaled power spectra were averaged across rats and plotted as group mean ± SEM.

4.2.6.3 Mismatch Response

Protocol

To investigate stimulus adaptation (SA) and deviance detection (DD), three sequences were used: (1) high-frequency deviant oddball sequence (DEV_{seq}); (2) high-frequency standard oddball sequence (STD_{seq}) and (3) Many-standard Control sequence (CTR_{seq}). All three sequences were played during one session, separated by at least 3 min, in two possible orders: (1) DEV_{seq} - CTR_{seq} - STD_{seq} or (2) STD_{seq} - CTR_{seq} - DEV_{seq} (**Figure 4.5A**) (Harms *et al.*, 2014, 2018; Harms, Michie and Näätänen, 2016). The order of the sequences was always the same for one animal, regardless of the treatment. Seven rats underwent the recording following the first order, and six animals followed the second order. The assignment of the order was random. Before the recording, the stimulus was played for 1 min to ensure that the responses were not corrupted by the previous sequence. All three sequences (DEV_{seq}, STD_{seq} and CTR_{seq}) consisted of 1600 trials of tone-stimuli with a 10 ms rise/fall time, duration of 100 ms, a stimulus onset asynchrony of 500 ms, and were presented at 80 dB SPL. In both oddball sequences (DEV_{seq} and STD_{seq}), 87.5% of the tones were standards (STD_{tone}), and 12.5% of the tones were deviants (DEV_{tone}). To maximize the MMRs, the oddball sequences were designed so that there were at least three STD_{tone} before each DEV_{tone} (Nakamura *et al.*, 2011; Jung *et al.*, 2013;

Harms *et al.*, 2014, 2018; Witten *et al.*, 2014; Lee *et al.*, 2018). In the DEV$_{seq}$, the DEV$_{tone}$ was an 8137 Hz tone, and the abundant tone was a 6636 Hz tone (**Figure 4.5B**). The STD$_{seq}$ sequence was a *flip-flop* sequence, i.e., the rare stimulus was at 6636 Hz, and the STD$_{tone}$ was 8137 Hz (**Figure 4.5C**). These frequencies were chosen based on previous studies that showed they could elicit deviance detection in rats (Nakamura *et al.*, 2011; Harms *et al.*, 2014, 2018; Harms, Michie and Näätänen, 2016; Lee *et al.*, 2018). CTR$_{seq}$ consisted of eight tone stimuli, all presented with equal 12.5% probability, differing on a logarithmic scale: 3600, 4414, 5412, 6636 (equivalent to STD$_{tone}$ in the DEV$_{seq}$, and DEV$_{tone}$ in the STD$_{seq}$), 8137 (equivalent to a DEV$_{tone}$ in the DEV$_{seq}$, and STD$_{tone}$ in the STD$_{seq}$) 9977, 12233, and 15000 Hz. The 8137 Hz control stimulus (CTR$_{tone}$) was presented in the exact temporal location (relative to the beginning of the sequence) as in the DEV$_{seq}$. The remaining tones were presented in pseudo-randomized order except that no tone was ever repeated (Winkler *et al.*, 1990; Jacobsen and Schröger, 2001; Jacobsen, Horenkamp and Schröger, 2003) (**Figure 4.5D**).
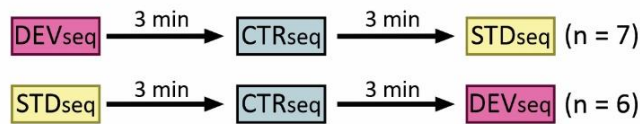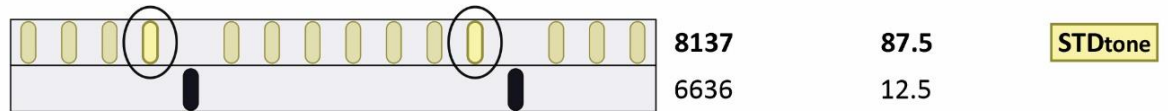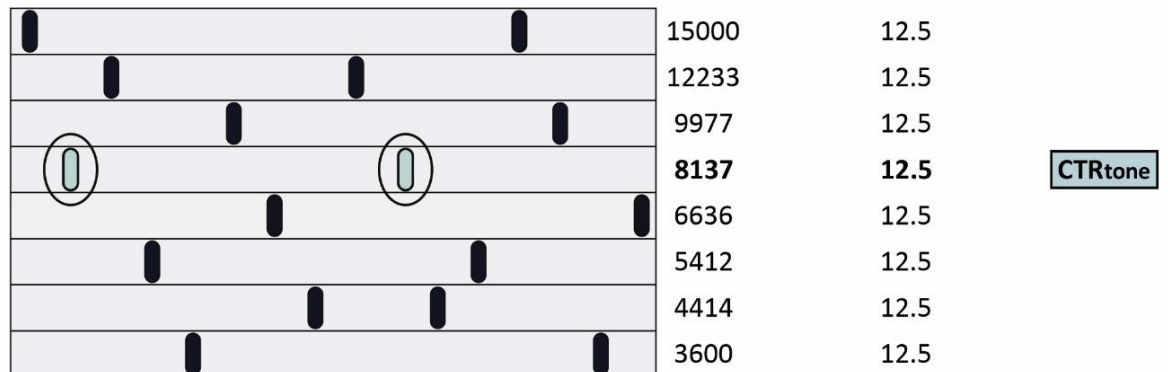
Figure 4.5 Overview of the Mismatch Response Experiment. (A) *Mismatch response protocols. The animals were divided into two groups and were subjected to the same order in all three recordings. **(B-D)** The schematic representation of the deviant (B), standard (C) and control (D) sequences. Depending on the sequence, the single 8137 Hz tone (i.e., 8 kHz) was presented as deviant, standard or control. In the standard sequence, the response to the last tone in the train was taken for analysis.*

Data analysis

The data analysis for the mismatch response protocol was performed offline in MATLAB (2019; MathWorks) using custom scripts. In the first step, epochs were extracted from the continuous LFP signal, consisting of a 100 ms pre-stimulus baseline and a 400 ms post-stimulus interval (Lauren Harms et al., 2014). Furthermore, the trials elicited by the 8137 Hz tone in each of the sequences, i.e. (1) DEV_{tone} in the DEV_{seq}, (2) the last STD_{tone} before the DEV_{tone} in the STD_{seq} and (3) CTR_{tone} in the CTR_{seq} (200 trials in each sequence) were extracted and inspected visually and then subjected to an automated artifact rejection using an algorithm that rejected signals exceeding two-thirds of the LFP amplitude range of the entire recording. Furthermore, an animal would be taken out of the study if the number of accepted trials was below 70% (i.e. below 140 trials) (Luck, 2014). Next, all the trials were baseline corrected over their 100 ms pre-stimulus interval, i.e., the average amplitude of the signal occurring 100 ms pre-stimulus onset was subtracted from the evoked response. Following these pre-processing steps, the value for N85 was calculated as the average response within the 40 ms window ranging from 65 – 105 ms (Harms *et al.*, 2014, 2018; Harms, Michie and Näätänen, 2016). Furthermore, the N85 responses elicited by the 8137 Hz tone in three different sequences (DEV_{tone}, STD_{tone} and CTR_{tone}) were compared in each of the pharmacological treatments. Finally, the prediction error (PE), repetition suppression (RS) and mismatch response (MR) were calculated as shown in equations 2.5-2.7 (Parras *et al.*, 2017).

Equation 4.6: Prediction Error

$$Prediction\ Error = \ DEV_{N85} - CTR_{N85}$$

Equation 4.7: Repetition Suppression

$$Repetition\ Suppression = \ STD_{N85} - CTR_{N85}$$

Equation 4.8: Mismatch Response

$$Mismatch\ Response =\ DEV_{N85} - STD_{N85}$$

4.2.7 Data Presentation and Statistics

Statistical analyses were performed using GraphPad Prism and included one-way and two-way repeated-measures analysis of variance (RM-ANOVA). Post hoc paired-samples t-tests with Bonferroni-corrected significance level were used to compare differences in the group means in the case of significant effects or interactions. Graphs were generated either by GraphPad Prism or MatLab and were edited and finalized for aesthetic purposes using CorelDRAW Graphics Suite 2020. The methods figures were built in CorelDRAW Graphics Suite 2020.

4.3 Results

4.3.1 Medial prefrontal cortex contributes to accurate sound detection ability, especially in noisy background

This experimental series investigated whether the mPFC contributes to the accuracy of detecting sounds in quiet versus noisy background conditions. Rats that had been previously trained to detect the *steady* from unsteady sounds then performed test sessions in quiet and background noise (50 dB SPL) following infusion of muscimol (0.5 and 1.0 mM) into their mPFC, and their performance metrics (*d'-score* and impulsivity) were compared to a control treatment (aCSF infusion). A two-way RM-ANOVA for treatment (aCSF, 0.5 mM muscimol; 1.0 mM muscimol) x background noise (quiet; 50 dB SPL) revealed a significant effect of treatment ($F_{(2,14)}$ = 23.50; $p < 0.001$) as well as background noise ($F_{(1,7)}$ = 27.96; $p = 0.001$) on the *d'-score* (**Figure 4.6 A**). Interestingly, post-hoc analysis showed that following infusion of 0.5 mM muscimol, the rats' performance was not affected in the quiet condition (*d'-score* aCSF: 2.50 ± 0.25 vs. 0.5 mM muscimol: 1.95 ± 0.25 p_{Bonf} = 0.40), but it was significantly worsened in the 50 dB SPL

background noise (d'-score aCSF: 2.23 ± 0.11 vs. 0.5 mM muscimol: 1.14 ± 0.16; p_{Bonf} = 0.014). Infusion of 1.0 mM muscimol into the mPFC had a more dramatic effect; the rats' performance, as compared to aCSF, was impaired in both quiet (d'-score: aCSF: 2.50 ± 0.25 vs. 1.0 mM muscimol: 1.60 ± 0.22; p_{Bonf} = 0.049) and in 50 dB SPL background noise (d'-score aCSF: 2.23 ± 0.11 vs. 1.0 mM muscimol: 0.84 ± 0.23; p_{Bonf} = 0.002), further indicating the importance of the mPFC during task performance. Together, these results show that the mPFC plays an important role in sound detection, especially in background noise, as even the lower concentration of muscimol led to detrimental effects on the rats' ability to detect the steady sound in the challenging listening environment.
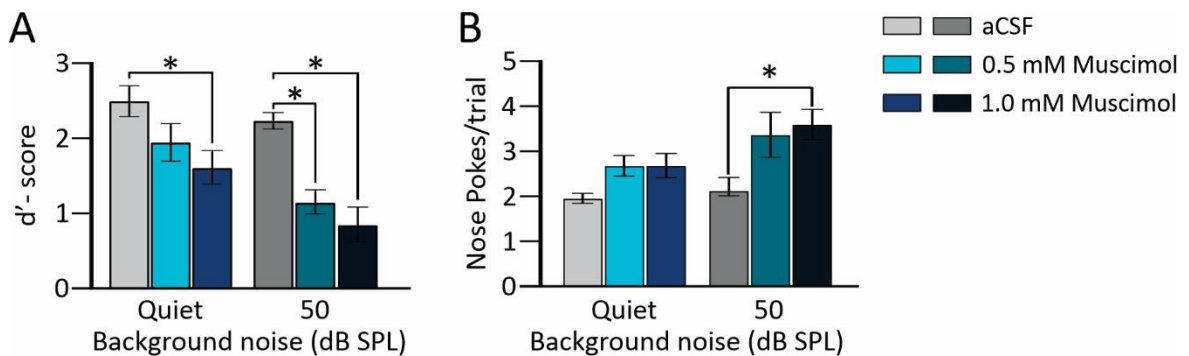
Figure 4.6 Inactivation of the medial prefrontal cortex (mPFC) decreased performance on the sound detection task and increased impulsivity in noisy background conditions. (A) As measured by their d'-score, the rats' performance on the sound detection task was dramatically worsened by mPFC infusion of 1.0 mM muscimol, both in quiet and 50 dB SPL background noise, whereas task performance was only significantly decreased in the noisy background condition following infusion of the lower concentration of muscimol (0.5 mM). (B) As measured by the average number of nose-pokes required to initiate a trial, the rats' impulsivity showed a trend to increase with muscimol infusion, ultimately demonstrating a significant increase in the most challenging task condition (i.e., 1.0 mM muscimol + 50 dB background noise). Data represent group mean ± SEM; n = 8 rats; *p_{Bonf} < 0.05

4.3.2 Impaired sound detection ability was correlated with increased impulsivity following medial prefrontal cortex inactivation.

To further examine the effects of mPFC inactivation via muscimol on the sound detection task in quiet and background noise, the average number of nose-pokes needed to initiate a single trial was calculated and used as a metric of impulsivity (Adriani *et al.*, 2003; Economidou *et al.*, 2009; Doremus-Fitzwater, Barreto and Spear, 2012). A two-way RM-

ANOVA for treatment (aCSF, 0.5 mM muscimol; 1.0 mM muscimol) x background noise (quiet; 50 dB SPL) revealed a significant effect of treatment ($F_{(2,14)}$ = 9.23; p = 0.003) but not the background condition ($F_{(1,7)}$ = 3.00; p = 0.127) (**Figure 4.6 B**). Furthermore, post-hoc analysis showed a significantly increased number of nose-pokes in the 50 dB SPL background noise following the treatment of 0.5 mM (aCSF: 2.23 ± 0.11 vs. 0.5 mM muscimol: 0.84 ± 0.23; p_{Bonf} = 0.002) and 1.0 mM muscimol (aCSF: 2.23 ± 0.11 vs. 1.0 mM muscimol: 0.84 ± 0.23; p_{Bonf} = 0.002). Overall, Pearson's correlation analysis revealed a significant relationship between the decrease in performance accuracy and increased impulsivity (R^2 = 0.340; $p < 0.001$) (**Figure 4.7**), suggesting that the poor performance on the sound detection task following the inactivation of the mPFC could be related to attentional deficits. Table 4.1 provides a summary of the statistical tests performed in this experimental series.
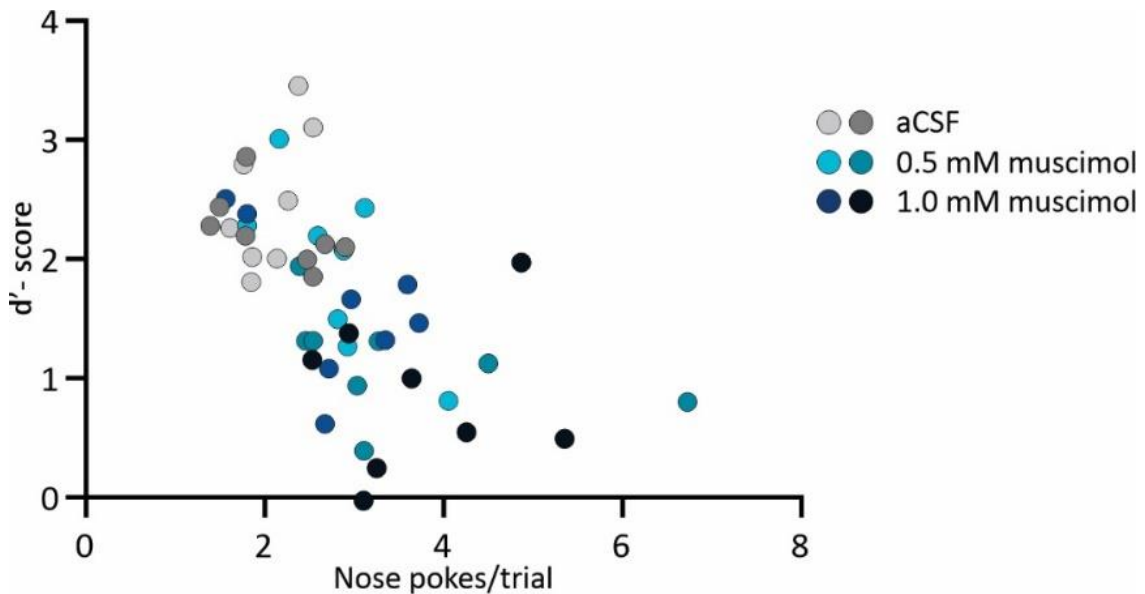
Figure 4.7 Impaired sound detection ability was correlated with increased impulsivity following medial prefrontal cortex inactivation*. The plot represents the performance on the sound detection task as measured by the d'-score in relation to the average number of nose-pokes required to initiate a single trial. The different colored dots represent the various treatments (grey = aCSF; teal = 0.5 mM muscimol; navy = 1.0 mM muscimol) and background conditions (lighter shades = quiet; darker shades = 50 dB SPL background noise).*

Test	Main effect/comparison	p-value	F-value/t-value; DF
Figure 4.6 Sound detection task			
Figure 4.6 A. d'-score			
2-way RM-ANOVA	Treatment (aCSF, 0.5 mM, 1.0 mM muscimol) *	<0.001	$F_{(2, 14)}$ = 23.50
	Background noise (quiet, 50 dB SPL) *	0.001	$F_{(1, 7)}$ = 27.96
	Interaction (treatment x background)	0.412	$F_{(2, 14)}$ = 0.95
Quiet background			
Post-hoc	aCSF vs. 0.5 mM muscimol	0.396 [B]	t= 1.77; DF = 14
Post-hoc	aCSF vs. 1.0 mM muscimol *	0.049 [B]	t= 2.88; DF = 14
50 dB SPL background noise			
Post-hoc	aCSF vs. 0.5 mM muscimol *	0.014 [B]	t= 3.52; DF = 14
Post-hoc	aCSF vs. 1.0 mM muscimol *	0.002 [B]	t= 4.49; DF = 14
Figure 4.6 Nose-pokes/trial			
2-way RM-ANOVA	Treatment (aCSF, 0.5 mM, 1.0 mM muscimol) *	0.003	$F_{(2, 14)}$ = 9.23
	Background noise (quiet, 50 dB SPL)	0.127	$F_{(1, 7)}$ = 3.00
	Interaction (treatment x background)	0.331	$F_{(2, 14)}$ = 1.20
Quiet background			
Post-hoc	aCSF vs. 0.5 mM muscimol	0.334 [B]	t= 1.86; DF = 14
Post-hoc	aCSF vs. 1.0 mM muscimol	0.326 [B]	t= 1.88; DF = 14
50 dB SPL background noise			
Post-hoc	aCSF vs. 0.5 mM muscimol *	0.017 [B]	t= 3.40; DF = 14
Post-hoc	aCSF vs. 1.0 mM muscimol *	0.005 [B]	t= 3.99; DF = 14
Figure 4.7 Correlation between d'-score and nose-pokes/trial			
Pearson's correlation	*d'-score* vs. nose-pokes/trial	<0.001	R^2 = 0.340

Table 4.1 Summary of the statistical tests performed to investigate the effects of medial prefrontal cortex inactivation on sound detection in quiet and background noise. [B] Bonferroni corrected p-value; * statistical significance.

4.3.3 Brainstem mediated acoustic startle response was not affected by the inactivation of the medial prefrontal cortex.

The effects of mPFC inactivation on the brainstem mediated auditory processing were assessed indirectly by investigating the acoustic startle response. A two-way RM-ANOVA was performed for stimulus sound intensity (70-110 dB SPL) x treatment (aCSF; 0.5 mM muscimol; 1.0 mM muscimol). As expected, the results revealed a significant effect of the stimulus sound intensity on the raw startle response ($F_{(1.93, 25.15)}$ = 207.9; p < 0.001), but failed to show a significant effect of the treatment ($F_{(1.88, 24.47)}$ = 2.54; p = 0.102) (**Figure 4.8 A**). Similarly, a separate two-way RM-ANOVA showed no significant effect of mPFC inactivation with muscimol on relative acoustic reactivity (i.e., normalized to its maximum

startle response on the given testing day) ($F_{(1.85, 24.02)}$ = 0.56; p = 0.562) (**Figure 4.8B**). Together, these findings suggest that increased activation of GABA$_A$ receptors within the mPFC did not significantly affect acoustic reactivity or the startle threshold.
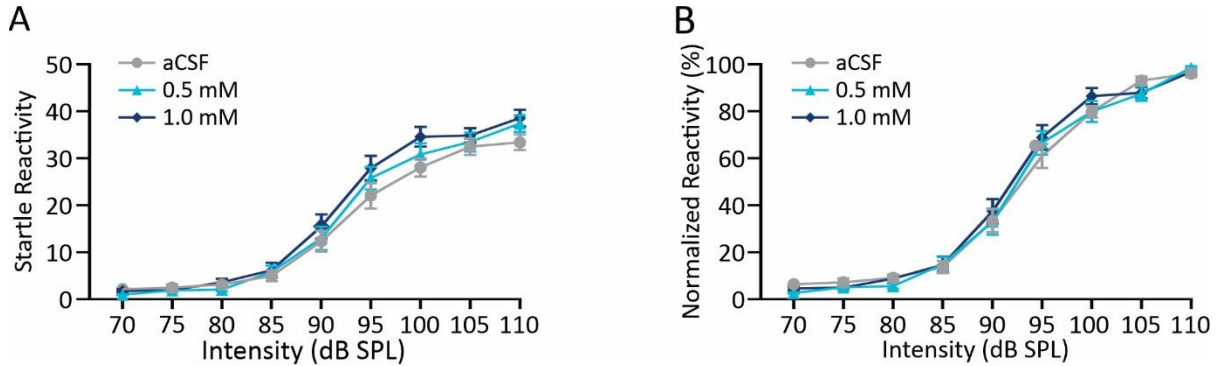
Figure 4.8 Medial prefrontal cortex (mPFC) inactivation did not affect acoustic reactivity. *The infusion of muscimol into the mPFC had no significant effect on raw acoustic startle response* ***(A)*** *nor normalized reactivity* ***(B).*** *Data represent group mean ± SEM; n= 13 rats.*

A one-way RM-ANOVA (aCSF; 0.5 mM muscimol; 1.0 mM muscimol) was used to compare the percent of the acoustic startle response attenuation due to the presence of the prepulse (i.e., % prepulse inhibition, or %PPI). Unlike the previous reports of decreased prepulse inhibition following prefrontal cortex lesions (Koch and Bubser, 1994), a one-way RM-ANOVA revealed no significant effect of muscimol treatment ($F_{(1.94, 25.20)}$ = 0.46; p = 0.459), (**Figure 4.9**); findings consistent with studies reporting a general lack of cortical contribution to sensorimotor gating (Davis and Gendelman, 1977; Fox, 1979; Ison, Peter Bowen and O'connor, 1991).
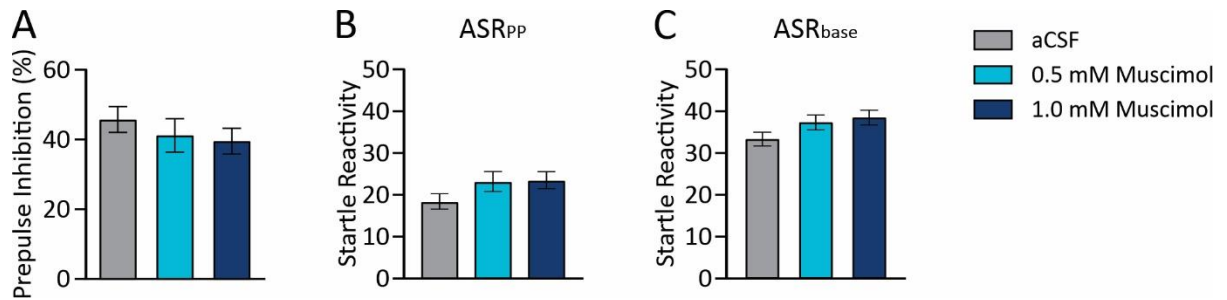
Figure 4.9 Medial prefrontal cortex (mPFC) inactivation did not affect sensorimotor gating. (A) *As assessed by prepulse inhibition of the acoustic startle response, sensorimotor gating was not affected by mPFC inactivation via local muscimol infusion. **(B** and **C)** The startle reactivity to a 110 dB SPL stimulus presented after a non-startling prepulse stimulus (ASR$_{PP}$ panel B) and the startle reactivity to a 110 dB SPL stimulus presented alone (ASR$_{base}$ panel C) were not affected by inactivation of the mPFC. Data represent group mean ± SEM; n= 13 rats.*

The mPFC inactivation on short-term habituation was studied by investigating the acoustic startle response to ten consecutive trials with a stimulus sound of 110 dB SPL. A two-way RM-ANOVA for trial (1-10) x treatment (aCSF; 0.5 mM; 1.0 mM muscimol) revealed as expected a significant effect of trials ($F_{(3.26, 42.42)}$ = 17.62; $p < 0.001$), meaning that the acoustic startle response was affected by the consecutive trials; an indication of the presence of short-time habituation. Surprisingly, however, the statistical analysis also revealed a significant effect of treatment ($F_{(1.49, 19.33)}$ = 5.0; $p = 0.025$), indicating that the magnitude of the acoustic startle response to ten consecutive 110 dB SPL stimuli was affected by the muscimol treatment (**Figure 4.10 A**). Bonferroni corrected post-hoc analysis revealed that inactivation of the mPFC with muscimol did not significantly affect the average startle response on the first two trials (α). However, the average acoustic startle response on the last two trials (ω) was significantly larger following the treatment with 1.0 mM muscimol as compared to the ω after aCSF infusions (aCSF: 30.5 ± 2.7 vs. 1.0 mM muscimol: 41.0 ± 2.6; p_{Bonf} = 0.025) (**Figure 4.10 B**), indicating that the mPFC inactivation decreased the effects of short-term habituation. These results were further confirmed by the *habituation score*, calculated as the percentage of ω attenuation compared to α. A one-way RM-ANOVA (aCSF, 0.5 mM muscimol; 1.0 mM muscimol) revealed a significant effect of treatment ($F_{(1.49, 19.31)}$ = 4.99; $p = 0.025$), showing decreased habituation score following infusion of 0.5 mM (aCSF: 26.7 ± 4.3 % vs. 0.5 mM muscimol:

9.0 ± 4.6 %; p_{Bonf} = 0.037) and 1.0 mM muscimol (aCSF: 26.7 ± 4.3 % vs. 0.5 mM muscimol: 14.8 ± 5.6 %; p_{Bonf} = 0.039) (**Figure 4.10 C**). A detailed summary of the statistical test is shown in table 4.2.
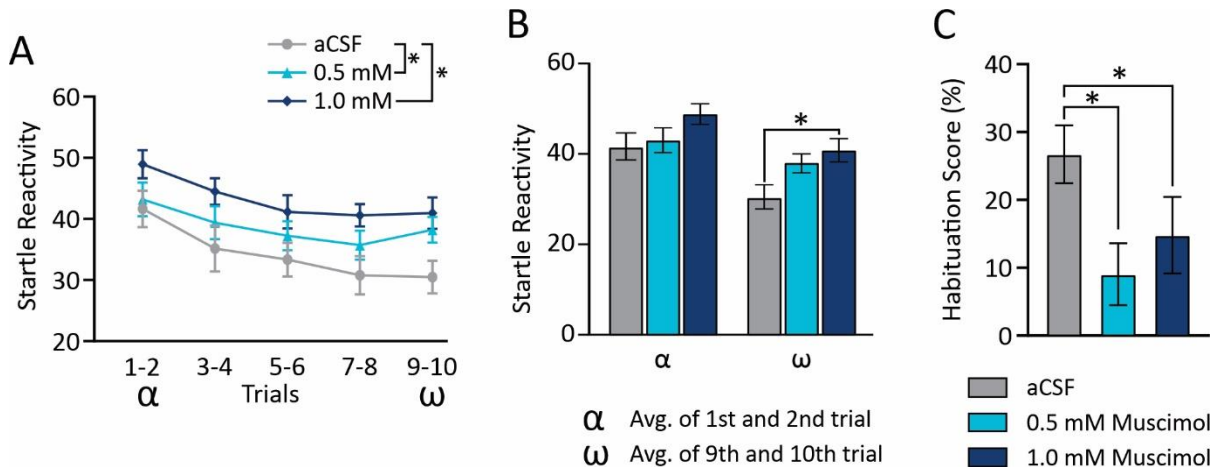
Figure 4.10 The effect of medial prefrontal cortex (mPFC) inactivation on short-term habituation. *(A) The acoustic startle response in the habituation block was significantly affected by the mPFC muscimol treatments. The graph shows the magnitude of the startle reactivity to ten consecutive startle-eliciting stimuli at 110 dB SPL. At each point of the graph, two consecutive trials were averaged. (B) Unlike the average of the first two trials (α), the mean startle response of the last two trials (ω) was significantly larger following the infusion of 1.0 mM muscimol as compared to the aCSF infusion, indicating deficits in short-term habituation. (C) The habituation score, expressed as the % of startle response attenuation of the last two trials (ω) compared to the first two trials (α), was significantly decreased following the infusion of 0.5 mM and 1.0 mM muscimol. Data represents mean ± SEM; n = 14; *p_{Bonf} < 0.05*

Test	Main effect/comparison	P-value	F-value/t-value; DF
Figure 4.8 Acoustic Startle Reactivity			
Figure 4.8 A. Acoustic Startle Reactivity (raw)			
	Treatment (aCSF, 0.5 mM, 1.0 mM muscimol)	0.102	$F_{(1.88, 24.47)} = 2.54$
2-way RM-ANOVA	Intensity (70 – 110 dB SPL) *	<0.001	$F_{(1.93, 25.15)} = 207.9$
	Interaction (treatment x intensity)	0.062	$F_{(4.52, 58.81)} = 2.31$
Figure 4.8 B. Normalized Acoustic Startle Reactivity			
	Treatment (aCSF, 0.5 mM, 1.0 mM muscimol)	0.562	$F_{(1.85, 24.02)} = 0.56$
2-way RM-ANOVA	Intensity (70 – 110 dB SPL) *	<0.001	$F_{(1.83, 23.78)} = 348.3$
	Interaction (treatment x intensity)	0.307	$F_{(4.58, 59.54)} = 1.23$
Figure 4.9 Sensorimotor Gating			
Figure 4.9 A. Prepulse inhibition (%)			
1-way RM-ANOVA	Treatment (aCSF, 0.5 mM, 1.0 mM muscimol)	0.459	$F_{(1.94, 25.20)} = 0.46$
Figure 4.9 B and C. Startle response elicited by the 110 dB base stimulus (B) or proceeded by a prepulse (C)			
	Treatment (aCSF, 0.5 mM, 1.0 mM muscimol)	0.035 *	$F_{(1.94, 25.22)} = 3.89$
2-way RM-ANOVA	Acoustic Startle Response type (ASR_{base}, ASR_{PP})	<0.001 *	$F_{(1.00, 13.00)} = 270.20$
	Interaction (treatment x ASR type)	0.857	$F_{(1.88, 24.44)} = 0.14$
Post hoc	ASR_{base} aCSF vs. 0.5 mM muscimol	0.324 [B]	t = 1.89; DF = 13
Post hoc	ASR_{base} aCSF vs. 1.0 mM muscimol	0.066 [B]	t = 2.75; DF = 13
Post hoc	ASR_{PP} aCSF vs. 0.5 mM muscimol	0.278 [B]	t = 1.98; DF = 13
Post hoc	ASR_{PP} aCSF vs. 1.0 mM muscimol	0.152 [B]	t = 2.31; DF =13
Figure 4.10 Short-Term Habituation			
Figure 4.10 A and B. Effect of prefrontal cortex inactivation on startle response of consecutive trials			
2-way RM- ANOVA	Habituation trials (1-10) *	<0.001	$F_{(3.26, 42.42)} = 17.62$
	Treatment (aCSF, 0.5 mM, 1.0 mM muscimol) *	0.025	$F_{(1.49, 19.33)} = 5.0$
	Interaction (trials x treatment)	0.676	$F_{(5.07, 65.91)} = 0.63$
Post hoc	α (avg. of first two trials) aCSF vs. 0.5 mM muscimol	>0.999 [B]	t = 0.48; DF = 13
Post hoc	α (avg. of first two trials) aCSF vs. 1.0 mM muscimol	0.158 [B]	t = 2.77; DF = 13
Post hoc	ω (avg. of last two trials) aCSF vs. 0.5 mM muscimol	0.192 [B]	t = 1.09; DF = 13
Post hoc	ω (avg. of last two trials) aCSF vs. 1.0 mM muscimol *	0.025 [B]	t = 3.12; DF = 13
Figure 4.10 C. Habituation score			
1-way RM-ANOVA	Treatment (aCSF, 0.5 mM, 1.0 mM muscimol) *	0.025	$F_{(1.49, 19.31)} = 4.99$
Post-hoc	Avg. startle to 110 dB aCSF vs 0.5 mM muscimol	0.037 [B]	t = 2.67; DF = 13
Post-hoc	Avg. startle to 110 dB aCSF vs 1.0 mM muscimol	0.039 [B]	t = 2.66; DF = 13

Table 4.2 *Summary of statistical tests performed during the investigation of the medial prefrontal cortex inactivation effects on acoustic startle response. [B] Bonferroni corrected p-value; * statistical significance; ASR_{base}: startle response elicited by a 110 dB startle stimulus alone; ASR_{PP}: startle response elicited by a 110 dB startle stimulus presented following a prepulse stimulus.*

4.3.4 Initial sound-evoked response within the auditory cortex was unaffected by medial prefrontal cortex inactivation.

To investigate the effects of the mPFC inactivation on sound-evoked responses within the auditory cortex, the initial response (N18) evoked by an acoustic stimulus was investigated in a group of rats (n=13). A one-way RM-ANOVA (aCSF, 0.5 mM muscimol; 1.0 mM muscimol) revealed that the local infusion of muscimol into the mPFC had no significant effect on N18 ($F_{(1.26, 15.08)}$ = 0.79; p = 0.417), (**Figure 4.11**). This finding suggested that increased activity of GABA$_A$ receptors within the mPFC does not affect initial sound-evoked responses within the auditory cortex. Considering the noise-exposure study results (Chapter 2) (i.e., increased ERP in auditory cortex post-noise exposure), the present findings suggest that the central gain enhancement observed in the auditory pathway following the noise-induced hearing loss was not likely an effect of increased inhibition within the mPFC.
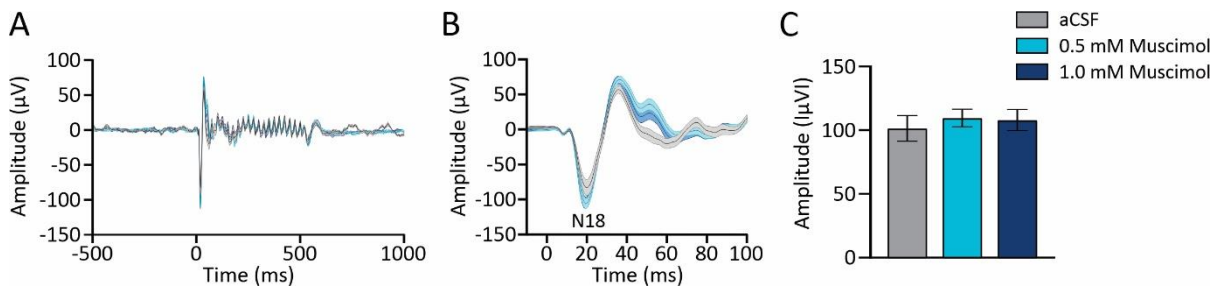
Figure 4. 11 Initial sound-evoked response in the auditory cortex was not affected by inactivation of the medial prefrontal cortex via local muscimol infusion. (A) The group mean profiles of auditory steady-state responses, (B) and zoomed-in window on the N18 (shading indicates SEM) of event-related potential in the treatment groups. (C) Group average of the N18 expressed as an absolute value, following the treatments with aCSF (grey), 0.5 (bright blue) and 1.0 mM (dark blue) muscimol. Compared to the control condition (aCSF), muscimol infusion did not alter the auditory cortex's evoked response. Data represent group mean ± SEM; n= 13 rats

4.3.5 Auditory Steady-State Response to the 40-Hz stimulus was unaffected by increased inhibition within the medial prefrontal cortex.

In addition to investigating the initial sound-evoked response in the auditory cortex, the present experiments examined how muscimol infusion into the mPFC would affect the ability of neurons within the auditory cortex to generate and sustain gamma oscillations,

which are known to be related to cognitive processing such as perception and attention (Joliot, Ribary and Llinás, 1994; Pritchett *et al.*, 2015; Sohal, 2016; Leonte *et al.*, 2018; Mock *et al.*, 2018). Compared to the control condition (aCSF), local infusion of 0.5 mM and 1.0 mM muscimol into the mPFC had no significant effect on evoked power (one-way RM-ANOVA: $F_{(1.64, 19.65)}$ = 0.48; p = 0.588), (**Figure 4.12**) or inter-trial coherence (one-way RM-ANOVA: $F_{(1.69, 20.24)}$ = 0.04; p = 0.938), (**Figure 4.13**) derived from the 40-Hz auditory steady-state response. These results suggest that inactivation of the mPFC, via increased GABAA receptors' activity, did not alter the ability of neurons within the auditory cortex to become entrained to an acoustic stimulus presented at 40-Hz frequency. For details of statistical analysis, see **Table 4.3**
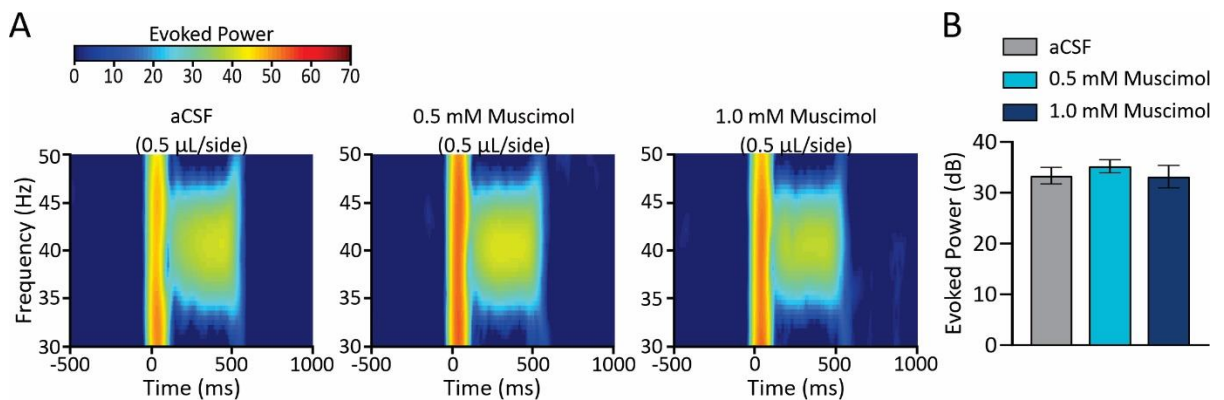
Figure 4.12 Magnitude of the evoked power of the 40-Hz auditory steady-state response within the auditory cortex was not affected following medial prefrontal cortex (mPFC) treatment with muscimol. (A) The heatmaps plot the group average of evoked power (EP) of the 40-Hz auditory steady-state response from the auditory cortex following infusion of aCSF (left), 0.5 (middle) and 1.0 mM muscimol (right) into the mPFC. (B) The group average magnitude of EP (35 – 45 Hz within 100 – 400 ms after stimulus onset) revealed no significant differences following the muscimol treatment. Data in bar graphs represent group mean ± SEM; n = 13 rats
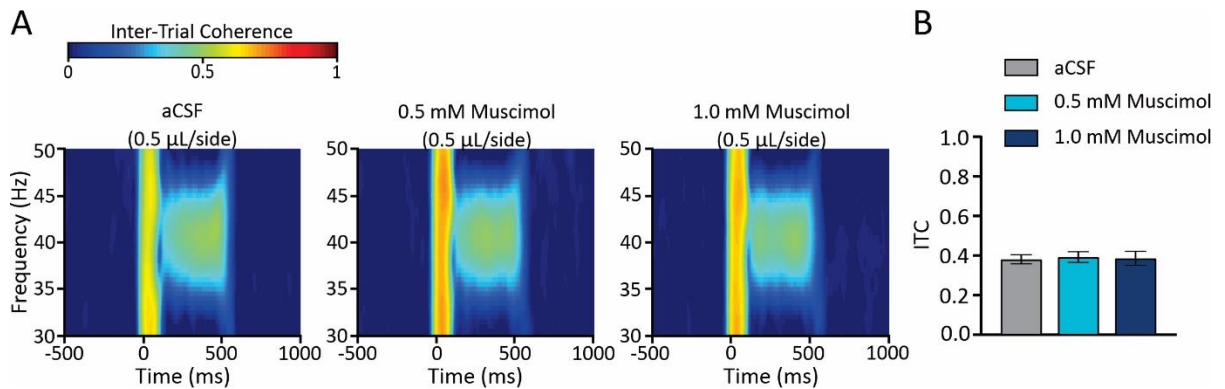
Figure 4.13 Inter-trial coherence of the 40-Hz auditory steady-state responses recorded from the auditory cortex was not affected following medial prefrontal cortex (mPFC) treatment with muscimol. (A) The heatmaps plot the group average of inter-trial coherence (ITC) of the 40-Hz auditory steady-state response from the auditory cortex following infusion of aCSF (left), 0.5 (middle) and 1.0 mM muscimol (right) into the mPFC. (B) The group average magnitude of ITC (35 – 45 Hz within 100 – 400 ms after stimulus onset) revealed no significant differences following the treatment with muscimol. Data in bar graphs represent group mean ± SEM; n = 13 rats

4.3.6 Inactivation of the medial prefrontal cortex via local infusion of muscimol resulted in decreased spontaneous gamma power within the auditory cortex.

To further investigate the role of the mPFC on the electrophysiological activity of the auditory cortex, the spontaneous oscillations within the gamma band were assessed. Gamma frequency is often correlated with higher-order cognitive functions, and it was found to be disrupted in neuropsychiatric conditions that exhibit auditory perceptual deficits, e.g., schizophrenia (Uhlhaas and Singer, 2010; Gonzalez-Burgos, Cho and Lewis, 2015; Hirano *et al.*, 2015; Grent-'t-Jong *et al.*, 2018; Baradits *et al.*, 2019), and autism spectrum disorder (Simon and Wallace, 2016), bipolar disorder (Özerdem *et al.*, 2010). In contrast to the lack of effect on sound-evoked oscillations discussed above, a one-way RM-ANOVA revealed a significant main effect of treatment on spontaneous gamma frequency ($F_{(1.72, 20.62)}$ = 6.59; p = 0.008), with Bonferroni corrected post-hoc analysis showing significantly decreased gamma oscillations within the auditory cortex following muscimol infusion into the mPFC (aCSF: 0.19 ± 0.01 vs. 0.5 mM muscimol 0.13 ± 0.02; p_{Bonf} = 0.015; vs. 1.0 mM muscimol: 0.13 ± 0.01; p_{Bonf} = 0.005) (**Figure 4.14; Table 4.3**).
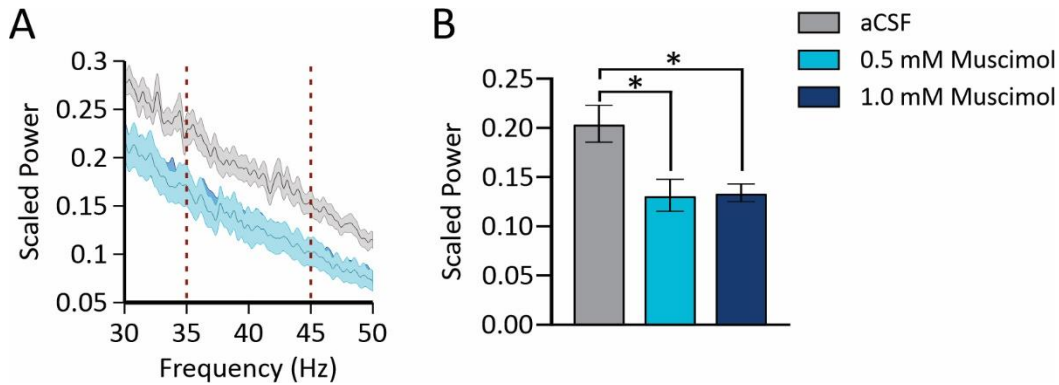
Figure 4.14 *Altered spontaneous gamma oscillations within the auditory cortex following the medial prefrontal cortex (mPFC) treatment with muscimol. (A) The group mean profile of scaled power (shading indicated SEM) of spontaneous oscillations within the gamma frequency range recorded from the auditory cortex following infusion of aCSF (grey), 0.5 mM (light blue) and 1.0 mM (navy blue) muscimol into the mPFC. (B) The average scaled power of spontaneous oscillations within the gamma frequency range (35-45 Hz), indicated by the red lines. Local infusion of muscimol into the mPFC significantly reduced the scaled power of gamma oscillations. Data represent group mean ± SEM; n= 13 rats;*$p_{Bonf} < 0.05$*

4.3.7 The deviant response typically observed in the auditory cortex during an oddball protocol was diminished following medial prefrontal cortex inactivation.

To determine the contribution of the mPFC to cognition-related information processing, the "Mismatch Negativity-like responses" (MMN) were recorded from the auditory cortex following infusion of aCSF, 0.5 mM and 1.0 mM muscimol. It is commonly believed that neurophysiological processes that give rise to deviance detection responses are extensively involved in higher cognitive function, such as recognition of categories and abstract patterns of stimulus sequences (Paavilainen *et al.*, 2001; Shestakova *et al.*, 2002; Paavilainen, 2013; Xiao *et al.*, 2018). Thus it serves as a good indicator of the unbiased cognitive assessment. Although the term "mismatch negativity" relates to a negative deflection at ~80ms following the deviant (DEV) stimulus onset in an oddball protocol, it is not uncommon to see responses with opposite polarity, especially in rodents (Harms, Michie and Näätänen, 2016). As expected, a two-way RM-ANOVA for stimulus type (DEV$_{tone}$, STD$_{tone}$, CTR$_{tone}$) x treatment (aCSF; 0.5 mM muscimol; 1.0 mM muscimol) showed a significant effect of the stimulus type (F $_{(1.92,\ 23.01)}$ = 14.69; p < 0.001), indicating a significant difference in the waveform elicited by 8 kHz tone stimulus presented in three

different scenarios as 1) deviant (DEV_{tone}) 2) standard (STD_{tone}) and 3) control (CTR_{tone}). Although there was no main effect of treatment ($F_{(1.43, 17.17)}$ = 0.04; p = 0.597), there was a significant interaction between the treatment and the stimulus type ($F_{(2.59, 31.06)}$ = 4.0; p = 0.02), indicating the possibility that the treatment had a differential effect on the same tone depending on its role (i.e. DEV_{tone}, STD_{tone}, CTR_{tone}). Therefore, an additional series of one-way RM-ANOVAs were performed to examine these effects more thoroughly. First, the effects of the stimulus type within each of the treatments were examined. As expected, in the control condition (i.e., following the mPFC infusion of aCSF), (**Figure 4.15 A, D**), there was a significant effect of the stimulus type ($F_{(1.93, 23.14)}$ = 14.57; p < 0.001), and Bonferroni corrected post-hoc analysis revealed a significant difference between the response to the 8 kHz tone stimulus presented as DEV vs. CTR (DEV: -0.63 ± 1.92 µV vs. CTR: -10.29 ± 2.20 µV; p_{Bonf} = 0.002) suggesting a prediction error (Nakamura *et al.*, 2011; Harms *et al.*, 2014, 2018; Harms, Michie and Näätänen, 2016; Lee *et al.*, 2018). Additionally, there was also a significant difference between the DEV and STD waveform (DEV: -0.63 ± 1.92 µV vs. STD: -9.32 ± 1.11 µV; p_{Bonf} = 0.001), consistent with a mismatch response that arose from the combined effects of prediction error and repetition suppression (Parras *et al.*, 2017).

Interestingly, following infusion of 0.5 mM muscimol into the mPFC, a one-way RM-measures ANOVA failed to reveal effects of stimulus type on the response recorded in the auditory cortex ($F_{(1.86, 22.31)}$ = 2.33; p = 0.124) (**Figure 4.15 B, E**). Surprisingly, following the infusion of 1.0 mM muscimol into the mPFC, a one-way ANOVA again showed a significant effect of the stimulus type ($F_{(1.71, 20.55)}$ = 5.89; p = 0.012) (Figure 4.15 C, F) again. However, contrary to the aCSF condition discussed above, post-hoc analysis with Bonferroni correction revealed a significant difference between the STD and CTR stimuli (STD -1.60 ± 1.78 µV vs. CTR -9.11 ± 2.40 µV; p_{Bonf} = 0.035), indicating the effect on repetition suppression. Interesting however, there was still no significant differences between the STD and DEV (STD -1.60 ± 1.78 µV vs. DEV -4.49 ± 2.48 µV; p_{Bonf} = 0.688) nor CTR and DEV

(CTR -9.11 ± 2.40 µV vs DEV -4.49 ± 2.48 µV; p_{Bonf} = 0.061). These collective results suggest that the DEV and STD stimulus might be affected differently by inactivation of the mPFC.
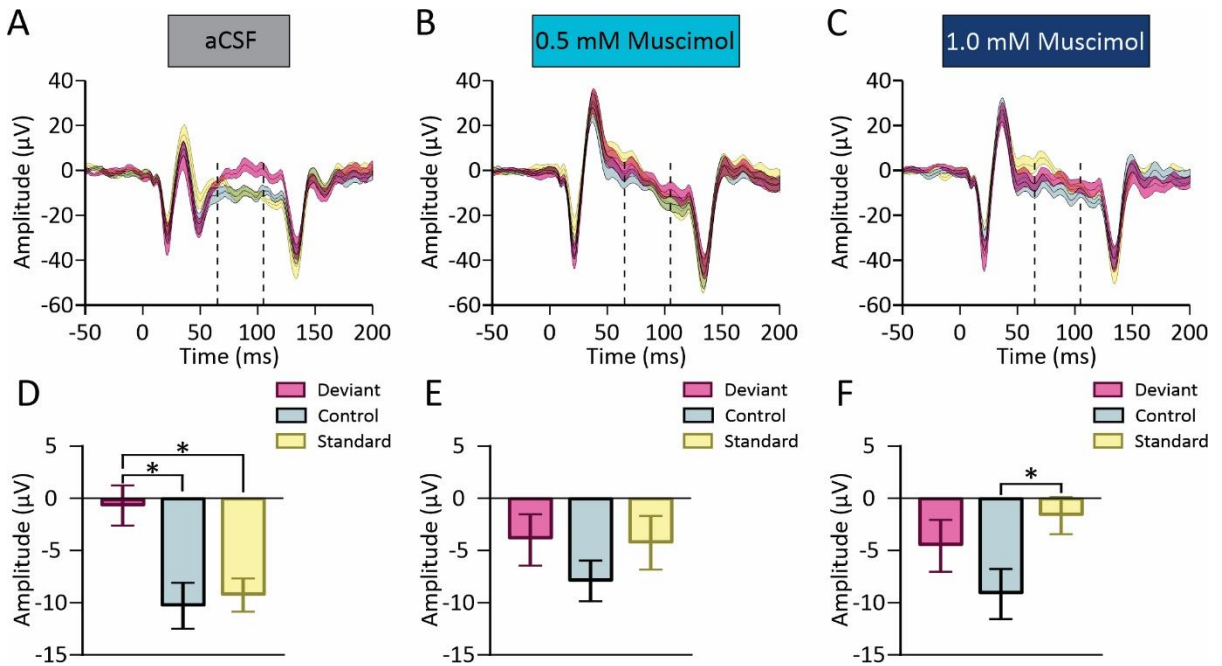
Figure 4.15 The deviant response typically observed in the auditory cortex during an oddball protocol was diminished following the inactivation of the medial prefrontal cortex (mPFC). (A-C) *The group mean profile of evoked responses to 8 kHz tone when presented as: deviant (DEV, pink), control (CTR, grey) and standard (STD, yellow), following the medial prefrontal cortex infusion (0.5 uL) of aCSF (A), 0.5 mM (B), and 1.0 mM muscimol (C). Shading indicates SEM, and dashed lines indicate the response between 65-105 ms, used for the group average.* ***(D-F)*** *Group average of the response to 8 kHz when presented as DEV, CTR, and STD. (D) As expected, following aCSF infusion, the DEV response was significantly different from the response elicited by the CTR and STD (*p_{Bonf} < 0.05). (E) Following the 0.5 mM muscimol infusion, there was no difference between the response to 8 kHz tone presented as DEV, CTR or STD. (F) Following the 1.0 mM muscimol infusion, there was a significant difference between the response to 8 kHz tone as CTR and STD (*p_{Bonf} < 0.05). Collectively, these data show that the deviant response observed in the auditory cortex in the aCSF condition was diminished following inactivation of the mPFC via muscimol. Data represent group mean ± SEM; n= 13 rats.*

4.3.8 Muscimol infusion into the medial prefrontal cortex had a differential effect on the response to an 8 kHz tone presented as a deviant versus a standard stimulus during an oddball protocol.

Although a one-way RM-ANOVA revealed a significant effect of the treatment on the DEV stimulus ($F_{(1.85, 22.26)}$ = 1.37; p = 0.009), the Bonferroni corrected post-hoc analysis did not show a significant difference between the control aCSF conditions and the treatments (**Figure 4.16A**). That said, there was a trend for this waveform to decrease (become more negative) following muscimol infusion. The waveform elicited by the CTR stimulus was not affected by the treatment as indicated by the lack of treatment effect in the one-way RM-ANOVA ($F_{(1.99, 23.94)}$ = 0.38; p = 0.689) (**Figure 4.16B**).The response to STD stimulus revealed a significant effect of treatment (one-way RM-ANOVA: $F_{(1.48, 17.80)}$ = 3.95; p = 0.049), and Bonferroni corrected post-hoc analysis revealed a significantly increased amplitude (more positive) of the STD response following infusion of 1.0 mM muscimol into the mPFC (aCSF: -9.32 ± 1.11 µV vs. 1.0 mM muscimol: -1.60 ± 1.78 µV; p_{Bonf} = 0.035) (**Figure 4.16C**).
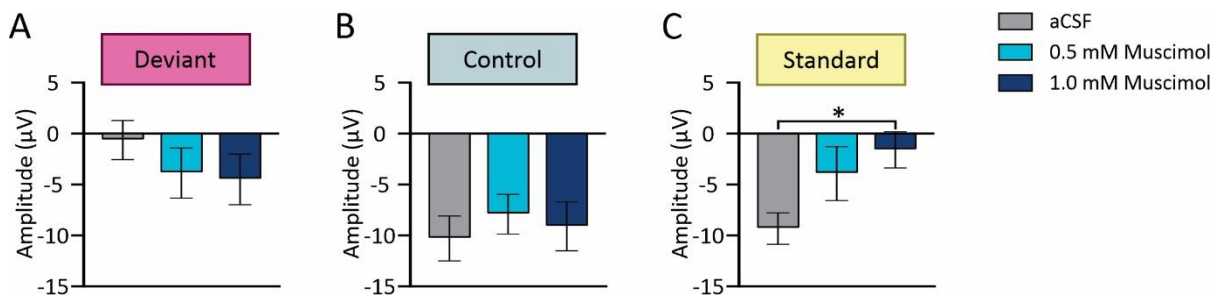
***Figure 4.16 Muscimol infusion into the medial prefrontal cortex (mPFC) had a differential effect on the response to an 8 kHz tone presented as a deviant versus a standard stimulus during an oddball protocol, indicating an altered mismatch response. (A)** One-way RM-ANOVA revealed a significant effect of the treatment on the 8 kHz tone presented as deviant (DEV). However, the post-hoc analysis failed to show a significant difference between the aCSF and muscimol conditions. **(B)** There was no significant effect of treatment on the response of the 8 kHz stimulus when it was presented as control (CTR). **(C)** The average response to 8 kHz tone presented as standard (STD) showed a significant treatment effect. Furthermore, the STD response following the infusion of 1.0 mM muscimol was significantly decreased compared with the response following aCSF infusion into the mPFC.*

Finally, to investigate the consequence of mPFC inactivation on different aspects of the MMN-like responses recorded in the auditory cortex, calculations were performed to

measure: prediction error (DEV response − CTR response); repetition suppression (STD − CTR) and mismatch response (DEV − STD) (Parras *et al.*, 2017). A two-way RM-ANOVA for measurement (Prediction Error; Repetition Suppression; Mismatch Response) x treatment (aCSF; 0.5 mM muscimol; 1.0 mM muscimol) revealed a main effect of measurement ($F_{(1.32, 15.90)}$ = 4.66; p = 0.038), as well as a significant interaction between the measurement and the treatment ($F_{(1.75, 21.04)}$ = 4.49; p = 0.028). Thus, the effects of the treatments (aCSF; 0.5 and 1.0 mM muscimol) on each of the measurements (Prediction Error; Repetition Suppression; Mismatch Response) were carried out separately using one-way RM-ANOVAs. Despite the above-mentioned loss of the DEV effect following infusion of 0.5 mM and 1.0 mM muscimol (**Figure 4.15**) the deviance detection measurement did not reveal a significant effect of the treatment ($F_{(1.89, 22.72)}$ = 2.91; p = 0.077) (**Figure 4.17A**).
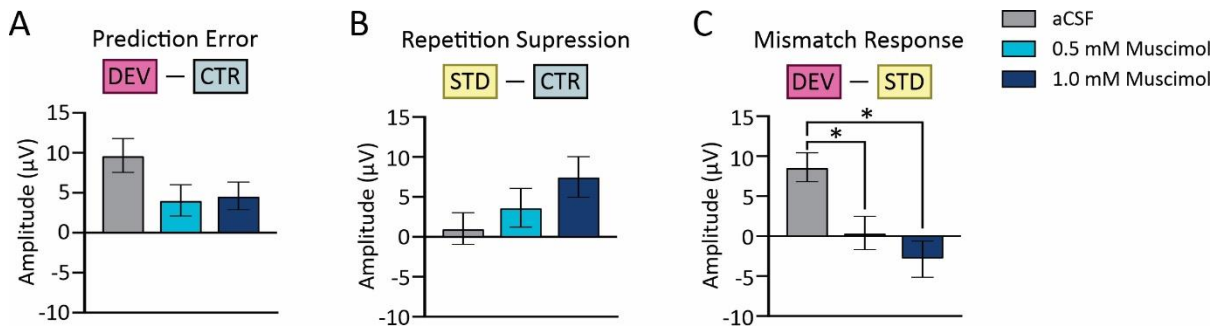
Figure 4.17 The loss of mismatch response following medial prefrontal cortex (mPFC) inactivation could be explained by a combined effect of decreased prediction error and increased repetition suppression. (A) Prediction Error (difference between the DEV and CTR) showed a trend to decrease following the infusion with muscimol; however, the statistical analysis did not show a significant treatment's main effect. *(B)* Repetition Suppression (difference between the STD and CTR) indicated a trend to increase the following infusion with muscimol, but a one-way RM-ANOVA did not show a significant treatment's main effect. *(C)* The Mismatch Response (difference between the DEV and STD) highlighted the differential effect of inactivation of the mPFC on DEV and STD, as it significantly decreased following muscimol infusion at 0.5mM and 1.0 mM. Data represent group mean ± SEM; n= 13 rats; (*p_{Bonf} < 0.05).*

Similarly, a one-way RM-ANOVA failed to reveal a significant effect of treatment on stimulus adaptation ($F_{(1.66, 19.92)}$ = 1.66; p = 0.22) (**Figure 4.17B**). However, consistent with the observations of a differential effect of the treatments on DEV and STD, a one-way RM-

ANOVA showed a significant effect of the muscimol infusion on the mismatch response ($F_{(1.64, 19.63)}$ = 8.24; p = 0.004), and post-hoc analysis with Bonferroni correction showed a drastic reduction in mismatch response (indicative of a decrease in the difference between the waveforms elicited by the DEV and STD) following muscimol infusion (aCSF 8.69 ± 1.78 μV vs 0.5 mM muscimol 0.06 ± 2.03 μV; p_{Bonf} = 0.005; aCSF 8.69 ± 1.78 μV vs 1.0 mM muscimol -2.88 ± 2.28 μV; p_{Bonf} = 0.005) (**Figure 4.17 C**). These results further suggest a differential effect of inactivation of the mPFC on the responses to 8 kHz stimuli recorded from the auditory cortex depending on whether it was presented as a deviant (DEV) or a standard (STD) during the oddball protocol. For detailed statistical information, see **Table 4.3.**

Test	Main effect/comparison	p-value	F-value/t-value; DF
Figure 4.11 Initial Sound-Evoked Response (N18)			
1-way RM-ANOVA	Treatment (aCSF, 0.5 mM, 1.0 mM muscimol)	0.417	$F_{(1.26, 15.08)} = 0.79$
Figure 4.12 ASSR Evoked power			
1-way RM-ANOVA	Treatment (aCSF, 0.5 mM, 1.0 mM muscimol)	0.588	$F_{(1.64, 19.65)} = 0.48$
Figure 4.13 ASSR Inter-trial coherence			
1-way RM-ANOVA	Treatment (aCSF, 0.5 mM, 1.0 mM muscimol)	0.938	$F_{(1.69, 20.24)} = 0.04$
Figure 4.14 Spontaneous gamma oscillations			
1-way RM-ANOVA	Treatment (aCSF, 0.5mM, 1.0mM muscimol) *	0.008	$F_{(1.72, 20.62)} = 6.59$
Post-hoc	Gamma aCSF vs. 0.5 mM muscimol *	0.015 [B]	t= 3.21; DF = 12
Post-hoc	Gamma aCSF vs. 1.0 mM muscimol *	0.005 [B]	t= 3.81; DF = 12
Figure 4.15 Deviant response effect			
	Treatment (aCSF, 0.5 mM, 1.0 mM muscimol)	0.597	$F_{(1.43, 17.17)} = 0.42$
2-way RM-ANOVA	Stimulus type (DEV, CTR, STD) *	<0.001	$F_{(1.92, 23.01)} = 14.69$
	Interaction (treatment x stimulus type) *	0.020	$F_{(2.59, 31.06)} = 4.00$
Figure 4.15 A&D. Deviant response effect aCSF			
1-way RM-ANOVA	Stimulus type (DEV, CTR, STD) *	<0.001	$F_{(1.93, 23.14)} = 14.57$
Post-hoc	aCSF DEV vs. CTR	0.002 [B]	t= 4.57; DF = 12
Post-hoc	aCSF DEV vs. STD	0.001 [B]	t= 4.87; DF = 12
Post-hoc	aCSF STD vs. CTR	>0.999 [B]	t= 0.48; DF = 12
Figure 4.15 B&E. Deviant response effect 0.5 mM muscimol			
1-way RM-ANOVA	Stimulus type (DEV, CTR, STD)	0.124	$F_{(1.86, 22.31)} = 2.33$
Figure 4.15 C&F. Deviant response effect 1.0 mM muscimol			
1-way RM-ANOVA	Stimulus type (DEV, CTR, STD) *	0.012	$F_{(1.71, 20.55)} = 5.89$
Post-hoc	1.0 mM muscimol DEV vs. CTR	0.061 [B]	t= 2.67; DF = 12
Post-hoc	1.0 mM muscimol DEV vs. STD	0.688 [B]	t= 1.27; DF = 12
Post-hoc	1.0 mM muscimol STD vs. CTR	0.035 [B]	t= 2.97; DF = 12
Figure 4.16 Differential effect of PFC treatment with muscimol on response to different stimuli types			
Figure 4.16 A. Deviant response			
1-way RM-ANOVA	Treatment (aCSF, 0.5 mM, 1.0 mM muscimol) *	0.009	$F_{(1.85, 22.26)} = 1.37$
Post-hoc	DEV aCSF vs. 0.5 mM muscimol	0.545 [B]	t= 1.15; DF = 12
Post-hoc	DEV aCSF vs. 1.0 mM muscimol	0.216 [B]	t= 1.74; DF = 12
Figure 4.16 B. Control response			
1-way RM-ANOVA	Treatment (aCSF, 0.5 mM, 1.0 mM muscimol)	0.689	$F_{(1.99, 23.94)} = 0.38$
Figure 4.16 C Standard response			
1-way RM-ANOVA	Treatment (aCSF, 0.5 mM, 1.0 mM muscimol) *	0.049	$F_{(1.48, 17.80)} = 3.95$
Post-hoc	STD aCSF vs. 0.5 mM muscimol	0.187 [B]	t= 1.82; DF = 12
Post-hoc	STD aCSF vs. 1.0 mM muscimol *	0.003 [B]	t= 4.11; DF = 12
Figure 4.17. Prediction Error, Repetition Suppression and Mismatch Response			
	Treatment (aCSF, 0.5 mM, 1.0 mM muscimol)	0.077	$F_{(1.89, 22.72)} = 2.91$
2-way RM-ANOVA	Measurement (DD, SA, MMR) *	0.038	$F_{(1.32, 15.90)} = 4.66$
	Interaction (treatment x measurement) *	0.028	$F_{(1.75, 21.04)} = 4.49$
Figure 4.17 A. Prediction Error			
1-way RM-ANOVA	Treatment (aCSF, 0.5 mM, 1.0 mM muscimol)	0.077	$F_{(1.89, 22.72)} = 2.91$
Figure 4.17 B. Repetition Suppression			
1-way RM-ANOVA	Treatment (aCSF, 0.5 mM, 1.0 mM muscimol)	0.216	$F_{(1.66, 19.92)} = 1.66$
Figure 4.17 C. Mismatch response (MMR)			
1-way RM-ANOVA	Treatment (aCSF, 0.5 mM, 1.0 mM muscimol) *	0.004	$F_{(1.64, 19.63)} = 8.24$
Post-hoc	MMR aCSF vs. 0.5 mM muscimol *	0.005 [B]	t= 3.84; DF = 12
Post-hoc	MMR aCSF vs. 1.0 mM muscimol *	0.005 [B]	t= 3.84; DF = 12

Table 4.3 *Summary of statistical tests performed during the electrophysiological recordings following the medial prefrontal cortex inactivation.*

4.4 Discussion

4.4.1 Sound detection deficits following the medial prefrontal cortex inactivation.

In line with the previous studies indicating the significant role of the mPFC in auditory selection task (Rodgers and DeWeese, 2014), the results of this study showed that the inactivation of the mPFC led to significantly impaired performance on a sound detection task. Interestingly, the lower dose of the muscimol resulted in significantly impaired sound detection in background noise but not in quiet. This novel finding indicates that the rodent mPFC might excrete an inhibitory effect on the auditory cortex to suppress the distracting information (i.e., background noise), to enhance the signalling of the target stimulus. In line with this proposal are the findings showing the effect of attention on cortical representation of targeted sound stimuli (Fritz, Elhilali and Shamma, 2007; Atiani *et al.*, 2009; Yin, Fritz and Shamma, 2014). A similar mechanism is observed in visual selective attention. Experiments with non-human primates revealed that the prefrontal cortex sends top-down "bias signals" to the sensory cortex to select the target stimulus, enhancing its neural representation while suppressing the representation of distractors (Miller and Cohen, 2001; Moore, Armstrong and Fallah, 2003).

A possible neurophysiological mechanism of this auditory selective attention, and its impairment following the inactivation of mPFC evident as decreased ability to detect sounds, could be altered cholinergic inputs to the auditory cortex. For example, studies showed that inactivation of the mPFC with muscimol abolishes the cortical acetylcholine release evoked by sensory stimulation in rats (Rasmusson, Smith and Semba, 2007). This neuromodulatory transmitter has been implicated in regulating various higher cortical functions, including working memory and attention (Sarter, Bruno and Givens, 2003; Dalley, Everitt and Robbins, 2011). Interestingly, a study in rodents reported that sound detection learning depends heavily on cholinergic inputs to the auditory cortex (Kudoh, Seki and Shibuki, 2004). Although the authors concluded that the decreased performance

on their task was due to impaired learning, it cannot be ruled out that the underlying reason for the poor performance lies in rats' possible inability to detect the sounds rather than learning. However, additional studies are needed to confirm or refute this possibility.

Consistent with the proposed auditory attention deficits underlying the reason for impaired sound detection, the results of this study showed a significant correlation between poor performance and increased impulsivity, assessed as the increased number of nose-pokes required to initiate the trial (Doremus-Fitzwater, Barreto and Spear, 2012). However, there are some that point to a significant distinction between impulsivity and attention. For example, a rodent study showed that mPFC inactivation with muscimol increased impulsive behaviour without affecting attention (Paine, Slipp and Carlezon, 2011). Therefore, future studies are needed to address this caveat and to further investigate the role of the mPFC in auditory selective attention.

4.4.2 Intact auditory processing along the primary auditory pathway following the inactivation of the medial prefrontal cortex.

Consistent with the view that the mechanisms underlying the acoustic startle response and prepulse inhibition are confined to the neural circuits within the brainstem (Davis and Gendelman, 1977; Fox, 1979; Li and Frost, 2000), the experiments in this study found that inactivation of the mPFC via local muscimol injection did not affect these pre-attentive responses. Considering these findings and current theories, it was somewhat unexpected to observe that muscimol infusion decreased the level of short-term habituation; a phenomenon often ascribed to synaptic depression within the primary startle pathway in the brainstem (Leaton, Cassella and Borszcz, 1985; Weber, Schnitzler and Schmid, 2002; Simons-Weidenmaier *et al.*, 2006; Zaman *et al.*, 2017). Although a potential top-down modulatory influence on acoustic stimulus processing cannot be ruled out with certainty (Koch and Schnitzler, 1997), it is essential to consider an alternative explanation for our results. The dual-process theory proposed by Groves and Thompson (1970) suggests that

following repeated exposure to a stimulus, the behavioural outcome is dependent on two opposing processes: habituation and sensitization, with the latter leading to enhancement of the response magnitude (Groves and Thompson, 1970; Pilz and Schnitzler, 1996; Bhandiwad *et al.*, 2018; Carnaghi and Starobin, 2019). Unlike the habituation processes that reside within the primary startle pathway, the sensitization occurs in a separate pathway (Groves and Thompson, 1970; Davis and Sheard, 1974; Davis and Gendelman, 1977; Fendt, Koch and Schnitzler, 1994a, 1994b; Pilz and Schnitzler, 1996). Ultimately, the input of these pathways is integrated within the primary startle circuitry, and the behavioural output equals the summative activity of these opposing processes. Although the neural circuitry underlying sensitization is not very well understood, studies suggest that regions outside of the brainstem, e.g., amygdala, might play an important role (Fendt, Koch and Schnitzler, 1994a). Notably, the interactions between the amygdala and the mPFC are crucial for emotional regulation and limbic activity (Blair *et al.*, 2008), and ex-vivo animal studies showed bidirectional connections between the amygdala and mPFC (Ghashghaei and Barbas, 2002; Ghashghaei, Hilgetag and Barbas, 2007). Furthermore, GABAerigc activity within the prefrontal cortex influences the autonomic response to threatening stimuli (Constantinidis, Williams and Goldman-Rakic, 2002; Akirav and Maroun, 2007; Chefer, Wang and Shippenberg, 2011; Moscarello and LeDoux, 2013; Courtin *et al.*, 2014). Thus, it suggests that the decrease in short-term habituation in the present study following mPFC inactivation might be a result of increased sensitization of the motor response to the acoustic stimulus, mediated through an amygdala – medial prefrontal cortex circuit, perhaps enhancing or inducing anxiety-like effects, rather than a consequence of the top-down modulation on sound processing within the primary auditory pathway at the level of the brainstem.

Of the three pre-attentive processes examined in the present study, it was short-term habituation (i.e., a form of sensory filtering) rather than acoustic reactivity or prepulse inhibition (i.e., sensorimotor gating) that was affected by inactivation of the mPFC. As such, the present findings may provide insight for studies on clinical populations, such as

schizophrenia and autism spectrum disorder, as these neurodevelopmental conditions are associated with impaired prepulse inhibition (Mena *et al.*, 2016; Cheng *et al.*, 2018; Scott *et al.*, 2018; Swerdlow *et al.*, 2018) as well as altered neural circuitry and neurotransmitter systems in the prefrontal cortex (Ajram *et al.*, 2017; Ferguson and Gao, 2018; Kehr *et al.*, 2018; Dienel and Lewis, 2019; Dienel *et al.*, 2020). Because inactivation of the mPFC did not alter prepulse inhibition in the present study, it is reasonable to question whether the clinically related deficits in the dorsolateral prefrontal cortex (the proposed homologue of the rodent mPFC) of individuals with schizophrenia or autism would be sufficient to underlie their commonly reported impairments in sensorimotor gating.

At the level of the auditory cortex, the present study found no effect of mPFC inactivation on sound-evoked responses related to primary sensory processing, as there were no changes in the amplitude of the N18 response of the event-related potential or the 40-Hz auditory steady-state response metrics (i.e., evoked power and inter-trial coherence) following muscimol infusion into the mPFC. These results appear to conflict with past studies which reported increased sound-evoked responses following prefrontal lesions (Knight, 1984; Knight *et al.*, 1999). Based on these past findings and the suggestion that the prefrontal cortex exerts a net inhibitory output that gates the input to the primary auditory cortex (Knight *et al.*, 1999), the present results were somewhat surprising. It was expected that local muscimol injection would decrease the activity of the pyramidal neurons of the mPFC, resulting in less inhibitory output to the auditory cortex, and this, in turn, would manifest as exaggerated sound-evoked responses reminiscent of central gain enhancement. Given that the muscimol doses used in the present study well exceed the physiological properties of muscimol binding at the receptor (DeFeudis, 1980; Madtes, Bashir-Elahi and Chader, 1986), it is not likely that the chosen does were too subtle to induce a significant physiological effect. Instead, perhaps the differences in results observed between the present pharmacological study and those of Knight and colleagues

(1999) were due to the immediate versus long-term nature of the disruption to the prefrontal cortex in the two studies.

To my knowledge, no previous study has investigated the effect of prefrontal cortex manipulation on auditory-state responses recorded from the auditory cortex. That said, a recent optogenetic study in mice did investigate the local consequences of mPFC disruption. More specifically, Toader *et al.*, (2020) reported that disinhibition of the mPFC via selective silencing of its fast-spiking (parvalbumin-expressing) inhibitory interneurons resulted in a local decrease of the 40-Hz auditory steady-state response recorded from the mPFC. Furthermore, they found that their optogenetic protocol also *increased* the spontaneous gamma oscillations in the mPFC; findings that conflict with an earlier report (Sohal, 2016), which showed that disrupting PV-expressing interneurons caused a local *decrease* in the synchronized activity in the gamma band. Given that the present study found a decrease in gamma oscillations in the auditory cortex following pharmacological inactivation of the mPFC, it would be interesting to investigate the effect of selective silencing of PV-expressing neurons in the mPFC on both the spontaneous oscillations and 40-Hz auditory steady-state responses recorded from the auditory cortex.

4.4.3 Higher-level auditory processing deficits may contribute to the impaired sound detection following medial prefrontal cortex inactivation.

As mentioned above, the inactivation of the mPFC did not affect neurons' ability in the auditory cortex to sustain the sound-evoked gamma oscillations; however, the spontaneous gamma oscillations were significantly decreased. Previous studies indicate that spontaneous gamma oscillations are crucial for short-range neuronal communication within a particular cortical region (Karakaş and Barry, 2017). Furthermore, these fast oscillations may be responsible for the coordination of multiple sensory stimuli into a single, cognitively relevant percept giving rise to a conscious awareness of the stimuli (Joliot, Ribary and Llinás, 1994; Pritchett *et al.*, 2015; Cardin, 2016; Sohal, 2016; Mock *et al.*, 2018). Although the inactivation of the mPFC did not disrupt basic auditory processing,

the decrease of spontaneous oscillation might imply perceptual deficits. In support of this suggestion, there was also a significant effect of mPFC inactivation on the mismatch response recorded from the auditory cortex. As previous studies indicate, the late latency response, like the one elicited by the mismatch response, results from higher-order auditory processing related to perceptual functions (Joos *et al.*, 2014). Considering that the mPFC inactivation was found to affect the deviant and the standard stimuli, it might suggest that the mPFC inactivation led to deficits in generating the perceptual prediction about the upcoming stimulus. Furthermore, several studies have indicated a relationship between the mismatch response amplitude and performance on auditory detection tasks (Sams *et al.*, 1985; Novak, Ritter and Vaughan, 1992). Therefore, the decreased ability for sound detection in background noise could result from the diminished deviant response effect following the mPFC inactivation or even be driven by the same underlying mechanism. However, considering that the mismatch response and sound detection task used different stimuli, further research on this topic is needed.

4.5 References

Adriani, W. *et al.* (2003) 'The spontaneously hypertensive-rat as an animal model of ADHD: evidence for impulsive and non-impulsive subpopulations', *Neuroscience & Biobehavioral Reviews*, 27(7), pp. 639–651. doi: 10.1016/j.neubiorev.2003.08.007.

Ajram, L. A. *et al.* (2017) 'Shifting brain inhibitory balance and connectivity of the prefrontal cortex of adults with autism spectrum disorder', *Translational Psychiatry*, 7(5), pp. e1137–e1137. doi: 10.1038/tp.2017.104.

Akirav, I. and Maroun, M. (2007) *The Role of the Medial Prefrontal Cortex-Amygdala Circuit in Stress Effects on the Extinction of Fear*, *Neural Plasticity*. Hindawi. doi: https://doi.org/10.1155/2007/30873.

Alexander, G. E., Newman, J. D. and Symmes, D. (1976) 'Convergence of prefrontal and acoustic inputs upon neurons in the superior temporal gyrus of the awake squirrel monkey', *Brain Research*, 116(2), pp. 334–338. doi: 10.1016/0006-8993(76)90913-6.

Alho, K. *et al.* (1994) 'Lesions of frontal cortex diminish the auditory mismatch negativity', *Electroencephalography and Clinical Neurophysiology*, 91(5), pp. 353–362. doi: 10.1016/0013-4694(94)00173-1.

Alho, K. (1995) 'Cerebral Generators of Mismatch Negativity (MMN) and Its Magnetic Counterpart (MMNm) Elicited by Sound Changes', *Ear and Hearing*, 16(1), pp. 38–51.

Atiani, S. *et al.* (2009) 'Task Difficulty and Performance Induce Diverse Adaptive Patterns in Gain and Shape of Primary Auditory Cortical Receptive Fields', *Neuron*, 61(3), pp. 467–480. doi: 10.1016/j.neuron.2008.12.027.

Baradits, M. *et al.* (2019) 'Alterations in resting-state gamma activity in patients with schizophrenia: a high-density EEG study', *European Archives of Psychiatry and Clinical Neuroscience*, 269(4), pp. 429–437. doi: 10.1007/s00406-018-0889-z.

Beaumont, K. *et al.* (1978) 'Muscimol binding in rat brain: Association with synaptic GABA receptors', *Brain Research*, 148(1), pp. 153–162. doi: 10.1016/0006-8993(78)90385-2.

Bhandiwad, A. A. *et al.* (2018) 'Noise-Induced Hypersensitization of the Acoustic Startle Response in Larval Zebrafish', *Journal of the Association for Research in Otolaryngology*, 19(6), pp. 741–752. doi: 10.1007/s10162-018-00685-0.

Bizley, J. K. and Cohen, Y. E. (2013) 'The what, where and how of auditory-object perception', *Nature Reviews Neuroscience*, 14(10), pp. 693–707. doi: 10.1038/nrn3565.

Blair, K. *et al.* (2008) 'Response to Emotional Expressions in Generalized Social Phobia and Generalized Anxiety Disorder: Evidence for Separate Disorders', *American Journal of Psychiatry*, 165(9), pp. 1193–1202. doi: 10.1176/appi.ajp.2008.07071060.

Cannon, T. D. *et al.* (2005) 'Association of DISC1/TRAX Haplotypes With Schizophrenia, Reduced Prefrontal Gray Matter, and Impaired Short- and Long-term Memory', *Archives of General Psychiatry*, 62(11), pp. 1205–1213. doi: 10.1001/archpsyc.62.11.1205.

Carbajal, G. V. and Malmierca, M. S. (2018) 'The Neuronal Basis of Predictive Coding Along the Auditory Pathway: From the Subcortical Roots to Cortical Deviance Detection', *Trends in Hearing*, 22, p. 2331216518784822. doi: 10.1177/2331216518784822.

Cardin, J. A. (2016) 'Snapshots of the Brain in Action: Local Circuit Operations through the Lens of γ Oscillations', *Journal of Neuroscience*, 36(41), pp. 10496–10504. doi: 10.1523/JNEUROSCI.1021-16.2016.

Carnaghi, M. M. and Starobin, J. M. (2019) 'Reaction-diffusion memory unit: Modeling of sensitization, habituation and dishabituation in the brain', *PLOS ONE*, 14(12), p. e0225169. doi: 10.1371/journal.pone.0225169.

Chefer, V. I., Wang, R. and Shippenberg, T. S. (2011) 'Basolateral Amygdala-Driven Augmentation of Medial Prefrontal Cortex GABAergic Neurotransmission in Response to Environmental Stimuli Associated with Cocaine Administration', *Neuropsychopharmacology*, 36(10), pp. 2018–2029. doi: 10.1038/npp.2011.89.

Cheng, C.-H. *et al.* (2018) 'Meta-analysis of sensorimotor gating in patients with autism spectrum disorders', *Psychiatry Research*, 262, pp. 413–419. doi: 10.1016/j.psychres.2017.09.016.

Constantinidis, C., Williams, G. V. and Goldman-Rakic, P. S. (2002) 'A role for inhibition in shaping the temporal flow of information in prefrontal cortex', *Nature Neuroscience*, 5(2), pp. 175–180. doi: 10.1038/nn799.

Courtin, J. *et al.* (2014) 'Prefrontal parvalbumin interneurons shape neuronal activity to drive fear expression', *Nature*, 505(7481), pp. 92–96. doi: 10.1038/nature12755.

Dalley, J. W., Cardinal, R. N. and Robbins, T. W. (2004) 'Prefrontal executive and cognitive functions in rodents: neural and neurochemical substrates', *Neuroscience & Biobehavioral Reviews*, 28(7), pp. 771–784. doi: 10.1016/j.neubiorev.2004.09.006.

Dalley, J. W., Everitt, B. J. and Robbins, T. W. (2011) 'Impulsivity, Compulsivity, and Top-Down Cognitive Control', *Neuron*, 69(4), pp. 680–694. doi: 10.1016/j.neuron.2011.01.020.

Damasio, A. R. and Anderson, S. W. (2003) 'The frontal lobes', in *Clinical neuropsychology, 4th ed*. New York, NY, US: Oxford University Press, pp. 404–446.

Davis, M. and Gendelman, P. M. (1977) 'Plasticity of the acoustic startle response in the acutely decerebrate rat', *Journal of Comparative and Physiological Psychology*, 91(3), pp. 549–563. doi: 10.1037/h0077345.

Davis, M. and Sheard, M. H. (1974) 'Habituation and sensitization of the rat startle response: Effects of raphe lesions', *Physiology & Behavior*, 12(3), pp. 425–431. doi: 10.1016/0031-9384(74)90120-6.

DeFeudis, F. V. (1980) 'Physiological and behavioral studies with muscimol', *Neurochemical Research*, 5(10), pp. 1047–1068. doi: 10.1007/BF00966163.

Dienel, S. J. *et al.* (2020) 'Markers of glutamate and GABA neurotransmission in the prefrontal cortex of schizophrenia subjects: Disease effects differ across anatomical levels of resolution', *Schizophrenia Research*, 217, pp. 86–94. doi: 10.1016/j.schres.2019.06.003.

Dienel, S. J. and Lewis, D. A. (2019) 'Alterations in cortical interneurons and cognitive function in schizophrenia', *Neurobiology of Disease*, 131, p. 104208. doi: 10.1016/j.nbd.2018.06.020.

Doremus-Fitzwater, T. L., Barreto, M. and Spear, L. P. (2012) 'Age-related differences in impulsivity among adolescent and adult Sprague-Dawley rats', *Behavioral Neuroscience*, 126(5), pp. 735–741. doi: 10.1037/a0029697.

Duque, A. and McCormick, D. A. (2010) 'Circuit-based Localization of Ferret Prefrontal Cortex', *Cerebral Cortex*, 20(5), pp. 1020–1036. doi: 10.1093/cercor/bhp164.

Economidou, D. *et al.* (2009) 'High Impulsivity Predicts Relapse to Cocaine-Seeking After Punishment-Induced Abstinence', *Biological Psychiatry*, 65(10), pp. 851–856. doi: 10.1016/j.biopsych.2008.12.008.

Edinger, H. M., Siegel, A. and Troiano, R. (1975) 'Effect of stimulation of prefrontal cortex and amygdala on diencephalic neurons', *Brain Research*, 97(1), pp. 17–31. doi: 10.1016/0006-8993(75)90911-7.

Fendt, M., Koch, M. and Schnitzler, H.-U. (1994a) 'Amygdaloid noradrenaline is involved in the sensitization of the acoustic startle response in rats', *Pharmacology Biochemistry and Behavior*, 48(2), pp. 307–314. doi: 10.1016/0091-3057(94)90532-0.

Fendt, M., Koch, M. and Schnitzler, H.-U. (1994b) 'Lesions of the central gray block the sensitization of the acoustic startle response in rats', *Brain Research*, 661(1), pp. 163–173. doi: 10.1016/0006-8993(94)91193-2.

Ferguson, B. R. and Gao, W.-J. (2018) 'PV Interneurons: Critical Regulators of E/I Balance for Prefrontal Cortex-Dependent Behavior and Psychiatric Disorders', *Frontiers in Neural Circuits*, 12. doi: 10.3389/fncir.2018.00037.

Fox, J. E. (1979) 'Habituation and prestimulus inhibition of the auditory startle reflex in decerebrate rats', *Physiology & Behavior*, 23(2), pp. 291–297. doi: 10.1016/0031-9384(79)90370-6.

Fritz, J. B. *et al.* (2010) 'Adaptive, behaviorally gated, persistent encoding of task-relevant auditory information in ferret frontal cortex', *Nature Neuroscience*, 13(8), pp. 1011–1019. doi: 10.1038/nn.2598.

Fritz, J. B., Elhilali, M. and Shamma, S. A. (2007) 'Adaptive Changes in Cortical Receptive Fields Induced by Attention to Complex Sounds', *Journal of Neurophysiology*, 98(4), pp. 2337–2346. doi: 10.1152/jn.00552.2007.

Fulcher, N. *et al.* (2020) 'Deciphering midbrain mechanisms underlying prepulse inhibition of startle', *Progress in Neurobiology*, 185, p. 101734. doi: 10.1016/j.pneurobio.2019.101734.

Ghashghaei, H. T. and Barbas, H. (2002) 'Pathways for emotion: interactions of prefrontal and anterior temporal pathways in the amygdala of the rhesus monkey', *Neuroscience*, 115(4), pp. 1261–1279. doi: 10.1016/S0306-4522(02)00446-3.

Ghashghaei, H. T., Hilgetag, C. C. and Barbas, H. (2007) 'Sequence of information processing for emotions based on the anatomic dialogue between prefrontal cortex and amygdala', *NeuroImage*, 34(3), pp. 905–923. doi: 10.1016/j.neuroimage.2006.09.046.

Gonzalez-Burgos, G., Cho, R. Y. and Lewis, D. A. (2015) 'Alterations in Cortical Network Oscillations and Parvalbumin Neurons in Schizophrenia', *Biological Psychiatry*, 77(12), pp. 1031–1040. doi: 10.1016/j.biopsych.2015.03.010.

Grent-'t-Jong, T. *et al.* (2018) 'Resting-state gamma-band power alterations in schizophrenia reveal E/I-balance abnormalities across illness-stages', *eLife*. Edited by R. B. Ivry, 7, p. e37799. doi: 10.7554/eLife.37799.

Groenewegen, H. J. and Uylings, H. B. M. (2000) 'The prefrontal cortex and the integration of sensory, limbic and autonomic information', in *Progress in Brain Research*. Elsevier (Cognition, emotion and autonomic responses: The integrative role of the prefrontal cortex and limbic structures), pp. 3–28. doi: 10.1016/S0079-6123(00)26003-2.

Groves, P. M. and Thompson, R. F. (1970) 'Habituation: A dual-process theory', *Psychological Review*, 77(5), pp. 419–450. doi: 10.1037/h0029810.

Harms, L. *et al.* (2014) 'Mismatch Negativity (MMN) in Freely-Moving Rats with Several Experimental Controls', *PLOS ONE*, 9(10), p. e110892. doi: 10.1371/journal.pone.0110892.

Harms, L. *et al.* (2018) 'Late deviance detection in rats is reduced, while early deviance detection is augmented by the NMDA receptor antagonist MK-801', *Schizophrenia Research*, 191, pp. 43–50. doi: 10.1016/j.schres.2017.03.042.

Harms, L., Michie, P. T. and Näätänen, R. (2016) 'Criteria for determining whether mismatch responses exist in animal models: Focus on rodents', *Biological Psychology*, 116, pp. 28–35. doi: 10.1016/j.biopsycho.2015.07.006.

Hayes, S. H. *et al.* (2020) 'Uncovering the contribution of enhanced central gain and altered cortical oscillations to tinnitus generation', *Progress in Neurobiology*, p. 101893. doi: 10.1016/j.pneurobio.2020.101893.

Hirano, Y. *et al.* (2015) 'Spontaneous Gamma Activity in Schizophrenia', *JAMA Psychiatry*, 72(8), pp. 813–821. doi: 10.1001/jamapsychiatry.2014.2642.

Ison, J. R., Peter Bowen, G. and O'connor, K. (1991) 'Reflex modification produced by visual stimuli in the rat following functional decortication', *Psychobiology*, 19(2), pp. 122–126. doi: 10.3758/BF03327181.

Jacobsen, T., Horenkamp, T. and Schröger, E. (2003) 'Preattentive Memory-Based Comparison of Sound Intensity', *Audiology and Neurotology*, 8(6), pp. 338–346. doi: 10.1159/000073518.

Jacobsen, T. and Schröger, E. (2001) 'Is there pre-attentive memory-based comparison of pitch?', *Psychophysiology*, 38(4), pp. 723–727. doi: https://doi.org/10.1111/1469-8986.3840723.

Joliot, M., Ribary, U. and Llinás, R. (1994) 'Human oscillatory brain activity near 40 Hz coexists with cognitive temporal binding', *Proceedings of the National Academy of Sciences*, 91(24), pp. 11748–11751. doi: 10.1073/pnas.91.24.11748.

Joos, K. *et al.* (2014) 'From sensation to percept: The neural signature of auditory event-related potentials', *Neuroscience & Biobehavioral Reviews*, 42, pp. 148–156. doi: 10.1016/j.neubiorev.2014.02.009.

Jung, F. *et al.* (2013) 'Mismatch Responses in the Awake Rat: Evidence from Epidural Recordings of Auditory Cortical Fields', *PLOS ONE*, 8(4), p. e63203. doi: 10.1371/journal.pone.0063203.

Karakaş, S. and Barry, R. J. (2017) 'A brief historical perspective on the advent of brain oscillations in the biological and psychological disciplines', *Neuroscience & Biobehavioral Reviews*, 75, pp. 335–347. doi: 10.1016/j.neubiorev.2016.12.009.

Kehr, J. *et al.* (2018) 'Effects of cariprazine on extracellular levels of glutamate, GABA, dopamine, noradrenaline and serotonin in the medial prefrontal cortex in the rat phencyclidine model of schizophrenia studied by microdialysis and simultaneous recordings of locomotor activity', *Psychopharmacology*, 235(5), pp. 1593–1607. doi: 10.1007/s00213-018-4874-z.

Kim, S. *et al.* (2019) 'Cortical volume and 40-Hz auditory-steady-state responses in patients with schizophrenia and healthy controls', *NeuroImage: Clinical*, 22, p. 101732. doi: 10.1016/j.nicl.2019.101732.

Knight, R. T. *et al.* (1981) 'The effects of frontal cortex lesions on event-related potentials during auditory selective attention', *Electroencephalography and Clinical Neurophysiology*, 52(6), pp. 571–582. doi: 10.1016/0013-4694(81)91431-0.

Knight, R. T. (1984) 'Decreased response to novel stimuli after prefrontal lesions in man', *Electroencephalography and Clinical Neurophysiology/Evoked Potentials Section*, 59(1), pp. 9–20. doi: 10.1016/0168-5597(84)90016-9.

Knight, R. T. *et al.* (1999) 'Prefrontal cortex regulates inhibition and excitation in distributed neural networks', *Acta Psychologica*, 101(2), pp. 159–178. doi: 10.1016/S0001-6918(99)00004-9.

Koch, M. (1999) 'The neurobiology of startle', *Progress in Neurobiology*, 59(2), pp. 107–128. doi: 10.1016/S0301-0082(98)00098-7.

Koch, M. and Bubser, M. (1994) 'Deficient Sensorimotor Gating After 6-Hydroxydopamine Lesion of the Rat medial Prefrontal Cortex is Reversed by Haloperidol', *European Journal of Neuroscience*, 6(12), pp. 1837–1845. doi: https://doi.org/10.1111/j.1460-9568.1994.tb00576.x.

Koch, M. and Schnitzler, H.-U. (1997) 'The acoustic startle response in rats—circuits mediating evocation, inhibition and potentiation', *Behavioural Brain Research*, 89(1), pp. 35–49. doi: 10.1016/S0166-4328(97)02296-1.

Kudoh, M., Seki, K. and Shibuki, K. (2004) 'Sound sequence discrimination learning is dependent on cholinergic inputs to the rat auditory cortex', *Neuroscience Research*, 50(1), pp. 113–123. doi: 10.1016/j.neures.2004.06.007.

Lacroix, L. *et al.* (2000) 'The effects of ibotenic acid lesions of the medial and lateral prefrontal cortex on latent inhibition, prepulse inhibition and amphetamine-induced hyperlocomotion', *Neuroscience*, 97(3), pp. 459–468. doi: 10.1016/S0306-4522(00)00013-0.

Leaton, R. N., Cassella, J. V. and Borszcz, G. S. (1985) 'Short-term and long-term habituation of the acoustic startle response in chronic decerebrate rats', *Behavioral Neuroscience*, 99(5), pp. 901–912. doi: 10.1037/0735-7044.99.5.901.

Lee, W. H. *et al.* (2018) 'A Computational Assessment of Target Engagement in the Treatment of Auditory Hallucinations with Transcranial Direct Current Stimulation', *Frontiers in Psychiatry*, 9. doi: 10.3389/fpsyt.2018.00048.

Leonte, A. *et al.* (2018) 'Supplementation of gamma-aminobutyric acid (GABA) affects temporal, but not spatial visual attention', *Brain and Cognition*, 120, pp. 8–16. doi: 10.1016/j.bandc.2017.11.004.

Li, L. and Frost, B. J. (2000) 'Azimuthal directional sensitivity of prepulse inhibition of the pinna startle reflex in decerebrate rats', *Brain Research Bulletin*, 51(1), pp. 95–100. doi: 10.1016/S0361-9230(99)00215-4.

Luck, S. J. (2014) *An Introduction to the Event-Related Potential Technique, second edition*. MIT Press.

Madtes, P., Bashir-Elahi, R. and Chader, G. J. (1986) 'Maximal GABA and muscimol binding to high-affinity sites differ in physiological and in non-physiological buffers', *Neurochemistry International*, 8(2), pp. 223–227. doi: 10.1016/0197-0186(86)90167-1.

Mena, A. *et al.* (2016) 'Reduced Prepulse Inhibition as a Biomarker of Schizophrenia', *Frontiers in Behavioral Neuroscience*, 10. doi: 10.3389/fnbeh.2016.00202.

Miller, E. K. and Cohen, J. D. (2001) 'An Integrative Theory of Prefrontal Cortex Function', *Annual Review of Neuroscience*, 24(1), pp. 167–202. doi: 10.1146/annurev.neuro.24.1.167.

Mock, V. L. *et al.* (2018) 'Phase shifts in high-beta- and low-gamma-band local field potentials predict the focus of visual spatial attention', *Journal of Neurophysiology*, 121(3), pp. 799–822. doi: 10.1152/jn.00469.2018.

Möhrle, D. *et al.* (2019) 'Enhanced Central Neural Gain Compensates Acoustic Trauma-induced Cochlear Impairment, but Unlikely Correlates with Tinnitus and Hyperacusis', *Neuroscience*, 407, pp. 146–169. doi: 10.1016/j.neuroscience.2018.12.038.

Moore, T., Armstrong, K. M. and Fallah, M. (2003) 'Visuomotor Origins of Covert Spatial Attention', *Neuron*, 40(4), pp. 671–683. doi: 10.1016/S0896-6273(03)00716-5.

Moscarello, J. M. and LeDoux, J. E. (2013) 'Active Avoidance Learning Requires Prefrontal Suppression of Amygdala-Mediated Defensive Reactions', *Journal of Neuroscience*, 33(9), pp. 3815–3823. doi: 10.1523/JNEUROSCI.2596-12.2013.

Nakamura, T. *et al.* (2011) 'Epidural Auditory Event-Related Potentials in the Rat to Frequency and duration Deviants: Evidence of Mismatch Negativity?', *Frontiers in Psychology*, 2. doi: 10.3389/fpsyg.2011.00367.

Novak, G., Ritter, W. and Vaughan, H. G. (1992) 'Mismatch Detection and the Latency of Temporal Judgments', *Psychophysiology*, 29(4), pp. 398–411. doi: https://doi.org/10.1111/j.1469-8986.1992.tb01713.x.

Oostenveld, R. *et al.* (2010) *FieldTrip: Open Source Software for Advanced Analysis of MEG, EEG, and Invasive Electrophysiological Data*, *Computational Intelligence and Neuroscience*. Hindawi. doi: https://doi.org/10.1155/2011/156869.

Özerdem, A. *et al.* (2010) 'Disturbance in long distance gamma coherence in bipolar disorder', *Progress in Neuro-Psychopharmacology and Biological Psychiatry*, 34(6), pp. 861–865. doi: 10.1016/j.pnpbp.2010.04.001.

Paavilainen, P. *et al.* (2001) 'Preattentive extraction of abstract feature conjunctions from auditory stimulation as reflected by the mismatch negativity (MMN)', *Psychophysiology*, 38(2), pp. 359–365. doi: https://doi.org/10.1111/1469-8986.3820359.

Paavilainen, P. (2013) 'The mismatch-negativity (MMN) component of the auditory event-related potential to violations of abstract regularities: A review', *International Journal of Psychophysiology*, 88(2), pp. 109–123. doi: 10.1016/j.ijpsycho.2013.03.015.

Paine, T. A., Slipp, L. E. and Carlezon, W. A. (2011) 'Schizophrenia-Like Attentional Deficits Following Blockade of Prefrontal Cortex GABA A Receptors', *Neuropsychopharmacology*, 36(8), pp. 1703–1713. doi: 10.1038/npp.2011.51.

Parras, G. G. *et al.* (2017) 'Neurons along the auditory pathway exhibit a hierarchical organization of prediction error', *Nature Communications*, 8(1), p. 2148. doi: 10.1038/s41467-017-02038-6.

Paxinos, G. and Watson, C. (2006) *The Rat Brain in Stereotaxic Coordinates: Hard Cover Edition*. Elsevier.

Pilz, P. K. D. and Schnitzler, H.-U. (1996) 'Habituation and Sensitization of the Acoustic Startle Response in Rats: Amplitude, Threshold, and Latency Measures', *Neurobiology of Learning and Memory*, 66(1), pp. 67–79. doi: 10.1006/nlme.1996.0044.

Pritchett, D. L. *et al.* (2015) 'For things needing your attention: the role of neocortical gamma in sensory perception', *Current Opinion in Neurobiology*, 31, pp. 254–263. doi: 10.1016/j.conb.2015.02.004.

Rasmusson, D. D., Smith, S. A. and Semba, K. (2007) 'Inactivation of prefrontal cortex abolishes cortical acetylcholine release evoked by sensory or sensory pathway stimulation in the rat', *Neuroscience*, 149(1), pp. 232–241. doi: 10.1016/j.neuroscience.2007.06.057.

Rodgers, C. C. and DeWeese, M. R. (2014) 'Neural Correlates of Task Switching in Prefrontal Cortex and Primary Auditory Cortex in a Novel Stimulus Selection Task for Rodents', *Neuron*, 82(5), pp. 1157–1170. doi: 10.1016/j.neuron.2014.04.031.

Salvi, R. *et al.* (2017) 'Inner Hair Cell Loss Disrupts Hearing and Cochlear Function Leading to Sensory Deprivation and Enhanced Central Auditory Gain', *Frontiers in Neuroscience*, 10. doi: 10.3389/fnins.2016.00621.

Sams, M. *et al.* (1985) 'Auditory frequency discrimination and event-related potentials', *Electroencephalography and Clinical Neurophysiology/Evoked Potentials Section*, 62(6), pp. 437–448. doi: 10.1016/0168-5597(85)90054-1.

Sarter, M., Bruno, J. P. and Givens, B. (2003) 'Attentional functions of cortical cholinergic inputs: What does it mean for learning and memory?', *Neurobiology of Learning and Memory*, 80(3), pp. 245–256. doi: 10.1016/S1074-7427(03)00070-4.

Scott, K. E. *et al.* (2018) 'Altered Auditory Processing, Filtering, and Reactivity in the *Cntnap2* Knock-Out Rat Model for Neurodevelopmental Disorders', *The Journal of Neuroscience*, 38(40), pp. 8588–8604. doi: 10.1523/JNEUROSCI.0759-18.2018.

Seamans, J. K., Lapish, C. C. and Durstewitz, D. (2008) 'Comparing the prefrontal cortex of rats and primates: Insights from electrophysiology', *Neurotoxicity Research*, 14(2), pp. 249–262. doi: 10.1007/BF03033814.

Selemon, L. D. (2001) 'Regionally Diverse Cortical Pathology in Schizophrenia: Clues to the Etiology of the Disease', *Schizophrenia Bulletin*, 27(3), pp. 349–377. doi: 10.1093/oxfordjournals.schbul.a006881.

Shestakova, A. *et al.* (2002) 'Abstract phoneme representations in the left temporal cortex: magnetic mismatch negativity study', *NeuroReport*, 13(14), pp. 1813–1816.

Shimamura, A. P. (2000) 'The role of the prefrontal cortex in dynamic filtering', *Psychobiology*, 28(2), pp. 207–218. doi: 10.3758/BF03331979.

Simon, D. M. and Wallace, M. T. (2016) 'Dysfunction of sensory oscillations in Autism Spectrum Disorder', *Neuroscience & Biobehavioral Reviews*, 68, pp. 848–861. doi: 10.1016/j.neubiorev.2016.07.016.

Simons-Weidenmaier, N. S. *et al.* (2006) 'Synaptic depression and short-term habituation are located in the sensory part of the mammalian startle pathway', *BMC Neuroscience*, 7(1), p. 38. doi: 10.1186/1471-2202-7-38.

Sivarao, D. V. *et al.* (2013) 'MK-801 disrupts and nicotine augments 40 Hz auditory steady state responses in the auditory cortex of the urethane-anesthetized rat', *Neuropharmacology*. doi: 10.1016/j.neuropharm.2013.05.006.

Skinner, J. E. (1984) 'Central Gating Mechanisms That Regulate Event-Related Potentials and Behavior', in Elbert, T. et al. (eds) *Self-Regulation of the Brain and Behavior*. Berlin, Heidelberg: Springer, pp. 42–55. doi: 10.1007/978-3-642-69379-3_4.

Sohal, V. S. (2016) 'How Close Are We to Understanding What (if Anything) γ Oscillations Do in Cortical Circuits?', *Journal of Neuroscience*, 36(41), pp. 10489–10495. doi: 10.1523/JNEUROSCI.0990-16.2016.

Spencer, K. M. *et al.* (2009) 'Left auditory cortex gamma synchronization and auditory hallucination symptoms in schizophrenia', *BMC Neuroscience*, 10(1), p. 85. doi: 10.1186/1471-2202-10-85.

Spencer, K. M. (2012) 'Baseline gamma power during auditory steady-state stimulation in schizophrenia', *Frontiers in Human Neuroscience*, 5. doi: 10.3389/fnhum.2011.00190.

Sullivan, E. M., Timi, P., Elliot Hong, L., *et al.* (2015) 'Effects of NMDA and GABA-A receptor antagonism on auditory steady-state synchronization in awake behaving rats', *International Journal of Neuropsychopharmacology*. doi: 10.1093/ijnp/pyu118.

Sullivan, E. M., Timi, P., Hong, L. E., *et al.* (2015) 'Effects of NMDA and GABA-A Receptor Antagonism on Auditory Steady-State Synchronization in Awake Behaving Rats', *International Journal of Neuropsychopharmacology*, 18(7). doi: 10.1093/ijnp/pyu118.

Swerdlow, N. R. *et al.* (2018) 'Deficient prepulse inhibition in schizophrenia in a multi-site cohort: Internal replication and extension', *Schizophrenia Research*, 198, pp. 6–15. doi: 10.1016/j.schres.2017.05.013.

Tada, M. *et al.* (2020) 'Gamma-Band Auditory Steady-State Response as a Neurophysiological Marker for Excitation and Inhibition Balance: A Review for Understanding Schizophrenia and Other Neuropsychiatric Disorders', *Clinical EEG and Neuroscience*, 51(4), pp. 234–243. doi: 10.1177/1550059419868872.

Thuné, H., Recasens, M. and Uhlhaas, P. J. (2016) 'The 40-Hz Auditory Steady-State Response in Patients With Schizophrenia: A Meta-analysis', *JAMA Psychiatry*, 73(11), pp. 1145–1153. doi: 10.1001/jamapsychiatry.2016.2619.

Toader, O. *et al.* (2020) 'Suppression of Parvalbumin Interneuron Activity in the Prefrontal Cortex Recapitulates Features of Impaired Excitatory/Inhibitory Balance and

Sensory Processing in Schizophrenia', *Schizophrenia Bulletin*, 46(4), pp. 981–989. doi: 10.1093/schbul/sbz123.

Uehara, T. *et al.* (2007) 'Effect of prefrontal cortex inactivation on behavioral and neurochemical abnormalities in rats with excitotoxic lesions of the entorhinal cortex', *Synapse*, 61(6), pp. 391–400. doi: https://doi.org/10.1002/syn.20383.

Uhlhaas, P. J. and Singer, W. (2010) 'Abnormal neural oscillations and synchrony in schizophrenia', *Nature Reviews Neuroscience*, 11(2), pp. 100–113. doi: 10.1038/nrn2774.

Vohs, J. L. *et al.* (2010) 'GABAergic modulation of the 40 Hz auditory steady-state response in a rat model of schizophrenia', *International Journal of Neuropsychopharmacology*. doi: 10.1017/S1461145709990307.

Vohs, J. L. *et al.* (2012) 'Auditory steady state responses in a schizophrenia rat model probed by excitatory/inhibitory receptor manipulation', *International Journal of Psychophysiology*. doi: 10.1016/j.ijpsycho.2012.04.002.

Weber, M., Schnitzler, H.-U. and Schmid, S. (2002) 'Synaptic plasticity in the acoustic startle pathway: the neuronal basis for short-term habituation?', *European Journal of Neuroscience*, 16(7), pp. 1325–1332. doi: https://doi.org/10.1046/j.1460-9568.2002.02194.x.

Weinberger, D. R. *et al.* (2001) 'Prefrontal neurons and the genetics of schizophrenia', *Biological Psychiatry*, 50(11), pp. 825–844. doi: 10.1016/S0006-3223(01)01252-5.

Weisz, N. *et al.* (2005) 'Tinnitus Perception and Distress Is Related to Abnormal Spontaneous Brain Activity as Measured by Magnetoencephalography', *PLOS Medicine*, 2(6), p. e153. doi: 10.1371/journal.pmed.0020153.

Weisz, N., Dohrmann, K. and Elbert, T. (2007) 'The relevance of spontaneous activity for the coding of the tinnitus sensation', in Langguth, B. et al. (eds) *Progress in Brain Research*. Elsevier (Tinnitus: Pathophysiology and Treatment), pp. 61–70. doi: 10.1016/S0079-6123(07)66006-3.

Winkler, I. *et al.* (1990) 'The effect of small variation of the frequent auditory stimulus on the event-related brain potential to the infrequent stimulus', *Psychophysiology*, 27(2), pp. 228–235. doi: 10.1111/j.1469-8986.1990.tb00374.x.

Wise, S. P. (2008) 'Forward frontal fields: phylogeny and fundamental function', *Trends in Neurosciences*, 31(12), pp. 599–608. doi: 10.1016/j.tins.2008.08.008.

Witten, L. *et al.* (2014) 'Auditory sensory processing deficits in sensory gating and mismatch negativity-like responses in the social isolation rat model of

schizophrenia', *Behavioural Brain Research*, 266, pp. 85–93. doi: 10.1016/j.bbr.2014.02.048.

Woods, D. L. and Knight, R. T. (1986) 'Electrophysiologic evidence of increased distractibility after dorsolateral prefrontal lesions', *Neurology*, 36(2), pp. 212–212. doi: 10.1212/WNL.36.2.212.

Xiao, X.-Z. *et al.* (2018) 'Detecting violation in abstract pitch patterns with mismatch negativity', *Psychophysiology*, 55(8), p. e13078. doi: https://doi.org/10.1111/psyp.13078.

Yin, P., Fritz, J. B. and Shamma, S. A. (2014) 'Rapid Spectrotemporal Plasticity in Primary Auditory Cortex during Behavior', *Journal of Neuroscience*, 34(12), pp. 4396–4408. doi: 10.1523/JNEUROSCI.2799-13.2014.

Zaman, T. *et al.* (2017) 'BK Channels Mediate Synaptic Plasticity Underlying Habituation in Rats', *Journal of Neuroscience*, 37(17), pp. 4540–4551. doi: 10.1523/JNEUROSCI.3699-16.2017.

Chapter 5

5. General Discussion

5.1 Summary of Main Findings

5.1.1 Medial Prefrontal Cortex Plasticity and Cognitive-Behavioural Deficits Following Noise Induced Hearing Loss (Chapter 2)

Overall, the results presented in Chapter 2 have helped reveal the varying degrees that behavioural tasks reliant on stimulus-response habit learning, cognitive flexibility, or spatial learning/memory are susceptible to noise exposure. Moreover, because performance on these chosen behavioural tasks is known to depend on specific brain regions, it is possible to identify the extent that areas outside of the auditory pathway appear to be either resilient or sensitive to noise exposure. For example, unlike reversal learning, tasks requiring spatial learning and reference memory and stimulus-response habit learning were significantly impaired in the noise-exposed rats; findings that suggest resilience of the orbitofrontal cortex and sensitivity of the hippocampus and striatum to noise exposure. With respect to the medial prefrontal cortex (mPFC), electrophysiological results demonstrated noise-induced changes in auditory processing. However, it is unclear whether the capacity of the mPFC to carry out non-auditory executive function was indeed compromised, as the seemingly unaffected set-shifting performance was perhaps confounded by initial learning deficits in the noise-exposed rats. Ultimately, the results in Chapter 2 provided a strong rationale for future investigations into the causal role of the mPFC in passive auditory processing and the impact of noise-induced mPFC plasticity on tasks known to be disrupted following the hearing loss, such as those requiring listening effort and auditory attention.

5.1.2 The Effects of Noise-induced Hearing Loss on Sounds Detection (Chapter 3)

This study successfully developed a novel operant-based two-alternative forced-choice sound detection task for rats that was sensitive to increasing background noise levels. This task was then used to investigate the possible behavioural effects of noise-induced hearing loss. This study showed that hearing loss was negatively correlated with detecting the sound in quiet and background noise, indicating the primary sensory processing deficits contributed to the impaired performance. The rats' impulsivity was not significantly affected by the noise exposure, as the group average results did not differ in either the quiet or in background conditions. That said, further analysis found a significant correlation between hearing loss and increased impulsivity. This finding indicates that impulsivity might be affected by noise exposure and thus, provides a rationale for further investigations of possible noise-induced attentional deficits.

5.1.3 The Effects of Medial Prefrontal Cortex Inactivation on Auditory Processing and Perception (Chapter 4)

The collective experiments in this study demonstrated that inactivation of the mPFC significantly influenced sounds processing (e.g., mismatch response) and perception (e.g., sound detection) while not affecting other functions (e.g., auditory-evoked potentials; 40-Hz auditory steady-state response). To my knowledge, this work represents the first direct investigation of top-down deficits leading to a decreased ability to detect sound in a noisy background. More specifically, these experiments are the first to report evidence of dysfunctional auditory perception in noise when the subject's basic auditory processing abilities were spared (i.e., no disruptions that affect bottom-up processing, such as cochlear trauma). Furthermore, despite the theorized involvement of the mPFC in the generation of the mismatch response during the oddball paradigm, its effects had not been investigated comprehensively. By pharmacologically inactivating the mPFC, the present results show for the first time that this brain region affects the late-latency response of the auditory cortex to deviant sounds. Ultimately, as these novel findings

could indicate deficits in the generation of the prediction about the upcoming sensory stimulus, further studies are warranted to investigate the neural basis of sensory prediction and the precise role of the mPFC in this phenomenon.

5.2 Experimental Limitations and Future Directions

The collective results of this thesis further our understanding of the effects of noise exposure on higher-order cortical regions and cognitive functions, as well as the role of the mPFC (made evident through its inactivation) on auditory processing and perception. That said, some experimental limitations should be addressed in future research. In the following sections, I discuss the main caveats of each study included in this thesis, as well as provide potential solutions to those limitations and suggest possible future directions.

5.2.1 Short-term versus long-term cortical plasticity following noise exposure

One of the experimental limitations of Chapter 2, which investigated noise-induced cortical plasticity, was the electrophysiological approach, as it did not allow for recording neural activity over longer durations of time to match the behavioural time points (i.e., >30 days post-noise exposure). The mPFC did not show the same degree of hyper-responsivity as the auditory cortex at seven days following noise exposure. However, it is possible that altered activity could manifest in the medial prefrontal cortex at later time points. The same could be said for the differential effects observed in the two cortical regions' ability to synchronize to the repetitive acoustic stimulus in the 40-Hz auditory steady-state protocol. Related to this, although there was no significant relationship between the degree of hearing loss and the magnitude of changes in neural activity that occurred in the week following noise exposure (i.e., increased event-related potentials in the auditory cortex; decreased inter-trial coherence in the mPFC; decreased phase-locking value), it is possible that the degree of hearing loss could eventually correlate with altered neural activity at later time points. Ultimately, given that this study provided the first evidence of differential plasticity in the auditory and prefrontal cortices post-noise exposure, it will be essential to carry out future longitudinal studies, particularly those in

which electrophysiology and behavioural measures are performed in the same animals, to draw specific conclusions regarding the extent that noise-induced changes in neural activity are associated with deficits in cognitive-behavioural performance.

5.2.2 Noise exposure effects on the striatum

The novel finding of impaired visual-cue discrimination following noise exposure (Chapter 2) raises exciting questions and future considerations regarding the effect of noise-induced hearing loss on the striatum. For example, given that neurons in both the auditory cortex and thalamus project to the dorsal striatum (Guo *et al.*, 2015; Chen *et al.*, 2019), and that dorsal striatal neurons are responsive to inputs from more than one sensory modality (Khibnik, Tritsch and Sabatini, 2014; Reig and Silberberg, 2014), it is possible that noise-induced plasticity within the auditory system could have a downstream effect on the dorsal striatum, and ultimately influence performance on non-auditory behavioural tasks by way of the multisensory nature of the striatal neurons. Ultimately, our current findings, coupled with past studies showing an effect of noise exposure on striatal neurotransmitter systems (Sembulingam, Sembulingam and Namasivayam, 1996; Samson *et al.*, 2006; Kazi and Oommen, 2014), motivate future investigations into how noise-induced plasticity may manifest in the striatal medium spiny projecting neurons and/or the tonically active cholinergic interneurons of the dorsal striatum. Related to this putative cellular plasticity, it will be important to determine whether there are distinct effects of noise-induced hearing loss on the various features of instrumental learning (e.g., goal-directed vs. habit learning) that are ascribed to regions of the striatum (e.g., anterior/posterior dorsomedial vs. dorsolateral; for review, see (Peak, Hart and Balleine, 2019)).

5.2.3 Relationship between noise-induced hearing loss and cognitive impairments?

The lack of correlation between the degree of hearing loss and the performance on the various cognitive-behavioural tasks (Chapter 2) is intriguing and warrants future

consideration. Consistent with these results, a previous study found a wide range of behavioural performance in the Morris water maze (i.e., from no deficit up to a large deficit) in mice with a similar degree of hearing loss following noise exposure (Liu *et al.*, 2016). These studies raise the question: if it is not the degree of hearing loss that determines the extent of cognitive impairment in non-auditory tasks, is it other factors (e.g. neuroendocrine dysregulation) associated with the noise exposure itself (Jafari, Kolb and Mohajerani, 2019; Hayes *et al.*, 2020), or simply the presence of *any* extent of sensory deprivation, that impacts cognition? This question remains pertinent as preclinical studies try to uncover the neural basis for the link between hearing loss and cognitive impairment reported in large-scale epidemiological studies (Taljaard *et al.*, 2016; Lee *et al.*, 2018).

5.2.4 Hearing testing

Throughout the research chapters in this thesis, the stimulus used to assess general hearing sensitivity was a 0.1 ms click stimulus. This stimulus was selected because it activates an extensive range of the cochlea (i.e., approximately 1-10 kHz) and provides consistent waveforms to assess the amplitude of each of the ABR waves. However, because a broadband noise was used for noise exposure (0.8 – 20 kHz), future studies should consider assessing hearing sensitivity using a noise burst stimulus to determine the change in hearing sensitivity concerning the frequencies presented during the noise exposure.

5.2.5 Functional connectivity and sound detection

As reported in Chapter 2, noise exposure disrupted the functional connectivity between the auditory cortex and the mPFC, as assessed by the decreased phase-locking value between these brain regions in response to the sound stimulus presented at 40-Hz. Previous studies in ferrets have shown that such functional connectivity is dynamically established during a sound detection task (Fritz *et al.*, 2010). Motivated by these findings and the noise-induced cortical plasticity observed in Chapter 2, the experiments outlined in Chapter 3 sought to investigate the rats' sound detection abilities following the same

noise exposure used in Chapter 2. Interestingly, it was revealed that rats with mild hearing loss did not exhibit sound detection deficits. Furthermore, unlike the deficits in the sound-evoked 40-Hz phase-locking value between the auditory cortex and mPFC (Chapter 2), the sound detection accuracy was correlated with the hearing loss assessed by the threshold shift (Chapter 3). Adding to the experimental limitations concerning the hearing testing itself (as mentioned in the previous section), it is crucial to notice that the measure of functional connectivity used in the first study (Chapter 2) was a passive electrophysiological recording, in which, although the rat heard the sound, it was not engaged with it behaviourally. In normal-hearing ferrets, Fritz and colleagues (2010) showed that the prefrontal cortex and auditory cortex engage dynamically in functional connectivity *during* a sound detection task. Thus, it would be worthwhile to study the effects of noise exposure on the ability of these brain regions to establish functional connectivity during a variety of sound detection tasks, including the one designed in Chapter 3.

Furthermore, the third study presented in this thesis (Chapter 4) revealed that the inactivation of the mPFC leads to significantly impaired sound detection. Interestingly, these results were dose-dependent, with the lower dose of muscimol only affecting the performance in background noise. Although this study showed no effect of the treatment on the 40-Hz ASSR measures within the auditory cortex, the phase-locking value assessing the passive functional connectivity between the auditory cortex and the mPFC has not been recorded. In the light of the collective results presented in this thesis, it would be interesting to investigate this aspect following the inactivation of the mPFC.

5.2.6 Impulsivity and attention following noise exposure and mPFC inactivation

In Chapter 4, it was found that inactivation of the mPFC with muscimol caused increased impulsivity during the sound detection task, with the degree of impulsivity significantly correlated with task performance (i.e., greater impulsivity was related to worsened

performance). Moreover, in Chapter 3, the rats' ability to discriminate sounds following the noise-induced hearing loss was also significantly correlated with impulsive behaviour. Consistent with the general methodological approach used in previous studies, this thesis recorded the number of nose-pokes necessary to initiate a trial as a premature response, thus a measure indicative of impulsive behaviour (Adriani *et al.*, 2006; Doremus-Fitzwater, Barreto and Spear, 2012; Hyatt *et al.*, 2019; Darling *et al.*, 2020; Jiménez-Urbieta, 2020). However, in these previous studies, the time that the animals were required to hold their noses before a trial was initiated was longer than in our experiments. Furthermore, unlike in the experiments presented in this dissertation, the previous studies were specifically designed to study impulsivity. Thus, the animals underwent rigorous condition-based training in which the goal was to hold the nose. Therefore, to better detect subtle changes in impulsivity, our future studies should attempt to optimize the assessment of impulsivity during behavioural testing. Motivated by the results of Chapter 2, which found neurophysiological changes in the mPFC following the noise exposure, it would be worthwhile to investigate the effects of noise exposure more comprehensively on impulsive behaviour with complementary and susceptible measures. In the short-term, a simple improvement would require that the rats wait longer before trial initiation, thereby increasing the task difficulty and providing us with the opportunity to detect even subtle differences in impulsivity.

It should be noted that, although impulsivity is often correlated with, and indicative of, attentional abilities (Kindlon, 1998; Bushnell and Strupp, 2009), past studies have shown that they are not necessarily the same, i.e., deficits in one trait do not necessarily result in deficits in the other. For example, Paine and colleagues (2011) found that inactivation of the prefrontal cortex with muscimol increased impulsive behaviour but did not affect attention (Paine, Slipp and Carlezon, 2011). Interestingly this study also showed that infusion of a $GABA_A$ antagonist, bicuculline, within the prefrontal cortex, i.e., increasing pyramidal neuron activity, decreased attention as assessed with a five-choice serial reaction time task. Considering that attention has been implicated in the ability to hear in

noise (Fritz, Elhilali and Shamma, 2007; Atiani *et al.*, 2009; Fritz *et al.*, 2010; Yin, Fritz and Shamma, 2014), it would be interesting to investigate its role in the sound detection, which could be accomplished by testing the animals following prefrontal cortex infusion with bicuculline. Furthermore, the experiments in Chapter 2 showed noise-induced plasticity decreased the ability of the prefrontal cortex to sustain the sound-evoked gamma oscillation, a finding that might imply GABAergic dysfunction (Bartos, Vida and Jonas, 2007; Volman, Behrens and Sejnowski, 2011; Buzsáki and Wang, 2012; Kujala *et al.*, 2015). Thus, in the future, it would be interesting to investigate the ability to sustain attention in a task that does not rely on auditory processing and perception (e.g., a visual sustained attention task).

5.3 References

Adriani, W. *et al.* (2006) 'Motor impulsivity in APP-SWE mice: a model of Alzheimer's disease', *Behavioural Pharmacology*, 17(5–6), pp. 525–533.

Atiani, S. *et al.* (2009) 'Task Difficulty and Performance Induce Diverse Adaptive Patterns in Gain and Shape of Primary Auditory Cortical Receptive Fields', *Neuron*, 61(3), pp. 467–480. doi: 10.1016/j.neuron.2008.12.027.

Bartos, M., Vida, I. and Jonas, P. (2007) 'Synaptic mechanisms of synchronized gamma oscillations in inhibitory interneuron networks', *Nature Reviews Neuroscience*, 8(1), pp. 45–56. doi: 10.1038/nrn2044.

Bushnell, P. J. and Strupp, B. J. (2009) 'Assessing attention in rodents', in *Methods of behavioral analysis in neuroscience, 2nd ed*. Boca Raton, FL, US: CRC Press/Routledge/Taylor & Francis Group (Frontiers in neuroscience), pp. 119–143.

Buzsáki, G. and Wang, X.-J. (2012) 'Mechanisms of Gamma Oscillations', *Annual Review of Neuroscience*, 35(1), pp. 203–225. doi: 10.1146/annurev-neuro-062111-150444.

Chen, L. *et al.* (2019) 'Medial geniculate body and primary auditory cortex differentially contribute to striatal sound representations', *Nature Communications*, 10(1), p. 418. doi: 10.1038/s41467-019-08350-7.

Darling, J. S. *et al.* (2020) 'Sex differences in impulsivity in adult rats are mediated by organizational actions of neonatal gonadal hormones and not by hormones acting at puberty or in adulthood', *Behavioural Brain Research*, 395, p. 112843. doi: 10.1016/j.bbr.2020.112843.

Doremus-Fitzwater, T. L., Barreto, M. and Spear, L. P. (2012) 'Age-related differences in impulsivity among adolescent and adult Sprague-Dawley rats', *Behavioral Neuroscience*, 126(5), pp. 735–741. doi: 10.1037/a0029697.

Fritz, J. B. *et al.* (2010) 'Adaptive, behaviorally gated, persistent encoding of task-relevant auditory information in ferret frontal cortex', *Nature Neuroscience*, 13(8), pp. 1011–1019. doi: 10.1038/nn.2598.

Fritz, J. B., Elhilali, M. and Shamma, S. A. (2007) 'Adaptive Changes in Cortical Receptive Fields Induced by Attention to Complex Sounds', *Journal of Neurophysiology*, 98(4), pp. 2337–2346. doi: 10.1152/jn.00552.2007.

Guo, Q. *et al.* (2015) 'Whole-Brain Mapping of Inputs to Projection Neurons and Cholinergic Interneurons in the Dorsal Striatum', *PLOS ONE*, 10(4), p. e0123381. doi: 10.1371/journal.pone.0123381.

Hayes, S. H. *et al.* (2020) 'Uncovering the contribution of enhanced central gain and altered cortical oscillations to tinnitus generation', *Progress in Neurobiology*, p. 101893. doi: 10.1016/j.pneurobio.2020.101893.

Hyatt, W. *et al.* (2019) 'Acute Administration of 3,4-Methylenedioxypyrovalerone (MDPV) Increases Motor Impulsivity in Rats', *The FASEB Journal*, 33(S1), p. 805.10-805.10. doi: https://doi.org/10.1096/fasebj.2019.33.1_supplement.805.10.

Jafari, Z., Kolb, B. E. and Mohajerani, M. H. (2019) 'Noise exposure accelerates the risk of cognitive impairment and Alzheimer's disease: Adulthood, gestational, and prenatal mechanistic evidence from animal studies', *Neuroscience & Biobehavioral Reviews*. doi: 10.1016/j.neubiorev.2019.04.001.

Jiménez-Urbieta, H. (2020) 'Motor impulsivity and delay intolerance are elicited in a dose-dependent manner with a dopaminergic agonist in parkinsonian rats', p. 13.

Kazi, A. I. and Oommen, A. (2014) 'Chronic noise stress-induced alterations of glutamate and gamma-aminobutyric acid and their metabolism in the rat brain', *Noise and Health*, 16(73), p. 343. doi: 10.4103/1463-1741.144394.

Khibnik, L. A., Tritsch, N. X. and Sabatini, B. L. (2014) 'A Direct Projection from Mouse Primary Visual Cortex to Dorsomedial Striatum', *PLOS ONE*, 9(8), p. e104501. doi: 10.1371/journal.pone.0104501.

Kindlon, D. J. (1998) 'The Measurement of Attention', *Child Psychology and Psychiatry Review*, 3(2), pp. 72–78. doi: https://doi.org/10.1111/1475-3588.00215.

Kujala, J. *et al.* (2015) 'Gamma oscillations in V1 are correlated with GABA A receptor density: A multi-modal MEG and Flumazenil-PET study', *Scientific Reports*, 5(1), p. 16347. doi: 10.1038/srep16347.

Lee, W. H. *et al.* (2018) 'A Computational Assessment of Target Engagement in the Treatment of Auditory Hallucinations with Transcranial Direct Current Stimulation', *Frontiers in Psychiatry*, 9. doi: 10.3389/fpsyt.2018.00048.

Liu, L. *et al.* (2016) 'Noise induced hearing loss impairs spatial learning/memory and hippocampal neurogenesis in mice', *Scientific Reports*, 6(1), p. 20374. doi: 10.1038/srep20374.

Paine, T. A., Slipp, L. E. and Carlezon, W. A. (2011) 'Schizophrenia-Like Attentional Deficits Following Blockade of Prefrontal Cortex GABA A Receptors', *Neuropsychopharmacology*, 36(8), pp. 1703–1713. doi: 10.1038/npp.2011.51.

Peak, J., Hart, G. and Balleine, B. W. (2019) 'From learning to action: the integration of dorsal striatal input and output pathways in instrumental conditioning', *European Journal of Neuroscience*, 49(5), pp. 658–671. doi: https://doi.org/10.1111/ejn.13964.

Reig, R. and Silberberg, G. (2014) 'Multisensory Integration in the Mouse Striatum', *Neuron*, 83(5), pp. 1200–1212. doi: 10.1016/j.neuron.2014.07.033.

Samson, J. *et al.* (2006) 'Biogenic amine changes in brain regions and attenuating action of Ocimum sanctumin noise exposure', *Pharmacology Biochemistry and Behavior*, 83(1), pp. 67–75. doi: 10.1016/j.pbb.2005.12.008.

Sembulingam, K., Sembulingam, P. and Namasivayam, A. (1996) 'Effect of Acute Noise Stress on Cholinergic Neurotransmitter in Corpus Striatum of Albino Rats', *Pharmacy and Pharmacology Communications*, 2(5), pp. 241–242. doi: https://doi.org/10.1111/j.2042-7158.1996.tb00602.x.

Taljaard, D. S. *et al.* (2016) 'The relationship between hearing impairment and cognitive function: a meta-analysis in adults', *Clinical Otolaryngology*, 41(6), pp. 718–729. doi: https://doi.org/10.1111/coa.12607.

Volman, V., Behrens, M. M. and Sejnowski, T. J. (2011) 'Downregulation of Parvalbumin at Cortical GABA Synapses Reduces Network Gamma Oscillatory Activity', *Journal of Neuroscience*, 31(49), pp. 18137–18148. doi: 10.1523/JNEUROSCI.3041-11.2011.

Yin, P., Fritz, J. B. and Shamma, S. A. (2014) 'Rapid Spectrotemporal Plasticity in Primary Auditory Cortex during Behavior', *Journal of Neuroscience*, 34(12), pp. 4396–4408. doi: 10.1523/JNEUROSCI.2799-13.2014.

Chapter 6

6 General Conclusion

Overall, the collective work in this thesis investigated the relationship between the auditory system and mPFC, using electrophysiological and behavioural approaches. The study presented in Chapter 2 demonstrated for the first time that noise exposure leads to noise-induced plasticity within mPFC, manifested as a decreased inter-trial coherence in the responses to the 40-Hz click train stimulus (indicative of reduced ability to synchronize sound-evoked gamma oscillations), and a loss of functional connectivity between the mPFC auditory cortex as assessed by the phase-locking value. Furthermore, this study confirmed that noise exposure caused hippocampal-dependent spatial memory deficits and revealed a noise-induced deficit in stimulus-response habit learning, which is thought to depend on the striatum. The study presented in Chapter 3 established a novel two-alternative forced-choice task to study the ability to detect sound following noise-induced hearing loss. Interestingly, this study showed that although the ability to detect sounds was correlated with the degree of hearing loss, it did not necessarily lead to deficits in quiet or background noise. Furthermore, these experiments also revealed a significant correlation between the hearing loss and increased impulsivity. Although this metric was not significantly affected by noise exposure, as revealed by the group average, the correlation analysis provides a rationale for further studies on possible attentional deficits following noise-induced hearing loss. Finally, using a battery of behavioural and electrophysiological techniques, the last study presented in Chapter 4 investigated a poorly understood topic; the direct effects of mPFC on auditory functional disruption. Interestingly, the results revealed evidence of deficits in higher-order auditory processing following mPFC inactivation, evident by the diminished deviant effect, decreased mismatch response and decreased spontaneous gamma oscillations. Furthermore, the mPFC treatment with a lower dose of muscimol led to sound detection deficits in noise, but not in quiet. These findings provide the first evidence of the higher-order auditory

function deficits following an mPFC insult, despite intact bottom-up sensory processing, as assessed by unaffected acoustic startle responses and a lack of change in sound-evoked responses and 40-Hz auditory steady-state responses recorded from the auditory cortex. Ultimately, the collective results of this thesis provide a solid rationale for using rodent models to further investigate the role of the mPFC in top-down modulation of auditory functions ranging from pre-attentive sound processing to sensory perception.

Appendix A: Ethics Approvals

AUP 2017-162

Brian Leonard Allman

From:	eSirius3GWebServer < ███████████████████
Sent:	Thursday, October 15, 2020 2:47 PM
To:	Brian Leonard Allman; ACC Office
Cc:	███████████████████
Subject:	eSirius3G Notification -- 2017-162 Modification Approved

Western 🛡

AUP Number: 2017-162
PI Name: Allman, Brian
AUP Title: Neurophysiological Basis of Multisensory Processing
Official Notification of ACC Approval: A MODIFICATION to Animal Use Protocol **2017-162** has been approved.

Please at this time review your AUP with your research team to ensure full understanding by everyone listed within this AUP.

As per your declaration within this approved AUP, you are obligated to ensure that:
    1) Animals used in this research project will be cared for in alignment with:
        a) Western's Senate MAPPs 7.12, 7.10, and 7.15
███████████████████

        b) University Council on Animal Care Policies and related Animal Care
Committee procedures
        c)
████████████████████████████████

   ~~2) As per UCAC's Animal Use Protocols Policy,~~
        a) this AUP accurately represents intended animal use;
        b) external approvals associated with this AUP, including permits and
scientific/departmental peer approvals, are complete and accurate;
        c) any divergence from this AUP will not be undertaken until the related
Protocol Modification is approved by the ACC; and
        d) AUP form submissions - Annual Protocol Renewals and Full AUP Renewals -
will be submitted and attended to within timeframes outlined by the
ACC ███████████████████
    3) As per MAPP 7.10 all individuals listed within this AUP as having any hands-on animal contact
will
        a) be made familiar with and have direct access to this AUP;
        b) complete all required CCAC mandatory training █████████████ nd
        c) be overseen by me to ensure appropriate care and use of animals.
    4) As per MAPP 7.15,
        a) Practice will align with approved AUP elements;
        b) Unrestricted access to all animal areas will be given to ACVS Veterinarians
and ACC Leaders;
        c) UCAC policies and related ACC procedures will be followed, including but not
limited to:
            i) Research Animal Procurement
            ii) Animal Care and Use Records
            iii) Sick Animal Response
            iv) Continuing Care Visits
    5) As per institutional OH&S policies, all individuals listed within this AUP who will be using or
potentially exposed to hazardous materials will have completed in advance

1

the appropriate institutional OH&S training, facility-level training, and reviewed related (M)SDS
Sheets,

Submitted by: Copeman, Laura
on behalf of the Animal Care Committee
University Council on Animal Care

The University of
Western Ontario
Animal Care Committee / University
Council on Animal Care
London, Ontario Canada

AUP 2018-006

From:	eSirius3GWebServer
Sent:	Thursday, October 15, 2020 2:48 PM
To:	Brian Leonard Allman; ACC Office
Cc:	mgr.smtgs@uwo.ca
Subject:	eSirius3G Notification -- 2018-006 Modification Approved

Western

AUP Number: 2018-006
PI Name: Allman, Brian
AUP Title: Effect of Noise Exposure and Chronic Stress on Auditory Processing
Official Notification of ACC Approval: A MODIFICATION to Animal Use Protocol **2018-006** has been approved.

Please at this time review your AUP with your research team to ensure full understanding by everyone listed within this AUP.

As per your declaration within this approved AUP, you are obligated to ensure that:
   1) Animals used in this research project will be cared for in alignment with:
        a) Western's Senate MAPPs 7.12, 7.10, and 7.15

        b) University Council on Animal Care Policies and related Animal Care Committee procedures
        c)
http://

   2) As per UCAC's Animal Use Protocols Policy,
        a) this AUP accurately represents intended animal use;
        b) external approvals associated with this AUP, including permits and scientific/departmental peer approvals, are complete and accurate;
        c) any divergence from this AUP will not be undertaken until the related Protocol Modification is approved by the ACC; and
        d) AUP form submissions - Annual Protocol Renewals and Full AUP Renewals - will be submitted and attended to within timeframes outlined by the ACC.

   3) As per MAPP 7.10 all individuals listed within this AUP as having any hands-on animal contact will
        a) be made familiar with and have direct access to this AUP;
        b) complete all required CCAC mandatory training (_____ and
        c) be overseen by me to ensure appropriate care and use of animals.
   4) As per MAPP 7.15,
        a) Practice will align with approved AUP elements;
        b) Unrestricted access to all animal areas will be given to ACVS Veterinarians and ACC Leaders;
        c) UCAC policies and related ACC procedures will be followed, including but not limited to:
             i) Research Animal Procurement
             ii) Animal Care and Use Records
             iii) Sick Animal Response
             iv) Continuing Care Visits
   5) As per institutional OH&S policies, all individuals listed within this AUP who will be using or potentially exposed to hazardous materials will have completed in advance

1

205

the appropriate institutional OH&S training, facility-level training, and reviewed related (M)SDS Sheets, ███████████████████████████

Submitted by: Copeman, Laura
on behalf of the Animal Care Committee
University Council on Animal Care

The University of Western Ontario

Animal Care Committee / University Council on Animal Care

London, Ontario Canada

h

Appendix B: Curriculum vitae

NAME	Krystyna Wieczerzak	

EDUCATION

<u>Doctor of Philosophy</u>	P.I. Dr. Brian Allman	**09/2016 – 04/2021**
Neuroscience	University of Western Ontario	
	London, Ontario (Canada)	
<u>Master of Science</u>	P.I. Dr. Timothy Cope	**09/2012 – 05/2015**
Neuroscience and Physiology	Wright State University	
	Dayton, Ohio (USA)	
<u>Bachelor of Science</u>	Wright State University	**09/2007 – 06/2012**
Major: Biology	Dayton, Ohio (USA)	
Major: Chemistry		
Minor: French		

SCHOLARSHIPS AND AWARDS

The Jonathan & Joshua Graduate Scholarship	**09/2019 – 08/2020**
Schulich School of Medicine Travel Award	**02/2019**
Association for Research in Otolaryngology Travel Award	**02/2019**
The Jonathan & Joshua Graduate Scholarship	**09/2018 – 08/2019**
Western Graduate Research Scholarship	**09/2016 – 12/2020**
National Collegiate Athletic Association Scholarship (swimming)	**08/2007 – 06/2012**
Wright State University Athletic Scholarship (swimming)	**08/2007 – 06/2011**

OTHER RESEARCH EXPERIENCE

<u>Research Technician</u>	P.I. Dr. Ashot Kozak	**06/2015 – 07/2016**
	Wright State University	
<u>Undergraduate Research Volunteer</u>	P.I. Dr. Daniel Ketcha	**01/2011 – 06/2012**
	Wright State University	

TEACHING EXPERIENCE

Undergraduate Thesis' Mentor	Student: Kelly Yeung Thesis: Electrophysiological Investigation of the Subtle Glutamatergic and Dopaminergic Dysfunction: Implication for Schizophrenia	**09/2019 – 04/2020**
Teaching Assistant	• Introductory Biology 1005 University of Western Ontario	**09/2020 – 12/2020**
	• Integrative Neuroscience University of Western Ontario	**09/2016 – 12/2019**

LEADERSHIP EXPERIENCE

Society of Neuroscience Graduate Students (SONGS)   **09/2017 – 06/2020**
Founder and President
International Graduate Student Issues Committee (IGSIC)   **05/2018 – 02/2020**
Chair
Western Psychology Undergraduate Journal (WPUJ)   **09/2017 – 08/2020**
Graduate reviewer
University of Western Medical Journal (UWMJ)   **09/2017 – 08/2020**
Peer reviewer
Western Science Rendezvous   **2017,2018,2019**
Leader of neuroscience group   2018, 2019

PUBLICATIONS

Wieczerzak, KB., Patel, S., MacNeil, H., Scott, KE., Schormans, AL., Hayes, SH., Herrmann, B., Allman, BL., **(2020)**, Differential Plasticity in Auditory and Prefrontal Cortices, and Cognitive-Behavioural Deficits Following Noise-Induced Hearing Loss. *Neuroscience*

Zhelay, T., **Wieczerzak, KB.,** Beesetty, P., Alter GM., Matsuchita, M., Kozak, JA., **2018.** Depletion of plasma membrane-associated phosphoinositides mimics inhibition of TRPM7 channels by cytosolic Mg2+, spermine, and pH. *Journal of Biological Chemistry* 293(47)

Beesetty, P., **Wieczerzak, KB**., Gibson, JN., Kaitsuka, T., Luu, CT., Matsuchita, M., Kozak, JA., **(2018).** Inactivation of TRPM7 kinase in mice results in enlarged spleens reduced T-cell proliferation and diminished store-operated calcium entry. *Scientific Reports* 8 p.1-21.

Vincent, JA., **Wieczerzak, KB**., Gabriel, HM., Nardelli, P., Rich, MM., & Cope, TC. **(2016).** A novel path to chronic proprioceptive disability with oxaliplatin: Distortion of sensory encoding. *Neurobiology of Disease*, 54-65

Jordan, C.A., **Wieczerzak, KB**., Knisley, KJ., Ketcha, DM. **(2014).** Expedited microwave-assisted N-alkylation of Isatins utilizing DBU. *Arkivoc IV*, 183-192 (2014)

POSTERS

Wieczerzak, KB., Scott, K., Herrmann, B., Hayes SH., Allman BL., 2019. Noise-Induced Plasticity in the Brainstem, Auditory Cortex, and Anterior Cingulate: Implications for Functional Connectivity and Acoustic Hyper-Activity. *(Association for Research in Otolaryngology Conference, Baltimore February 2019).*

Wieczerzak, KB., Desai S., Rajakumar, N., Allman, BL., 2018 *Unraveling the Role of NMDA* Receptor Hypofunction in Aberrant Cortical Oscillation and Cognitive Dysfunction: Implication for Schizophrenia. (*London Health Research Day, London Ontario, May 2018*)

TALKS

Wieczerzak, KB., MacNeil H., Scott, K., Herrmann, B., Allman BL., Electrophysiological and Behavioural Consequences of Noise-Induced Hearing Loss Along Auditory Pathway and Anterior Cingulate*; (Presented at London Health Research Day, April 2019)*